Investigating the murine meiotic telomere complex TERB1-TERB2-MAJIN: spatial organization and evolutionary history

Dissertation zur Erlangung des naturwissenschaftlichen Doktorgrades
der Julius-Maximilians-Universität Würzburg

vorgelegt von

Irene María da Cruz Güerisoli

aus Salto, Uruguay

Würzburg, 2020

Eingereicht am: ……..……..

Mitglieder der Promotionskommission:

Vorsitzender: ……..

Gutachter: Prof. Dr. Ricardo Benavente

Gutachter: Prof. Dr. Christian Stigloher

Tag des Promotionskolloquiums: ……..…

Doktorurkunde ausgehändigt am: …….

Table of Content

List of Figures

List of Table

Zusammenfassung

Einess der faszinierenden Merkmale der meiotischen Prophase I sind die hochkonservierten kräftigen Bewegungen homologer Chromosomen. Diese Bewegungen sind entscheidend für den Erfolg von Schlüsselereignissen wie die Ausrichtung, Paarung und Rekombination der homologen Chromosomen. Mehrere bisher untersuchte Organismen, darunter Säugetiere, Würmer, Hefen und Pflanzen, erreichen diese Bewegungen, indem sie die Chromosomenenden an spezialisierten Stellen in der Kernhülle verankern. Diese Verankerung erfordert Telomer-Adapterproteine, die bisher in der Spalthefe und der Maus identifiziert wurden.

Die meiosespezifischen Telomer-Adapterproteine der Maus, TERB1, TERB2 und MAJIN, sind an der Verankerung des ubiquitären Telomer-Shelterin-protein an den LINC-Komplex beteiligt, mit einem analogen Mechanismus, wie er die Spalthefe beschrieben wird. Obgleich die meiose-spezifischen Telomer-Adapterproteine eine wesentliche Rolle spielen, ist der genaue Mechanismus der Verankerung der Telomere an die Kernhülle sowie ihre evolutionäre Geschichte bisher noch wenig verstanden. Das Hauptziel dieser Arbeit ist daher die Untersuchung der Organisation des meiosespezifischen Telomer-Adapterkomplexes TERB1-TERB2-MAJIN der Maus und dessen Evolutionsgeschichte.

Im ersten Teil dieser Arbeit wurde die Organisation des TERB1-TERB2-MAJIN Komplexes mittels hochauflösender Mikroskopie (SIM), an Mausspermatozyten untersucht, sowie die Lokalisation in Bezug auf TRF1 des Telomer-Shelterin-Komplexes und die telomerische DNA analysiert. In den Stadien Zygotän und Pachytän zeigten die Fluoreszenzsignale eine starke Überlappung der Verteilung der meiotischen Telomer-Komplex-Proteine, wobei die Organisation von TERB2 an den Chromosomenenden heterogener war als die von TERB1 und MAJIN. Außerdem konnte die TRF1-Lokalisation an den Enden der Lateralelemente (LEs) mit einer griffartigen Anordnung um die TERB1- und MAJIN-Signale im Zygotän- und Pachytän-Stadium gezeigt werden. Interessanterweise erwies sich die telomerische DNA als lateral verteilt und teilweise überlappend mit der zentralen Verteilung der meiotischen Telomer-Komplex-Proteine an den Enden der LEs. Die Kombination dieser Ergebnisse erlaubte die Beschreibung eines

alternativen Modells der Verankerung der Telomer an die Kernhülle während der meiotischen Prophase I.

Der zweite Teil dieser Arbeit analysiert die Evolutionsgeschichte der Mausproteine von TERB1, TERB2 und MAJIN. Die fehlende Übereinstimmung zwischen den Meiose-spezifische Telomer-Adapteproteinen der Maus und der Spalthefe hat die Frage nach dem evolutionsbedingten Ursprung dieses spezifischen Komplexes aufgeworfen. Um vermeintliche Orthologen der Mausproteinevon TERB1, TERB2 und MAJIN über Metazoen hinweg zu identifizieren, wurden computergestützte Verfahren und phylogenetische Analysen durchgeführt. Darüber hinaus wurden Expressionsstudien implementiert, um ihre potenzielle Funktion während der Meiose zu testen. Die Analysen haben ergeben, dass der Meiose-spezifische Telomer-Komplex der Maus sehr alt ist, da er bereits in den Eumetazoen entstand, was auf einen einzigen Ursprung hindeutet. Das Fehlen jeglicher Homologen des meiosespezifischen Telomerkomplexes in Nematoden und die einigen wenigen in Arthropoden nachgewiesenen Kandidaten, deuten darauf hin, dass die Telomer-Adapterproteine in diesen Abstammungslinien verloren/ersetzt oder stark diversifiziert worden sind. Bemerkenswerterweise zeigten Proteindomänen von TERB1, TERB2 und MAJIN, die an der Bildung des Komplexes sowie an der Interaktion mit dem Telomer-Shelterin-Protein und den LINC-Komplexen beteiligt sind, eine hohe Sequenzähnlichkeit über alle Kladen hinweg. Abschließend lieferte die Genexpression im Nesseltier *Hydra vulgaris* den Beweis, dass der TERB1-TERB2-MAJIN-Komplex selektiv in der Keimbahn exprimiert wird, was auf die Konservierung meiotischer Funktionen über die gesamte Metazoen-Evolution hinweg hindeutet.

Zusammenfassend bietet diese Arbeit bedeutende neue Erkenntnisse hinsichtlich des Meiose-spezifischen Telomer-Adapterkomplex, seines Mechanismus zur Verankerung der Telomer an die Kernhülle und die Entschlüsselung seines Ursprungs in den Metazoen.

Summary

One of the fascinating features of meiotic prophase I, is the highly conserved vigorous movements of homologous chromosomes. These movements are critical for the success of essential events as homologs alignment, synapsis and recombination. Several organisms studied so far, including mammals, worms, yeast and plants achieve these movements by anchoring the chromosome ends to specialized sites in the nuclear envelope (NE). This attachment requires telomere adaptor proteins which have to date been identified in fission yeast and mice.

The mouse meiosis-specific telomere adaptor proteins TERB1, TERB2, and MAJIN are involved in the attachment of ubiquitous shelterin telomere to the LINC complex, in an analogous mechanism as those described in fission yeast. Despite the essential role of meiosis-specific telomere adaptor proteins, the precise mechanism of anchorage of telomeres to the nuclear envelope, as well as their evolutionary history, are still not well understood. Therefore, the main aim of this thesis is to investigate the organization of the mouse meiosis-specific telomere adaptor complex TERB1-TERB2-MAJIN and its evolutionary history.

In the first part of this thesis high-resolution Structured Illumination Microscopy (SIM), indirect immunofluorescence and Telo-FISH on mouse spermatocytes were used to determine precisely how the telomere complex proteins are localized with relation to the shelterin telomeric TRF1 protein and telomeric DNA. During zygotene and pachytene stages staining patterns revealed extensively overlapping of meiotic telomere complex proteins distributions in which TERB2 organization is more heterogeneous than TERB1 and MAJIN at the chromosome ends. Further, TRF1 localization was shown at the side of lateral elements (LEs) ends with grasp-like distribution surrounding the TERB1 and MAJIN signals in zygotene and pachytene stages. Interestingly, telomeric DNA was shown to be laterally distributed and partially overlapping with the more central distribution displayed by meiotic telomere complex proteins of LEs ends. The combination of these results allowed to describe an alternative model of the telomere attachment to the NE during meiotic prophase I.

The second part of this thesis, analyses mouse TERB1, TERB2, and MAJIN evolutionary history. The lack of similarity between mouse and fission yeast meiotic-specific telomere adaptor proteins has raised the question about the origin of this specific complex through evolution. To identify mouse TERB1, TERB2, and MAJIN putative orthologues, computational approaches and phylogenetic analyses were performed. Besides, to test their potential function during meiosis, expression studies were conducted. From these analyses, it was revealed that mouse meiosis-specific telomere complex is ancient, as it originated as early as eumetazoans pointing to a single origin. The absence of any homologs in Nematoda and only a few candidates detected in Arthropoda for meiosis-specific telomere complex, seemed, that these proteins have been lost/replaced or highly diversified in these lineages. Remarkably, TERB1, TERB2, and MAJIN protein domains involved in the formation of the complex as well as those required for the interaction with the telomere shelterin protein and the LINC complexes revealed high sequence similarity across all clades. Finally, gene expression in the cnidarian *Hydra Vulgaris* provided evidence that the TERB1-TERB2-MAJIN complex is selectively expressed in the germline suggesting conservation of meiotic functions across metazoan evolution.

In summary, this thesis provides significant *insights* into the meiosis-specific telomere complex mechanism to engage telomeres to the nuclear envelope and the elucidation of its origin in metazoans.

Chapter 1 General Introduction

1.1 Meiosis is key for gametogenesis and sexual reproduction

Sexual reproduction involves the fusion of haploid gametes from two individual organisms to produce an offspring with diploid nuclear content. Therefore, the first indispensable event in sexually reproducing organisms is to produce maternal and paternal gametes capable of fertilization. In male individuals, gametogenesis is called spermatogenesis and originates in the particular environment provided by the gonads, or sex organs. When the spermatogonia (2n) receives the right signals to enter meiosis, culminates in four haploids (n) spermatozoa or gametes that have half the content of DNA within them. Hence, meiosis is a specialized cell division type that accomplishes reduction of ploidy from a diploid germ cell (2n), through two sequential rounds of nuclear division (known as meiosis I and meiosis II) following a single series of DNA replication (S-phase) resulting in four haploids (n) cells (Figure 1-1).

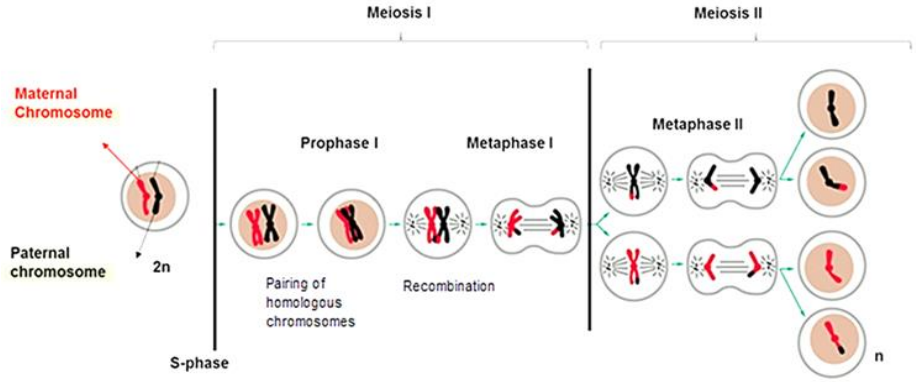

Figure 1-1 Events during meiosis cell cycle.

Schematic representation of a diploid germ cell with maternal (red) and paternal (black) chromosomes that have been duplicated. Upon prophase I, homologous chromosomes pair and synapse thereby forming a structure containing four chromatids known as a bivalent. In prophase I homologous chromosomes pair and synapse leading to recombination events such as reciprocal exchange of chromosome arms. In metaphase I bivalents can move to the opposite spindle poles while in metaphase II each sister chromatids moves to opposite poles leading to the generation of haploid cells (Image modified from Alberts et al., 2002).

Cytological and genetic data published so far suggested that meiosis evolved from mitosis (Wilkins & Holliday 2009) or paralleled to it (Cavalier-Smith, 2010). Consequently, the division stages of meiosis I and II are analogous to the events of mitosis and the same names are assigned for meiotic division I and II (prophase, metaphase, anaphase, and telophase).

At the onset of the meiotic prophase I, duplicated homologous chromosomes recognize each other and get into physical contact. In many organisms, this initial homologous chromosome association is called pairing and culminates with full connection along their length. This connection is reinforced by the formation of the synaptonemal complex (SC) between the two homologous chromosomes, promoting the exchange of chromosomes segments between non-sister homologous chromatids, known as crossover (CO). These events are the source of genetic variation due to the reciprocal exchange of equivalent DNA between homologous chromosomes.

Towards the end of prophase I, crossovers are cytologically observable as chiasmata (Jones, 1987) that hold pairs together until the spindle separates them at anaphase I. The arms of the sister chromatids for each duplicated homologous chromosome are glued together along their length by proteins called cohesins. At the start of anaphase I, the cohesins that hold sister chromatids together are degraded, allowing the homologous chromosome to be pulled to opposite poles of the spindle.

In Meiosis II, the daughter cells follow a segregation pattern that resembles the standard equatorial division of mitosis. Before anaphase II, each sister chromatid attaches to microtubules by an individual kinetochore formed from opposite poles. Subsequently, in anaphase II, the sister chromatid's cohesion is released, and each chromatid is dragged apart to opposite poles by the spindle fibres. In telophase II chromosomes begin to decondense and progressively arrive at opposite poles. Finally, Cytokinesis takes place dividing the cytoplasm of the two cells, producing four daughter cells, each with a haploid set of chromosomes. After meiosis, these haploid cells (gametes or sperm) are genetically unique due to crossover between maternal and paternal segments of chromosomes that occurs during meiotic recombination.

Overall, meiosis is a highly complex process that depends on timely-coordinated events, including the recruitment of meiosis-specific cohesins on sister chromatids, pairing, synapsis, recombination of homologous chromosomes and dynamic chromosome movements. These finely coordinated events occur during meiotic prophase I thus, guaranteeing the success of halving the genome. Chromosomes that fail to segregate normally into the four haploid cells can lead to infertility, miscarriage during pregnancy and severe congenital disabilities.

1.2 Dynamics of homologous chromosome during meiotic prophase I

The prophase of meiotic division I is the longest and most complex phase of meiosis. Conventionally it is divided into five sequential stages—leptotene, zygotene, pachytene, diplotene, and diakinesis—defined by morphological changes associated with the assembly (synapsis) and disassembly (desynapsis) of the synaptonemal complex.

The Prophase I begins with the leptotene (Greek "leptos" = thin) stage, characterized by the progressive condensation of duplicated homologous chromosomes. During leptotene, telomeres attach to the inner nuclear membrane (INM) and the decondensed chromatin starts to be organized via the formation of a protein axes (axial elements; AEs) along the replicated sister chromatids. In mammals, SYCP2 and SYCP3 form the AEs during leptonema (Offenberg et al., 1998; Schalk et al., 1998). Simultaneously the genome undergoes numerous DNA double-strand breaks (DSBs) introduced by topoisomerase-like enzyme Spo11 (Keeney et al., 1997). DSB formation and subsequent repair (Keeney, 2001) is the core of meiotic recombination. Cytological studies in mouse and yeast revealed Spo11 forming discrete staining structures ("foci") on chromatin early in leptotene (Romanienko & Camerini-Otero 2000; Storlazzi et al., 2003; Prieler et al., 2005). Also, the Spo11 recombination pathway involves a protein complex that repairs meiotic DSBs. Among them, Rad51 (the eukaryotic version of the RecA protein) and Dmc1 have a role in repairing DSBs and homologous pairing in *S. cerevisiae*, mouse and maize (Weiner et al. 1994; Franklin et al. 1999; Pawlowski et al. 2003; Yoshida et al., 1998). Rad51 and Dmc1 localization to chromosome cores, has

been postulated as a marks of initial DNA-DNA interactions sites after DSB induction (Moens et al., 2002; Tarsounas et al., 1999). These sites are called early nodules (EN), which can be detected as an electron-dense structure associated with the chromosome axis (Moens et al., 2002). These multiple EN can be further subdivided into two categories: those found on asynapsed axes and those found on synapsed axes (Ashley, 2007). The second stage of meiosis prophase I is the zygotene (Greek "zygos" = pair). In this stage, stable pairing initiates between the homologous chromosomes due to the assembly of transverse filaments between AEs (now called lateral elements; LEs) terminating in the appearance of a central element (CE) of the SC (von Wettstein et al., 1984; Hunter, 2003). At the same time, telomeres move and cluster on a single site through the NE forming the so-called "telomere bouquet" (von Wettstein et al., 1984; Zickler & Kleckner, 1998; Scherthan, 2001). The presence of a bouquet-stage is conserved among plants, mammals, and fungi in concomitant relation with chromosome pairing events (Chikashige et al., 1994; Schertan et al., 1996; Trelles-Sticken et al., 1999). However, it was reported that homologous chromosomes are brought together earlier via global and/or local pairing after which DSB-mediated co-alignments occur, during leptotene (Goldman & Lichten, 2000; Kleckner & Weiner, 1993; Klutstein & Cooper 2014). For instance, in budding yeast, sordaria, mouse, and some plants, the bouquet does not display until after homologs are already co-aligned (Zickler & Kleckner, 1998; 2015). It was also suggested that once the pairing process is ongoing, telomere movement could help full-length pairing of homologous chromosomes or prevent entanglements by removing non-homologous interactions (Zickler, 2006; Koszul et al., 2008; Kleckner et al., 2011; Klutstein & Cooper 2014; Koszul & Kleckner, 2009). As the SC is assembled, the number of ENs decreases as they processed into transitional nodules (TNs) in mammals (Moens et al., 2002). The TNs localize in synapsed axes proteins and contain RPA, MSH4, BLM helicase and topoisomerase, which are implicated in the initial DSB processing (Moens et al., 2002).

Once the CE spread into both directions to connect homologous chromosomes axes along their entire length, they are said to have synapsed; thus the cell has reached the third substage of prophase I, known as pachynema Greek "pakhus"

= thick). Upon pachytene stage the SC is fully assembled in a highly conserved tripartite ladder-like organization with two lateral elements (LEs) and central element (CE) consists of transverse filaments (TFs) (Petronczki et al., 2003; Schmekel & Daneholt 1995; Heyting, 2005; Fraune et al., 2012). In mammals, the LEs are connected by TFs composed mainly of SYCP1 (Meuwissen et at., 1992). Upon the localization of SYCP1, it recruits other proteins to the CE, such as SYCE1, SYCE2, SYCE3, and TEX12 (Costa et al., 2005; Hamer et al., 2006; Schramm et al., 2011).

In pachytene stage, electron-dense nodules in association with the fully established SCs are referred as late recombination nodules (LNs). From the initial several hundred of DSBs, only few and non-randomly distributed LNs on the fully synapsed SC presumably represent the sites of the processed into crossing-overs in mammals (Plug et al., 1998).

The diplotene (Greek "diplos" = double) stage begins when homologous chromosomes start to desynapse due to the disassembly of SC. Telomeres begin to detach from the INM, and the recombination-associated proteins are generally not present in this stage, but homologs remain attached through chiasmata. Finally, the last stage is called diakinesis (Greek "kinesis" = movement) in which the homologous chromosomes undergo their highest degree of condensation to transit into metaphase I.

Altogether prophase I is a complex process in which pairing, synapsis and recombination are a tightly coordinated. The establishment of this coordinated process requires both telomere attachment and regulated movement for accurate homologous chromosome pairing, thus recombination and segregation of homologous chromosomes.

1.3 Chromosome movements: a universal feature of meiotic prophase I

Chromosome movement displayed during meiotic prophase I is vital for proper pairing, synapsis and recombination events (Alleva & Smolikove, 2017). Upon meiosis, chromosome ends (telomeres) attach to the NE and follow a dynamic conserved choreography (For mouse see Figure 1-2) during prophase I.

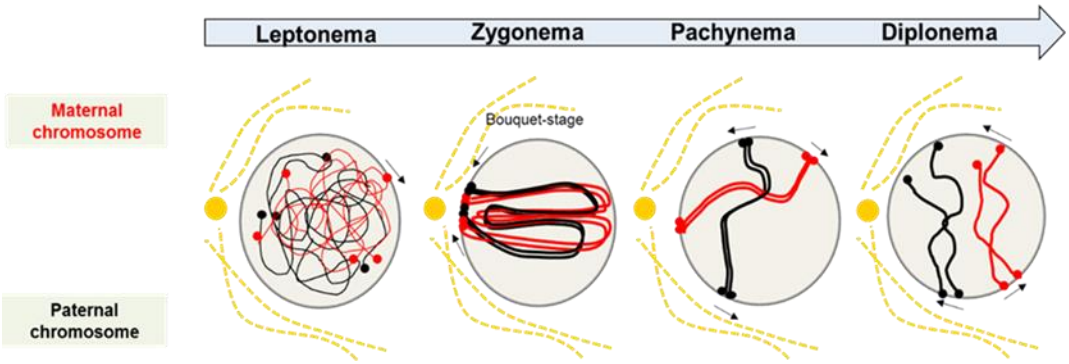

Figure 1-2 Meiotic telomere dynamics during prophase I in mouse.
Upon leptonema mouse homologous chromosomes (red and black), starts to condense and a protein axes start to assemble (axial elements; AEs). Telomeres (red and black circles) begins to attach and transit (black arrow) through the nuclear envelope (NE) mediated by cytoplasmic microtubules (in yellow) originated in the centrosome (yellow circle). At the transition to zygonema telomeres are congregated in a confined region of the NE towards the centrosome. This configuration is called bouquet. At the same time stable pairing initiate between homologous chromosomes due to the assemblage of proteinaceous transverse filaments between AEs (now called lateral elements; LEs). In pachynema telomeres are active dispersed within the NE and lengthwise synapsed by the complete assembly of the synaptonemal complex (SC). The synapsis allows meiotic recombination events. During diplotene the SC start to disassemble, and homologous chromosomes association is released. Telomeres begin to detach from the NE and homologous chromosomes are associated by the crossing-over sites at the chiasmata.

Another widespread feature during early prophase I is the telomere bouquet or chromosome end clustering. In animals and fungi, telomere clusters orientate towards the centrosome or spindle pole body (SPB), respectively (Zickler & Kleckner, 1998). In plants, telomeres cluster opposite to the area with a higher concentration of cytoplasmic microtubules (Cowan et al., 2001).
Despite the conservation of bouquet in mammals, plants and yeast, the arrangement and time are likely to be species-specific. For instance, in mouse, bouquet formation occurs briefly during the leptotene/zygotene transition (Scherthan et al., 1996), while in *S. pombe* it can persist for much longer in Prophase I (Cooper & Hiraoka, 2006). In maize, bouquet formation is at the end of leptotene and continues throughout zygotene (Bass et al., 1997). In *C.*

elegans, one single end of the chromosome is attached to the NE. Although *C. elegans* does not form a bouquet configuration, the chromosome ends to acquire a polarized organization at the NE during leptotene/zygotene stages (Dernburg et al. 1998; Goldstein & Slaton, 1982).

While clustering of chromosome ends brings homologs closer together (Harper et al., 2004; Ding et al., 2004), the role proposed in promoting the initiation of pairing has been debated. Several lines of evidence in mouse, yeast and plants showed that defects in bouquet generation alter pairing, synapsis and reparation of the DSBs of homologous chromosome (Niwa et al., 2000; Chikashige et al., 2007; Liebe et al., 2004; Carlton & Cande 2002, Harper et al., 2004). Studies that used mutations that specifically disrupt the bouquet in fission yeast showed that telomere bouquet plays a crucial role in controlling the spindle pole body (SPB) maturation and proper meiotic spindle formation (Tomita & Cooper 2007). Interestingly a recent report in zebrafish showed that bouquet stage is necessary to increase the chances to find homologs chromosome and initiate of pairing by the non-specific association of telomeres (Blokhina et al., 2019). At this time, homology chromosomes gather together in a non-homology-driven fashion that promotes pairing and crossover formation similar to that which has been found in several other organisms (Blokhina et al., 2019).

In general, the dynamics of homologous chromosomes in prophase I is widely conserved and the relative importance of their motion and chromosome interaction in bouquet formation seems to be species-specific but key for the faithful homolog alignment and, consequently, are essential for prophase I progression.

1.4 Meiosis-specific nuclear envelope adaptations for telomere attachment site

1.4.1 Ultrastructure of meiotic chromosome ends attachment to the NE

The association of the meiotic chromosome ends with the NE was shown to be mechanically stable due to the resistance to harsh spreading techniques and dragging forces applied by micromanipulation or centrifugation (Alsheimer et

al., 1998; Scherthan et al., 2007). Significant progress from studies that were aimed at identifying the molecules involved in the attachment complex of meiotic chromosome ends have revealed that the NE has a key role (Kracklauer et al., 2013). Earlier electron microscopy (EM) studies in crayfish spermatocyte samples described for the first time that chromosomes ends were terminally associated with the NE (Moses, 1956). Later it was shown that SCs are attached to the NE at both ends (Wettstein & Sotelo 1967). This association was described in rodents as a conical thickening of the LEs structure embedded in the NE (Esponda & Gimenez-Martin, 1972). Several years afterwards Liebe et al., (2004) uncover telomere attachment to the NE in mouse deficient for Sycp3, the major structural protein component of the LEs (Lammers et al., 1994; Yuan et al., 1998). In contrast with wildtype mice, the ultrastructure analysis of Sycp3 knockout mouse showed that, the conical thickness of AEs were absent, but telomeric DNA is still attached to the INM via attachment plates, i.e. highly dense structures of the INM. At the level of attachment plate the NE is more dense and thin filaments that project from both INM and ONM likely connect chromosomal ends and cytoplasmic structures (Figure 1-3) (Liebe et al., 2004). These studies provided for the first-time strong evidence that telomere sites are connected to the cytoplasm because the typical membrane traversing filaments seen in the wild type were also detected in mice Sycp3-/- demonstrating that functional attachment complex is formed even though SCs are absent (Liebe et al, 2004).

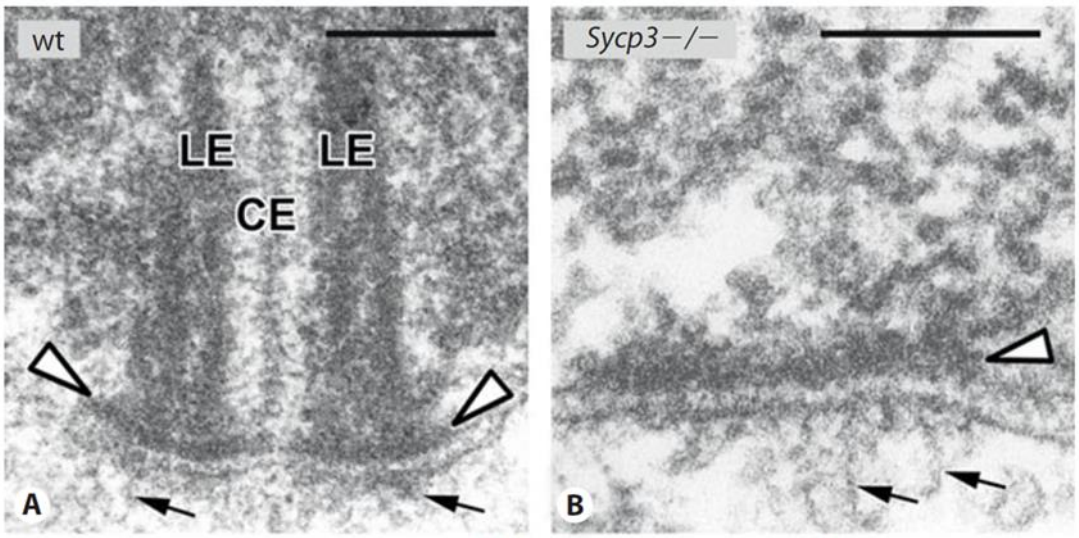

Figure 1-3 Ultrastructure of mouse meiotic telomere attachment.
Electron micrograph of the attachment plate of a wildtype mouse pachytene stage (A) in which the two lateral elements (LEs) and the central element (CE) is shown. Towards the site of the telomeres, the highly dense attachment plate connects the conical thickening end of the LEs with the inner nuclear membrane (INM) (white arrows). Thin filament bundles project between the telomere attachment plates and the black arrows indicate the INM through the outer nuclear membrane (ONM) to the cytoplasm. (B) Transmission electron microscopy of a section of a telomere attachment of a Sycp3 -/- mouse spermatocyte showing the highly dense region at the attachment plate but not the conical thickening. Also is visible the same fibrillar material as in wild type that traverses the nuclear envelope and extends to the cytoplasm (black arrows). (Figure from Liebe et al., 2004).

1.4.2 Meiosis-specific splice variant Lamin C2 is enriched at the sites of telomere attachment

It was argued that the association of chromosomes ends with the NE must be dynamic to allow the chromosome movements to take place during meiotic prophase I.

The NE is a double membrane system composed of two membrane bilayers, the inner nuclear membrane (INM) and the outer nuclear membrane (ONM) which are perforated by the nuclear pore complex. The endoplasmic reticulum (ER) is associated with the ONM layer as if it forms an extension of the outer face. Between the ONM and INM lies the perinuclear space (PNS), which is

continuous with the ER lumen. Additionally, the INM of metazoans nucleus is composed of an organized mesh of proteins known as the lamina, assembled form intermediate filaments. Although these intermediate filaments are members of a large family of cytoplasmic and nuclear proteins that polymerize into stable threads, they are not conserved in plants and fungi. In metazoans, nuclear lamins form a meshwork between the INM and the DNA, which also connects nuclear pores (Mekhail & Moazed, 2010).

In mammals, A-type and B-type lamins are encoded by three genes: LMNA; LMNB1 and LMNB2. The LMNA gene encodes two somatically expressed isoforms A and C lamins (Lin & Worman, 1993). However, an alternative splice variant also originated from the LMNA gene is the meiosis-specific lamin C2 which found specifically expressed in male and female meiotic germ cells (Alsheimer & Benavente, 1996, Alsheimer et al., 1998; Furukawa et al., 1994). Several observations indicate that the attachment sites of telomeres in the NE involves lamin C2 (Alsheimer et al., 1999). Lamin C2 appears to reduce the mechanical stiffness of the NE, playing a role in the dynamic reposition of meiotic telomeres (Link et al., 2013).

To summarize, Lamin C2 directly involved the attachment of meiotic telomeres probably by the local influence on the NE properties thereby facilitating the conserved dynamic of telomere movements within the NE during prophase I.

1.4.3 The meiotic LINC complex: Linker of Nucleoskeleton and Cytoskeleton

Telomere regions anchoring to the NE involves highly conserved LINC complex (Linker of Nucleoskeleton and Cytoskeleton). LINC-complexes are an essential component of the NE composed of two classes of proteins: Sad1p/Unc84 (SUN) and Klarsicht/Anc1/Syne1 homology (KASH) domain. The SUN domain proteins reside in the INM and interact with proteins that bind the chromosome ends to the NE (Kracklauer et al., 2013). The KASH domain is embedded in the outer nuclear membrane and interacts with the cytoskeleton of meiotic cells (Kracklauer et al., 2013). Through SUN-KASH interactions in the perinuclear space, the LINC complex can transduce forces generated by the cytoskeleton enabling meiotic chromosomes to move (Kracklauer et al., 2013; Link et al., 2015).

SUN domain-containing proteins exhibit a highly conserved structure and function among different species (Starr, 2009). The N-terminus of SUN proteins resides in the INM, and it is separated from the C-terminus by at least one transmembrane domain. Also, the N-terminal domain interacts with the nucleoskeleton components such as lamins and indirectly with telomeres. Conversely, the C-terminus contains the conserved SUN domain that extends to the perinuclear space.

The KASH proteins show a conserved motif localized in its C-terminal domain and resides in the PNS to interact with SUN domain proteins specifically. In contrast, KASH N-terminus resides in the ONM and is less conserved among the species, reflecting the variety of the cytoskeleton proteins that can connect including actin, microtubules components, and plectin (Razafsky & Hodzic, 2009; Starr, 2009; Starr & Fischer, 2005).

In the course of evolution, SUN genes have undergone diversification across different species, and the expression of the individual SUN proteins depends on the cell-type, suggesting cell-type adaptations of LINC-complexes to cope with different physiological requirements (Table 1-1). For instance, mammals encode five SUN domain-containing proteins (SUN1, SUN2, SUN3, SUN4 and SUN5). Of these, only the SUN1 and SUN2 (Crisp et al., 2006; Ding et al., 2007; Morimoto et al., 2012; Schmitt et al., 2007) are ubiquitously expressed and have an essential role in tethering meiotic telomeres in prophase I. Also, their INM partners, the A-type lamins, interact with both Sun1 and Sun2 both (Schmitt et al., 2007). On the other hand, the expression of SUN3, SUN4 and SUN5 seems to be restricted to spermiogenesis (Göb et al., 2010; Frohnert et al., 2011). Similarly, in *C. elegans*, UNC-84 is expressed in all cells; meanwhile, SUN-1/Matefin expression is restricted to germ cells (Malone et al., 2003; Tzur et al., 2006; Penker et al., 2007; Sato et al., 2009). The same situation was identified in *A. thaliana* and maize, in which five SUN domain-containing proteins were identified. Only two of them, AtSUN1, AtSUN2 for *A. thaliana* and ZmSUN1, ZmSUN2 for the maize have a specific role in tethering meiotic telomeres to the NE (Graumann et al., 2010; Zhou et al., 2015; Varas et al., 2015; Murphy et al., 2014). The situation is different in lower eukaryotes such as *S. pombe* and *S. cerevisiae* in which only one SUN domain-containing protein is enough to

meet the cell's requirements (Miki et al., 2004; Chikashige et al., 2006; Ding et al., 2007; Jaspersen et al., 2006; Conrad et al., 2008; Wanat et al., 2008).
Likewise, KASH domain proteins have also been identified somatically expressed in widespread model organisms (Zhang et al., 2001; Starr & Han, 2002). In most of them, at least one KASH domain protein is specifically expressed during meiosis. For instance, to date, KASH5 in mammals (Morimoto et al., 2012); ZYG-12 in *C. elegans* (Malone et al., 2003; Sato et al., 2009; Zhou et al., 2009) and Kms1, Kms2, Csm4 in yeast (Miki et al., 2004; Chikashige et al., 2006; King et al., 2008; Conrad et al., 2008; Koszul et al., 2008) have been confirmed to be involved in meiosis (Table 1-1).
In summary, LINC complexes are components of the NE that facilitate chromosome dynamics through the direct association of INM meiotic chromosome ends with cytoplasmic structural elements residing outside the nucleus. LINC complexes function in a highly conserved manner from yeast to mice and thereby critical for fertility.

Table 1-1 SUN-KASH proteins of the meiotic LINC complex in different species

	S. pombe	***S. cerevisiae***	***C. elegans***	***M. musculus***	***A. thaliana***
SUN domain proteins	Sad 1	Mps3	Matefin/SUN-1	SUN1 SUN2	AtSUN1 AtSUN2
KASH domain protein	Kmas1 Kms2	Csm4	ZYG-12	KASH5	unknown
Motor	Dynein, Dynactin, Kinesin	Actin motors	Dynein	Dynein, Dynactin	unknown

1.5 Telomere associated proteins and meiosis specific adaptor proteins

1.5.1 Telomere sequences associated protein complex

The chromosome ends of eukaryotes, or telomeres, are specialized nucleoprotein complexes that protect DNA from degradation, end fusions and recombination. In most eukaryotes, telomeres are comprised of double-stranded short tandem DNA repeats (the length of repeats can vary between

species) and are maintained by telomerase. Vertebrates, like most metazoans, use the sequence motif (TTAGGG)n at their chromosomes ends (Palm & de Lange, 2008). These double-stranded telomere repeats (20-50 kb) terminate in an evolutionarily conserved single-stranded 3'-protution of the G-strand known as the 3'-overhang (50-500 nt) (Moyzis et al., 1988, Palm & de Lange, 2008). Conversely, the lineages leading to Nematodes and Arthropods in Metazoans possess a different telomere motif sequence. For instance, the chromosome capping in *C. elegans* is achieved by 4-9 kb of a (TTAGGC)n sequence motif. At the same time, *D. melanogaster* uses arrays of telomerase independent retrotransposons at the chromosome ends (Gomes et al., 2011). In plants like Arabidopsis, the telomeric motif found consists of TTAGGG repeats (Richards & Ausubel, 1988). The Arabidopsis-type telomere has been found in most angiosperms, but several reports indicate that this sequence is absent in related species (Pich et al., 1996). On the other hand, telomeric repeats in *S. pombe* consist of the sequence GGTTACA (Hiraoka et al., 1998) while the telomere sequence in *S. cerevisiae* is C1-3 A/TG1-3 (Förstemann & Lingner, 2001).

Telomeres associate with a conserved DNA-binding protein complex known as shelterin, the primary function of which is to protect telomeres from the aberrant activation of DNA damage response. Mammalian telomeres associate with six proteins known as the telomere shelterin complex (de Lange et al., 2005). From the shelterin proteins, telomeric repeat TRF1 and TRF2 specifically recognize the double-stranded DNA via its C-terminal SANT/MYB DNA-binding domain which is part of the homeodomain-like superfamily (Bilaud et al., 1996). Also, both proteins share a domain structure that consists of a TRF homology (TRFH) domain through which they bind the DNA as homodimers formed through their homotypic interactions (Bianchi et al., 1997; Broccoli et al., 1997). TRF1 and TRF2 recruit the other four shelterin components: TIN2, RAP1, TPP1 and POT1 (de Lange et al., 2005) to the telomeres. Among them, POT1 (POT1a and POT1b in mice) can bind the single-stranded telomere DNA. Besides, the TRFH domains of TRF1 and TRF2 encompass a versatile peptide-docking site through which other target proteins are recruited to contribute in the maintenance and protection of chromosome ends (Chen et al., 2008). The motif F/YxLxP on target proteins is critical for their recognition by the TRFH domain.

Therefore, the TRFH domains of TRF1 and TRF2 can recruit and recognize different specific target proteins to telomeres according with the necessities of the cell (Palm & de Lange, 2008).

Similarly, in *C. elegans*, telomerase and shelterin proteins regulate telomere length (Malik et al., 2000; Cheung et al., 2006; Meier et al., 2006; Shtessel et al., 2013). Previous work has illustrated that *C. elegans* homologous to mammalian POT1 the POT-1 and POT-2 can interact with single-stranded telomeric DNA in vitro (Raices et al. 2008).

Remarkably, several aspects of the mammalian telomere shelterin complex are highly conserved in fission yeast somatic telomere complex. *S. pombe* Taz1 is an ortholog of human TRF1 and TRF2 and binds directly to telomere repeat sequence (Zhong et al., 1992; Bilaud et al., 1997; Broccoli et al., 1997; Cooper et al., 1998; Ferreira & Cooper 2001, Nakamura et al. 1998). Also, Rap1 protein is an ortholog of human RAP1 (Li et al., 2000) that interact with the telomeres through the binding with Taz1 (Chikashige & Hiraoka, 2001; Kanoh & Ishikawa, 2001). *S. cerevisiae* lacks a TRF-like telomeric protein, however, have been demonstrated that Rap1 interact and regulate telomeres length (Marcand et al. 1997a, Marcand et al. 1997b, McEachern et al. 2000). Notably, vertebrate POT1 and TPP1 are orthologs of the *S. pombe* Pot1 and Tpz1.

In summary, evolutionary conservation of the roles of telomere shelterin proteins seems to occur at the level of functional domains that enable their binding to single-stranded DNA, and telomere-sequence recognition.

1.5.2 Meiosis-specific adaptors between Telomeres/PC and LINC complex

Besides telomeres vital functions, they have also been implicated as key players during meiosis. Several lines of evidence in mice, yeast and plants suggested that interference with telomere structure compromises the passage through meiosis (Voet et al., 2003; Carlton & Cande 20002; Lundblad & Szostak, 1989). Also, it has been demonstrated that the deletion of telomeres or rings as results of of linear chromosomes rearrangement impedes the process of meiosis (Naito et al., 1998; Ishikawa & Naito, 1999; Nimmo et al., 1998).

To reinforce the connection between telomeres and the meiotic LINC complex and their subsequent movement within the NE during prophase I, different

organisms engage unique meiotic adaptor proteins, which are not well conserved (Figure 1-4).

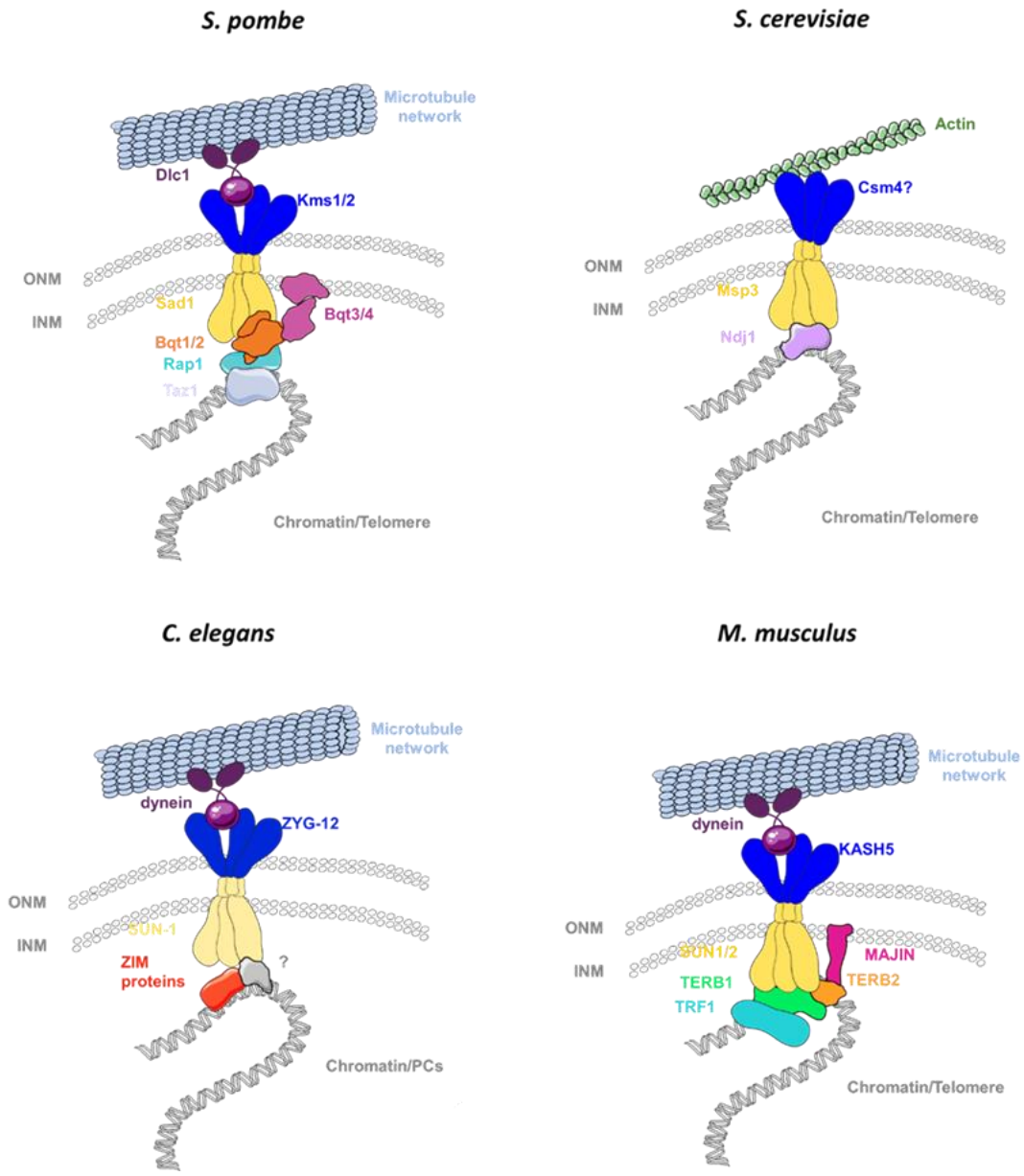

Figure 1-4 Schematic representation of the molecular components that tether telomeres to LINC complexes in different species.

The LINC complex in different model organisms is composed of a highly conserved SUN domain protein in the inner nuclear envelope (INM) and a KASH domain protein in the outer nuclear envelope (ONM). The complex functions to connect the telomeres indirectly with cytoplasmic microtubules. In fission yeast (*S. pombe*), the proteins Bqt1-4 connect the Rap1 and Taz1 somatic telomeric proteins with the SUN domain protein Sad1. In budding yeast (*S. cerevisiae*) the telomere-associated protein Ndj1 interact with SUN domain protein Mps3 attach telomeres to Csm4. In the case of *C. elegans* a

set of four zinc finger proteins (ZIM-1/2/3 and HIM-8) specifically associate to sub-telomeric chromosome regions known as pairing centers (PCs), but the direct connectors to the LINC complex is still unknown. In the mouse TERB1-TERB2-MAJIN meiotic adaptor proteins cooperate with TRF1 telomere shelterin protein to interact with the SUN1/2 proteins.

In a screen for budding yeast meiotic genes, Ndj1 was the first gene linked to bouquet formation in *S. cerevisiae* (Conrad et al. 1997). Cytological analysis of a Ndj1 mutant showed that telomeres fail to tether to the NE in early meiotic prophase (Conrad et al. 1997). Ndj1 is a meiosis-specific telomere protein that interacts with the NE Mps3 (Conrad et al. 2007; 2008). Mps3 is a conserved SUN family protein of the INM and interacts with Cms4 in the space between the inner and outer nuclear membranes. Cms4 associates with cytoskeletal actin filaments and thus enables the formation of a linker complex involving Mps3 and Ndj1 to move chromosome ends within the nucleus (Trelles-Sticken et al., 2005; Conrad et al., 2007, 2008; Scherthan et al., 2007; Kosaka et al., 2008; Koszul et al., 2008; Wanat et al., 2008).

As for *S. pombe*, meiosis-specific proteins Bqt1 and Bqt2 were identified essential in the telomere clustering pathway (Chikashige et al., 2006). Bqt1 and -2 connect the Taz1-Rap1 telomere somatic protein to the Sad1–Kms1 (LINC complex) located in the NE. The Sad1–Kms1 complexes tether telomeres to the SPB through the nuclear membranes using cytoplasmic microtubules through an interaction between Kms1 and dynein (Chikashige et al., 2007). In addition to Bqt1, -2 the Bqt3 and -4 INM proteins are necessary to connect telomeres to the NE during both vegetative growth and meiosis (Chikashige et al., 2009). It was shown that in *S. pombe* vegetative cells telomeres are anchored to the NE through direct interaction between the protein Bqt4 and telomeric protein Rap1 (Chikashige et al., 2009). A recent report characterized the crystal structure of the N-terminus of Bqt4 which contain an APSES DNA-binding domain found in a family of fungal transcription factors (with diverse roles) (Iyer et al., 2002; Zhao et al., 2015), which can bind double-stranded DNA (Hu et al., 2018). Also, it was shown that structural features of Bqt4 could potentially interact with Sad1 (Hu et al., 2019). Bqt3 supposedly is required to protect Bqt4 from protein degradation by a yet-unknown mechanism (Chikashige & Hiraoka, 2001). In the

absence of Bqt3 or -4, telomeres fail to associate with the nuclear membrane (Chikashige et al., 2009).

On the other hand, the nematode *C. elegans* couples chromosomes to the NE by sub-telomeric chromosome regions called pairing centers (PCs). PCs are composed of short repetitive sequences and have localized to one end of each chromosome (Herman & Kari, 1989; Phillips et al., 2009; Sanford & Perry, 2001). The leading role of PCs is to stabilize pairing, alignment and synapsis of homologous by promoting assembly of the synaptonemal complex and probably through their central role in chromosome end attachment (MacQueen et al., 2005; Woglar & Jantsch, 2014). A family of four paralogous proteins of zinc fingers, (ZIM-1/2/3 and HIM-8) specifically associated with the PCs (Phillips et al., 2005; Phillips & Dernburg, 2006). Interestingly the pentameric motif recognized by the HIM-8 and ZIM zinc finger cores (TTGGC) is closely related to the telomeric repeat in *C. elegans* (TTAGGC) (Phillips et al., 2009). The four members of this zinc finger protein family are essential for coupling chromosome ends to the LINC complex (SUN-1-ZYG-12) (Phillips & Dernburg, 2006; Penkner et al., 2007) thereby interacting with cytoplasmic microtubule-associated dynein (Wynne et al., 2012). However, the direct connectors to the LINC complex (Link & Jantsch, 2019) in *C. elegans* are still unknown.

Significant progress was made in the identification of mammalian meiosis-specific telomere proteins involved in the tethering of telomeres during meiosis. In mice, meiotic TERB1, TERB2 (telomere repeat-binding bouquet formation proteins 1 and 2) (Daniel et al., 2014; Shibuya et al., 2014; Shibuya & Watanabe, 2014; Shibuya et al., 2015) and MAJIN proteins (membrane-anchored junction protein) lead telomere binding between the LINC-complex and shelterin complex (Shibuya et al., 2015). Although the mouse mutants of all three proteins are viable, they displayed abnormal bouquet organization and telomere distribution, loss of chromosomal movements, and aberrant chromosomal synapsis resulting in sterility (Shibuya et al., 2015; Shibuya et al., 2014).

A series of cytological and biochemical studies have dissected the assembly mechanism between meiotic telomere complex and shelterin protein complex

to achieve telomere attachment to the INM this mechanism in mice (Shibuya et al., 2015). From early meiosis, the meiotic telomere complex assembly is formed by TERB2 bridging the interaction with TERB1 at its C-terminus and with MAJIN through its N-terminus domain. Simultaneously, MAJIN protein connects with the INM via its transmembrane helix domain (Shibuya et al., 2015). Subsequently, the TERB1-TERB2-MAJIN complex recruit telomeres to the INM via direct interaction between TRF1 (Telomeric Repeat binding Factor 1, a shelterin component) and TERB1, thereby establishing the first bond between the telomere and the INM (Shibuya et al., 2015). With the progression of meiosis I, TERB1-TERB2-MAJIN complex released shelterin complex and matured into a ring structure in which the telomere and the NE are directly bound. Interestingly, the INM MAJIN protein possesses DNA binding activity likely required to stabilize telomeric DNA tethering to the INM and resist the forces of chromosome movement (Shibuya et al., 2015; Dunce et al., 2018).

Summarizing, meiosis-specific telomere adaptor proteins are essential to accomplish the attachment and movement of chromosomes in prophase I. The most prominent examples of how meiotic telomeres attach to the nucleoplasm side of the LINC complex comes from fission yeast studies and the recent identification of responsible in the mouse. However, it seems that meiosis-specific telomere complex proteins are not conserved.

Chapter 2 Aims of the thesis

Meiotic chromosome dynamics is a conserved feature of early prophase I progression during evolution and is indispensable for initial chromosome interactions and recombination. Although previous studies in mice unveiled the meiosis telomere complex adaptor proteins TERB1-TERB2-MAJIN responsible for assisting chromosomal end connection to the cytoskeletal machinery via the NE, many aspects are still not well understood. Therefore, the main aim of this thesis is to provide a better understanding of their role, spatial organization and evolutionary history of the mouse meiosis specific-telomere adaptor proteins TERB1-TERB2-MAJIN.

2.1 Investigation of the spatial localization and relationship of TERB1-TERB2-MAJIN with shelterin protein TRF1 at chromosome ends during mouse prophase I using Structured Illumination Microscopy

The organization of the meiotic telomere complex and its association with the shelterin and LINC complexes play a crucial role in the proper meiotic telomere attachment and movement. Despite recent advances in the identification of the multiprotein complex TERB1-TERB2-MAJIN and its interaction with TRF1, their spatial organization/relationship at the chromosome end has been limited by the imaging resolution of conventional microscopy methods. Hence, this thesis aims to investigate the spatial localization and organization of TERB1, TERB2 and MAJIN proteins and its relationship with the shelterin protein TRF1 using high-resolution Structured Illumination Microscopy (SIM) in mouse spermatocytes during Prophase I. This would consequently allow gaining deeper insights into the mechanism of mammalian meiotic telomere attachment.

2.2 Investigation of the evolutionary history of mouse meiosis-specific telomere adaptor proteins

Comparative studies from yeast to mouse have demonstrated that conserved protein families such as SUN and KASH are able to direct chromosome

movements during prophase I. However, the attachments of telomeres to the SUN domain in the INM requires telomere meiosis-specific adaptors proteins, (i.e. Ndj1 in budding yeast, Bqt1-4 in fission yeast and TERB1, TERB2, and MAJIN in mouse) whose sequences are highly divergent.

Thus, a further aim of this thesis is to elucidate, the evolutionary history of meiosis-specific telomere adaptors genes of the mouse. This would contribute our understanding in key cellular functions of meiotic telomere, that have been conserved throughout metazoan evolution.

Chapter 3 Analysis of the spatial organization of mice meiotic telomere complex with TRF1 protein

3.1 Introduction

At the onset of meiotic prophase I, the movement of chromosomes is achieved through the association of telomeres with specialized sites in the NE called attachment plates. These structures contain LINC complexes composed of SUN-KASH domain binding-partners (Alsheimer, 2009). The INM protein SUN interacts with telomeres while KASH domain interacts with cytoplasmic motor proteins at the ONM (Alsheimer, 2009; Bhalla & Dernburg, 2008; Sheehan & Pwlowski, 2009; Woglar & Jantsch, 2014; Pradillo et al., 2019). Consequently, cytoskeletal forces are transduced via LINC complexes to telomeres enabling chromosome movement (Hiraoka & Dernburg, 2009; Link et al., 2016; Starr & Fridolfsson, 2010).

Considerably progress made in recent years has led to the identification of the mammalian meiosis-specific telomere complex TERB1-TERB2-MAJIN (Shibuya et al., 2014; 2015), responsible for INM tethering of telomeres. Within the meiotic telomere complex, TERB1 simultaneously interacts with the telomeric shelterin protein TRF1 and TERB2 through its C-terminus (Shibuya et al., 2015) (Figure 3-1). On the other hand, MAJIN interacts with TERB2 at its N-terminal domain and with the INM at its C-terminal by a transmembrane helix (Shibuya et al., 2015) (Figure 3-1).

Furthermore, TERB1 and MAJIN possess DNA binding properties that may stabilize the INM tethering of telomeres. In this regard, TERB1 protein sequence includes a MYB domain at its C-terminal (mouse aa 715-760), which plays a specific role in accumulating meiotic cohesin subunit SA3 and to specifically interact with double-stranded DNA telomeric sequences (Daniel et al., 2014; Shibuya et al., 2014; 2015; Bilaud et al., 1996) (Figure 3.1). Alternatively, MAJIN confers DNA binding activity independent of the sequence by a basic segment adjacent the transmembrane helix at its C-terminal (Shibuya et al., 2015; Dunce et al., 2018, Wang et al., 2019).

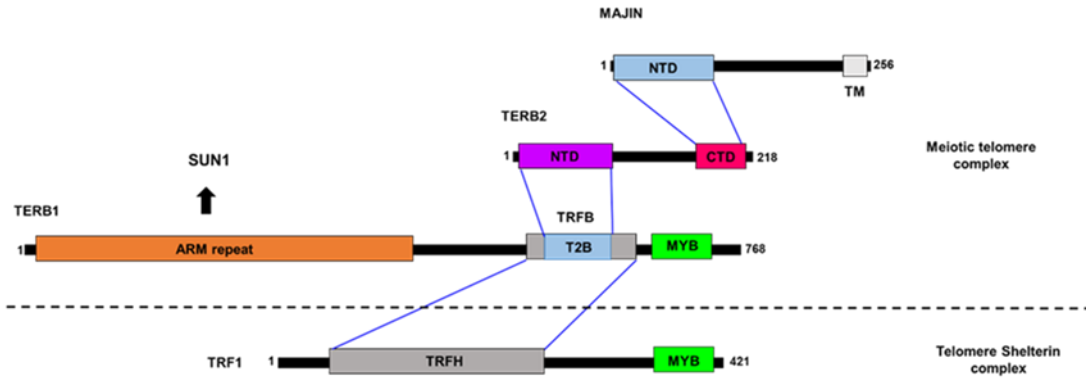

Figure 3-1 Schematic representation of the interacting domains mediating the simultaneous binding of TERB1-TERB2-MAJIN, telomeric shelterin protein TRF1, and the SUN1 protein of the LINC complex in mice.

The MAJIN C-terminus contains a trans-membrane binding domain (TM, aa 233-251) and interacts via its N-terminal domain (NTD, aa 1-120) with a specific C-terminal domain of TERB2 (CTD, aa 169-202). The TERB2 N-terminal domain (NTD, aa 2-194) interacts with the C-terminal domain of TERB1 (T2B, aa 594-626) encompassed by the TRF1-binding domain (TRFB, aa 523-699) which interacts in turn with the TRF homology domain of TRF1 (TRFH, aa 54-251). The TERB1 N-terminus contains an armadillo repeat (ARM repeat, aa 16-384) domain that is suggested to interact with SUN1/2. Both TERB1 and TRF1 also possess a MYB domain (MYB, aa 715-760; aa 367-416 respectively) that binds telomeric DNA (Shibuya et al., 2014; 2015; Long et al., 2017; Pendlebury et al., 2017; Zhang et al., 2017).

The mechanism of how meiotic telomere complex is recruited in prophase I to anchor telomeres to the INM is still poorly understood. Using mutation analysis in vivo, immunofluorescence microscopy and extensive biochemistry, a model for the process of telomere INM anchoring was proposed (Shibuya et al., 2015; Shibuya et al., 2014). Prior to leptotene, TRF1 shelterin protein directly interacts with TERB1 promoting the initial recruitment of telomere bound TRF1 to the INM (Shibuya et al., 2015) (Figure 3-2). After the priming attachment in leptotene-zygotene stages, detected TRF1 co-localization with TERB1-TERB2-MAJIN (Shibuya et al., 2015). However, in the pachytene stage, TRF1 was dissociated and distributed in the surrounding area forming a ring-shaped structure (Shibuya et al., 2015). At this time, telomere DNA co-localized with

complex TERB1-TERB2-MAJIN but not with TRF1 shelterin protein. The process in which TRF1 released telomeric DNA to bound TERB1-TERB2-MAJIN complex was termed cap exchange (Shibuya et al., 2015). Further studies on the mechanism of cap exchange suggested that the interaction between TERB1-TRF1 is potentially regulated by a CDK (Shibuya et al., 2014; 2015; Pendlebury et al., 2017; Long et al.. 2017). The binding region between TERB1-TRF1 overlaps with a predicted CDK phosphorylation site, and a phosphomimetic mutation was shown to affect the interaction with TRF1 (Pendlebury et al., 2017; Long et al., 2017).

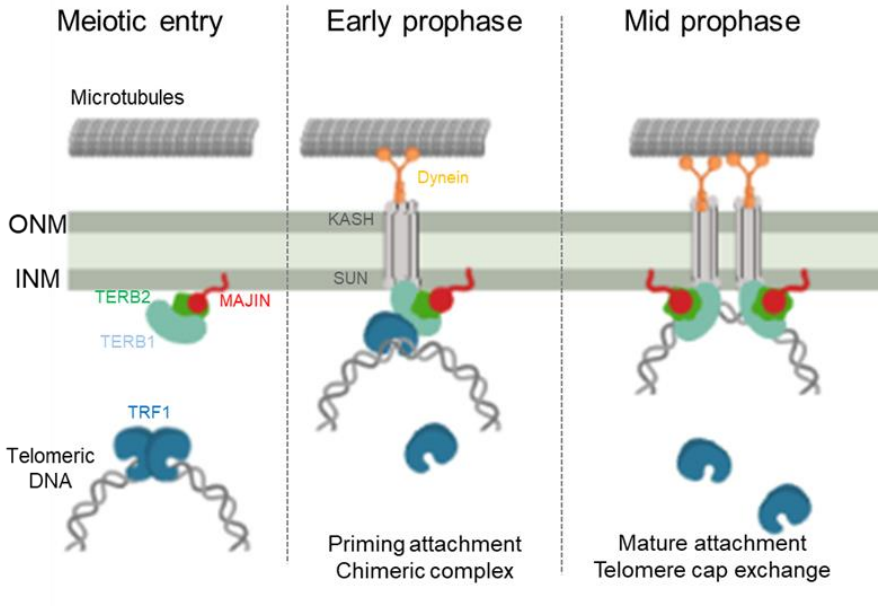

Figure 3-2 Illustration process of telomere INM anchoring of cap exchange during prophase I in mouse.

Before the cell enters meiotic prophase I, the meiosis telomere complex is sequestered to the INM through MAJIN by transmembrane helix at its C-terminal. Early on prophase I, the priming attachment is achieved via the interaction of TRF1-TERB1 forming the chimeric complex TRF1-TERB1-TERB2-MAJIN. This interaction is critical for SUN1-KASH5 recruitment in the attachment site of telomeres. The process of attachment maturates by mid pachytene with the dissociation of TRF1 allowing the direct interactions of telomeres with meiotic telomere complex (telomere cap exchange). (Shibuya et al., 2015).

Previous studies analyzed the mouse meiotic telomere complex in relation with TRF1 by conventional microscopy (Shibuya et al., 2015) in which the resolution achieved is limited by the diffraction of light (lateral resolution of 200 nm). Because the molecular complex responsible for INM tethering of telomeres are close in size to the diffraction limit of conventional light microscopy, their spatial relationships during cap exchange remain to be further characterized. The present thesis aims to understand the role of meiotic telomere complex in zygotene and pachytene stages by better knowledge of their spatial relationships with the shelterin protein TRF1. To this end, we analyzed the localization of meiotic telomere complex either alone or with TRF1 by performing indirect immunofluorescence assay in intact (3D preservation) and spread nuclei (2D) from mouse spermatocytes using super-resolution SIM microscopy.

3.2 Results

3.2.1 SIM provides mouse detailed of somatic shelterin distribution compared to CLSM

We started evaluating the suitability of Confocal Laser Scanning Microscopy (CLSM) and Structured Illumination Microscopy (SIM) to study the spatial organization of meiosis-specific telomere proteins in mice. To this end, we did proceed to do indirect immunofluorescence (IF) assays on spermatocyte spreads of young animals (14-18 days old). This selection of young mice was optimal for spermatocytes spreads because there is an absence of many spermatozoa and a relative higher percentage of cells undergoing meiosis in the testis (de Boer et a., 2009). The reference molecules selected for co-immunostaining were SYCP3 (antibody raised on full-length SYCP3 protein of Hamster) that detects explicitly AE/LEs of the SC and TRF1 (antibody raised on 19 amino acids of mouse N-terminal protein) telomeric shelterin protein (Figure 3-3). Figure 3-3 A shows the reconstructed 2D SIM image obtained for late pachytene where the LEs of each homologous chromosome is resolved as two distinct structures twisted into each other. Besides, a well-defined TRF1 ring-like structure was observed in some of the chromosomes ends (Figure 3-3 A).

This result is consistent with the previously described ring shape structure of TRF1 in late pachytene (Shibuya et al., 2015).

Furthermore, when the line profile of signal arrangements at the end of the SC was analyzed, we observed discontinuity of the TRF1 signal into two peaks (Figure 3-3 B-C). Moreover, when the SC structure was analyzed, we identify the presence of two well-defined peaks with bimodal distribution (Fig 3-3 B-D). For comparison, the same immunofluorescence experiment was visualized with CLSM (Figure 3-4). The images obtained showed less detail compared to SIM when fluorescent line profile scanning for the SC and TRF1 were analyzed. In this case, the analysis revealed only one single peak suggesting a single continuous structure for both SC and TRF1 signal (Fig. 3-4 A-D).

Overall, after these experiments, we conclude that SIM is more suitable to study the meiotic telomere complex compared to CLSM because it displays the structure with much higher resolution thus allowing precise and comprehensive investigation of its spatial organization.

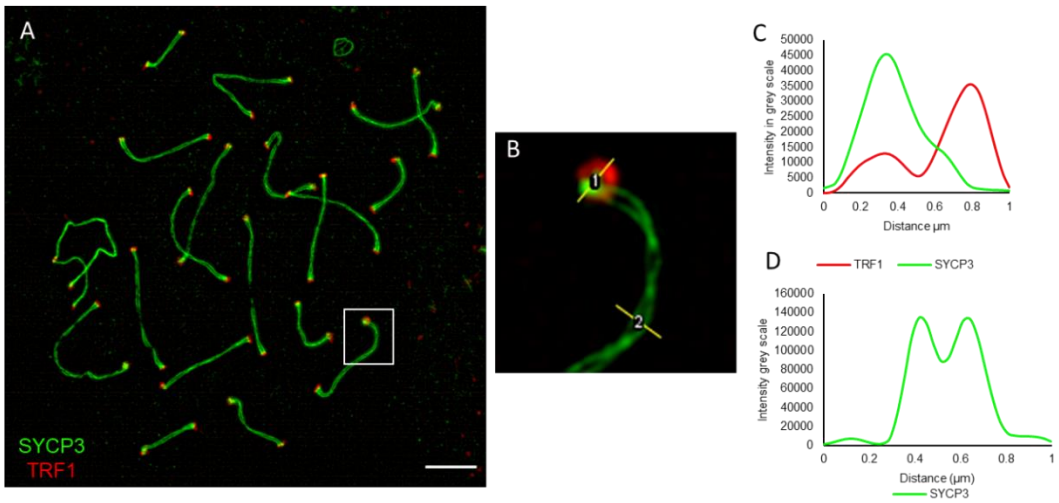

Figure 3-3 SIM image of immunofluorescence with SYCP3 and TRF1.

(A) Representative image showing spread spermatocytes from late pachytene stage labelled with SYCP3 (green) and TRF1 (red) antibodies. The white arrowhead marks the XY body. (B) Magnified view of one chromosome end (inset in A). Line profile of intensities was recorded at the end of the SC (C) and the middle of the chromosome (D). (Scale: 5 µm). Figure adopted from Eva-Maria Minarsch (Bachelor thesis, 2017).

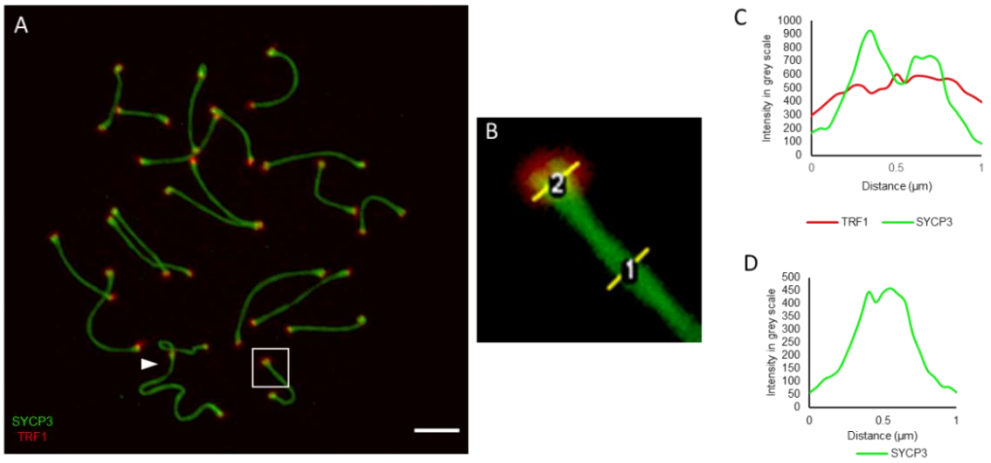

Figure 3-4 CSLM image of immunofluorescence with SYCP3 and TRF1.

(A) Representative image showing spread spermatocytes from late pachytene stage labeled with SYCP3 antibody marked with Alexa 488 (green) and TRF1 marked with Alexa 647 (red). (B) Magnified view of the SC end (inset in A). Line profile of intensities was recorded at the end of the SC (C) and the middle of the chromosome (D). (Scale: 5 µm). Figure adopted from Eva-Maria Minarsch (Bachelor thesis, 2017).

3.2.2 TERB2 signal distribution is heterogeneous in comparison with TERB1 and MAJIN binding partners at chromosome ends

To determine how MAJIN, TERB2, and TERB1 proteins are localized their immunostaining patterns in zygotene and pachytene stages in mouse spermatocytes were examined by SIM imaging (Figure 3-5 a-c and 3-6 a-d).

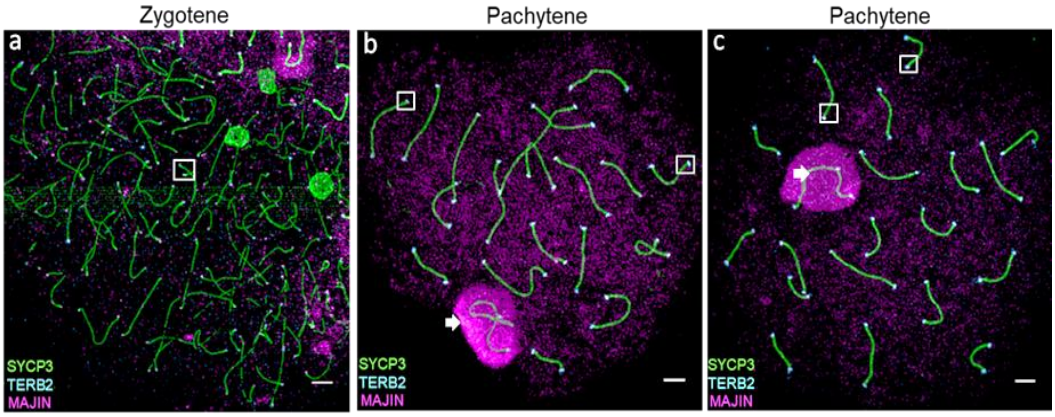

Figure 3-5 SIM image of immunofluorescence with SYCP3, TERB2, and MAJIN.

SIM image of (a) mouse zygotene spermatocyte chromosome spread, (b-c) mouse pachytene spermatocyte chromosome spread with anti-SYCP3 (green), anti-TERB2 (cyan) and anti-MAJIN (magenta). Scale bar 3 μm. White squares represent the telomere ends used for display and analysis in Figure 3-7 A-C.

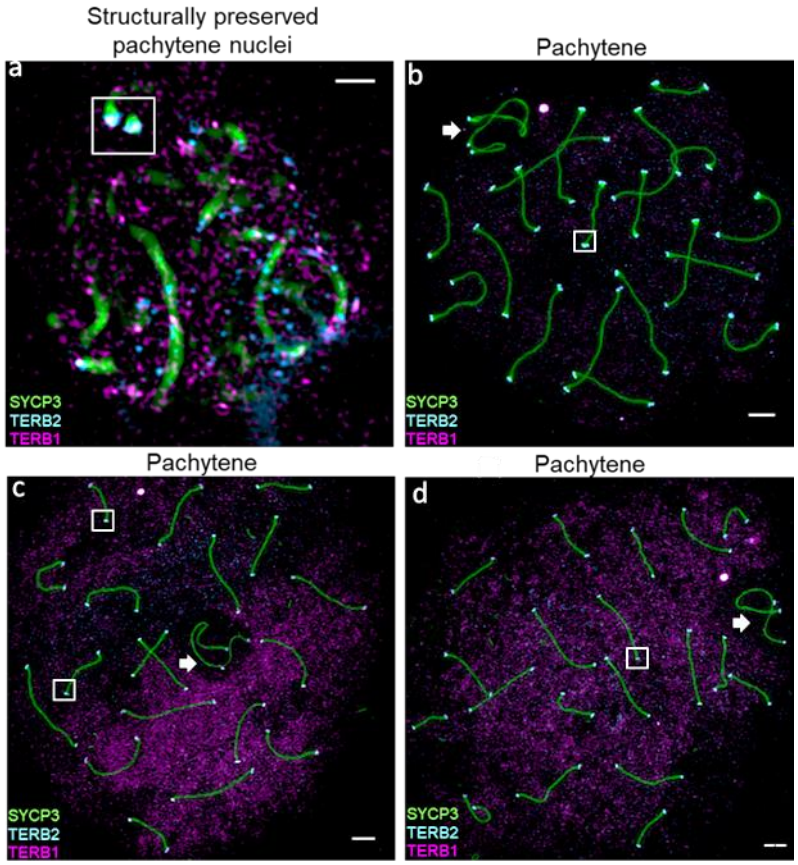

Figure 3-6 SIM image of immunofluorescence with SYCP3, TERB2, and TERB1.

SIM image of (a) structurally preserved mouse pachytene nuclei and (b-d) mouse pachytene spermatocyte chromosome spread stained with anti-SYCP3 (green), anti-TERB2 (cyan) and anti-TERB1 (magenta). Scale bars 5 μm (a) and 3 μm (b-d). White squares represent the telomere ends used for display and analysis in Figure 3-8 A-C.

Early zygotene spermatocytes were evidenced by largely unpaired AEs positive staining for SYCP3 (Figure 3-5 a and 3-7 A). In this stage, MAJIN (antibody raised against mouse amino acids 18-30) exhibited one punctate signal often located at the centre of each chromosome ends (Figure 3-7 A). By contrast, TERB2 (antibody raised against mouse full-length) staining revealed a signal split in two enclosing the one dense MAJIN per chromosome end (Figure 3-7 A). Subsequently, pachytene stage spermatocytes were evidenced by the fully synapsed of homologous chromosomes axis (Figure 3-5 b-c and Figure 3-7 B). MAJIN localization in pachytene stage revealed dense dots signal in frontal and lateral views of the LEs ends (Figure 3-7 B). Conversely, TERB2 signal exhibited

a semi-hoop configuration surrounding the MAJIN signal in different top views (Figure 3-7 B).

To better understand the fluorescence distribution of co-staining with MAJIN and TERB2 line profiles of their intensity fluorescence were performed in top and frontal views. As a result, in top views, the intensity signal distribution of MAJIN is rarely reduced, while TERB2 signal intensity is more heterogeneous (Figure 3-7 C). However, frontal views line profiles (obtained from 26 chromosomes ends) revealed overlapping of the signal distributions (Figure 3-7 C) in accordance with its ability of TERB2 to interact with MAJIN (Shibuya et al., 2015).

Next, the spatial distribution of TERB1, TERB2, and SYCP3 by SIM was analyzed in pachytene cells (Figure 3-6 a-d). TERB2 localization signal was distributed lying outer more to the chromosome axis in comparison with the compact TERB1 signal (antibody raised against mouse amino acids 525-540) in structurally conserved nuclear samples, (Figure 3-8 A).

When double immunolabeling of TERB2 and TERB1 was performed in pachytene spreads cells TERB1 localized distally at the end of the LEs. At the same time, TERB2 distribution is proximal to the chromosome axis in both lateral and top views (Figure 3-8 B).

Noticeably the analysis of frontal views (25 chromosome ends) TERB2 and TERB1 intensity line profiles indicated that their signals overlap (Figure 3-8 C). Similarly, single line profiles of lateral and top views suggested that TERB2 and TERB1 overlap in a significant fraction (Figure 3-8 C) in line with their mutual dependency interaction (Shibuya et al., 2015).

In conclusion, TERB2 localized more proximal to the chromosome axis and adopt a more heterogeneous signal distribution in comparison with MAJIN and TERB1 in both zygotene and pachytene stages.

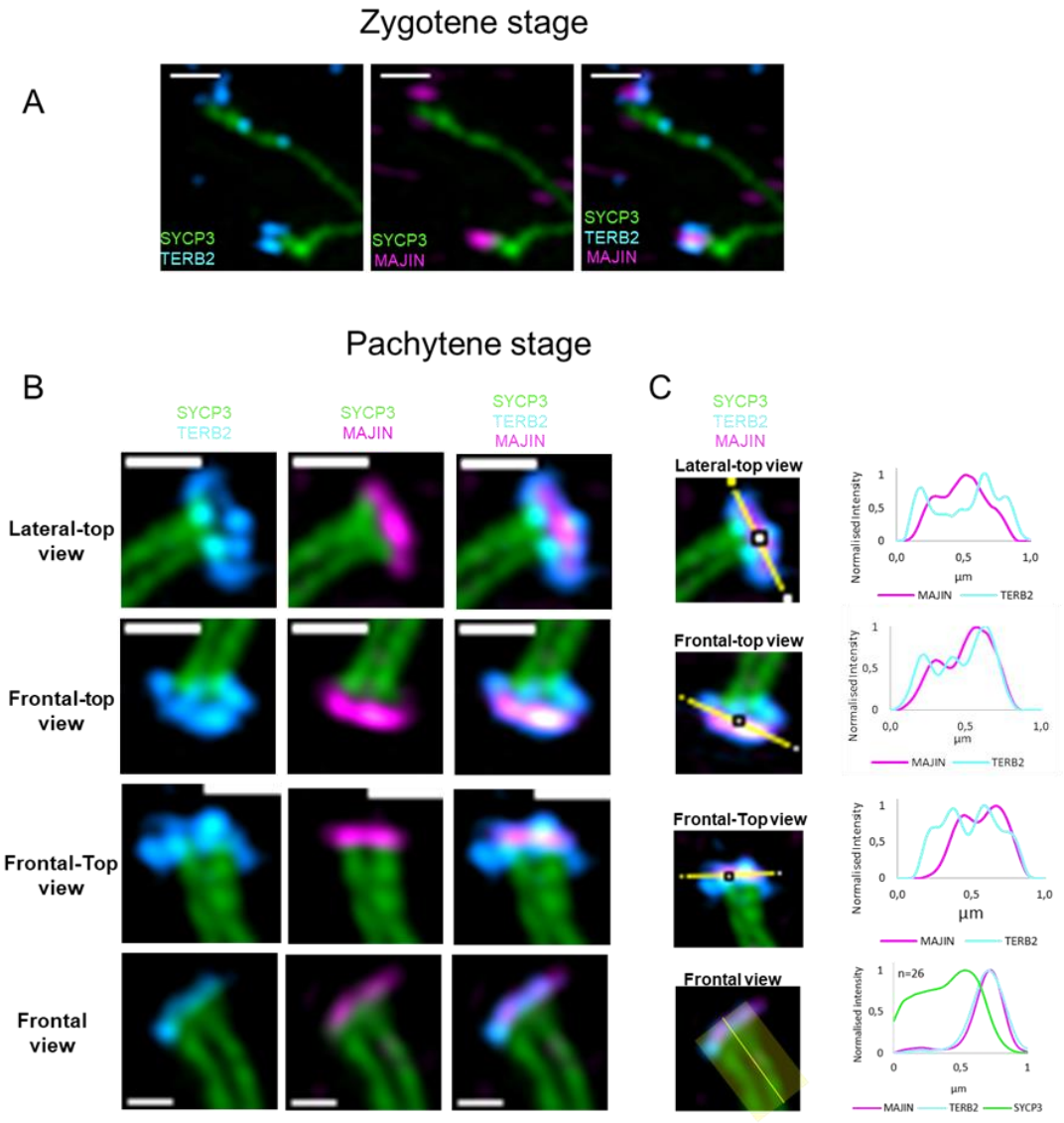

Figure 3-7 ***Super-resolution microscopy of the meiotic telomere complex TERB2-MAJIN and SYCP3.***

Structured illumination microscopy of mouse zygotene and pachytene spermatocyte chromosomes spread preparation stained with anti-SYCP3 (green), anti-TERB2 (cyan) and anti-MAJIN (magenta). Scale bars, 0.3 and 0.5 µm. Full images are shown in Figure 3.4. Higher magnification image of separated telomeres in zygotene-spermatocytes (A). Higher magnification of late pachytene-spermatocytes, in frontal and lateral top views of spread chromosomes (B). Line scans corresponding to the yellow line of TERB2 and MAJIN signals distribution (C). The figure is adopted from Dunce et al., 2018.

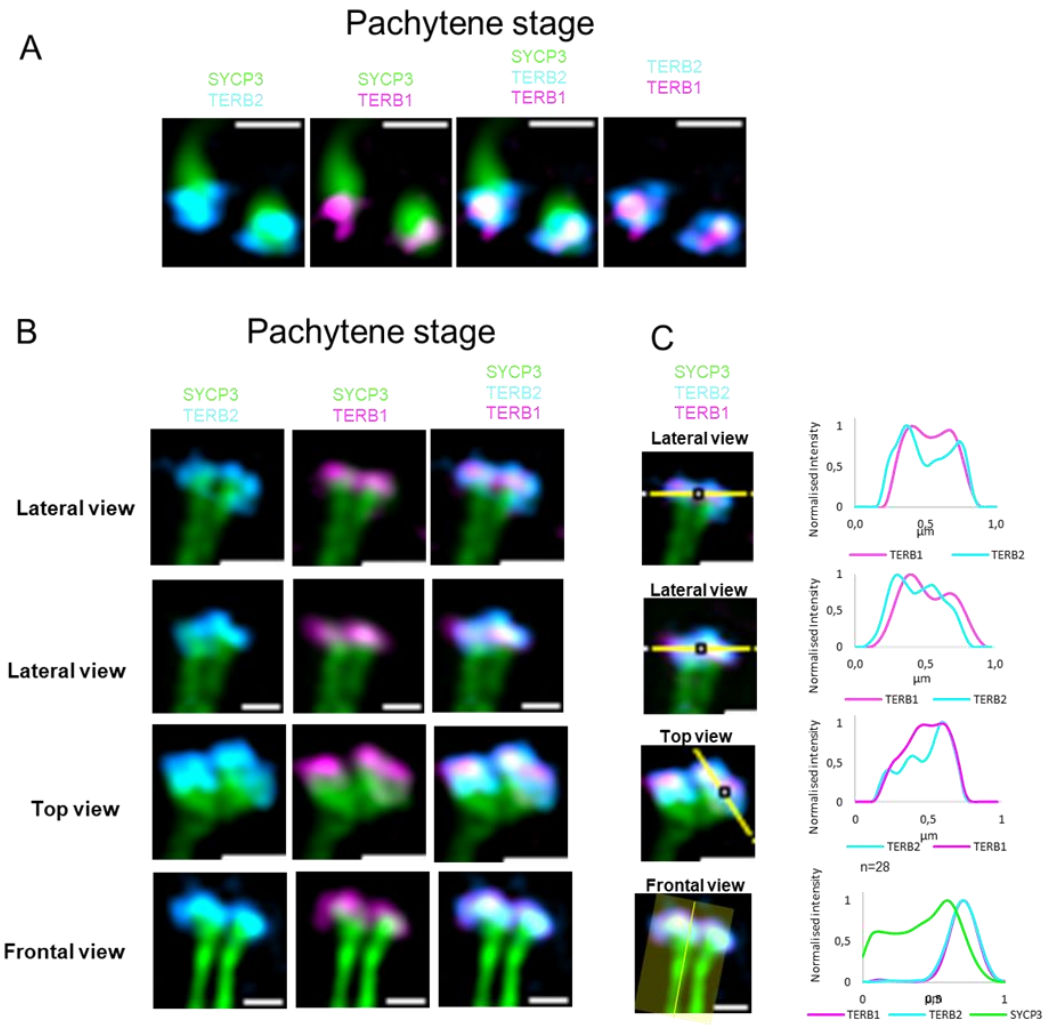

Figure 3-8 Super-resolution microscopy of the meiotic telomere complex TERB1-TERB2 and SYCP3.

Structured illumination microscopy of mice zygotene and pachytene spermatocyte chromosomes of spreading and preserved nuclei structure preparation stained with anti-SYCP3 (green), anti-TERB2 (cyan) and anti-TERB1 (magenta). Full images are shown in Figure 3.6. Scale bars, 0.3 and 0.5 µm. Higher magnification image of preserved nuclei structure preparation pachytene-spermatocytes separated (A). Higher magnification, in frontal and lateral top views of spread pachytene-spermatocytes chromosomes (B). Line scans corresponding to the yellow line of TERB2 and TERB1 signals distribution (C). The figure is adopted from Dunce et al., 2018.

3.2.3 TRF1 protein exhibit grasp-like distribution surrounding the meiotic telomere complex.

During meiosis, the somatic telomere shelterin complex is modified to associate with TERB1-TERB2-MAJIN complex to accomplish chromosome movement. It has been postulated that in pachytene stage the telomere shelterin complex is exchanged to enable telomeric DNA interactions with meiotic telomere complex in a process called cap exchange. The dissociation of shelterin proteins (cap exchange) has been cytologically observed using conventional microscopy methods as a ring-shaped structure in the pachytene stage (Shibuya et al., 2015). To provide a more accurate description of the spatial relationships between meiotic telomere complex and TRF1, their localizations were analyzed in both zygotene and pachytene stages by SIM imaging (Figure 3-9 a-f; and Figure 3-10 a-e).

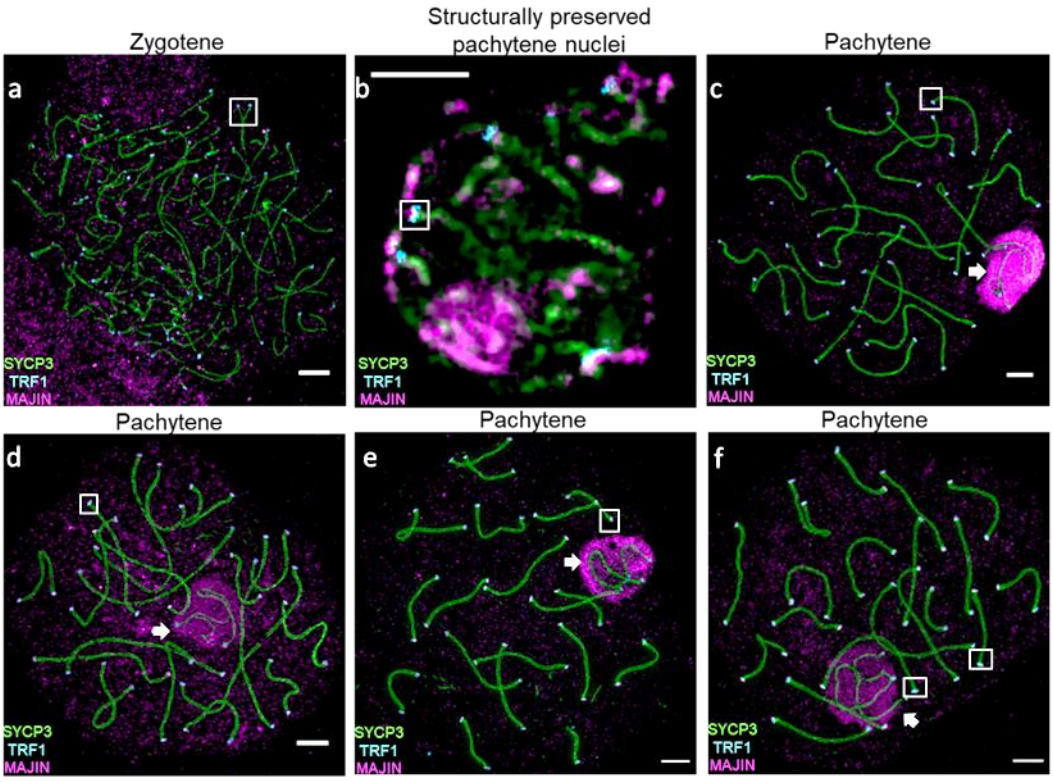

Figure 3-9 SIM image of immunofluorescence with SYCP3, TERB1, and TRF1. Widefield SIM image of mice spermatocyte zygotene spread cells (a), structurally preservation of pachytene nuclei (b) and pachytene spread cells (c-f) stained with anti-SYCP3 (green), anti-TRF1 (cyan) and anti-TERB1 (magenta). The white square indicates the telomere ends analyzed in Figure 3-11 A-C and E. Scale bars 3 μm

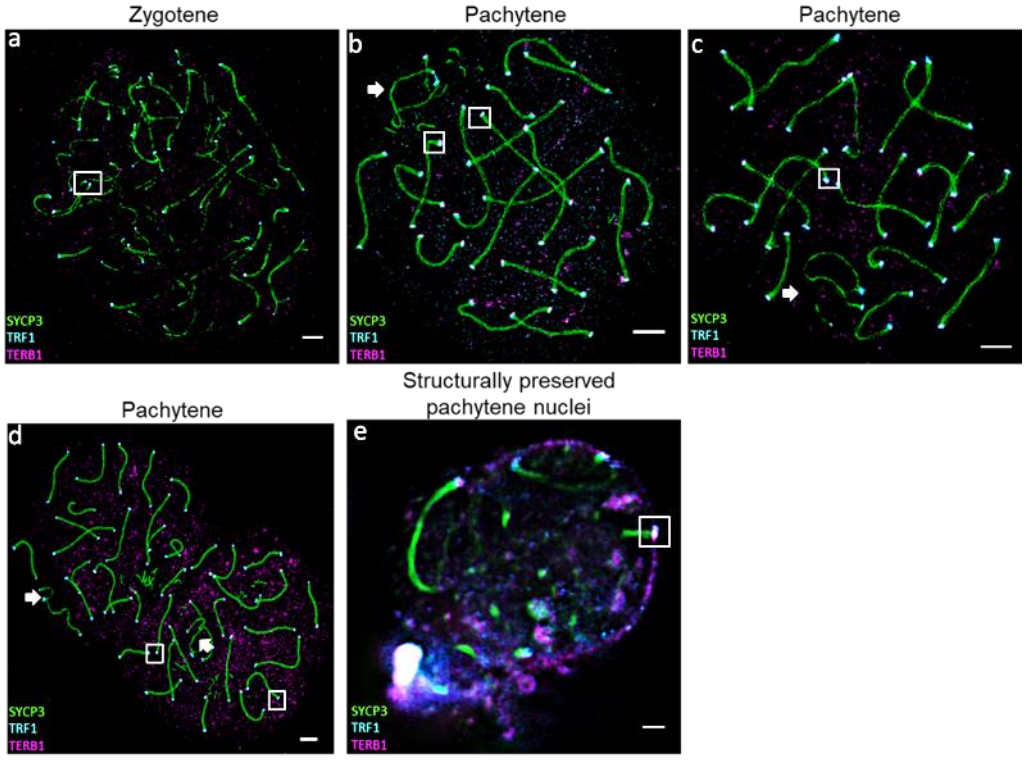

Figure 3-10 SIM image of immunofluorescence with SYCP3, MAJIN, and TRF1

SIM reconstructed images of mice Zygotene spread cells (a), pachytene spermatocytes spread cells (b-d), and structurally preserved nuclei pachytene cells (e) co-stained with anti-SYCP3 (green), anti-TRF1 (cyan) and anti-MAJIN (magenta). The white square indicates the telomere ends analyzed in Figure 3-12 a-c. Scale bar 0.3 µm and 0.5 µm (b).

Staining showed a substantial degree of overlap between the localization of TRF1 and TERB1 at the end of the unpaired AEs at the zygotene stage (Figure 3-11 A). As evident from Figure 3-12 a, a similar pattern was visualized in zygotene spermatocytes co-stained for TRF1 and MAJIN. In contrast to previous findings (Shibuya et al., 2015), these results indicate that signal distribution between TERB1 or MAJIN with TRF1 in zygotene stage are closely adjacent but not directly co-localizing.

Subsequently, when co-staining of TRF1 and TERB1 were analyzed in late pachytene stage, TRF1 signal revealed two elongated dots or semi-ring-like pattern distributions localized at the sides of the end of each LE surrounding the dense TERB1 signal (Figure 3-11 B and D). A similar pattern was detected when co-staining with antibodies against MAJIN and TRF1 in cell spreads or

nuclei preserved samples. As indicated in Figure 3-12 b and d, TRF1 signal distribution localized at the side and more proximal to the chromosome axis enclosing the MAJIN signal distribution more distally localized at the end of chromosomes.

In agreement with previous findings (Shibuya et al., 20015), TRF1 ring-like shape structure was observed in pachytene stage and distributed at outer portions of LEs ends in comparison with the relative central position of TERB1 or MAJIN at LEs ends (Figure 3-11 C and Figure 3-12 c).

From these results, it seems that TRF1 adopt a grasp-like distribution enclosing TERB1 and MAJIN within the end of LEs. Such a distribution pattern between TRF1 and meiotic telomere complex appears to be independent of the presence or not of TRF1 ring-like arrangement. In support of this observation, top views line profiles revealed that the maximum intensity distribution of TERB1 and MAJIN are located in the regions of reduced intensities of TRF1 suggesting different relative positions of these proteins within the end of LEs (Figure 3-11 E and Figure 3-12). Finally, to further examine the signal distribution between TRF1 and meiotic telomere complex in pachytene stages, line profiles of 25 chromosome ends from frontal views were analyzed. The resulting data showed that the signal distribution between TRF1 and MAJIN or TERB1 are slightly separated but still overlapping in a significant fraction (Figure 3-11 E and Figure 3-12 e). This result may reflect a reorganization of TRF1 instead of a complete dissociation to enable telomeric DNA interactions with meiotic telomere complex as described in the process of cap exchange (Shibuya et al., 2015).

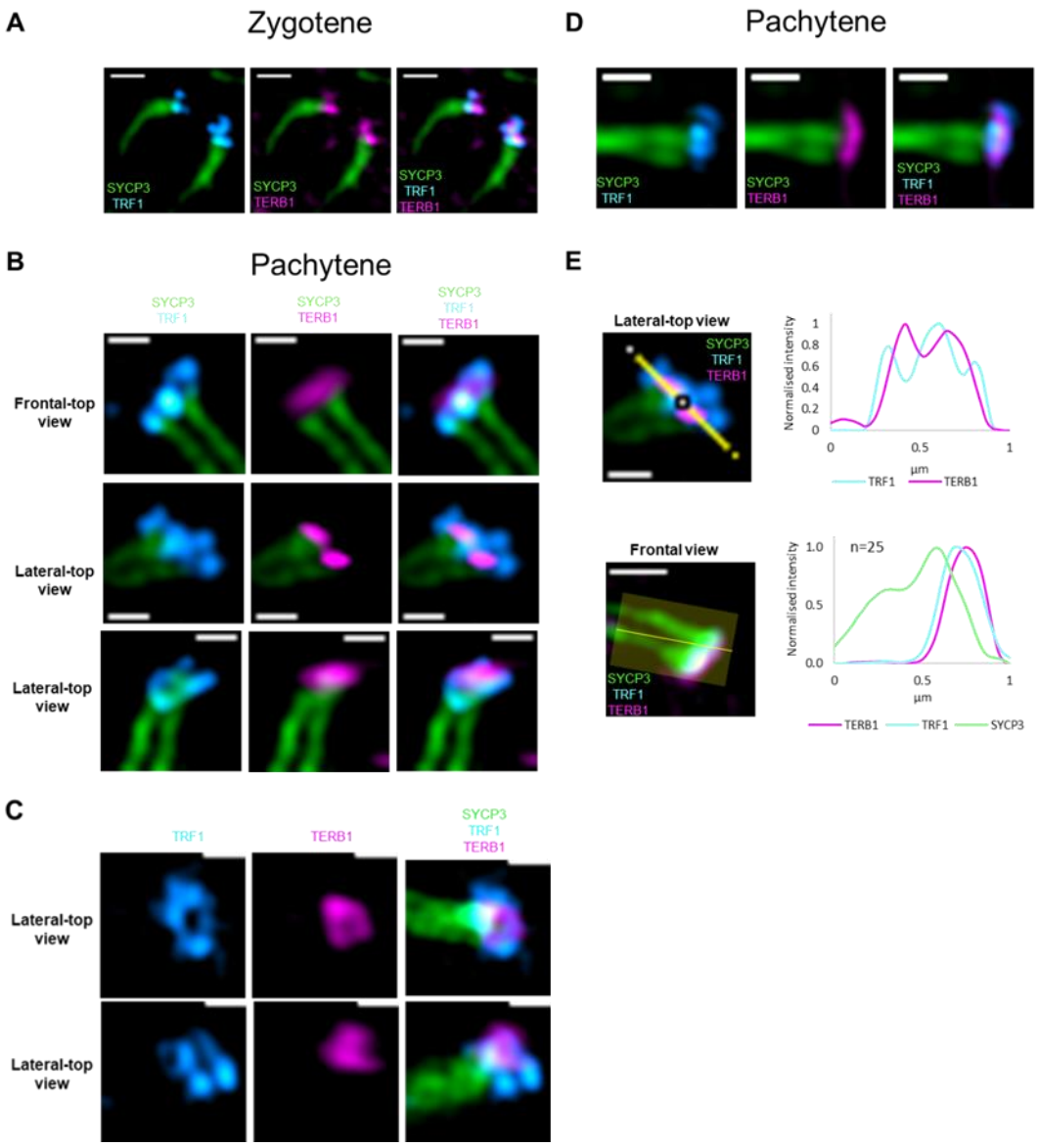

Figure 3-11 Super-resolution microscopy of the meiotic telomere complex TERB1-TRF1 and SYCP3.

Higher magnification of SIM image from co-immunostaining of TERB1 (magenta), TRF1 (hot-cyan) and SYCP3 (green) in zygotene (A) and pachytene-spermatocytes spread cells (B-C), and spermatocytes of preserved nuclei structure (D) preparations. Evaluation of average line profile of frontal view (n=25) and a sole line profile showing the distribution of Lateral-top view signal (E). Scale bars, 0.3 and 0.5 µm. The figure is adopted from Dunce et al., 2018.

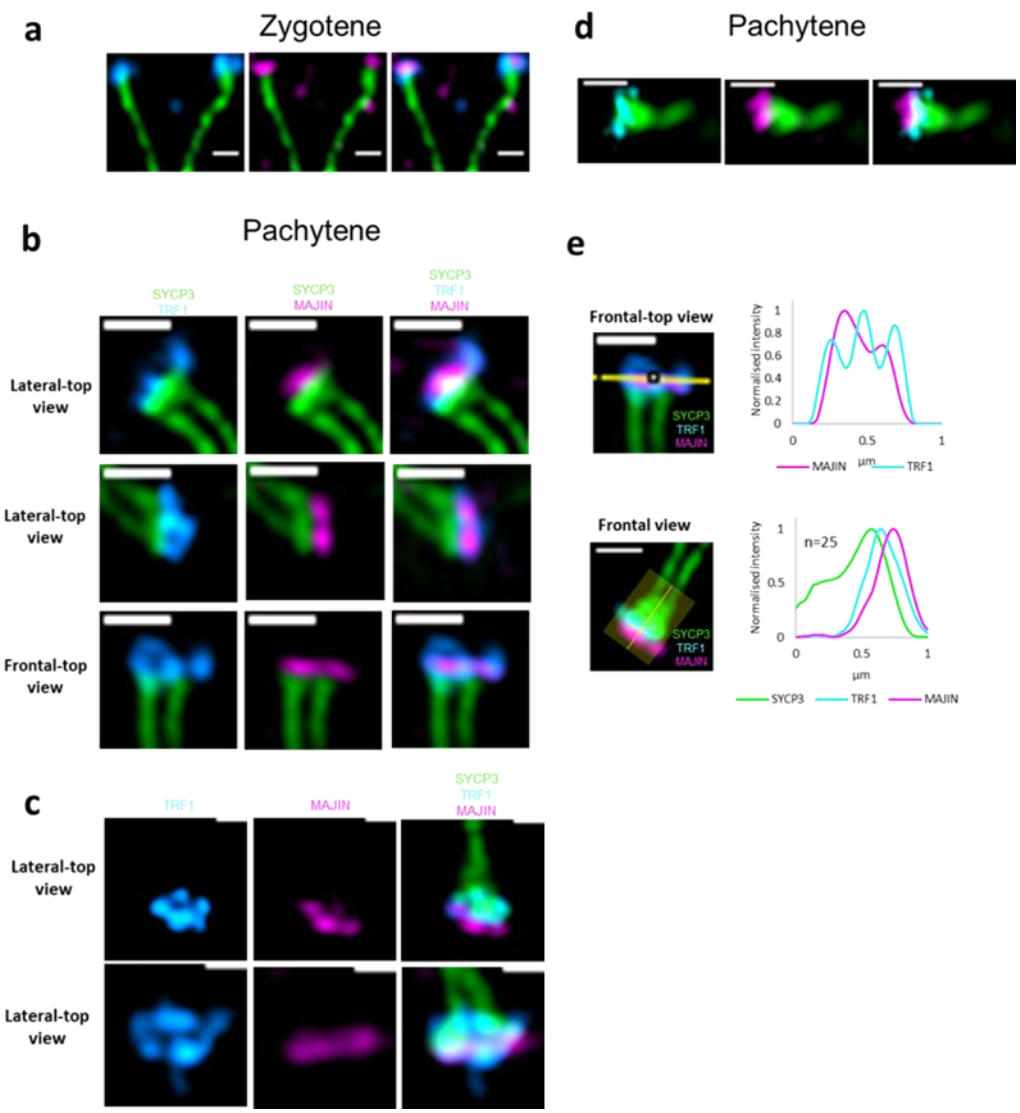

Figure 3-12 Super-resolution microscopy of the meiotic telomere complex MAJIN, TRF1 and SYCP3.

Higher magnification of SIM image from co-immunostaining of MAJIN (magenta), TRF1 (hot-cyan) and SYCP3 (green) in zygotene (a) and pachytene- spread spermatocytes (b-c) and (d) spermatocytes of preserved nuclei structure preparations. Average line profile of frontal view (n=25) and a single line profile showing the distribution of Frontal-top view signal (e). Scale bars, 0.3 and 0.5 µm. The figure is adopted from Dunce et al., 2018.

3.2.4 Telomeric DNA localization and its relationship with the meiotic telomere complex

As mentioned earlier, in the maturation process of cap exchange shelterin complex dissociates from telomeric DNA leading to its association with TERB1-TERB2-MAJIN in pachytene stage (Shibuya et al., 2015). The critical question raised is how meiotic telomere complex might engage telomere DNA during cap exchange. To determine how meiotic telomere proteins and telomeric DNA are distributed at chromosome ends, we performed immunofluorescence assays in combination with DNA FISH in spermatocytes cell spreads (Figure 3-13 A). In contrast to the findings of Shibuya et al., (2015), TERB2 and telomeric DNA staining pattern partially overlap. A complete co-localization was not observed (Figure 3-13 B). Of note, telomeric DNA signal showed two dots laterally distributed at each LEs ends, whereas TERB2 signal displayed more central distribution at LEs ends (Figure 3-13 B). Moreover, in some orientations, the localization of telomeric DNA is distal to TERB2 signal, which is more proximal to the chromosome axis. These results reflect an association of meiotic telomere complex and telomeric DNA but likely occupy distinct areas with some overlap.

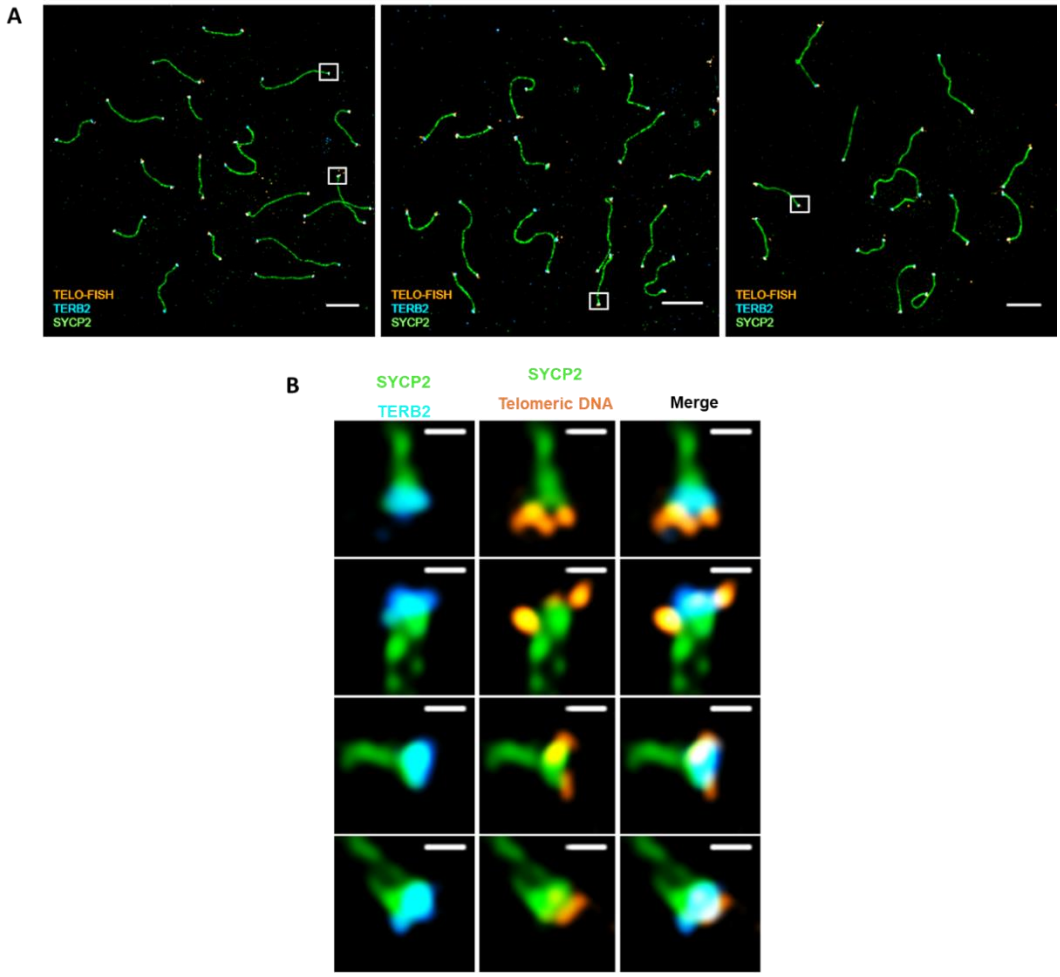

Figure 3-13 SIM of Immuno-TeloFISH with TERB2 and SYCP3.
Representative SIM image of a cell spreading preparation stained for SYCP2 protein (green), TERB2 protein (hot cyan) and Telomeric DNA (hot orange). Scale bar 0.5µm

3.3 Discussion

3.3.1 SIM provides information about meiosis specific protein localization that cannot be obtained by conventional CLSM

Previous research has identified in mammals the TERB1, TERB2, and MAJIN proteins to form a specialized meiotic telomere complex that is responsible for chromosome anchoring to the nuclear envelope (Shibuya et al., 2014; 2015). However, these studies have used conventional microscopy techniques, in which spatial resolution is limited by diffraction to approximately half the wavelength of light (Abbe, 1873). In this study, we used super-resolution

microscopy (SIM) to provide insightful structural details of the meiotic telomere complex and the shelterin complex.

In contrast, with conventional optical microscopes such as CLSM which are limited to a lateral resolution ~220 nm, SIM gives a twofold increase in lateral resolution ~110 nm and provides optical sectioning without discarding any light by a pinhole or other mask (Gustafsson et al., 2008). Moreover, the SIM method uses the so-called interference effect to reveal hidden spatial information of the fluorescence signal, which is then calculated through mathematical Fourier transformation (Langhorst et al., 2009). Following computational reconstruction of the recovered high spatial frequency information contained within these moiré fringes, the resolution achieved is beyond the limit of conventional light microscopes.

SIM imaging data revealed a separation between the LEs (about 100 nm) as a twisted, double-stranded structure. The results are in general agreement with other reports (Yoon et al., 2018) in which SIM provided more detailed information of the SC morphology compared to the CLSM. Also, SIM imaging is advantageous when performing triple immunolocalization due to its compatibility with currently available dyes and robustness in sample preparation. Thus, SIM imaging provides more detailed information on the spatial relationships between TRF1 and the meiotic telomere complex compared to conventional light microscopy.

3.3.2 Relative position and signal morphology of TERB1-TERB2-MAJIN within the meiotic telomere complex.

Previous works have recently shown the molecular interaction between TERB1-TERB2-MAJIN using knock out mice strains, cellular, and genetic approaches (Shibuya et al., 2015; Zhang et al., 2017). Although these studies have provided valuable information on protein-protein interactions that mediate meiotic telomere complex, the spatial organization in the context of meiotic telomeres is poorly resolved. In the present thesis, SIM imaging in spread cells and structurally preserved nuclei of mice spermatocytes were performed to examine the distribution pattern of TERB1-TERB2-MAJIN within the end of LEs.

SIM imaging recognized closely association between TERB1-TERB2-MAJIN in consistence with the mutual dependency for telomere attachment to the NE (Shibuya et al., 2015). It was noticeable that MAJIN and TERB1 displayed in zygotene and pachytene stages dense punctuate signals distally localized at the LEs ends (Figure 3-14 A-B).

In contrast, SIM imaging revealed two dots signal per LEs end for TERB2 in zygotene and more heterogeneous signal distribution in the pachytene stage. Although in frontal views MAJIN and TERB1 clearly overlap with TERB2 signal, in top-views TERB2 appeared to surround MAJIN and cap TERB1 (Figure 3-14 A-B). Such an arrangement of TERB2 could act as a platform for association with TERB1 and MAJIN or other binding partners still not identified. Previous crystallographic studies have shown that TERB2 interacting region with MAJIN form a 2:2 heterotetrameric and can adopt greatly extended conformations. In contrast, the interacting region with TERB1 can form a 1:1 complex providing a molecular scaffold to link the interacting domains of MAJIN and TERB1. Furthermore, it has been demonstrated that MAJIN is highly unstable in the absence of TERB2, implying that its presence is essential for MAJIN dimerization (Dunce et al., 2019).

It is conceivable although that the staining patterns for TERB1 and MAJIN observed in this study may represent primarily the positions of the C-terminus and the N-terminus (peptide antigens used to raise the antibodies) respectively and may not reflect the entire protein distribution. Further studies are required to reveal the details of meiotic telomere complex distribution using the full-length protein for manufacturing antibodies against TERB1 and MAJIN.

In conclusion, the relative positions of TERB2 with TERB1 and MAJIN indicate extensively overlapping of their distribution in zygotene and pachytene stages. The signal morphology of TERB2 is broader and more proximal to the chromosome axis than the discrete signal morphology for TERB1 and MAJIN at LE ends of pachytene spermatocytes.

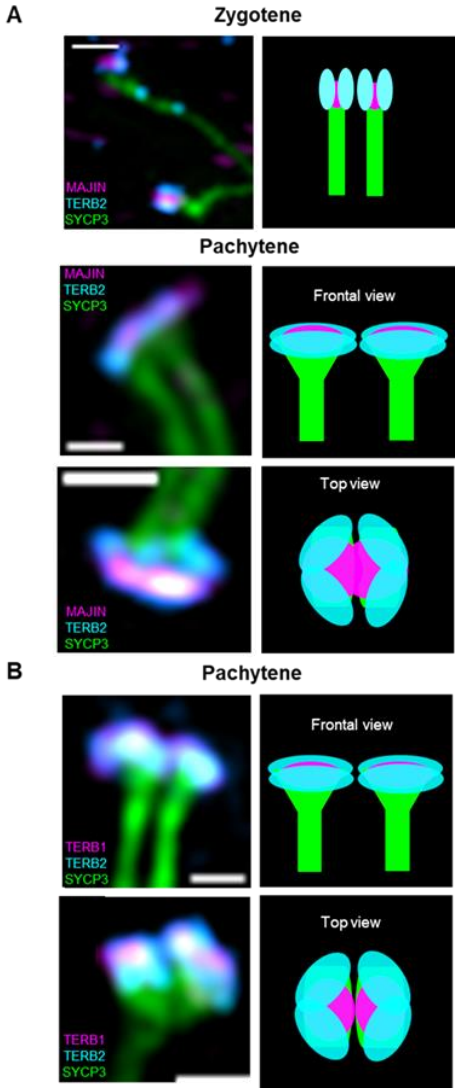

Figure 3-14 Schematic model for the distribution of meiotic telomere complex in frontal and top views of LEs ends.

A) Distribution of MAJIN (magenta) and TERB2 (cyan) at LEs end (green) in zygotene and pachytene stages. B) Distribution of TERB1(magenta) and TERB2 (cyan) at LEs end (green) in pachytene stage

3.3.3 TRF1 is partially displaced from telomeric DNA and not fully dissociated in the process of INM telomere attachment.

In early meiotic prophase I, telomeres associate with meiotic telomere complex via TRF1 shelterin protein (Shibuya et al., 2015). As the process of attachment maturates in pachytene stage, TRF1 dissociates telomeric DNA to bind TERB1-TERB2-MAJIN. This process termed cap exchange supposedly involves the

rearrangement of the shelterin complex components into an annular structure in close vicinity of telomeres (Shibuya et al., 2015).

In this thesis, SIM imaging was applied to understand better the spatial relationship of TRF1 with meiotic telomere complex in mouse spermatocytes. In contrast to previous findings (Shibuya et al., 2015) the double staining of TRF1 with TERB1 or MAJIN suggested that TRF1 may occupy distinct areas within the unpaired chromosome ends in zygotene stage (Figure 3-15 A).

As meiosis progressed, TRF1 arrangements were observed in frontal or lateral views as two elongated dot signals, and semi-ring structures at the side of LE ends with grasp-distribution enclosing the relative centralized TERB1 and MAJIN signals in pachytene stage (Figure 3-15 B).

In line with previous findings (Shibuya et al., 2015), TRF1 ring-like arrangement was identified. However, since such TRF1 ring-like arrangement was mostly observed at fully synapsed chromosomes ends, it may reflect the lateral overlapping of semi-ring-like structures of TRF1. Thus, the data obtained does not determine whether the arrangement in a ring-like structure of TRF1 and other shelterins is essential for the maturation process of telomeric DNA interactions with meiotic telomere complex (Shibuya et al., 2015). Nevertheless, the telomeric DNA staining pattern revealed a discrete distribution at the side of the LEs ends (Figure 3-15 C), which nicely correlates with the relative position described for TRF1. Also, it was demonstrated that the localization of telomeric DNA partially overlaps with the relatively centralized location of TERB2 at LEs ends (Figure 3-15 C). Based on these observations, it is likely that TRF1 is partially displaced from telomeric DNA rather than showing a complete dissociation. This last would allow reinforcing the interaction of telomeric DNA with the meiotic telomere complex. In line with these observations, previous biochemical experiments demonstrated that the ability of TERB1-TERB2-MAJIN to bind DNA is inhibited by the presence of TRF1´s TRFH domain suggesting competitive inhibition of DNA binding upon recruitment of TRF1 by TERB1 (Dunce et al., 2018).

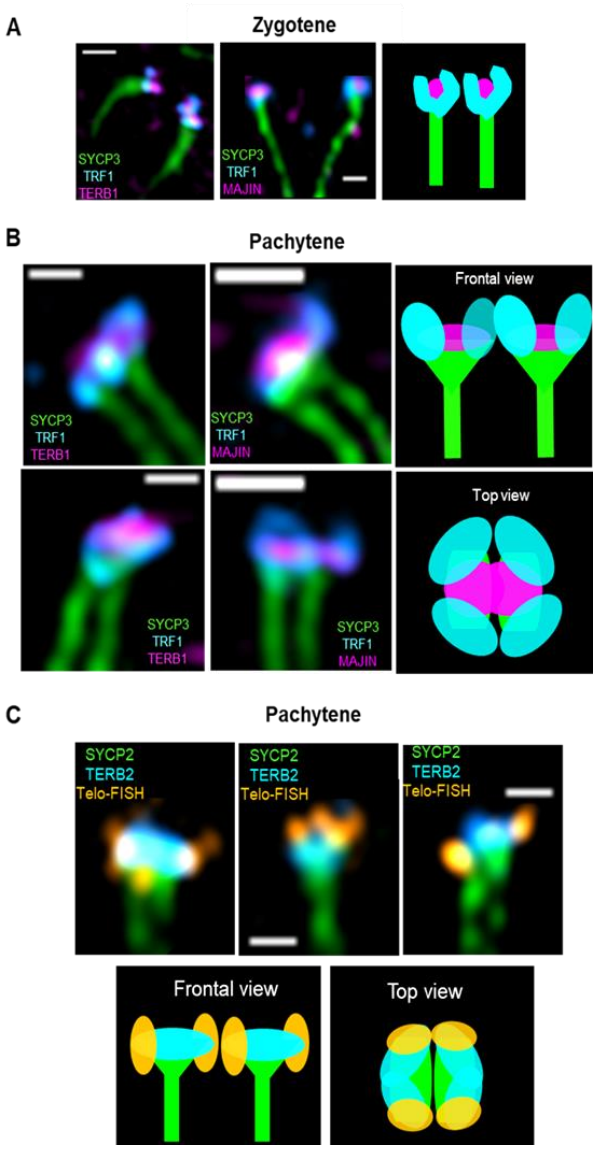

Figure 3-15 Schematic model of the relative distribution of TRF1, meiotic telomere complex and telomeric DNA at the end of LEs ends.

Staining patterns and relative distribution of TRF1 (cyan), MAJIN (magenta) and TERB1 (magenta) at the end of LEs ends of frontal and top views in zygotene (A) and pachytene (B) stage. Localization of telomeric DNA (orange) and TERB2 (cyan) at the LEs end (green) and their relative distribution position in frontal and top views (C).

Chapter 4 Evolutionary history of the mouse meiotic telomere complex

4.1 Introduction

Telomeres-led chromosome movement along the NE is an evolutionarily conserved meiotic process essential for pairing and recombination of homologous chromosomes. As described earlier, the forces required for chromosome movement are generated in the cytoplasm and transduced into the nucleus via SUN-KASH proteins (LINC complex), which are widely conserved in animals, yeast, and plants (Link & Jantsch, 2019; Pradillo et al., 2019; Zeng et al., 2018). Furthermore, to establish the connection between telomeres and the LINC complex, different organisms engaged different meiotic protein adaptors. In mouse TERB1, TERB2, and MAJIN telomere adaptor proteins associate with somatic telomeric protein TRF1 to establish the connection of telomeres to the meiotic LINC complex (Shibuya et al., 2014; 2015; Daniel et al., 2014). A similar mechanism in *S. pombe* involves the Bqt1-2 meiosis-specific telomere adapter that connects the Taz1-Rap1 telomere proteins to Sad1 SUN domain protein in a complex with nuclear membrane proteins Bqt3-4 (Chikashige & Hiraoka, 2001; Chikashige et al., 2006; 2009; Miki et al., 2004; Cooper et al., 1998). However, no protein sequence similarity was detected between mouse and yeast telomere adaptor proteins suggesting that meiotic specific telomere adaptor proteins are highly divergent. Therefore, the purpose of this study is to unravel the evolutionary origin of the mouse TERB1-TERB2-MAJIN complex and conservation of the mechanism to anchor telomeres to the NE.

4.2 Results

4.2.1 Mouse TERB1, TERB2, MAJIN are restricted to metazoans

The study started with the identification of mouse TERB1, TERB2, and MAJIN homologs in distant lineages using PSI-BLAST (Altschul et al., 1997). As a result,

the survey of public databases identified putative homologous proteins among metazoans (Supplementary Table 10-1, Table 10-3, and 10-3). Most of the putative homologous proteins obtained were in Deuterostomes, particularly in Vertebrata, but also in Cephalochordata, Echinodermata, and Hemichordata. Also, homologs were detected in Lophotrochozoa in Mollusca, Annelida and Brachiopoda representatives. In contrast, only a few putative homologs were found in the Ecdysozoan representatives Priapulida and Arthropoda.

Remarkably, we detected putative homologs of mouse TERB1, TERB2, and MAJIN in non-bilateral invertebrates in Cnidaria, Placozoans and Porifera lineages. Also, we noted that TERB1, TERB2, and MAJIN homologs were present in one single copy, in the metazoan lineages, even in the case of vertebrate genomes which underwent two rounds of duplication (Dehal & Boore, 2005). This result suggests that paralogs of TERB1, TERB2, and MAJIN were not retained during the evolution. As expected, we were not able to detect homologous sequences in Choanoflagellates, Fungi and Plants.

In general, these results strongly suggest that mice TERB1, TERB2, and MAJIN are likely originated before the formation of bilaterian in metazoan diversification.

4.2.2 The evolutionary history of mouse TERB1-TERB2-MAJIN complex

To understand the origin and evolutionary history of mouse TERB1, TERB2, and MAJIN, taxonomically balanced Bayesian trees were built, and nodes were evaluated with posterior probabilities. For simplicity, only posterior probabilities < 0.75 are shown in the trees. Although a small number of sites were kept for phylogenetic analysis, particularly for MAJIN (39 sequences; 57 amino acid positions kept) and TERB2 (41 sequences; 71 amino acids positions kept) the topologies of the Bayesian trees showed that members belonging to Cnidaria, Lophotrochozoa and Deuterostome are more closely related to each other than any of them are to any non-member (Figure 4-1 and Figure 4-3). In the case of TERB1, more positions could be kept for the analysis (42 sequences; 232 amino acid positions kept), resulting in a robust resolution and nodes with higher statistical support (Figure 4-1). These results indicate a lack of phylogenetic signal instead of a true conflicting signal and are consistent with

the commonly accepted view of the metazoan tree (Philippe et al. 2009; Telford et al., 2015).

Furthermore, within the clade of Vertebrata, the relation among sequences are considerably consistent with the systematics (Meyer & Zardoya, 2003) (Figure 4-1, 4-2, and 4-3), and the resolution within the vertebrates is confirmed by enough statistical support in most of the nodes. In contrast, for Ecdyzosoa, long branches were detected for the Arthropoda candidates corresponding to TERB1 and TERB2, indicating high rates of divergence (Figure 4-1 and 4-2).

Overall, these results clearly indicate that TERB1, TERB2, and MAJIN date back to the antecessor of all present-day metazoans.

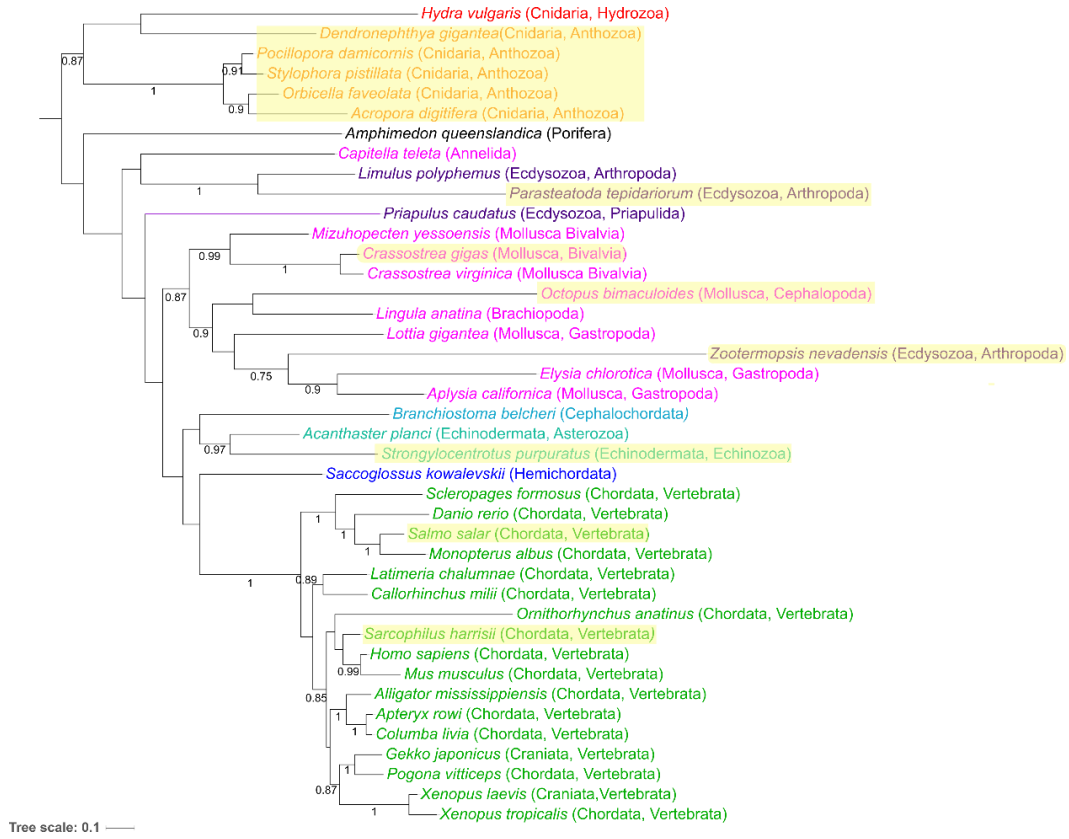

Figure 4-1 Evolutionary history of metazoan TERB1 proteins.

Unrooted Bayesian tree of TERB1 proteins inferred with MrBayes. The values > 0.75 represent posterior probabilities at the branch. The taxa lacking a MYB domain for TERB1 are highlighted in yellow. The length of each branch is proportional to the number of amino acid substitutions per site that have occurred. The scale at bottom left, displays the average number of substitutions per site. The dataset and the

computational tree calculation was supported and confirmed by Céline Brochier-Armanet

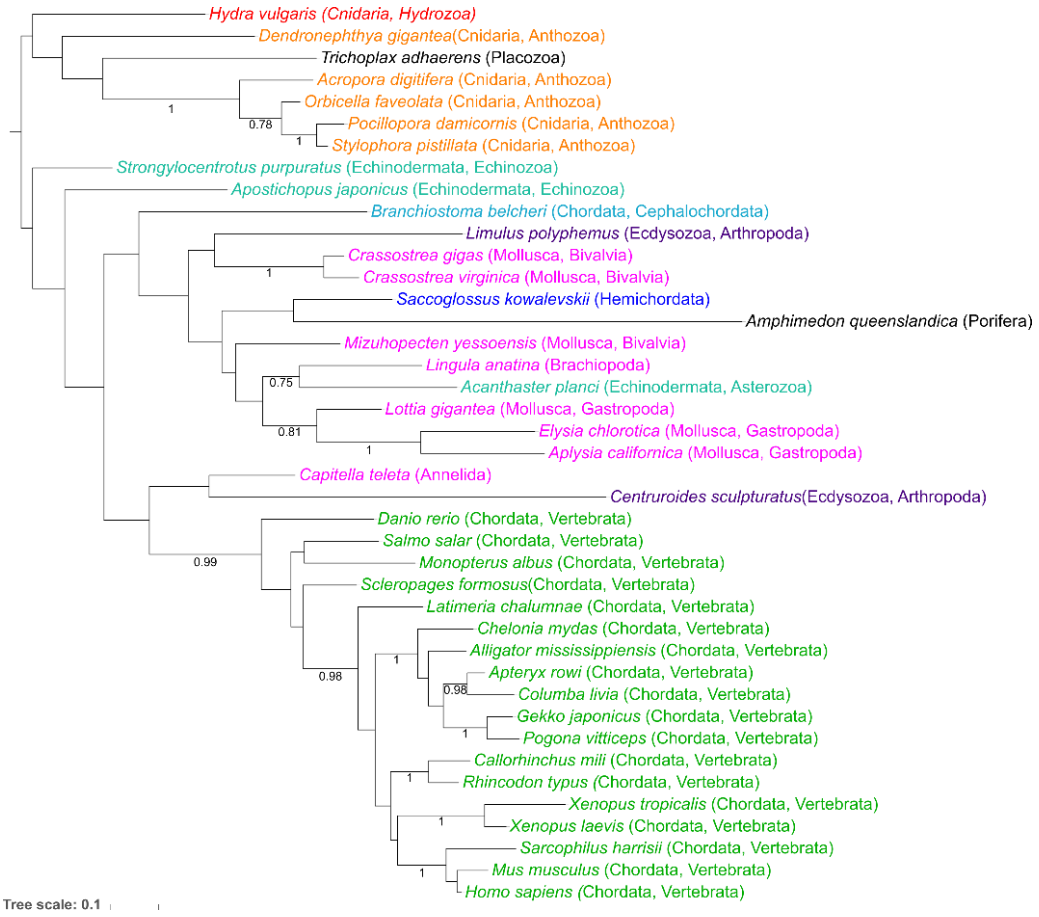

Figure 4-2 Evolutionary history of metazoan TERB2 proteins.

Bayesian phylogenetic tree constructed for TERB2 proteins. Bayesian posterior probabilities >0.75 are indicated at the branches. The length of each branch is proportional to the number of amino acid substitutions per site that have occurred. The scale at bottom left, displays the average number of substitutions per site. The dataset and the computational tree calculation was supported and confirmed by Céline Brochier-Armanet.

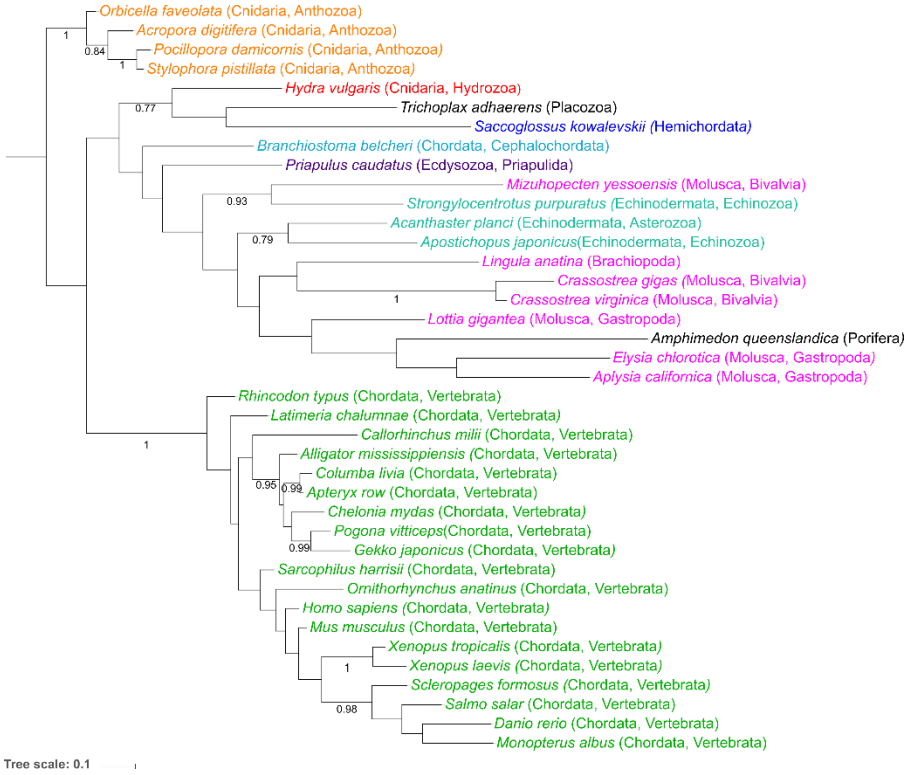

Figure 4-3 Evolutionary history of metazoan MAJIN proteins.

Bayesian phylogenetic tree from MAJIN proteins. Branch robustness is indicated by posterior probabilities > 0.75. The length of each branch is proportional to the number of amino acid substitutions per site that have occurred. The scale at bottom left, displays the average number of substitutions per site. The dataset and the computational tree calculation was supported and confirmed by Céline Brochier-Armanet

4.2.3 Binding sites between TERB1-TERB2-MAJIN are conserved among metazoans

To gain further information of the most conserved domains within the TERB1-TERB2-MAJIN complex, multiple sequence alignment of the representative homologous sequences were performed using PROMALS3D (Pei et al., 2008). PROMALS3D enhanced the database searches incorporating secondary structure prediction in distantly related homologs (Pei et al., 2008).

The amino acid sequence alignment of TERB1 revealed conserved domain architecture of N-terminal ARM repeat (aa 16-384 of mice) and C-terminal MYB (aa 715-747 of mice) domain among Porifera, Cnidaria (Hydrozoans), Annelida, Mollusca, Brachiopod, Echinodermata (Asterozoa) and Vertebrata (Figure 4-4,

Supplementary Figure 10-1). Furthermore, the specific region in the C-terminus of TERB1 necessary for the interaction with TERB2 (T2B) (aa 593 -622 of mice) (Zhang et al., 2017) was conserved in almost all the candidates analyzed (Supplementary Figure 10-2). However, candidate species of Cnidaria (Anthozoa), Arthropoda, Priapulida, Cephalopoda, Hemichordate and Cephalochordate sequences appear to lack the MYB-domain. The apparent lack of MYB domain probably derives from poorly sequence annotation.

In addition, the C-terminal region of the TERB1 contains a motif (IxLxP) (aa 646-650 of mice) essential for the interaction surface of TRF1 protein in vertebrates (Long et al., 2017). Nevertheless, this region was not detectable within invertebrate taxa suggesting that TERB1 may be targeted differently to TRF1 outside the lineage of Vertebrata (Figure 4-4).

As for TERB2, the most highly conserved region falls into the N-terminal domain (aa 1-116 of mice). Although several gaps were introduced in the alignment because of variations in amino acid sequences, a considerably smaller region of the C-terminus of TERB2 (aa 174-209 of mice) revealed a high level of conservation (Figure 4-5, Supplementary Figure 10-3). These results imply that from human to cnidarians the most conserved parts of TERB2 come from the regions necessary for the interaction of both TERB1 and MAJIN. Remarkably, towards the N-terminus on all TERB2 sequence analyzed, a conserved motif (FxLxP) (aa 86-90 of the mouse) was found which resembles the canonical binding motif of shelterin-associated to interact with TRF1 and TRF2 in mammals (Chen et al., 2008). This result suggests that TERB2 may potentially recognize the TRFH domain of shelterin telomere proteins.

Finally, the MAJIN multiple sequence alignment identified high similarity on the N-terminal domain in all taxa (aa 1-112 of mice) which is a necessary region for the interaction with TERB2 (Shibuya et al., 2015) (Figure 4-6, Supplementary Figure 10-4). The C-terminal part of the mouse MAJIN protein ends in a trans-membrane binding domain (TM, aa 233-251) characterized by hydrophobic amino acids involved in the anchoring of MAJIN to the INM. Small stretches of similarity and helix structure predictions in inside the hydrophobic TM domain this region were detected (Supplementary Figure 10-4). These results suggest

the presence of a potential transmembrane domain at the end of the C-terminal domain of the taxa analyzed.

As a final point, the multiple sequence alignment showed a high similarity of the interacting region between TERB1-TERB2-MAJIN, suggesting conservation of functional domains from a common ancestor.

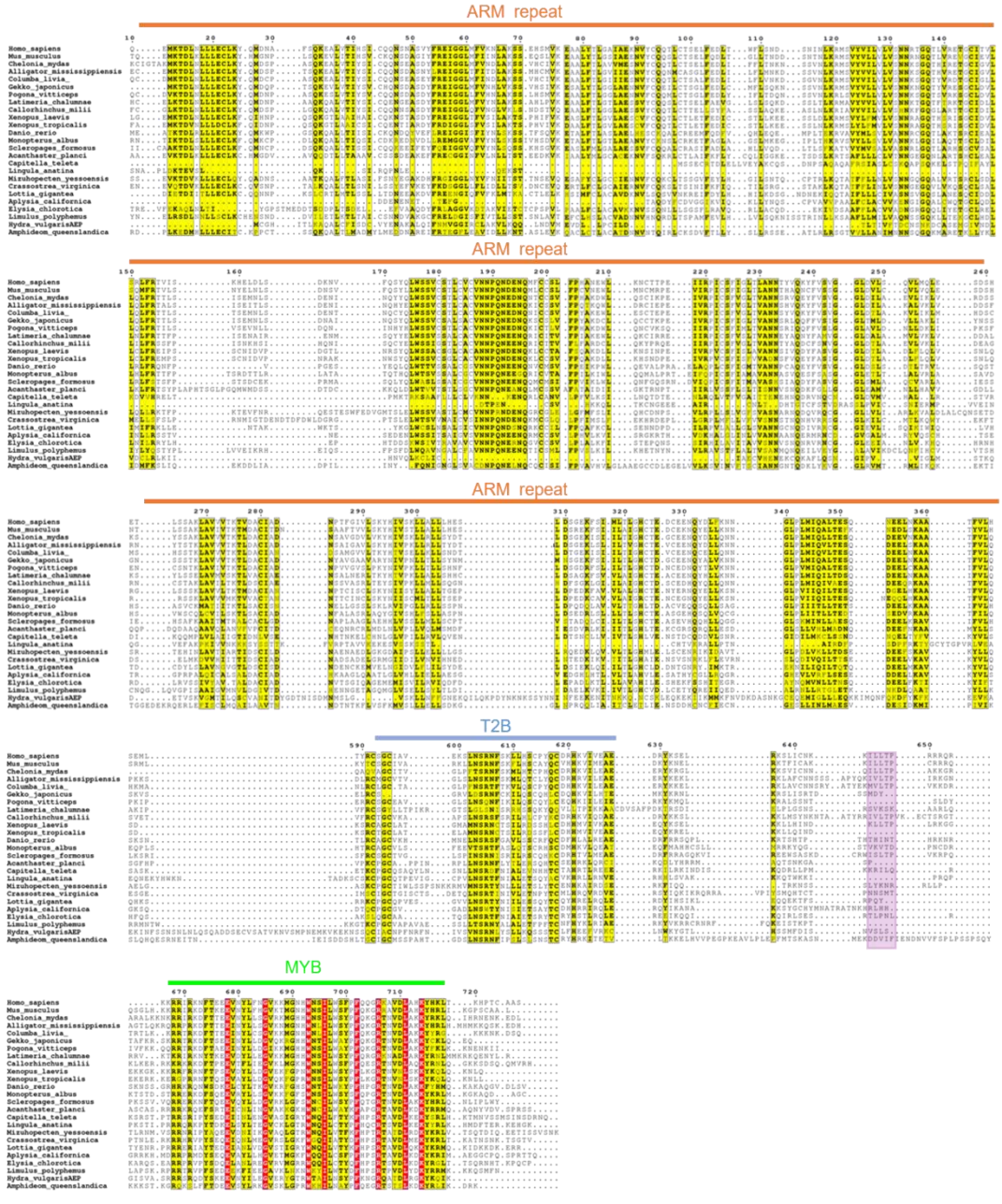

Figure 4-4 Multiple sequence alignment of candidate TERB1 metazoan proteins revealed highly conserved domain organization

TERB1 multiple sequence alignment with various representative metazoan species using PROMALS3D and annotated using ESPrit 3.0. The threshold for grouping of the residues was set to 70% and is depicted in yellow. Amino acid positions conserved in

all taxa are highlighted in red. Species names are shown on the left. The horizontal lines above the alignment indicate domain boundaries. Armadillo repeat; ARM repeat (aa 16-384 of mouse), T2B; binding site of TERB2 (aa 594-626 of mice) and MYB; homeodomain (aa 715-760 of mouse). The violet square indicates the docking site of TERB1 (IxLxP) to bind TRF1.

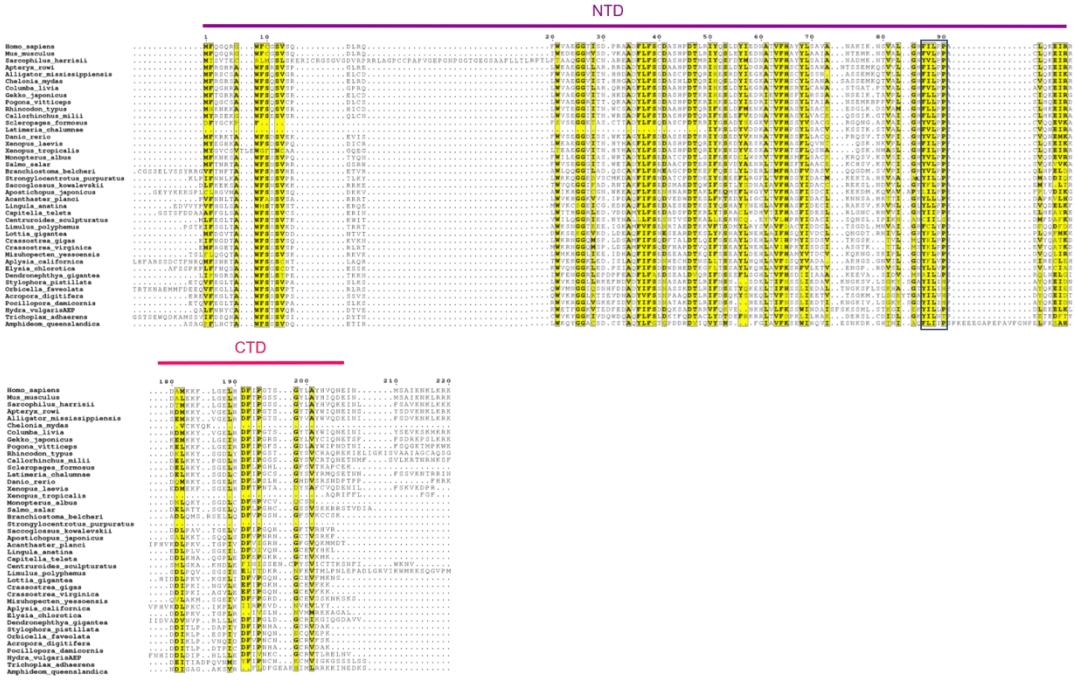

Figure 4-5 Multiple sequence alignment of candidate TERB2 metazoan proteins showed conservation at regions which interact with TERB1 and MAJIN.

Multiple sequence alignment of putative orthologs of mouse TERB2 among metazoans representatives through PROMALS3D. The annotation was performed with ESPrit 3.0 and the threshold for grouping of the residues was set to 70% highlighted in yellow. Species names are shown on the left. The horizontal lines above the alignment indicate domain N-terminal (NTD) (aa 2-194 of mouse) and C-terminal (CTD) (aa 169-202 of mouse) of TERB2. The motif [F/YxLxP] detected in all TERB2 sequences is shown in the dark blue rectangle

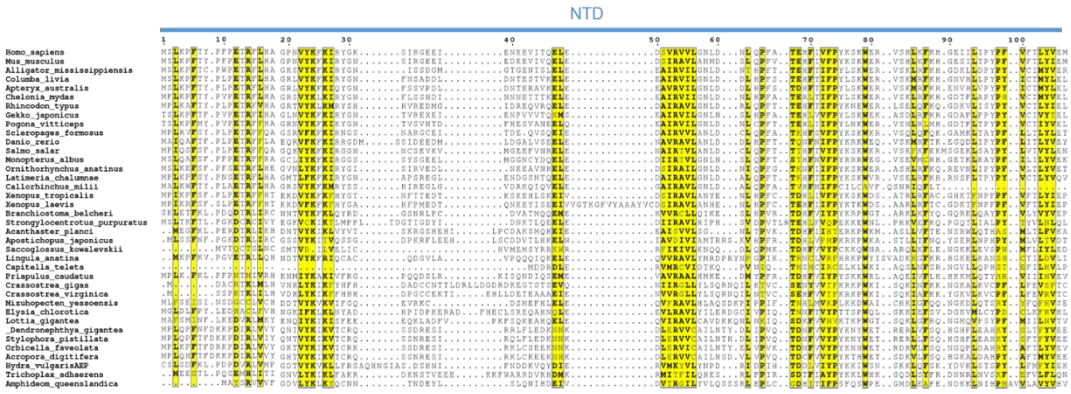

Figure 4-6 Multiple sequence alignment of candidate MAJIN metazoan proteins revealed prominent conservation at its N-terminal domain.

Above the alignment the light blue denotes that the N-terminal domain (NTD) (aa 1-120 of mouse) is the most conserved in all the taxa. The alignments were annotated using ESPrit 3.0. The threshold for grouping of the residues was set to 70% and is visualized in yellow. Species names are shown on the left.

4.2.4 Insights into a meiotic role for TERB1, TERB2, and MAJIN in the ancient phylum Cnidaria

To provide insights into an early origin of the meiotic telomere complex, we conducted expression analysis in *Hydra vulgaris*. In terms of evolution, *Hydra vulgaris* represents the old phylum Cnidaria and is the sister group of bilateral lineages leading the metazoan tree before the Urbilaterian comes into existence.

Firstly, was checked whether the mouse counterpart, hydra homolog transcript model TERB1 (GenBank ID: XM_01270454), TERB2 (GenBank ID: XM_012706454) and MAJIN (GenBank ID: XM_01270399) have a complete open reading frame. Only the model transcript for hydra TERB1 lacked the 3´UTR; thus, the predicted protein lacks the stop codon. Therefore, blastn analysis was performed with hydra meiotic telomeres transcripts models, in assembled transcript (e.g. est, tsa) databases at NCBI and Compagen (http://www.compagen.org/datasets). This last allowed to target the full-length coding region (ORF) and make primer design more robust. The resulting analysis detected a putative ORF of hydra Terb1 from an assembled transcript

sequence (GenBank ID: GGKF01021594). Also, an assembled transcript (GenBank ID: GEVZ01007256.1) which contained a complete ORF for Hydra Terb2 was identified which was used to strengthen our primer design in combination with its the transcript model. After the designed of specific primers (Table 7-3), the cDNA from total mRNA of approximately 50 *Hydra vulgaris* individuals from the AEP strain were amplified by RT-PCR.

As shown in Figure 4-7 A-C, the hydra Terb1, Terb2, and Majin were found to be expressed in *Hydra vulgaris* with the expected fragment size. The corresponding amplified sequences were isolated, sequenced and verified for the obtained full-length or nearly full-length cDNA compared with the transcript reference sequence (Supplementary Figure 10-5, 10-6, and 10-.7).

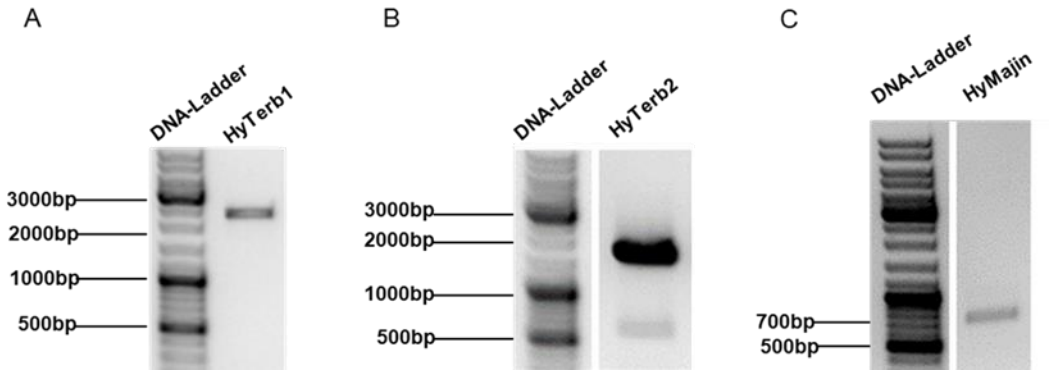

Figure 4-7 Expression of meiotic telomere complex in *Hydra vulgaris*.
RT-PCR analysis of the complete ORFs of identified hydra Terb1 (A), Terb2 (B) and Majin (C). The expected size of the full ORF: 2380 bp (HyTerb1), 1780 bp (HyTerb2), and 699 bp (HyMajin). DNA-Ladder refers to the molecular-weight size marker

To discern a possible meiotic role, we analyzed the expression patterns of hydra Terb1, Terb2, and Majin in four different body fractions by RT-PCR. Approximately 80 hydras were used to isolate head, body-column, testes, and foot total RNA. Equal amounts of RNA were used for cDNA synthesis. The primers were designed to span exon-exon boundaries using the genomic information of hydra Terb1 (GenBank ID: NW_004171015), Terb2 (GenBank ID: NW_0041710153), and Majin (GenBank ID: NW_004173123) to reduce the chances of amplifying DNA contaminants from the process of RNA isolation (Table 8-2). As is indicated in the Figure 4-8 A, all three transcripts are predominately or exclusively found in the testes fraction while a slight

amplification in the body-column could be contamination from testes pieces that were not completely removed.

In contrast, no amplification was detectable in head and foot fractions. Hydra Actin was used as an internal control. As is shown in Figure 4-8 A, equal amounts of mRNA amplification were detected for hydra Actin. These expression patterns of Hydra putative meiotic telomeres transcripts strongly suggest a role in meiosis.

Besides, to confirm this expression pattern, we evaluated the spatial localization by whole mount in situ hybridization (WMIH) of hydra Terb1, Terb2, and Majin. To this end, we used hydra Sycp3 (HySycp3) as a meiotic expression marker (Fraune et al., 2012). As expected, hydra Terb1, Terb2, and Majin expression were localized at the basal layer of testes (Figure 4-8 B), in which meiotic cells reside (Kuznetsov et al., 2001; Fraune et al., 2013).

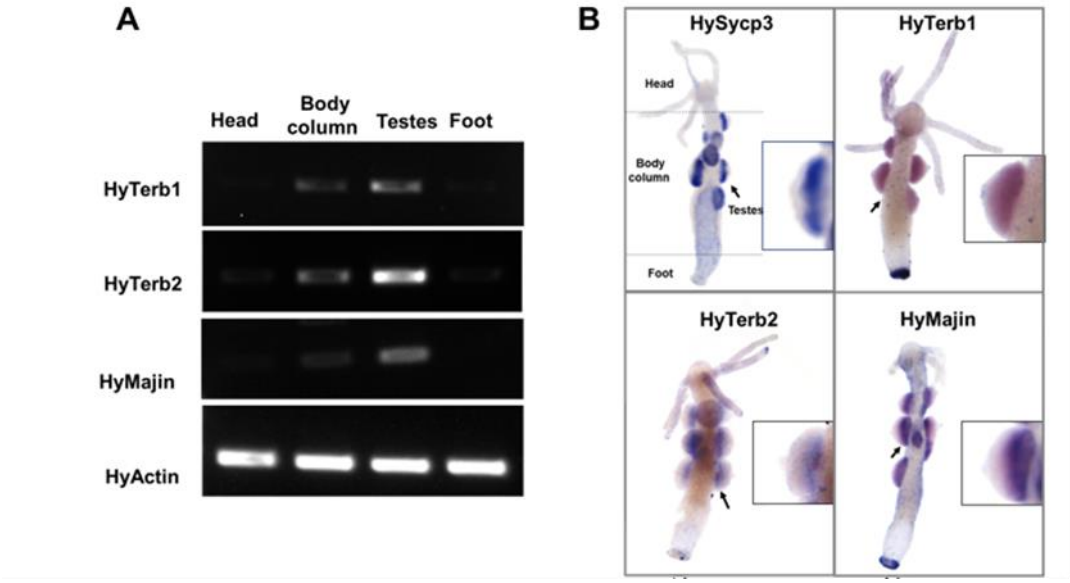

Figure 4-8 Expression pattern of *Hydra vulgaris* Terb1, Terb2, and Majin revealed gonad specificity.

(A) Expression of *Hydra vulgaris* AEP Terb1, Terb2, Majin and Actin were detected in hydra tissues by RT-PCR. Actin was used as a control and (B) Whole-mount in situ hybridization to detect for HySycp3, HyTerb1, HyTerb2, HyMajin transcripts. Arrows indicate the regions shown enlarged in the insets and high magnification of testis shows expressing cells at the base.

As the predicted translation of hydra Terb1, Terb2, and Majin, were obtained a detailed comparison with the respective (GenBank ID: NP_851289; NP_083190, and NP_001159391) mouse meiotic telomere proteins were performed. As detailed in Figure 4-9 A, the N-terminus of mouse and hydra MAJIN share 29% identity and 46% similarity (aa 1-108 of mice; aa 3-117 of hydra). The putative hydra TERB1 similarly to the mouse protein displayed an ARM repeat domain (aa 6-182 of hydra, aa 16-384 of mice) (23% identity; 41% similarity) and a MYB domain (aa 665-710 of hydra; 715-760 aa of mice) (50% identity; 73% similarity) (Figure 4-9 B). Also, we detected 23% identity and 35% similarity between hydra TERB1 aa 382-454 and mouse region aa 557-623, known to be essential for TERB2 binding (T2B) (Figure 4-9 B). Lastly, the comparison between mouse TERB2 and hydra showed that the N-terminus (aa 8-107; aa 1-98 of mice hydra) is conserved with 27% identity and 52% similarity (Figure 4-9 C). However, the C-terminus of hydra TERB2 is notably longer than the mouse and the other metazoan candidates analyzed in this study but not longer than in other Cnidarias candidates.

Recent studies reported the human crystal structure of the subcomplex consisting of the N-terminus of MAJIN (aa 1-112) and C-terminus of TERB2, (aa 168-220) (Dunce et al., 2018, Wang et al., 2019). The structure of MAJIN-TERB2 displayed a 2:2 heterotetrameric in which two chains of TERB2 surrounded the surface of a core globular MAJIN dimer (Figure 4-10 a). The MAJIN protomers adopt a ß-grasp fold around a core amphipathic MAJIN α-helix (Dunce et al., 2018). The ß-grasp fold dimer interface contains highly conserved MAJIN residues that have been shown to contribute to MAJIN dimerization and to provide a large basic surface to interact with the DNA (Dunce et al., 2018). To analyze the structural similarities of hydra MAJIN its 3D structure was modelled using the experimental structure of the human complex (PDB ID: 6gny) (Dunce et al., 2018), using Swiss Model. The resulting model of N-terminal hydra MAJIN showed an acceptable quality (QMEAN > -4) (Figure 4-10 b). Remarkably, in the hydra MAJIN model, highly conserved amphipathic residues on the α-helix and those that contribute to the dimerization of MAJIN (residues P64, F73 and Y75 in human and P66, L78, and Y81 in hydra) (4-10 c) were identified. In addition, it was detected in the hydra

MAJIN model conservation of the basic surface on the ß-grasp and linkers (Figure 4-10 d) necessary for DNA interaction.

Overall, the obtained provide convincing evidence that hydra meiotic telomere genes appear to be orthologs of mammalian genes due to the high similarity of functional domains residues, suggesting that TERB1-TERB2-MAJIN has been conserved throughout ~500 million years of metazoans history.

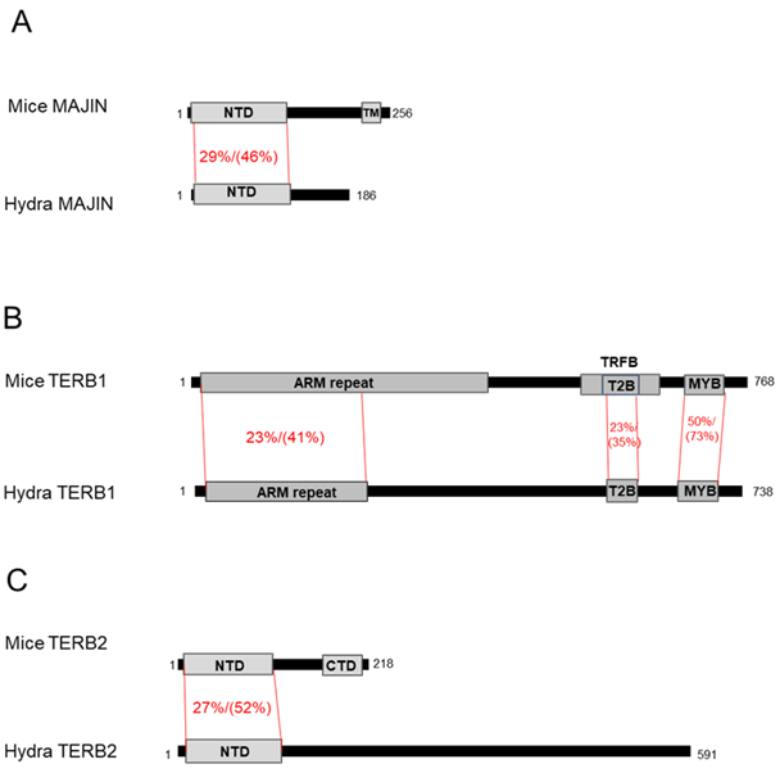

Figure 4-9 Schematic comparison of mouse and hydra MAJIN (A), TERB1 (B) and TERB2 (C) proteins through blastp.

The mouse sequence accession IDs are: MAJIN (GenBank ID:BAT24489), TERB1 (GenBank ID: (GenBank ID: NP_851289). We used predicted translation product for hydra from our full-length cDNA experiments. Sequence identity and similarity (in parenthesis) at the amino acid level are given (%). The gray boxes represent domains. NTD, N-terminal domain; TM, trans-membrane domain; ARM repeats, armadillo repeats; T2B, binding region of TERB2 in TERB1 protein.

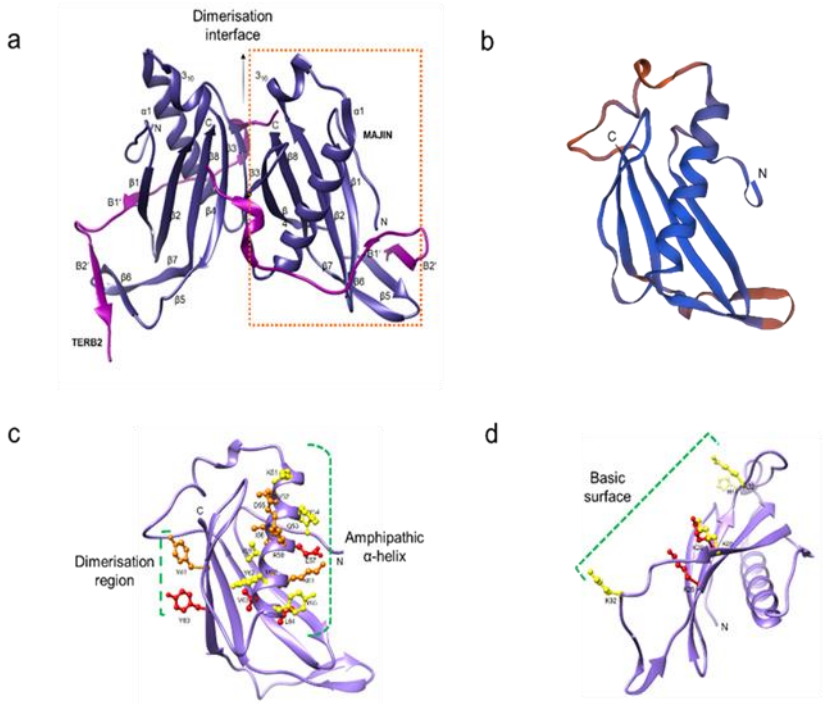

Figure 4-10 Hydra MAJIN N-terminal domain models retain the structural elements needed for homodimerization and DNA binding.

Crystal structure representation of human MAJIN NTD and TERB2 CTD (PDB ID: 6gny) 2:2 heterotetrametric. Model of hydra MAJIN NTD using the template (PDB ID: 6gny.1.A) (punctate box in red). Results of quality assessment can be visualized onto the model with color gradient, from blue to orange indicating high and low quality respectively through QMEAN estimations using SWISS MODEL (b). Hydra MAJIN NTD model showing residues necessary for dimerization (Y79 and Y81) and amphipathic composition of the main alpha helix. The identical residues are denoted in red, similar in orange and non-conserved in yellow (c). Composition of basic amino acid on the surface of hydra NTD MAJIN model. The residues are shown according to identity (red), similarity (orange), and non-conservative but amphipathic amino acid (yellow) (d).

4.3 Discussion

4.3.1 The mouse TERB1-TERB2-MAJIN complex dates back to a metazoan common ancestor

Vigorous chromosome movements during prophase I are conserved in almost all eukaryotes and crucial for faithful homologous chromosome pairing, recombination and segregation into daughter cells. The stable attachment of

telomeres achieves the move to the highly conserved LINC complexes that couple the chromosomes ends from the INM to cytoplasmic cytoskeletal forces. However, another pre-requisite for attachment of chromosome ends or telomeres are the meiotic telomere adapter protein that is highly divergent between yeast and mammals.

The core of this analysis strongly suggests that the origin of mouse TERB1, TERB2, and MAJIN dates back to the common ancestor of metazoans. We have found that TERB1, TERB2, and MAJIN are widely distributed but restricted to metazoans. In addition, the results showed the specific expression of hydra Terb1, Terb2, and Majin in testis and selective synthesis in the basal cells of hydra testis. The last agrees with the general organization of meiotic cells in hydra testis (Kuznetsov et al., 2001). It appears that meiotic telomere genes are not an innovation of mammals; instead, they arose only once in metazoan evolution.

The few candidates as homologous sequences identified in Ecdysozoan belong to Priapulida and Arthropoda. The phylogenetic trees showed long branches indicating that meiotic telomere genes have highly diverged especially for Arthropoda. It seems that meiotic telomere genes in Nematoda and Arthropoda have diversified to the degree that standard homology algorithms cannot detect the homology. Indeed, several lines of evidence showed that many gene families in mammals were lost in *C. elegans* and *D. melanogaster* and this loss can be traced back to pre-bilaterian times (Raible & Arendt, 2004; Kortschak et al., 2003).

The mechanism that uses *C. elegans* to anchor chromosomes to the NE is through a sub-telomeric region of the chromosome, consisting of short repetitive sequences at one end of each chromosome called pairing centers (PC) (Phillips et al., 2009). A set of four zinc fingers, (ZIM-1/2/3 and HIM-8) associate with the PCs (Phillips et al., 2005; Phillips & Dernburg, 2006) and recognize a (TTGGC) motif, which is closely related to the telomeric repeat in *C. elegans* (Phillips et al., 2009). The leading role of this zinc finger family is to couple chromosome ends to the LINC complex (SUN-1-ZYG-12) (Phillips & Dernburg, 2006; Penkner et al., 2007). However, it is still unknown the direct connectors to the LINC complex are still unknown (Link & Jantsch, 2019).

Previous hybridization experiments of telomere probes to worm gonads has indicated the absence of a telomere-mediated meiotic bouquet (Phillips & Dernburg, 2006). Given the drastically change in the genome of *C. elegans* and telomere binding proteins, seems more likely that the ancient meiotic telomere adaptor protein in *C. elegans* was lost and replaced by a non-homologous mechanism to couple the PC to the NE.

4.3.2 TERB1, TERB2, and MAJIN share functional domains across metazoans.

TERB1-TERB2-MAJIN complexes are known to establish protein-protein interactions with two independent protein complexes to anchor telomeres to the NE: telomeric shelterin and LINC complex (Shibuya et al., 2014; 2015; Long et al., 2017; Zhang et al., 2017; Dunce et al., 2018; Wang et al., 2019). The present data showed overall conservation of the general organization of mouse TERB1, TERB2, and MAJIN among taxa analyzed.

The same N-terminus ARM repeat and C-terminus MYB domain of mouse TERB1 protein domain organization were detected in several lineages including Chordata (Vertebrata), Arthropoda (Chelicerata), Mollusca (Gastropod and Bivalves), Annelida, Brachiopod, *Hydra vulgaris* (Hydrozoa, Cnidaria) and *Amphideom queenslandica* (Porifera). However, in diverse taxa belonging to Cnidaria (Anthozoa), Priapulida, Hemichordata, Cephalochprdata and some Vertebrata, the MYB domain seems to be absent. The MYB domain or telobox consensus specifically binds double-stranded telomeric DNA and associates with meiosis-specific cohesion SA3 (Billaud et al., 1996; Shibuya et al., 2014; Daniel et al., 2014). Therefore, a possible explanation is that the sequences that lack the MYB domain could be genome assembly errors.

Furthermore, the TERB1, C-terminus (aa 590-649 of the mouse) interacts with the N-terminus of TERB2 (Shibuya et al., 2015; Zhang et al., 2017). The obtained results have shown that almost all TERB1 sequences, including the ones that lack the MYB domain, possess stretches of conserved residues that span the binding region necessary for TERB2. These results suggest that the physical interaction between TERB1 and TERB2 protein was established in the eumetazoan ancestor.

Previous studies identified a sequence motif in TERB1 (LxLxP; aa 645-648 of mouse/human) that establish the association with TRF1 with a similar strategy adopted by TRF2 (Chen et al., 2008, Long et al., 2017). Despite mutations in this motif abolishing or substantially impairing the binding of TRF1 leading to a decreased fertility in male mice (Long et al., 2017), the present analysis found this motif conserved only in the Vertebrata clade. The fact that outside Vertebrata this motif is not conserved suggests a specific adaptation in this lineage. Further studies are needed to reveal the association with shelterin complex outside the clade of Vertebrata.

Unexpectedly, the analysis of TERB2 sequences revealed a motif [F/YxLxP] proximal to the N-terminus sequences (aa 86-90 of the mouse) taxa that bear highly similarity with the motif employed by shelterin proteins to bind TRHF's domain of TRF1 and TRF2 (Chen et al., 2008). These findings led to the interpretation that TERB2 could intrinsically be recruited and/or interact with shelterin TRFH surfaces. Also, a conserved stretch at the C-terminus of TERB2 alignment (aa 169-202 of the mouse) it was detected conserved which corresponds to the interacting region with the N-terminus of MAJIN.

Also, the present analysis identified that the N-terminal domain of MAJIN is highly conserved among metazoans. As previously discussed, crystallographic studies on the interacting region of human MAJIN (aa 1-112) and TERB2 (aa 168-220) have revealed a 2:2 composition form through aromatic interactions in MAJIN dimerization interface (Dunce et al., 2018). The folding of MAJIN-TERB2 provides extensive DNA binding surfaces (Dunce et al., 2018). In support of these studies, the hydra N-terminus 3D model shows structural properties for MAJIN dimerization and DNA binding of telomeres of the human counterpart structure (Dunce et al., 2018). However, the present analysis detected moderate conservation among taxa in the stretch harboring the TM domain of mouse on its C-terminus (TM, aa 232-251), the TM domain in other species remains to be identified.

Collectively, these findings suggest that the functional domains of meiotic telomere complex proteins were established in the eumetazoan ancestor and likely functioned together to anchor telomeres to the NE during meiotic prophase I.

4.3.3 General evolution of the meiotic telomere complex in sexually reproducing multicellular organisms

Here, we have answered the question about the evolutionary origin of the mouse meiotic telomere complex. However, the general evolution of the meiotic telomere complex in sexually reproducing multicellular organisms remains unknown. So far, the pathways that regulate telomere movements and bouquet formation are most well-characterized in fission yeast and (partially) in budding yeast but not in plants.

The overall amino acid sequence between yeast and mouse meiosis-specific telomere complexes do not reveal any evolutionary relationship. This lead to consider two possible evolutionary scenarios. First, telomere meiotic adaptors proteins could have two distinct origins in Fungi and Metazoan (they are real analogues), or second, they derived from an ancestral sequence but evolved beyond recognition (they are very divergent homologues).

It is evident that yeast and mouse meiosis-specific telomere proteins specifically interact with shelterin telomeres complex TRF-family proteins such as Taz1 and TRF1, respectively. Regarding fission yeast, Taz1 and Rap1 are constitutive telomere-associated proteins. Taz1, the ortholog of human TRF1 and TRF2 (Zhong et al., 1992; Bilaud et al., 1997; Broccoli et al., 1997) can directly bind the duplex telomeric DNA (Cooper et al., 1998) as in mammals.

Also, even though Bqt4 is not meiosis-specific, it is similar to MAJIN in that it has a single transmembrane segment and double-stranded DNA (dsDNA)-binding activity with no sequence selectivity for DNA binding (Shibuya et al., 2015; Dunce et al., 2018; Hu et al., 2019).

From this standpoint, it seems, that yeast and mouse meiotic telomere adaptors derived from an ancestral sequence that evolved beyond recognition probably because telomere adaptors are fast-evolving and very specific due to the significant variability of telomeric sequences across eukaryotes. In this scenario, the ancient inventory of the meiosis telomere adaptor protein pathway may have recruited a set of proteins that co-evolve with the telomere somatic complex and with nuclear envelope proteins to anchor telomeres to the NE during meiosis. However, during the evolution of the different lineages, this set

of proteins might have changed by strong diversification, losses and replacement of individual components.

Chapter 5 General Discussion

5.1 Summary of findings and implications

The overall objective of this thesis was to further our understanding of the mouse meiotic telomere INM-tethering mechanism and how conserved are its components in the course of evolution.

In the first part of the thesis, super-resolution SIM microscopy was used to examine the spatial organization/relationships of mouse TERB1-TERB2-MAJIN complex with TRF1 shelterin protein during meiotic prophase I. By increasing the resolution with SIM imaging the present study showed novel architectural features of the meiotic telomere complex in relationship with TRF1 and telomeric DNA compared to previous findings using conventional light microscopy.

In agreement with their mutual dependency, the staining patterns of TERB1-TERB2-MAJIN complex strongly suggested that they are interacting together during meiotic prophase I (Shibuya et al., 2015). TERB2 showed a broader distribution pattern at the distal end of LEs compared to the globular arrangement of TERB1 and MAJIN in both zygotene and pachytene stages. In support of the TERB2 staining pattern observed, an interaction model for TERB1-TERB2-MAJIN based on structural data have shown that TERB2 flexible linkers could stretch out owing to provide physical separation between the interacting domains with TERB1 and MAJIN (Dunce et al., 2018).

Furthermore, the data obtained using SIM have demonstrated that during late pachytene, a large fraction of the TRF1 is likely associated with telomeric DNA instead of a complete dissociation in the process of cap exchange. This finding supports an alternative model for meiotic telomere attachment to the NE (Figure 5-1) in which TRF1 displacement represents a reorganization event that merely displaced to the surrounding unattached telomeric DNA.

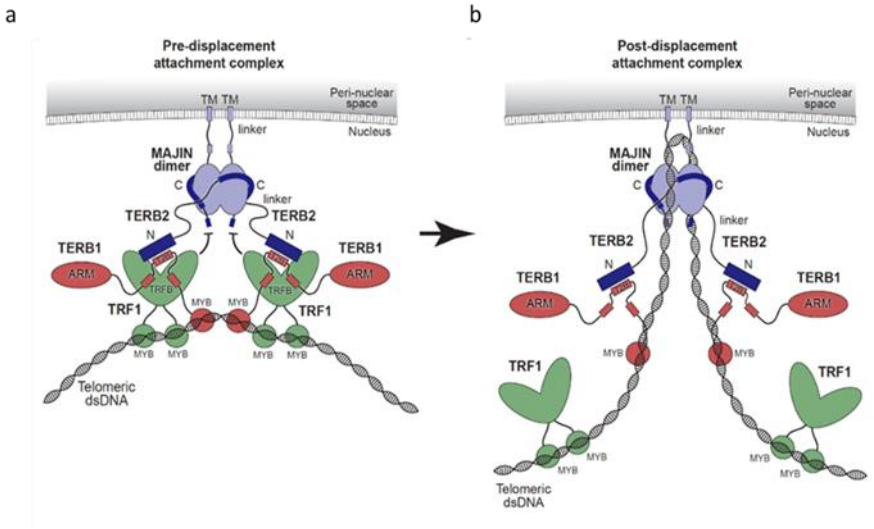

Figure 5-1 Model of meiotic attachment to the nuclear envelope.
a) Initially telomeres are recruited through TRF1, which interacts with TERB1 and thus with the meiotic telomere complex. (b) TRF1 is subsequently displaced, leading the meiotic telomere complex to bind directly to telomeric DNA, with TRF1 associating with surrounding telomeric DNA. (Image modified from Dunce et al., 2018).

The second part of this thesis aimed to answer a major question of how conserved the mouse meiotic telomere complex components in evolution are.
The present study demonstrated that the mouse meiotic telomere complex is not an invention of mammalian lineages but instead originated as early as eumetazoans (Figure 5-2). Despite the fact that two rounds of whole-genome duplication occurred during the evolutionary history of Vertebrata TERB1, TERB2, and MAJIN are present in a single copy as the other taxa outside the clade of Vertebrata analyzed, indicating that paralogs resulting from these events were not retained during evolution.
Furthermore, related sequences of TERB1, TERB2 and MAJIN were detected in ancient on-bilateral clades such as Cnidaria, Placozoa, and Porifera. Therefore, it seems likely that the ancestral meiotic telomere complexes have emerged even earlier, in the ancestor of Metazoans. However, the absence of any homologs in Nematoda and only a few candidates detected in Arthropoda for TERB1 and TERB2 but not MAJIN, suggest that these complexes have been either secondarily lost or diverged beyond recognition in lineages leading to *C. elegans* and *D. melanogaster*.

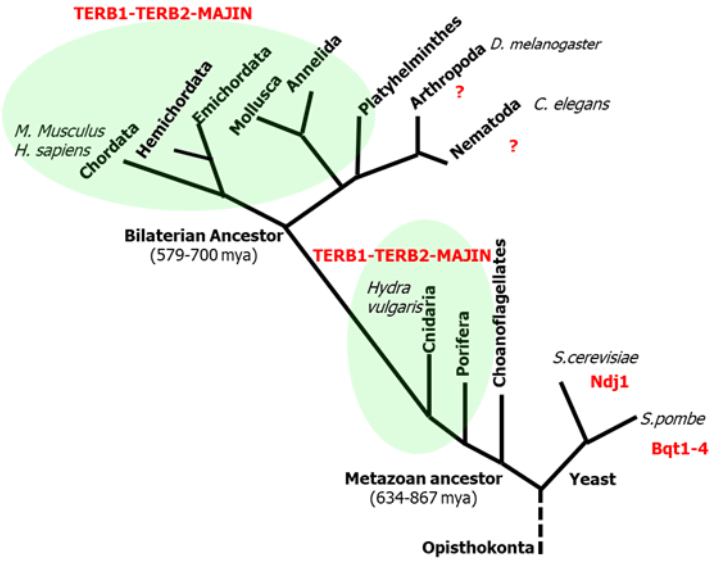

Figure 5-2 Conservation of meiosis-specific telomere adaptor in metazoans. Simplified phylogenetic tree of Metazoans which include yeast as outgroup forming the supergroup Opisthokonta in evolution. The ancient TERB1-TERB2-MAJIN (in red) originated before the bilaterian ancestor come into existence approximately 500 Mya ago, since homologs were found in Cnidaria and Porifera. During the evolution TERB1-TERB2-MAJIN complex remain in the present day Bilaterians but seems to have and been lost/replaced or highly diversified in lineages leading to Arthropoda and Nematoda. Is denoted for *S. cerevisiae* and *S. pombe* in red the protein names of their respective meiosis specific telomere complex.

Moreover, the detected highly conserved protein domains among taxa belongs to the functional domains associated with mouse meiotic telomere complex assembly. In support of this view, the expression pattern of putative orthologs of mouse TERB1, TERB2, and MAJIN in the basal metazoans *Hydra vulgaris* were specifically observed in the testes where spermatocytes reside suggesting a meiotic role for these genes that have been conserved throughout metazoan evolution.

As previously discussed, the mammalian TERB1 localized at telomeres through the interaction with the shelterin protein TRF1. Of note, the domain boundaries for the interaction of TRF1 in TERB1 were shown not as highly conserved as the other functional domains discussed above. Also, TRF1-TERB1 directly interact in mammals through a sequence motif (aa 645-648 in human/mouse

TERB1) that is comparable to the docking site adopted by TIN2 to bind TRFH domain of TRF1 (Chen et al., 2008; Long et al., 2017). The presented results failed to find similar sequence motif of TERB1 outside the clade of Vertebrata, suggesting a new adaption in this lineages to interact with TRF1.

On the other hand, a F/YxLxP motif was conserved in all TERB2 N-terminus sequences analyzed. So far, it is known that Vertebrata TRF1 or TRF2 TRFH´s domains are capable of recruiting and binding other telomere-associated proteins through a highly similar motif (Chen et al., 2008) as the one detected for TERB2. The presence of such a motif in TERB2 sequences points to a novel mechanism into the meiotic telomere complex regulation. It is tempting to speculate that TERB2 could be recruited to telomeres by the interaction with the TRFH domain of the telomeric shelterin proteins.

Worth mentioning, the data obtained highlight the conservation of features necessary to mediate interaction with telomeric DNA. Teloboxes are conserved in plant, yeast and animals somatic telomeric proteins to bind double-strand telomeric DNA specifically. The detection of MYB or telobox domain at the C-terminus of TERB1 sequences strongly suggests that they play a role in directly binding with telomeres. Other structure-function information obtained modelling the N-terminal hydra MAJIN using human the counterparts structure revealed high similarity of the folding necessary for dimerization and DNA binding. It could be suggested that the DNA-binding properties of TERB1 and MAJIN are retained between metazoans.

As a final point, it seems that before the emergence of metazoans the ancient meiosis-specific telomere proteins of eukaryotes could have evolved adaptively beyond recognition to exert telomeric function. It is well-known that somatic telomeric proteins have exquisite specificity for telomeric repeat motif (de Lange et al., 2005 Bianchi et al., 1997; Court et al., 2005, Hnaoka et al., 2005) and possibly meiotic telomere proteins co-evolved with telomeric repeats and telomere binding proteins. This last could explain why despite the similarity in both yeast and mouse mechanism for telomere INM-tethering, their protein components are strongly diversified.

In conclusion, the results presented in this thesis provides new insight into the molecular architecture of the mammalian meiotic telomere complex. The data supports functional conservation over evolutionary time of TERB1-TERB2-MAJIN complex, implicating that is the critical mediator of meiotic chromosome attachment in metazoans.

Chapter 6 Future work

This chapter reviews some of the provided results which are worth further investigation.

In Chapter 3, the results obtained strongly suggest that TRF1 merely displaces to the adjacent unattached telomeres that may represent a reorganization event to allow the interaction of TERB1-TERB2-MAJIN complex with telomeric DNA. However, the presented data with SIM leaves open the possibility that these reorganization events involves the specific interaction of meiotic telomere complex with telomeric structures (for example t-loops), subtelomeric regions or chromatin state. Other methods such as expansion microscopy (ExM) (Chen et al., 2015) that can increase the achievable resolution imaging on a standard fluorescence microscope could be implemented to provide a more detailed protein localization map of meiotic telomere complex and its relationship with telomeric DNA. This last would give a better understanding of the ultrastructural organization adopted by the ubiquitous sheltering and meiotic telomere complexes to address the INM-telomere attachment during prophase I.

As for Chapter 4, the findings presented in this thesis strongly suggest functional conservation of mouse meiotic telomere complex across Metazoans. As discussed previously, the direct interaction between mouse TERB1-TRF1 is vital to initiate the mechanism of INM-telomere attachment during prophase I. From the data obtained it seems that the TERB1 motif required to bind with TRF1 directly is a new adaptation from the Vertebrata clade. An important question for future studies is to determine the interaction mechanism between telomere shelterin complex and meiotic telomere complex outside the clade of Vertebrata. Furthermore, a novel conserved motif identified in TERB2 N-terminus is comparable to the motif required in mammalian telomere-associated proteins to bind TRF1. This finding point to a new mechanism in the regulation of TERB2 probably to ensure its recruitment to telomeres by telomere shelterin proteins as TERB1 upon prophase I. Further studies are needed to confirm the functionality of this motif in the context of meiosis.

Chapter 7 Materials

7.1 Organism used

7.1.1 Mice

Male wild-type mice C57BL/6 strain was used in this study. The mice were bred in the animal facility of the Biocenter at the University of Würzburg.

7.1.2 *Hydra vulgaris* strain AEP

Hydra vulgaris strain AEP (Hemmrich et al., 2007) were grown in hydra medium (HM) according to the standard procedures at 18°C (Lenhoff & Brown, 1970). The animals were fed three times per week with Artemia salinas, (Silver Star Artemia dehydrated cysts, Inter Ryba GmbH). The Artemia cyst (two tee spoons) were incubated overnight in 500 mL aerated bottles with saltwater (concentration of 34 g NaCl/L) for two days. The sexual differentiation was induced when required, by starving the animals for several days after one week of intensive feeding.

Hydra medium (HM):

- Solution 1: 42 g/L CaCl2·2H2O in ddH2O; working concentration 1:1000 in ddH2O
- Solution 2: 8.112 g/L MgSO4·7H2O, 4.238 g/L NaHCO3, 1.0958 g/L K2CO3 in ddH2O, working concentration 1:100 in ddH2O

7.1.3 Bacteria

- StrataClone SoloPack Competent Cells

The bacteria strain StrataClone SoloPack Competent Cells is part of the StrataClone Blunt PCR Cloning Kit (Agilent Technologies, Böblingen) used for the cloning of PCR products into the StrataClone PCR cloning vector pSC-B-

amp/kan (7.2.1). Transformation of bacteria was performed according to manufacturer's instructions.

- Escherichia coli XL1-blue (Agilent Technologies, Böblingen)

The Escherichia coli XL1-blue bacteria strain was used to isolate its genomic DNA for telomeric in situ hybridization experiments.

7.2 Antibodies

The primary and secondary antibodies used in this study are listed in Table 7-1 and Table 7-2, respectively. The antibodies were ordered from commercial sources or produced for our lab by Bioscience (Göttingen).

Table 7-1 List of primary antibodies used in this thesis

Primary antibodies	Antigen	Host	Dilution	Application/Incubation	Suppliers
MAJIN (Membrane-anchored junction protein)	N-terminal aa 18-30 mouse HAGPNVYKFKIR YGN GenBank accession number: BAT24489	Guinea pig	1:10 3rd bleeding serum	Immunofluorescence / 1 hr. at room temperature	SeqLab, Göttingen
TERB1 (Telomere repeats-binding bouquet formation protein 1)	C-terminal aa 525-540 aa mouse LDKEKTFDQKDS VSQ GenBank accession number: NP_851289	Guinea pig	1:30 3rd bleeding serum	Immunofluorescence / 1 hr. at room temperature	SeqLab, Göttingen
TERB1 (Telomere repeats-binding bouquet formation protein 1)	and against 103-aa from the C-terminal of mouse	Guinea pig		Immunofluorescence / 1 hr. at room temperature	Daniel et al., 2014.
TERB2 (Telomere repeats-binding bouquet formation protein 2)	Whole protein from mice GenBank accession: LC068588	Rabbit	1:100	Immunofluorescence / 1 hr. at room temperature	Shibuya et al., 2015
TRF1 (Telomeric repeat binding factor 1)	N-terminal 19 aa mouse	Rabbit	1:100	Immunofluorescence / 1 hr. at room temperature	Alpha Diagnostic; TRF12-A),

SYCP3	Recombinant full-length protein corresponding to Hamster SCP3 aa 1 to the C-terminus.	Mouse	1:100	Immunofluorescence / 1 hr. at room temperature	Abcam; ab 97672
SYCP2	C-terminal aa 1095-1585 from rat	Guinea pig		Immunofluorescence / 1 hr. at room temperature	Seqlab; Göttingen
α-anti-digoxigenin Fab fragment	Digoxigenin	Mouse	1:50	In situ hybridization / overnight at 4°C	Roche, Mannheim
α-anti-digoxigenin-POD	Digoxigenin	Mouse	1:1000	Dot blot /1 hr. at room temperature	Roche, Mannheim
α-anti-digoxigenin-AP	Digoxigenin	Sheep	1:600	In situ hybridization / overnight at 4°C	Roche, Mannheim

Table 7-2 Secondary antibodies used in this study

Secondary Antibodies	Host	Dilution	Application/Incubation	Suppliers
α guinea pig IgG (H+L) Alexa Fluor 647 conjugated	Goat	1:200	Immunofluorescence/ 30 min at room temperature	Thermo scientific A-21450
α rabbit IgG (H+L) Alexa Fluor 488 conjugated	Goat	1:200	Immunofluorescence/ 30 min at room temperature	Thermo scientific
α mouse IgG (H+L) Alexa Fluor 488 conjugated	Goat	1:200	Immunofluorescence/ 30 min at room temperature	Thermo scientific ,A-11017
α guinea pig IgG (H+L) Alexa Fluor 568 conjugated	Goat	1:200	Immunofluorescence/ 30 min at room temperature	Thermo scientific

7.3 Molecular materials

7.3.1 Plasmid

- Strata pSC-B-amp/kan (Agilent Technologies, Böblingen)

The Strata pSC-B-amp/Kan vector is part of the StrataClone Blunt PCR Cloning Kit (Agilent technologies). This vector was used for capable cloning of a non-phosphorylated blunt end PCR product. The selection of the positive clones is possible because of its inherent resistance for ampicillin and kanamycin as well as a lacZ' complementation for blue-white selection cassettes. For colony PCR

standard primers (M13 forward, M13 revers, T7, T3) (Table 7-3) can be used as well as for sequencing.

7.3.2 Oligonucleotides

The oligonucleotides used in this study were synthesis from Simga-Aldrich (Steinheim) or Biomers (Ulm).

Table 7-3 Oligonucleotide used in this study

Application	Primer Sequence	Fragment length	Annealing Temperature
Cloning full-length cDNA			
Hydra vulgaris AEP Terb11	HyTerb1_FL_Fwd 5′ TCAATCATATCCAAACCAACAA 3′ Hy_Terb1_FL_Rev 5′ AGTTGGAATGGCGATTCTTC 3′	2400 bp	61 °C
Hydra vulgaris AEP Terb2	HyTerb2_FL_Fwd 5′ ATGATGCAGCCAGAAAACCA 3′ Hy_Terb2_FL_Rev 5′ TCAAACATTCAATTCACGCA 3′	2000 bp	60 °C
Hydra vulgaris AEP Majin	Hy_MAJIN_FL_Fwd 5′ CATGACGTGTAGTTTGTCTGATT 3′ Hy_MAJIN_FL_Rev 5′ TCAGTGGTGCTATCAACTTTTTTC 3′	739 bp	63 °C
RT-PCR			
Hydra vulgaris AEP Terb1	HyTerb1_RT_Fwd 5′ TTTTCTACGCCTGAGCACAAT 3′ HyTerb1_RT_Rev 5′ GAGGTTCCAGTCGAAGCAAG 3′	497 bp	63°C
Hydra vulgaris AEP Terb2	HyTerb2_RT_Fwd 5′ TGACTTCGAAAAATGGCAGA 3′ HyTerb2_RT_Rev 5′ CCATCAAGAAAGTTCTCGCC 3′	447 bp	64°C
Hydra vulgaris AEP Majin	HyMajin_RT_Fwd 5′ CATGACGTGTAGTTTGTCTGATT 3′ HyMajin_RT_Rev 5′ TCAGTGGTGCTATCAACTTTTTTC 3′	369 bp	60 °C
Hydra vulgaris AEP Actin	HyActin_Fwd 5′ AGGAGTCATGGTTGGTATGGGA 3′ HyActin_Rev 5′ AATCTCGTCCTGCTAAATCCA 3′	448 bp	63 °C
Whole Mount In Situ Hybridization			
Hydra vulgaris AEP TERB1	HyTerb1_WMIH_Fwd 5′ TTTTCTACGCCTGAGCACAAT 3′ HyTerb1_WMIH_Rev 5′ TTCCACGTAAATCTGTTGCTTG 3′	649 bp	67 °C
Hydra vulgaris AEP TERB2	HyTerb2_WMIH_Fwd 5′ TGACTTCGAAAAATGGCAGA 3′ HyTerb2_WMIH_Rev 5′ CCATCAAGAAAGTTCTCGCC 3′	447 bp	64°C

Hydra vulgaris AEP MAJIN	HyMajin_WMIH_Fwd 5' CATGACGTGTAGTTTGTCTGATT 3' HyMajin_WMIH_Rev 5' AAAGATCCGGTCGGTCAGACA 3'	739 bp	63 °C
Hydra vulgaris AEP SYCP3	HySycp3_Fwd 5' GTCCGCAATTAGTGCAGCAATGAACGA 3' HySycp3_Rev 5'GACTTAAACACTGTGTAGCAAGCTTTGAAG CGA 3'	714 bp	64°C
Telomere probe synthesis			
Telo 1	5'TAACCCTAACCCTAACCCTAACCCTAACCCT AACCCTAACCC 3'		77 °C
Telo 2	5'GGGTTAGGGTTAGGGTTAGGGTTAGGGGT TAGGGTTAGGGTTA 3'		77 °C
Colony PCR/ sequencing in Strata pSB-amp/kan			
M13	Fwd 5'TGTAAAACGACGGCCAGT3'		54°C
M13	Rev 5'CAGGAAACAGCTATGACC3'		54°C
T3	Fwd. 5'ATTAACCCTCACTAAAGGGA3'		54°C
T7	Fwd. 5'TAATACGACTCACTATAGGG3'		54°C

7.3.3 DNA ladder

- GeneRuler DNA Ladder Mix (Thermo Scientific, Schwerte)
- GeneRuler 1kb DNA Ladder (Fermentas, St. Leon-Roth)

7.3.4 Kits

- NucleoSpin Gel and PCR Clean-up (Macherey-Nagel, Düren)
- NucleoSpin Plasmid (Macherey-Nagel, Düren)
- StrataClone Blunt PCR Cloning Kit (Agilent Technologies, Böblingen)
- peqGOLD TriFast (PeqLab, Erlangen)
- RNeasy mini Kit (Quiagen, Hilden)

7.3.5 Enzymes

- Terminal transferase (Tdt) (Thermo Scientific Waltham, MA)
- Phusion High-Fidelity DNA-Polymerase (Thermo Scientific, Schwerte)
- Reverse Transcriptase M-MLV (Promega, Mannheim)
- Taq DNA-Polymerase (Manufactured in the laboratory by the Technician Silke Braune.)
- EcoRV (Thermo Scientific, Schwerte)
- SmaI (Thermo Scientific, Schwerte)
- Proteinase K (Serva Heidelberg)

7.3.6 Chemicals

The Chemicals used in this study were purchased from AppliChem (Darmstadt), Merck (Darmstadt), Roth (Karlsruhe), Serva (Heidelberg) and Sigma-Aldrich (Steinheim).

7.4 Computer software and Online Tools

Special equipment and software used in this study are listed in Table 7-4.

Table 7-4 Special equipment used in this study

Equipment	Suppliers
Binocular SZ 61, equipped with Camera EC3	Olympus (Hamburg) and Leica (Wetzlar)
Centrifuge MIKRO 200/ MIKRO 200R	Hettich (Tuttlingen)
Centrifuge 6-16K	Sigma (Osterode)
Confocal laser scanning microscope TCS-SP2 AOBS	Leica (Wetzlar)
Electrophoresis Power Supply	Peqlab (Erlangen)
Elyra S1 microscope	Carl Zeiss Microscopy GmbH (Jena)
Gradient Thermocycler T100	Bio-Rad (Munich)
Heating block	Liebisch (through Hartenstein, Würzburg)
Hybridization Oven MINI 10	MWG Biotech (Ebersberg)
Hybridization Oven/ Incubator	Memmert (Schwabach)
Infinite M200	Tecan (Männedorf)
Thermocycler Primus 25 advanced	Peqlab (Erlangen)
UV Stratalinker 1800	Stratagene (Heidelberg)
Fine spring scissors	FST GmbH (Heidelberg)
Software and online tools	**Application**
Leica Confocal Software TCS SP2	Image acquisition
CLC DNA Workbench v.7	DNA and protein sequence analysis
Fiji	Image analysis
ZEN 2012	Image acquisition
PSI-BLAST at NCBI (https://www.ncbi.nlm.nih.gov/)	Identification of homologues
tBLASTn at NCBI (https://www.ncbi.nlm.nih.gov/)	Identification of homologues
with PROMALS3D web server (http://prodata.swmed.edu/promals3d/)	Multiple protein sequence alignment
Seaview v. 4.4.0	Multiple protein sequence alignment
ESPript3 (http://espript.ibcp.fr/ESPript/ESPript/)	Multiple protein sequence alignment annotator

the Eukaryotic Linear Motif (ELM) (http://elm.eu.org/index.html)	Identification of protein motifs
Superfamily web server (http://supfam.org/)	Identification of protein domains families
MAFFT v.7.309	Multiple sequence alignment
BMGE v.1.12	Multiple alignments trimmer
MrBayes v.3.2.6	Trees construction
iToL v4	Trees draw or edition
BLAST at Compagen http://www.compagen.org/	Transcriptome analysis of *Hydra vulgaris* AEP
T-Coffee (www.t-coffee.org)	Protein alignment assessment

Chapter 8 Methods

8.1 Microbiological methods

8.1.1 Culturing bacteria

8.1.1.1 Culturing of bacteria in liquid culture

- LB-medium (1L):10 g tryptone; 10 g NaCl; 5 g yeast extract; pH 7.4, autoclave
- Antibiotics stock solution: ampicillin (50 mg/mL in ddH2O) and kanamycin 50 mg/mL in ddH2O)

The recombinant bacteria were cultured in 10 mL liquid sterile LB-medium using Greiner tubes (50 ml), and antibiotics were added to the appropriate working concentration (ampicillin 100 µg/mL and/or kanamycin 50 µg/mL). The bacterias were cultured overnight at 37 °C with continuous agitation.

8.1.1.2 Bacterial Glycerol stock

The liquid bacterial culture of interest was stored as a glycerol stock culture to ensure the viability of the culture over in an extended period. The glycerol infuses into the bacterial cells, making them structurally stable and allowing them to be stored safely. 850 µL of a liquid culture and 150µL glycerol were mixed gently in a 2 mL Eppendorf tube. After mixing, the samples were frozen at −80 °C..

8.1.1.3 Culturing of bacteria on agar plates

For cultivation of bacteria on agar plates, 1.5% agar (w/v) was suspended in autoclaved LB medium. After the medium was cooled down approximately to 50 °C, the suitable antibiotic was added at the appropriate working concentration (ampicillin: 100 µg/mL and/or kanamycin 50 µg/mL). The solution of 1.5% agar in LB was poured into sterile Petri dishes under in a safety cabinet and left to dry for several hours. About 70-200 µL of a liquid bacteria culture

could be plated with a glass Pasteur pipette and incubated at 37°C overnight with the plate turned upside down to prevent condensed water from dripping onto the nutrient medium, the selection plates are stored upside down at 4 ° C for 3 to 4 weeks.

8.1.2 Transformation of competent bacteria

- StrataClone Blunt PCR Cloning Kit (7.2.1)
- 2 % X-gal: 0.02 g/mL X-Gal in 10 mL of dimethylformamide (DMF)
- LB medium (8.1.1.1)

The transformation of StrataClone SoloPack competent cells was carried out following the manufacturer instructions of StrataClone Blunt PCR Cloning Kit (Agilent Technologies, Böblingen). First, a tube of competent bacteria was thawed on ice and gently mixed with complete ligation mix. An additional ligation mixture could be done with 2 µL of a Control Insert ligation to check the ligation efficiency. Afterwards, the competent cells were heat-shocked for 1 min at 45 °C. Immediately after the heat shock, the bacteria were incubated on ice for 20 min, following which 900 µL of pre-warmed (37°C) LB medium was added. Then the bacteria were incubated at 37°C for at least 1.5 h under continuous agitation. Finally, 70- 200 µL of the liquid culture was streaked onto an agar plate, which contains ampicillin (working concentration 100 µg/mL), and 2% X-Gal in DMF for the blue-white screening of the competent bacteria.

8.2 Molecular methods

8.2.1 RNA isolation

- peqGOLD TriFast kit (PeqLab, Erlangen)
- Gel Loading Buffer II (Ambion).

Total RNA of hydra was isolated using peqGOLD TriFast kit (PeqLab, Erlangen) following the manufacture's protocol. Approximately 50-80 hydras were taken for one preparation. The RNA quality was evaluated by non-denaturing agarose gel electrophoresis using the Gel Loading Buffer II (Ambion).

8.2.2 cDNA synthesis by reverse transcription

- RiboLockTM ribonuclease inhibitor (Fermentas, St. Leon Roth)
- Reverse Transcriptase M-MLV and M-MLV RT 5x buffer (Promega, Mannheim)
- dNTPs (Fermentas, St. Leon Roth)
- Oligo(dT)18 primer (Fermentas, St. Leon Roth)

The synthesize of complementary DNA (cDNA) from isolated mRNA is through RNA-dependent DNA polymerase. This enzyme operates on a single strand of mRNA, to generate its complementary DNA based on the pairing of RNA base pairs to their DNA complements. Eukaryotic cells transcribe DNA (genes) into RNA and process them by removing introns and adding a poly-A and 5' Methyl-Guanine cap. The poly-A tail of the mature mRNA is used to hybridize with a poly-T oligonucleotide primer in a reaction with the reverse transcriptase and deoxynucleotide triphosphates (A, T, G, C). Therefore, the resulting DNA from the original mRNA is suitable for cloning of specific genes into vectors because cDNA contains a reading frame without introns that codes for the functional protein.

The reverse transcription for 20 µL preparation was carried out as follows:

- 1 µg RNA in a sterile RNase-free microcentrifuge tube
- 1.25 µL Oligo(dT)18 (500 µg/mL) primer
- 1 µL RNase inhibitor (40 U/µL)
- 5 µL 5x RT-buffer
- 1.25 µL dNTPs (10 mM/nucleotide)
- 1 µL reverse transcriptase (200 U/µL)
- RNase free water to a final volume of 20 µL

The tubes were gently mixed and incubated for 1 hr at 37°C. Subsequently the tubes were incubated at 95°C for 5 minutes to inactivate the enzymatic reaction. The resulting cDNA was stored at -20°C.

8.2.3 Polymerase chain reaction (PCR)

PCR is an enzyme-based in vitro method for amplifying a specific region of a DNA or cDNA strand. The procedure consists of three key reaction steps:

1. Denaturation of the double-stranded DNA template by breaking the hydrogen bonds between complementary bases, to yield two single-stranded DNA molecules. This step is the first regular cycling event and consists of heating the reaction to 95–98 °C for 20–30 seconds.
2. Annealing is the step in which a precise temperature is required for specific primers or oligonucleotides (forward and reverse) to anneal to the respective single-stranded DNA templates. Therefore, it is critical to determine the proper temperature to allow specificity and avoid false positives. The ideal temperature is not so low that the primer may bind non-specifically, but not so high that the primer does not bind at all. The typical annealing temperature is 50 °C-70 °C or about 3–5 °C below the melting temperature (Tm) of the primers used.
3. Elongation is the step in which a new DNA strand is synthesized in the 5'-3 'direction by thermostable DNA polymerase at 72 °C. The synthesis proceeds from the 3'-end primers and require the addition of deoxyribonucleoside triphosphates (dNTPs). The elongation time depends on the processivity of the enzyme and the length of the DNA fragment to be amplified.

8.2.4 Amplification of cDNA with Phusion DNA polymerase

- PhusionTM DNA polymerase and 5x Phusion HF buffer (Thermo Scientific, Schwerte)
- dNTPs (Fermentas, St. Leon Roth)
- specific primer pairs (Sigma-Aldrich, Steinheim)

PCR reactions were performed using PhusionTM High-Fidelity DNA Polymerase (Thermo Scientific, Schwerte) for cloning experiments. PhusionTM High-Fidelity DNA Polymerase offers high accurate performance due to its 5´-3´DNA

polymerase activity and 3´-5´ exonuclease activity, generating blunt-ended products ideal for cloning.

Protocol for 50 µL preparation:

- 5-10 ng template DNA or 0.5-1 µL cDNA
- 1 µL 5' primer (10 pmol/µL)
- 1 µL 3' primer (10 pmol/µL)
- 1 µL dNTPs (10 mM/nucleotide)
- 1.5 µL DMSO
- 10 µL 5x HF reaction buffer
- 0.3 µL PhusionTM DNA polymerase (2 U/µL)
- ddH2O to 50 µL

Table 8-1 Cycling protocol

Steps	Temperature	Time	
Initial Denaturation	98 °C	2 min	
Denaturation	98 °C	20 sec	35 cycles
Annealing	X°C	30 sec	
Elongation	72°C	1Kb/15 sec	
Final Elongation	72°C	10 min	
Cooling down	4°C		

8.2.5 Semi-quantitative RT-PCR analysis

Semi-quantitative RT-PCR was performed to evaluate expression levels of genes from four different *Hydra vulgaris* AEP body regions: head, body column, testes and foot. The RNA isolation, integrity and cDNA synthesis were performed as section 8.2.1 and 8.2.2. All the samples were prepared identically and added to the PCR with primers against the gene of interest (Table 8-2). We amplify hydra actin as housekeeping gene (30 PCR cycles) to control for RNA amounts.

Table 8-2 Cycling protocol

Steps	Temperature	Time	
Initial Denaturation	95 °C	5 min	
Denaturation	95 °C	30 sec	30 cycles
Annealing	X°C	30 sec	
Elongation	72°C	1Kb/1 min	
Final Elongation	72°C	7 min	
Cooling down	4°C		

8.2.6 Colony PCR with Taq polymerase

Colony PCR is a method for fast screening of colonies of bacteria that have grown up on selective media following a transformation step, to verify that the chosen genetic construct is present. The Taq DNA polymerase (self-manufactured by Silke Braun) from the thermophilic bacterium *Thermus aquaticus* was used to amplify colonies by PCR. This polymerase has no proof-reading function and can incorporate 1000 bp per min. We picked ten single bacterial colonies from the agar LB plate (8.1.2.1) and resuspended in the PCR mix. Subsequently, on a back-up plate containing ampicillin, the tested colonies were cultured in a numbered order and incubated upside down overnight at 37 ° C.

The reaction includes:

- Taq DNA polymerase and 10x Taq buffer
- dNTPs (Fermentas, St. Leon Roth)
- specific primer pairs (Table 4)

Protocol for 25 µL preparation:

- 100 ng template DNA or one bacteria colony
- 0.25 µL 5’ primer (10 pmoL/µL)
- 0.25 µL 3’ primer (10 pmol/µL)
- 0.5 µL dNTPs (10 mM/nucleotide)

- 1.5 µL MgCl2 (25 mM)
- 2.5 µL 10x Taq buffer
- 0.5 µL Taq DNA polymerase (5 U/µL)
- ddH2O to 25 µL

8.2.7 Agarose gel electrophoresis

- 1x TAE Electrophoresis Running Buffer: 40 mM Tris-Acetate; 1 mM EDTA, adjusted to pH 8.
- PeqGOLD Universal Agarose (PeqLab, Erlangen)
- 6x DNA Loading Dye (Thermo Scientific)
- Gene Ruler DNA Ladder Mix (0.5 µg/µL; 50 ng) (Thermo Scientific)
- ethidium bromide

The conventional technique of agarose gel electrophoresis is used to separate DNA fragments based on their size. The polymer agarose can form a three-dimensional matrix gel with pores through which DNA molecules can travel. The pore size of agarose can increase or decrease depending on its concentration in a buffer, making it suitable to separate DNA of different sizes. For instance, a 0.8 % agarose gel is used to separate large fragments between 300-1500 bp, while 1.2 % agarose is used to separate shorter DNA molecules. The agarose gel was prepared in 1x TAE buffer with 1.2 % (w/v) agarose. After heating and dissolving the agarose in 1xTAE buffer was poured into a gel chamber. At the top of the chamber, there is an attached comb to form pocket-like indentations in the gel called wells, into which samples can be loaded after the get solidifies. The agarose gel was polymerized for 30 minutes, and the electrophoresis chamber was filled with 1x TAE buffer. In the first well of each gel, 6 µL of the DNA Ladder was loaded and then in the rest of the wells. The samples were loaded containing 1x DNA loading buffer. The DNA ladder was used for determination of size and amount of the applied DNA fragment. 90-120 V was applied to the electrophoresis chamber for 30-45 minutes, causing the negatively charged DNA molecules to migrate in the electric field to the positive pole. For the visualization of the DNA, we placed the gel for 10-20 min in an ethidium bromide bath (50 µL EtBr in 150 mL ddH2O) under the hood. The dye

ethidium bromide (EtBr) intercalates into nucleic acids, changing its absorption spectrum, and the nucleic acids can be visualized through UV light.

8.2.8 DNA cloning

- StrataClone Blunt PCR Cloning Kit (Agilent Technologies, Böblingen)

The cloning was performed with the pSC-B-amp/kan vector (7.2.1) provided with the StrataClone Blunt PCR Cloning Kit. The StrataClone blunt PCR cloning vector mix contains two blunt-ended DNA arms, each charged with topoisomerase I on one end and carrying a loxP recognition sequence on the other end. This method enables the blunt-ended cDNA PCR products which were generated by PhusionTM DNA polymerase (8.2.4) to be ligated to these vector arms in a 5-minute ligation reaction by topoisomerase I-mediated strand ligation. The ligation was conducted following the instructions of the manufacturer, with the exception that only half of the recommended reaction mix was used per cloning attempt. The transformation of competent bacterial is described in 8.1.3.

8.2.9 Purification of plasmid DNA

- Nucleospin Plasmid Kit (Macherey-Nagel, Düren)

Plasmid DNA purification was performed using Nucleospin Plasmid Kit according to the manufacturer's instructions. We started the purification using 10 mL overnight culture from the respective bacterial transformant of interest. The isolated DNA was eluted in 50 µL ddH2O and the concentration of DNA was measured using Tecan infiniteM200 (Männedorf, Switzerland).

8.2.10 Preparative DNA gel electrophoresis and gel extraction

- NucleoSpin Gel and PCR Cleanup Kit (Macherey-Nagel, Düren)

When the amplified specific DNA fragment of interest was needed for cloning or sequencing it was excised with a scalpel on a UV table and therefore isolated from the gel. Afterwards, the purification of the DNA fragment from the gel

piece was done with the NucleoSpin Gel and PCR Cleanup Kit over a silica membrane according to the manufacturer. The concentration and purity of the isolated DNA was measured with the Tecan infiniteM200 (Männedorf, Switzerland).

8.2.11 Generation of a labeled, single-stranded antisense RNA probe

We designed RNA probes for spatial expression analysis (Table 7-3). Gel-purified PCR products of interest were used for probe preparation and individually cloned into the vector pSC-B-amp/kan (7.2.1). The vector pSC-B-amp/kan contains RNA polymerase promoter sites (T3 and T7 sites) from which the enzyme T7 or T3 RNA polymerase can start to synthesize single-stranded antisense RNA probes. To obtain an antisense RNA probe, the cDNA needed to be in 5'-3' orientation having the T7 or T3 promotor of the vector at its 3' end. The first step in the synthesis of the probes was linearizing of the vector and then incubation with RNA polymerase and nucleotides labelled with Digoxigenin for subsequent detection.

The protocol to linearize pSC-B-amp/kan was as follows:

- 1.2 µg vector with the transcript cDNA in pSC-B-amp/kan
- 1 µL EcoRV (10 U/µL, 2000 U) or 1.5 µL SmaI (10 U/µL, 2000 U) (Thermo Scientific)
- 2 µL Buffer R or Tango (Thermo Scientific)
- ddH2O to final volume of 20 µL

The mixture was incubated for 1.5 hrs. at 37 °C. Then the enzyme was inactivated for 30 min at 80°C. Afterwards the linearized vector was purified according to (8.2.9).

The protocol of the in vitro transcription for 20 µL:

- 1 µg linearized vector DNA
- 2 µL DIG-RNA labelling Mix, 10 x conc. (Roche)
- 4 µL Transcription buffer 5x (Thermo Scientific)
- 1 µL Ribolock RNase inhibitor (40 U/µL) (Thermo Scientific)

- 2 µL T7 (20 U/µL) or T3 (20 U/µL) RNA polymerase (Thermo Scientific)
- RNase free water to 20 µL

The mixture was incubated at 37 ˚C for 2 h. Then 2µL (2U) DNase I was added for 30 min at 37°C to digest the DNA. At the end, the RNA probes were purified using the RNeasy mini Kit (Qiagen) and quality control was done by non-denaturing agarose gel electrophoresis using the Gel Loading Buffer II (Ambion). The RNA probes were diluted 1:2 with hybridization buffer (See 8.3.1) and stored at -20 °C

8.2.12 DNA sequencing

To validate the sequence of the purified DNA molecules we sent them to GATC Biotech (Konstanz) who performed Sanger sequencing.

8.2.13 Isolation of bacterial genomic DNA

- TE buffer: 10 mM Tris-Cl (pH 8.0); 1mM EDTA (pH 8.0)
- Lysis buffer (10 mL): 9.34 mL TE buffer; 600 µL of 10% SDS; 60µl of 20 mg/mL proteinase K in 10 mM CaCl2; 5M sodium acetate in ddH2O (adjust pH with diluted acetic acid to 5.2)
- Phenol/Chloroform (1:1)

The genomic DNA from E. coli XL1-blue (7.2.1) was used as a competitor DNA for use in the telomeric hybridization protocols (See 8.3.1) as a blocking agent to reduce the non-specific binding of the hybridization probe. The DNA is typically used at a concentration of 250 µg/mL in the hybridization solutions. First E. coli XL1-blue was cultured in LB-medium (50 mL) (8.1.1.1). Then cultured bacteria were centrifuged at 3000 g for 10 min at 4 °C. The pellet was resuspended in 4 mL lysis buffer and incubated for 1 hr, at 37 °C. Afterwards, an equal volume of phenol/chloroform (1:1) was added until the phases were thoroughly mixed. The mixture was centrifuged at max speed for 5 min at room temperature. The upper aqueous phase (contain the DNA) was carefully transferred to a new tube using 1 mL pipette to avoid disturbing the interface and centrifuged for 10 min at 10000 g at 4°C. The aqueous phase was resuspended in 500 µL of 5M sodium acetate and mixed gently. To precipitate

the DNA, 2.5 or 3 volumes of cold 100 % ethanol (stored in -20 °C freezer) were added and gently mixed. The tubes were incubated for 30 min or overnight at -20 °C. After this step, the tubes were centrifuged at maximum speed for 5 min, and the DNA pellet was washed with 1 ml of 70% EtOH. After the washing step, the tubes were centrifuged at maximum speed for 2 min, and DNA pellet was air-dried. Finally, we resuspend the DNA in ddH2O and measure the concentration in Tecan infiniteM200.

8.2.14 Generation of Telomere probes

- Dig-ddUTP (Roche, Mannheim)
- terminal transferase (Tdt) (Thermo Scientific, Waltham, MA).
- Telo1 (TAACCC)7 and Telo2 (GGGTTA)7 (Sigma-Aldrich, Steinheim)
- Telomere-specific probes for Telo-FISH were generated by 3´-end-labeling of the two 42mer synthetic telomere oligonucleotides (each of the two oligonucleotides in a separate reaction).

The protocol for 20 µL was as follows:

- 100 pmol oligonucleotide (Telo1 or Telo2)
- 4 µL 5x TdT buffer
- 1 µL Dig-ddUTP (1 mM stock)
- 2 µL TdT enzyme
- Fill with ddH20 to 20 µL

The mixture was prepared on ice and then incubated at 37°C for 20 min to 1 hr. The labelled probes were store at -20 °C until use.

8.2.15 Dot-Blot

- membrane PVDF-Plus, 0.45 Micron, Catalog No PV4HY000GL
- anti-Digoxigenin-POD (Peroxidase) (Roche, Mannheim)
- 1xTBS: 150 mM NaCl, 10 mM Tris-HCl, pH 7.4
- TBS/BR: 0.5% Roche Blocking reagent (Roche, Mannheim), pH 7.4
- Western Lightning® Plus-ECL Enhanced Chemiluminescence Substrate (PerkinElmer,Waltham)

A dot-blot was performed to test the efficiency of the labelling with Dig-ddUTP for the synthesis of Telomere probes. First dilutions of labelled Telomere probes we prepare (5ng, 500pg, 50pg, 5pg, 500fg and 50fg) in water and 2 µL of each dilution was loaded on a membrane PVDF-Plus. The membrane was auto-cross-linked (12000 µJ x 100; UV-Stratalinker 1800) and then incubated for 30 min at 80 °C. Afterwards, the membrane was washed in 1x TBS for 5 min and blocked in 0.5% blocking reagent in TBS for 30 min. Following the blocking, the membrane was washed in TBS three times for 5 min, followed by incubation with anti-Digoxigenin-POD (Peroxidase) 1:1000 in 0.5 % blocking reagent in TBS for 1 h. Then the membrane was washed three times for 5 min, followed by detection on X-ray film. In a dark room, 1 mL of each Western Lightning Plus-ECL solution was mixed in a 2 mL tube, and the membrane was incubated for 1 min in the Lightning solution. Then the membrane was placed between plastics sheets in a box, and the X-ray film was set on top. After incubating for 3 min, the X-ray film was placed in the developer solution for 2 min. Finally, the X-ray film was washed in ddH2O and incubated in the fixation solution for 5 min.

8.3 Histochemistry

8.3.1 Whole mount in situ hybridization

Whole mount in situ hybridization (WMIH) is a technique that allows the detection and localization of specific RNA sequences in an entire tissue by the hybridization of a complementary nucleotide probe. The nucleotide probe in this study was synthesized based on the target mRNA of *Hydra vulgaris* AEP to examine the expression of meiotic genes in the hydra body (See 8.2.11). The synthesized probe contained digoxigenin (DIG) which can be detected by an antibody conjugated to alkaline phosphatase. The enzymatic activity of alkaline phosphatase results in the local generation of a coloured blue precipitate upon the addition of a chromogenic substrate. As a consequence, the localization of target mRNA can be visualized in the tissue by a coloured signal using light microscopy. This method of in situ hybridization was modified from Grens et al., (1996).

- Hydra medium (HM) (7.2.1)
- 2% (w/v) urethane in HM
- 4% formaldehyde in HM, pH 7.4
- PBS (140 mM NaCl; 2.6 mM KCl; 6.4 mM Na2HPO4; 1.4 mM KH2PO4; pH 7.4).
- 4% formaldehyde in PBS, pH 7.4
- PBST (0.1% (v/v) Tween 20 in 1x PBS)
- PBSTX (1 % (v/v) Triton X-100 in 1x PBS)
- Proteinase K (0.05 mg/mL) in PBST
- 2mg/mL glycine in PBST
- 20x SSC (3M NaCl; 300 mM trisodium citrate, pH 7.8)
- 2x SSC, pH 7.4
- 1M of triethanolamine
- Acetic anhydride (0.25% and 0.5 %)
- Hybridization buffer (50% Formamide; 25% 20x SSC; 0.1% Tween 20; 0.15 mg/mL Heparin; 5 mg/mL Torula RNA)
- digoxigenin-labeled probes (7.2.8)
- Maleic acid buffer (100 mM Maleic acid; 150 mM NaCl adjust to pH 7.5
- 1% Blocking reagent (Roche, Mannheim) in MAB
- Anti-DIG-AP-Fab fragment (150 U, 200µL) (Roche, Mannheim) (Table 7-1)
- NTM buffer: (100 mM NaCl, 100 mM Tris pH 9,5)
- 2% NBT/BCIP (Roche, Mannheim)
- 90% Glycerol/1XPBS
- Micro pestle (Hartenstein)

The protocol of the in-situ hybridization takes at least four days and consists of the following steps:

1. Fixation of the animals (day 1)
2. Permeabilization of the tissue and hybridization of the probe (day 2)
3. Probe detection (day 3)
4. Visualization (day 4)

About 50 hydras were starved for a few days before the experiment and kept at 18 ˚C. On the first day, the hydras were relaxed in 2% urethane for 1 min

and then fixed in 4% formaldehyde in HM at 4°C overnight. The next day (day 2), the hydras were places in 4 mL glass sample vials (Hartenstein) before proceeding to the permeabilization and hybridization steps. At room temperature, the hydras were washed in 100% ethanol for 10 min and then were rehydrated in a declining alcohol series (75 % EtOH / 25 % ddH2O, 50 % EtOH / 50 % PBS, 25 % EtOH / 75 % PBS) for 5 min each. The hydras were washed in PBST three times for 5 min to remove the ethanol. Subsequently, the tissue was permeabilized to increase the accessibility of the probe by digesting the proteins with proteinase K (0.05 mg/mL) for 20 min. To halt tissue digestion, the animals were incubated with 2 mg/mL glycine solution for 10 min. Then the hydras were incubated in 0.1 M of triethanolamine and acetic anhydride (0.25% and 0.5 % in 0.1 M triethanolamine) for 10 min each. This step is to prevent binding of the negatively charged RNA probe to positively charged amino groups of proteins in the samples and minimize background in the detection step. Afterwards, the samples were re-fixed with 4% formaldehyde for 1 h at room temperature followed by a series of three wash steps with PBST for 20 min. Subsequently, the hydras were washed with hybridization buffer at room temperature for 10 min and with pre-heated hybridization buffer at 57°C for 1 hr. Finally, during the last 10 min, the digoxigenin-labelled probes (See 8.2.11) were denatured in hybridization solution to a final concentration of 100 ng/mL and incubated for 20 hrs, at 57°C. During the time of hybridization, the anti-DIG-AP-Fab fragments were preabsorbed to reduce the excessive background. We collected ca. 20 hydras in 2 ml Eppendorf tube and washed them three times in 1x PBS. Then we homogenized the hydra tissue using a micro pestle and added 1 ml 1x PBS with 10 µl Anti-DIG-AP-Fab fragment (150 U, 200µL). The hydras homogenates were incubated overnight with the antibody on a shaker at 4°C at with continuous agitation. Afterwards, the samples were centrifuged at minimum velocity for 5 min to pellet the homogenized hydra tissue, and the supernatant was filtered using a 0.22 µm syringe filter membrane (VWR international). The filtered supernatant was added to the filtered 1xPBS to achieve 1:600 dilution and give an antibody working concentration of 7500-1500 mU/mL. The preabsorbed anti-DIG-AP-Fab fragments were stored at 4 °C.

On day 3 the samples were washed with pre-warmed (57°C) 100% hybridization solution, followed by 75% hybridization solution/25% 2x SSC 50% hybridization solution/50% 2x SSC and 25% hybridization solution/75% 2x SSC, all at 57 °C, for 10 min each. Then the hydras were blocked in 1% blocking reagent in MAB to saturate unspecific binding sites for 1 h at room temperature followed by the staining reaction with the preabsorbed 1:600 anti-Dig antibody coupled to alkaline phosphatase in 1X PBS, pH 7.5 at 4°C overnight. On day 4 the unbound antibody was washed out approximately 15 times, each for 20 min in 1X PBSTX. The detection of the signal was achieved by first equilibrating the animals with NTM buffer for 10 min at room temperature and then incubating in 2% NBT/BCIP in the dark. After reaching the optimal signal to background ratio, the reaction was stopped by washing the animals in ddH2O, followed by dehydration and mounting on microscopic slides in 90% glycerol/1XPBS. Digital images were acquired using a Leica EC3 digital camera incorporated into an Olympus SZ61 Zoom Stereo Microscope.

8.4 Microscopic techniques

8.4.1 Synthesis of specific antibodies

In the case of TERB1 and MAJIN, there were no commercial antibodies against the mouse proteins available; thus, we raised our own. We selected a suitable antigen using their protein sequences (TERB1, GenBank ID: NP_851289 and MAJIN GenBank ID: NP_001159391) (Table 7-1). CLC Genomic Workbench v7.0 software was used to select adequate antigenic polypeptides (10-20 residues) considering sequence and structural features such as hydrophilicity, accessibility and antigenic propensity. The corresponding peptides were used to immunize animals to produce polyclonal antibodies. The immunization was carried out by SeqLab (Götting) in a 2-month protocol 2-month protocol with three injections of the antigen at day 0, 21 and 49. Blood serum, which contains the polyclonal antibodies, was taken at day 35 (1st bleeding), 53 (2nd bleeding) and 60 (final bleeding) and forwarded by SeqLab.

8.4.2 Testis tissue dissection

- 1x PBS (140mM NaCl, 2.6mM KCl, 6.4mM Na2HPO4, 1.4mM KH2PO4, pH 7.4).

The testes were isolated by a cut across the lower abdomen of a mouse. Testes were then exposed by pulling out the fatty tissue. After separation from the fatty tissue and cutting off the epididymis, the testes were quickly rinsed in ice-cold PBS and further processed as needed.

8.4.3 Spreading spermatocytes from testicular seminiferous tubules

- PBS (8.4.2)
- 1% (w/v) paraformaldehyde (PFA), pH 9.2 + 0.15% (v/v) Triton X-100
- Hypotonic buffer: (30mM Tris-HCl; 17mM trisodium citrate; 5mM EDTA; 50mM sucrose; 5mM dithiothreitol, pH 8.2)
- 100 mM sucrose in ddH2O
- SuperFrost Plus slide (Thermo Scientific)

For the preparation of mice, meiotic chromosome spreads, we followed the protocol described by de Boer et al., (2009) with minor modifications. Wild type mice (7.1.1) (30 days old) were anaesthetized and euthanized with CO2. After the removal and decapsulation of mouse testes, seminiferous tubules were suspended in hypotonic buffer. After 30 min, the swollen tubules from the hypotonic buffer were transferred to a new slide into a drop of 100mM sucrose. The tubules were disrupted with two fine forceps until a cell suspension was achieved. Immediately, a SuperFrost Plus slide (Thermo Scientific) were dipped into the 1% (w/v) (PFA), pH 9.2, 0.15% (v/v) Triton X-100 solution. Excess solution was drained carefully by dripping it onto a tissue paper. The last droplet was finally kept in one corner of the slide, so the cell suspension was placed into this droplet. The suspension was dispersed over the entire slide by gently swinging the slide. The slides were then placed in a moist chamber where it was incubated with the lid closed for 2 hours, with the lid ajar for a further 1 h and finally with the lid completely removed until it was dry. Finally, the slide was wrapped in aluminium foil and could be stored at -80°C for a long period.

8.4.4 Immunofluorescence of spreading meiotic cells

- PBS (8.4.2)
- Blocking solution: 5% (w/v) milk, 5% (v/v) fetal calf serum (FCS) in PBS pH 7.4. Before use centrifuge at 16000 x g for 30 min and use only supernatant.
- Antibodies against protein of interest (Table 7-1)
- Hoechst stock solution: 5 µg 5 Hoechst 33258 (Roche) in ddH2O (working dilution: 1:333 in PBS)
- Mounting medium: 50% (v/v) glycerol; 50% (v/v) PBS

Slides of spread spermatocytes cells were washed in PBS (3x 5m min). After this washing step, the slides were covered with blocking solution in a moist chamber for at least 30 min. The primary antibodies were diluted in blocking solution and centrifuged at 16000 g and 4°C for 30 min. Subsequently, the antibody dilution was applied to the slide from which the blocking solution had been removed by tilting it, and a coverslip was placed on top to ensure equal dispersion of the antibody across the entire slide. The incubation of the primary antibodies was performed in a closed, moist chamber at room temperature for at least 1 hour. After the incubation step, samples were washed three times for 5 min in PBS. Before the incubation with the secondary antibodies, the slides were again incubated in blocking solution (5% (w/v) milk 5% (v/v) FCS in PBS, pH 7.4) in the moist chamber for 30 min. The secondary antibodies were diluted in blocking solution (1:200) and centrifuged at 16000 g and 4°C for 30 min as for the primary antibodies. The secondary antibody dilution was applied to the sample in the moist chamber for 30 min. Then the coverslips were removed, and a few drops of Hoechst 33258 working dilution 1:333 in PBS were added. After 10 min incubation, the slides were rewashed in PBS three times for 5 min and mounted with glycerol/PBS.

8.4.5 Immunofluorescence on meiotic cell suspension

- 1x PBS (7.4.2).
- 1% (w/v) paraformaldehyde in ddH2O
- 0.1 % (v/v) Triton X-100 in ddH2O
- nylon filter (Hartstein)

- Lab-Tek II chamber slide system (Nunc, Thermo Scientific)
- 0.01% poly-L-lysine in ddH2O
- Blocking solution: 5% (w/v) milk, 5% (v/v) fetal calf serum (FCS) in PBS pH 7.4. Before use centrifuge at 16000 g for 30 min and use only supernatant.
- Antibodies against protein of interest (Table 7-1)
- Hoechst stock solution: 5 µg 5 Hoechst 33258 (Roche) in ddH2O (working dilution: 1:333 in PBS)

For the preparation of meiotic cell suspension, we followed Alsehimer et al., (2005), with minor modifications. Wild type mouse strain C57BL/6J (30 days old) (7.1.1) were anaesthetized and euthanized with CO2. After the removal and decapsulation of mice testes, seminiferous tubules were disrupted with two razor blades until a cell suspension was achieved in cold 1x PBS. The suspension was filtered through a nylon filter (mesh size 25-30 µm) (Hartstein) and then centrifuged for 10 min at 500 g at 4 °C. Afterwards, the pellet was resuspended and incubated in 8 well Lab-Tek II chamber slide system (Nunc, Thermo Scientific) chambers for 1 h at room temperature. During this time, the cells could sink to the bottom of the chambers and adhere to the surface by previous treatment of the chambers with 0.01% poly-L-lysine in ddH2O for 1 h, at room temperature. The cells were fixed with 1% paraformaldehyde in ddH2O for 5 min at room temperature. Subsequently, the cells were permeabilized with 0.1% Triton-X100 solution, for 10 min at room temperature. Immediately the cells were blocked with 5% milk powder and 5% FCS in PBS (pH 7.4) for at least 30 min. The incubation of the primary antibodies was at room temperature for at least 1 h. After the incubation step, samples were washed (3x 5 min) in PBS. Before the incubation with the secondary antibodies, the slides were again incubated in blocking solution (5% milk powder and 5% FCS in PBS, pH 7.4) for 30 min. During the last 10 min of the secondary antibody incubation, a few drops of Hoechst 33258 working dilution 1:333 in PBS were added. Samples were again washed (3x 5 min) and incubated with PBS and stored at 4°C.

8.4.6 Telomere fluorescence in-situ hybridization (TeloFISH)

- 2x SCC: 0.3 M NaCl, 0.03 M Na-Citrate, pH 7.4

- Hybridization solution: 30 % (v/v) Formamide; 10% (v/w) Dextran Sulfate; 250 µg/mL E.coli DNA (7.2.10) in 2x SSC)
- TBS buffer:150 mM NaCl; 10 mM Tris-HCl pH 7.4
- TBS/BR: 0.5% blocking reagent, pH 7.4 (Roche, Mannheim)
- Telomeric probes (7.2.1.1)

The combined TeloFISH with immunofluorescence protocol for mouse spread preparations was performed according to Link et al., (2016), with minor modifications.
Firstly, testis cell spreads (8.4.3) were dehydrated in an alcohol series (70%, 85% and 100%) for 5 min each. In parallel, 6 µl of each labelled telomere probe reaction (8.2.14) was added to 80 µL pre-heated hybridization solution at 95 °C for 15 min. Right before hybridization, 40 µL of the pre-heated hybridization solution with the telomere probes was quickly pipetted onto the slides in a moisture chamber. Immediately, the moisture chamber was placed in a pre-heated (95 °C) oven and incubated for 20 min.
Subsequently, hybridization was performed at 37 °C overnight in a humid chamber. Then, slides were washed two times in 2× SSC at 37 °C for 10 min each and blocked with 0.5% blocking reagent (Roche, Mannheim, Germany) in TBS (150 mM NaCl, 10 mM Tris/HCl; pH 7.4). Samples were incubated with mouse anti-digoxigenin antibodies according to the manufacturer's protocol, and bound antibodies were detected with Alexa488 anti-mouse secondary antibodies (Table 7-1 and Table 7-2). Following the TeloFISH procedure, samples were prepared for immunofluorescence as described in (8.4.6).

8.4.7 Confocal laser scanning microscopy (CLSM)

The immunofluorescence preparations of mice spermatocyte cell spread were visualized and imaged on a Leica TCS-SP2 AOBS confocal laser scanning microscope (CLSM) (Leica, Bensheim). The microscope was equipped with a 63x/1.40 HCX PL APO oil-immersion objective and laser lines of 405 nm, 488 nm, 561 nm and 633 nm.

The images were scanned using Z-stacks at 800 Hz and 1024x1024 pixels for the best focal plane. In addition, 4-fold frame averaging was used to minimize background noise.

8.4.8 Structured illumination microscopy (SIM) and data processing

Intact mouse spermatocyte nuclei or cell spread from immunofluorescence preparation were imaged at high resolution in 2D and 3D with a SIM Zeiss Elyra S.1 (Carl Zeiss Microscopy GmbH). The microscope was equipped with a 63x/1.4 oil Plan-Apochromat DICM27 and 63x/1.2 W KorrM27 objective DICIII, X-cite (LED) illumination lamp; 405, 488, 592 and 647 nm lasers with 5 grid rotation and 5 shifts and a PCO Edge 5.5 sCMOS camera (Zeiss). Immersion oils ranging in refractive index from 1.33 (water) to 1.518 were used, depending on the objective and sample conditions analyzed.

Chromatic shifts introduced by different optical parts (dichroic and emission filters) along the z-axis were corrected using multicolour imaging of 200 nm TetraSpeck beads (Life Technologies, Catalog # T7280). The beads were placed on spread cells, or cell suspension samples were mounted at a dilution of 1:500 (v/v) in ethanol or ddH2O and left to completely dry until the samples were mounted, to ensure identical conditions of the oil and mounting medium. To acquire bead images, we made a Z-stack (interval=90nm, Z-range=3.5 µm) for each colour present in the sample of interest. The images were processed using ZEN 2012 software (Carl Zeiss Microscopy GmbH) algorithms for channel alignment. The created correction template (.bin file) was used in each image to compensate for any chromatic aberrations and offsets between channels in SIM.

The image acquisition was performed, adjusting for each sample the laser power, camera exposure time, and camera gain (if applicable) to fill a significant portion of the dynamic range of the camera. We avoided saturating any pixels and amplifying noise from non-specific staining and autofluorescence as much as possible. To prevent bleaching, the individual fluorochromes in the sample were imaged in succession from the longest to the shortest wavelength. Z-stacks of each image was performed using the following settings: Interval of 0.1 µm, Resolution in bits: 16 and Format in 1024x1024. After the acquisition,

we used the function 'Average in Frame' provided by the software ZEN 2012 (Carl Zeiss Microscopy GmbH) to minimize background noise. The image reconstruction was done using the software ZEN 2012 (Carl Zeiss Microscopy GmbH) based on the structured illumination algorithms developed by Heintzmann and Cremer (1999). The negative values were not discarded in the reconstruction process, to utilize the full dynamic range and 16-bit colour depth.

8.4.9 Intensity profile measurements of meiotic telomeres

The signal distribution of meiotic telomere proteins from immunofluorescence preparations of spermatocyte cell spread were analyzed in FIJI (Schindelin et al., 2012). Late pachytene-spermatocytes were selected by the marker pair XY chromosomes (Moses, 1980), and zygotene-like cells. For each image stack, maximum intensity projections were used for the analysis. In addition, the background was subtracted by measuring the average intensity in an ROI outside the sample area and subtracting this fixed intensity value from each in the image equally. Telomeres are orientated differently in space so to measure the intensity profile we drew an ROI of fixed length (1 µm) and width (10) along the last part of each telomere to follow its direction and perpendicular to the staining orientation. For each colour channel, the intensity along the selected ROI was recorded. Then the highest intensity value was used to assign the position of the peak along the line in µm. The distal along the axial axis between two protein signals were calculated as the separation distance between the maxima of their corresponding intensity peaks.

8.5 Bioinformatics

8.5.1 Homology search

To identify distantly homologous sequences of mouse TERB1, TERB2 and MAJIN protein sequences PSI-BLAST (Position-Specific Iterative Basic Local Alignment Search Tool) (Altschul et al., 1997) were performed using the NCBI server https://blast.ncbi.nlm.nih.gov/Blast.cgi

The advantage of PSI-BLAST is that it derives a position-specific scoring matrix (PSSM) or profile from the multiple sequence alignment of sequences detected

above a given score threshold using protein-protein BLAST. This PSSM is used to further search the database for new matches and is updated for subsequent iterations with these newly detected sequences.
PSI-BLAST was executed using the default parameters (expected threshold 10, word size 3, Gap cost Existence: 15 Extension: 2). The hits with better statistical significance than the threshold e-value 0.005 were used for the next PSI-BLAST iteration. Iterations were repeated for newly detected homologue sequences until the search converged. The sequences retrieved were used for reciprocal BLAST analyses to ensure that they represented putative homologs and not false positives.

8.5.2 Multiple sequence alignment

Multiple sequence alignments of putative homologs of mouse TERB1-TERB2-MAJIN candidates were performed with PROMALS3D web server (http://prodata.swmed.edu/promals3d/). PROMALS3D integrate advanced alignment techniques such as probabilistic consistency of profile–profile comparisons and predicted secondary and tertiary structures (Pei & Grishin, 2007; Pei et al., 2008). Available structures from the Protein Data Bank (PDB) (Berman et al., 2003) for TERB1 (PDBI: 1x58_chainA and 6j07_chainB), TERB2 (6j07_chainA) and MAJIN (6j08_chainA) were uploaded in PROMALS3D. The resulting multiple sequence alignments were annotation using ESPript3 (Robert & Gouet 2014). In order to predict functional motifs or functional domains we scanned the sequences through the Eukaryotic Linear Motif (ELM) (http://elm.eu.org/index.html) (Dinkel et al., 2016) and Superfamily web server (http://supfam.org/) (Gough et al., 2001) respectively.

8.5.3 Phylogenetic tree construction

To estimate the relationship between the sequences and their hypothetical common ancestor, we built a phylogenetic tree. The phylogenetic tree was constructed based on a taxonomically balanced subset of homologous sequences which represent a wide range of animal phyla. First, the multiple sequence alignment was performed using MAFFT v.7.309 (Katoh & Standley, 2013) with the iterative accurate option L-INS-I. Then, the resulting multiple

alignments were trimmed to include only the regions that suited for phylogenetic inference with BMGE ("Block Mapping and Gathering with Entropy" software) v.1.12 (option -m BLOSUME45) (Criscuolo & Gribaldo, 2010). This step edits the unambiguously aligned regions and inserts or deletes gaps to more accurately reflect the probable evolutionary process that leads to divergence between the sequences. Subsequently, MrBayes v.3.2.6 (Ronquist et al., 2012) was used to compute Bayesian trees with a mixed model of amino acid substitution, including a gamma distribution (4 discrete categories). The gamma distribution assigns a substitution probability to sites (e.g. the third codon position tends to be much more variable). Also, MrBayes was run with four chains for 1 million generations, and trees were sampled every 100 generations. To construct the consensus tree, the first 2,000 trees were discarded as "burn-in". The robustness of the tree nodes was assessed with Bayesian posterior probabilities (BPP > 70). The final trees were drawn with iToL v4 (Letunic & Bork, 2019).

8.5.4 Protein structure homology modeling

Homology modelling of hydra MAJIN proteins was performed with the SWISS-MODEL program (https://swissmodel.expasy.org/) (Biasini et al., 2014) using human N-terminal MAJIN (Swiss-Prot id: Q9D992 1-112 aa.; PDB id: 6gny) as a template. The model quality is estimated using the scoring function QMEAN, based on different geometrical properties. It provides both global (i.e. for the entire structure) and local (i.e. per residue) absolute quality estimates. The QMEAN Z-score indicates if the QMEAN score of the model is comparable to what one would expect from experimental structures of similar size. QMEAN Z-scores around 0 indicates good agreement between the model structure and experimental structure of similar size. Scores of -4 or below are an indication of models with low quality. The model .pdb file was retrieved and visualized in Chimera v1.13.1 (Pettersen et al., 2004).

Chapter 9 Bibliography

Abbe, E. (1873). Beiträge zur Theorie des Mikroskops und der mikroskopischen Wahrnehmung. Archiv für mikroskopische Anatomie, 9(1), 413-418.

Agarwal, S., & Roeder, G. S. (2000). Zip3 provides a link between recombination enzymes and synaptonemal complex proteins. Cell, 102(2), 245-255.

Alberts, B., Johnson, A., Lewis, J., Raff, M., Roberts, K., & Walter, P. Molecular Biology of the Cell 4th edition,(2002). Garland Science New York.

Alleva, B., & Smolikove, S. (2017). Moving and stopping: Regulation of chromosome movement to promote meiotic chromosome pairing and synapsis. Nucleus, 8(6), 613-624.

Alsheimer, M. (2009). The dance floor of meiosis: evolutionary conservation of nuclear envelope attachment and dynamics of meiotic telomeres. In Meiosis (Vol. 5, pp. 81-93). Karger Publishers.

Alsheimer, M., Drewes, T., Schütz, W., & Benavente, R. (2005). The cancer/testis antigen CAGE-1 is a component of the acrosome of spermatids and spermatozoa. European journal of cell biology, 84(2-3), 445-452.

Alsheimer, M., & Benavente, R. (1996). Change of karyoskeleton during mammalian spermatogenesis: expression pattern of nuclear lamin C2 and its regulation. Experimental cell research, 228(2), 181-188.

Alsheimer, M., Fecher, E., & Benavente, R. (1998). Nuclear envelope remodelling during rat spermiogenesis: distribution and expression pattern of LAP2/thymopoietins. Journal of Cell Science, 111(15), 2227-2234.

Alsheimer, M., von Glasenapp, E., Hock, R., & Benavente, R. (1999). Architecture of the nuclear periphery of rat pachytene spermatocytes: distribution of nuclear envelope proteins in relation to synaptonemal complex attachment sites. Molecular biology of the cell, 10(4), 1235-1245.

Altschul, S. F., Madden, T. L., Schäffer, A. A., Zhang, J., Zhang, Z., Miller, W., & Lipman, D. J. (1997). Gapped BLAST and PSI-BLAST: a new generation of protein database search programs. Nucleic acids research, 25(17), 3389-3402.

Ashley, T. (2007). Synaptic and recombination nodules in mammals: structural continuity with shifting protein composition. In Recombination and Meiosis (pp. 153-194). Springer, Berlin, Heidelberg.

Plug, A. W., Peters, A. H., Keegan, K. S., Hoekstra, M. F., de Boer, P., & Ashley, T. (1998). Changes in protein composition of meiotic nodules during mammalian meiosis. Journal of Cell Science, 111(4), 413-423.

Bass HW, Marshall WF, Sedat JW, Agard DA and Cande WZ (1997) Telomere cluster de novo before the initiation of synapsis: a three-dimensional spatial analysis of telomere positions before and during meiotic prophase. J Cell Biol, 137, 5–18.

Berman, H., Henrick, K., & Nakamura, H. (2003). Announcing the worldwide protein data bank. Nature Structural & Molecular Biology, 10(12), 980.

Bhalla, N., & Dernburg, A. F. (2008). Prelude to a division. Annual review of cell and developmental biology, 24, 397-424.

Bianchi, A., Smith, S., Chong, L., Elias, P., & De Lange, T. (1997). TRF1 is a dimer and bends telomeric DNA. The EMBO journal, 16(7), 1785-1794.

Biasini, M., Bienert, S., Waterhouse, A., Arnold, K., Studer, G., Schmidt, T., Kiefer, F., Cassarino, T. G., Bertoni, M., Bordoli, L., & Schwede, T. (2014). SWISS-MODEL: modelling protein tertiary and quaternary structure using evolutionary information. Nucleic acids research, 42(W1), W252-W258.

Bilaud, T., Koering, C. E., Binet-Brasselet, E., Ancelin, K., Pollice, A., Gasser, S. M., & Gilson, E. (1996). The telobox, a Myb-related telomeric DNA binding motif found in proteins from yeast, plants and human. Nucleic acids research, 24(7), 1294-1303.

Blokhina, Y. P., Nguyen, A. D., Draper, B. W., & Burgess, S. M. (2019). The telomere bouquet is a hub where meiotic double-strand breaks, synapsis, and stable homolog juxtaposition are coordinated in the zebrafish, Danio rerio. PLoS genetics, 15(1), e1007730.

Broccoli, D., Smogorzewska, A., Chong, L. and de Lange, T. (1997) Human telomeres contain two distinct Myb-related proteins, TRF1 and TRF2. Nat. Genet., 17, 231–235.

Carlton, P. M., & Cande, W. Z. (2002). Telomeres act autonomously in maize to organize the meiotic bouquet from a semipolarized chromosome orientation. The Journal of cell biology, 157(2), 231-242.

Cavalier-Smith, T. (2010). Origin of the cell nucleus, mitosis and sex: roles of intracellular coevolution. Biology direct, 5(1), 7.

Chen, F., Tillberg, P. W. and Boyden, E. S. (2015). Optical imaging. Expansion microscopy. Science 347, 543-8.

Chen, Y., Yang, Y., van Overbeek, M., Donigian, J. R., Baciu, P., de Lange, T., & Lei, M. (2008). A shared docking motif in TRF1 and TRF2 used for differential recruitment of telomeric proteins. Science, 319(5866), 1092-1096.

Cheung, I., Schertzer, M., Rose, A., & Lansdorp, P. M. (2006). High incidence of rapid telomere loss in telomerase-deficient Caenorhabditis elegans. Nucleic acids research, 34(1), 96-103.

Chikashige, Y., & Hiraoka, Y. (2001). Telomere binding of the Rap1 protein is required for meiosis in fission yeast. Current Biology, 11(20), 1618-1623.

Chikashige, Y., Ding, D. Q., Funabiki, H., Haraguchi, T., Mashiko, S., Yanagida, M., & Hiraoka, Y. (1994). Telomere-led premeiotic chromosome movement in fission yeast. Science, 264(5156), 270-273.

Chikashige, Y., Haraguchi, T., & Hiraoka, Y. (2007). Another way to move chromosomes. Chromosoma, 116(6), 497-505.

Chikashige, Y., Tsutsumi, C., Yamane, M., Okamasa, K., Haraguchi, T., & Hiraoka, Y. (2006). Meiotic proteins bqt1 and bqt2 tether telomeres to form the bouquet arrangement of chromosomes. Cell, 125(1), 59-69.

Chikashige, Y., Yamane, M., Okamasa, K., Tsutsumi, C., Kojidani, T., Sato, M., Haraguchi, T., & Hiraoka, Y. (2009). Membrane proteins Bqt3 and-4 anchor telomeres to the nuclear envelope to ensure chromosomal bouquet formation. The Journal of cell biology, 187(3), 413-427.

Conrad, M. N., Dominguez, A. M., & Dresser, M. E. (1997). Ndj1p, a meiotic telomere protein required for normal chromosome synapsis and segregation in yeast. Science, 276(5316), 1252-1255.

Conrad, M. N., Lee, C. Y., Chao, G., Shinohara, M., Kosaka, H., Shinohara, A., Conchello, J. A., & Dresser, M. E. (2008). Rapid telomere movement in meiotic prophase is promoted by NDJ1, MPS3, and CSM4 and is modulated by recombination. Cell, 133(7), 1175-1187.

Conrad, M. N., Lee, C. Y., Wilkerson, J. L., & Dresser, M. E. (2007). MPS3 mediates meiotic bouquet formation in Saccharomyces cerevisiae. Proceedings of the National Academy of Sciences, 104(21), 8863-8868.

Cooper, J. P., Watanabe, Y., & Nurse, P. (1998). Fission yeast Taz1 protein is required for meiotic telomere clustering and recombination. Nature, 392(6678), 828.

Costa, Y., Speed, R., Öllinger, R., Alsheimer, M., Semple, C. A., Gautier, P., Maratou, K., Novak, I., Höög, C., Benavente, R., & Cooke, H. J. (2005). Two novel

proteins recruited by synaptonemal complex protein 1 (SYCP1) are at the centre of meiosis. Journal of cell science, 118(12), 2755-2762.

Court, R., Chapman, L., Fairall, L., Rhodes, D. (2005). How the human telomeric proteins TRF1 and TRF2 recognize telomeric DNA: a view from high-resolution crystal structures. EMBO Rep, 6(1), 39-45.

Cowan, C.R., Carlton, P.M., and Cande, W.Z. (2001). The polar arrangement of telomeres in interphase and meiosis. Rabl organization and the bouquet. Plant Physiol. 125, 532–538.

Criscuolo, A., & Gribaldo, S. (2010). BMGE (Block Mapping and Gathering with Entropy): a new software for selection of phylogenetic informative regions from multiple sequence alignments. BMC evolutionary biology, 10(1), 210.

Crisp, M., Liu, Q., Roux, K., Rattner, J. B., Shanahan, C., Burke, B., Stahl, P.D., & Hodzic, D. (2006). Coupling of the nucleus and cytoplasm: role of the LINC complex. J Cell Biol, 172(1), 41-53.

Daniel, K., Tränkner, D., Wojtasz, L., Shibuya, H., Watanabe, Y., Alsheimer, M., & Tóth, A. (2014). Mouse CCDC79 (TERB1) is a meiosis-specific telomere associated protein. BMC cell biology, 15(1), 17.

de Boer, E., Lhuissier, F. G., & Heyting, C. (2009). Cytological analysis of interference in mouse meiosis. In Meiosis (pp. 355-382). Humana Press, Totowa, NJ.

de Lange, T. (2005). Shelterin: the protein complex that shapes and safeguards human telomeres. Genes & development, 19(18), 2100-2110.

Dehal, P., & Boore, J. L. (2005). Two rounds of whole genome duplication in the ancestral vertebrate. PLoS biology, 3(10), e314.

Dernburg, A. F., McDonald, K., Moulder, G., Barstead, R., Dresser, M., & Villeneuve, A. M. (1998). Meiotic recombination in *C. elegans* initiates by a conserved mechanism and is dispensable for homologous chromosome synapsis. Cell, 94(3), 387-398.

Ding, D. Q., Yamamoto, A., Haraguchi, T., & Hiraoka, Y. (2004). Dynamics of homologous chromosome pairing during meiotic prophase in fission yeast. Developmental cell, 6(3), 329-341.

Ding, X., Xu, R., Yu, J., Xu, T., Zhuang, Y., & Han, M. (2007). SUN1 is required for telomere attachment to nuclear envelope and gametogenesis in mice. Developmental cell, 12(6), 863-872.

Dinkel, H., Van Roey, K., Michael, S., Kumar, M., Uyar, B., Altenberg, B., Milchevskaya, V., Schneider, M., Kühn, H., Behrendt, A., Dahl, S. L., Damerell, V., Diebel, S., Kalman, S., Klein, S., Knudsen, A. C., Mäder, C., Merrill, S., Staudt, A., Thiel, V., Welti, L., Davey, N. E., Diella F., & Dahl, S. L. (2015). ELM 2016—data update and new functionality of the eukaryotic linear motif resource. Nucleic acids research, 44(D1), D294-D300.

Dunce, J. M., Milburn, A. E., Gurusaran, M., da Cruz, I., Sen, L. T., Benavente, R., & Davies, O. R. (2018). Structural basis of meiotic telomere attachment to the nuclear envelope by MAJIN-TERB2-TERB1. Nature communications, 9(1), 5355.

Esponda, P., & Gimenez-Martin, G. (1972). The attachment of the synaptonemal complex to the nuclear envelope. Chromosoma, 38(4), 405-417.

Ferreira, M. G., & Cooper, J. P. (2001). The fission yeast Taz1 protein protects chromosomes from Ku-dependent end-to-end fusions. Molecular cell, 7(1), 55-63.

Förstemann, K., & Lingner, J. (2001). Molecular basis for telomere repeat divergence in budding yeast. Molecular and cellular biology, 21(21), 7277-7286.

Franklin, A. E., McElver, J., Sunjevaric, I., Rothstein, R., Bowen, B., & Cande, W. Z. (1999). Three-dimensional microscopy of the Rad51 recombination protein during meiotic prophase. The Plant Cell, 11(5), 809-824.

Fraune, J., Brochier-Armanet, C., Alsheimer, M., & Benavente, R. (2013). Phylogenies of central element proteins reveal the dynamic evolutionary history of the mammalian synaptonemal complex: ancient and recent components. Genetics, 195(3), 781-793.

Fraune, J., Schramm, S., Alsheimer, M., & Benavente, R. (2012). The mammalian synaptonemal complex: protein components, assembly and role in meiotic recombination. Experimental cell research, 318(12), 1340-1346.

Frohnert, C., Schweizer, S., & Hoyer-Fender, S. (2010). SPAG4L/SPAG4L-2 are testis-specific SUN domain proteins restricted to the apical nuclear envelope of round spermatids facing the acrosome. Molecular human reproduction, 17(4), 207-218.

Furukawa, K., Inagaki, H., & Hotta, Y. (1994). Identification and cloning of an mRNA coding for a germ cell-specific A-type lamin in mice. Experimental cell research, 212(2), 426-430.

Göb, E., Schmitt, J., Benavente, R., & Alsheimer, M. (2010). Mammalian sperm head formation involves different polarization of two novel LINC complexes. PloS one, 5(8), e12072.

Goldman, A. S., & Lichten, M. (2000). Restriction of ectopic recombination by interhomolog interactions during Saccharomyces cerevisiae meiosis. Proceedings of the National Academy of Sciences, 97(17), 9537-9542.

Goldstein, P., & Slaton, D. E. (1982). The synaptonemal complexes of Caenorhabditis elegans. Chromosoma, 84(4), 585-597.

Gomes, N. M., Ryder, O. A., Houck, M. L., Charter, S. J., Walker, W., Forsyth, N. R., Austad S. N., Venditt, C., Pagel, M. Shay, J. W. & Wright, W. E. (2011). Comparative biology of mammalian telomeres: hypotheses on ancestral states and the roles of telomeres in longevity determination. Aging cell, 10(5), 761-768.

Gough, J., Karplus, K., Hughey, R., & Chothia, C. (2001). Assignment of homology to genome sequences using a library of hidden Markov models that represent all proteins of known structure. Journal of molecular biology, 313(4), 903-919.

Graumann, K., Runions, J., & Evans, D. E. (2010). Characterization of SUN-domain proteins at the higher plant nuclear envelope. The Plant Journal, 61(1), 134-144.

Grens, A., Gee, L., Fisher, D. A., & Bode, H. R. (1996). CnNK-2, an NK-2 homeobox gene, has a role in patterning the basal end of the axis in hydra. Developmental biology, 180(2), 473-488.

Gustafsson, M. G., Shao, L., Carlton, P. M., Wang, C. R., Golubovskaya, I. N., Cande, W. Z., Agard, D. A., & Sedat, J. W. (2008). Three-dimensional resolution doubling in wide-field fluorescence microscopy by structured illumination. Biophysical journal, 94(12), 4957-4970.

Hanaoka, S., Nagadoi, A., & Nishimura, Y. (2005). Comparison between TRF2 and TRF1 of their telomeric DNA-bound structures and DNA-binding activities. Protein science, 14(1), 119-130.

Hamer, G., Gell, K., Kouznetsova, A., Novak, I., Benavente, R., & Höög, C. (2006). Characterization of a novel meiosis-specific protein within the central element of the synaptonemal complex. Journal of cell science, 119(19), 4025-4032.

Harper, L., Golubovskaya, I., & Cande, W. Z. (2004). A bouquet of chromosomes. Journal of Cell Science, 117(18), 4025-4032.

Heintzmann, R., & Cremer, C. G. (1999, January). Laterally modulated excitation microscopy: improvement of resolution by using a diffraction grating. In Optical Biopsies and Microscopic Techniques III (Vol. 3568, pp. 185-196). International Society for Optics and Photonics.

Hemmrich, G., Anokhin, B., Zacharias, H., & Bosch, T. C. (2007). Molecular phylogenetics in Hydra, a classical model in evolutionary developmental biology. Molecular phylogenetics and evolution, 44(1), 281-290.

Herman, R. K., & Kari, C. K. (1989). Recombination between small X chromosome duplications and the X chromosome in Caenorhabditis elegans. Genetics, 121(4), 723-737.

Heyting, C. (2005). Meiotic transverse filament proteins: essential for crossing over. Transgenic research, 14(5), 547-550.

Hiraoka, Y., Henderson, E., & Blackburn, E. H. (1998). Not so peculiar: fission yeast telomere repeats. Trends in biochemical sciences, 23(4), 126.

Hu, C., Inoue, H., Sun, W., Takeshita, Y., Huang, Y., Xu, Y., Kanoh, J., & Chen, Y. (2018). Structural insights into chromosome attachment to the nuclear envelope by an inner nuclear membrane protein Bqt4 in fission yeast. Nucleic acids research, 47(3), 1573-1584.

Hu, C., Inoue, H., Sun, W., Takeshita, Y., Huang, Y., Xu, Y., Kanoh, J., & Chen, Y. (2019). The Inner Nuclear Membrane Protein Bqt4 in Fission Yeast Contains a DNA-Binding Domain Essential for Telomere Association with the Nuclear Envelope. Structure, 27(2), 335-343.

Hunter, N. (2003). Synaptonemal complexities and commonalities. Molecular cell, 12(3), 533-535.

Ishikawa, F., & Naito, T. (1999). Telomeres and sexual reproduction. Protein, nucleic acid, enzyme, 44(12 Suppl), 1674.

Iyer, L. M., Koonin, E. V., & Aravind, L. (2002). Extensive domain shuffling in transcription regulators of DNA viruses and implications for the origin of fungal APSES transcription factors. Genome biology, 3(3), research0012-1.

Jaspersen, S. L., Martin, A. E., Glazko, G., Giddings, T. H., Morgan, G., Mushegian, A., & Winey, M. (2006). The Sad1-UNC-84 homology domain in Mps3 interacts with Mps2 to connect the spindle pole body with the nuclear envelope. The Journal of cell biology, 174(5), 665-675.

Jones, G. H. (1978). Giemsa C-banding of rye meiotic chromosomes and the nature of "terminal" chiasmata. Chromosoma, 66(1), 45-57.

Kanoh, J., & Ishikawa, F. (2001). spRap1 and spRif1, recruited to telomeres by Taz1, are essential for telomere function in fission yeast. Current Biology, 11(20), 1624-1630.

Katoh, K., & Standley, D. M. (2013). MAFFT multiple sequence alignment software version 7: improvements in performance and usability. Molecular biology and evolution, 30(4), 772-780.

Keeney, S. (2001). Mechanism and control of meiotic recombination initiation. Curr Top Dev Biol, 52, 1-53.

Keeney, S., Giroux, C. N., & Kleckner, N. (1997). Meiosis-specific DNA double-strand breaks are catalyzed by Spo11, a member of a widely conserved protein family. Cell, 88(3), 375-384.

King, M. C., Drivas, T. G., & Blobel, G. (2008). A network of nuclear envelope membrane proteins linking centromeres to microtubules. Cell, 134(3), 427-438.

Kleckner, N., & Weiner, B. M. (1993). Potential advantages of unstable interactions for pairing of chromosomes in meiotic, somatic, and premeiotic cells. In Cold Spring Harbor Symposia on Quantitative Biology, 58, 553-565.

Kleckner, N., Zhang, L., Weiner, B., & Zickler, D. (2011). Meiotic chromosome dynamics. Genome Organization and Function in the Cell Nucleus, 487-533.

Klutstein, M., & Cooper, J. P. (2014). The chromosomal courtship dance—homolog pairing in early meiosis. Current opinion in cell biology, 26, 123-131.

Kortschak, R. D., Samuel, G., Saint, R., & Miller, D. J. (2003). EST analysis of the cnidarian Acropora millepora reveals extensive gene loss and rapid sequence divergence in the model invertebrates. Current Biology, 13(24), 2190-2195.

Kosaka, H., Shinohara, M., & Shinohara, A. (2008). Csm4-dependent telomere movement on nuclear envelope promotes meiotic recombination. PLoS genetics, 4(9), e1000196.

Koszul, R., & Kleckner, N. (2009). Dynamic chromosome movements during meiosis: a way to eliminate unwanted connections?. Trends in cell biology, 19(12), 716-724.

Koszul, R., Kim, K. P., Prentiss, M., Kleckner, N., & Kameoka, S. (2008). Meiotic chromosomes move by linkage to dynamic actin cables with transduction of force through the nuclear envelope. Cell, 133(7), 1188-1201.

Kracklauer, M. P., Link, J., & Alsheimer, M. (2013). LINCing the nuclear envelope to gametogenesis. In Current topics in developmental biology (Vol. 102, pp. 127-157). Academic Press.

Kuznetsov, S., Lyanguzowa, M., & Bosch, T. C. (2001). Role of epithelial cells and programmed cell death in Hydra spermatogenesis. Zoology, 104(1), 25-31.

Lammers, J. H., Offenberg, H. H., Van Aalderen, M., Vink, A. C., Dietrich, A. J., & Heyting, C. (1994). The gene encoding a major component of the lateral elements of synaptonemal complexes of the rat is related to X-linked lymphocyte-regulated genes. Molecular and cellular biology, 14(2), 1137-1146.

Langhorst, M. F., Schaffer, J., & Goetze, B. (2009). Structure brings clarity: structured illumination microscopy in cell biology. Biotechnology Journal: Healthcare Nutrition Technology, 4(6), 858-865.

Letunic, I., & Bork, P. (2006). Interactive Tree Of Life (iTOL): an online tool for phylogenetic tree display and annotation. Bioinformatics, 23(1), 127-128.

Lenhoff, H. M., & Brown, R. D. (1970). Mass culture of hydra: an improved method and its application to other aquatic invertebrates. Laboratory Animals, 4(1), 139-154.

Li, B., Oestreich, S., & De Lange, T. (2000). Identification of human Rap1: implications for telomere evolution. Cell, 101(5), 471-483.

Liebe, B., Alsheimer, M., Hoog, C., Benavente, R., & Scherthan, H. (2004). Telomere attachment, meiotic chromosome condensation, pairing, and bouquet stage duration are modified in spermatocytes lacking axial elements. Molecular biology of the cell, 15(2), 827-837.

Lin, F., & Worman, H. J. (1993). Structural organization of the human gene encoding nuclear lamin A and nuclear lamin C. Journal of Biological Chemistry, 268(22), 16321-16326.

Link, J., & Jantsch, V. (2019). Meiotic chromosomes in motion: a perspective from Mus musculus and Caenorhabditis elegans. Chromosoma, 1-14.

Link, J., Benavente, R., & Alsheimer, M. (2016). Analysis of meiotic telomere behavior in the mouse. In The Nuclear Envelope (pp. 195-208). Humana Press, New York, NY.

Link, J., Jahn, D., Schmitt, J., Göb, E., Baar, J., Ortega, S., Benavente, R. & Alsheimer, M. (2013). The meiotic nuclear lamina regulates chromosome dynamics and promotes efficient homologous recombination in the mouse. PLoS genetics, 9(1).

Link, J., Jahn, D., & Alsheimer, M. (2015). Structural and functional adaptations of the mammalian nuclear envelope to meet the meiotic requirements. Nucleus, 6(2), 93-101.

Long, J., Huang, C., Chen, Y., Zhang, Y., Shi, S., Wu, L., & Lei, M. (2017). Telomeric TERB1–TRF1 interaction is crucial for male meiosis. Nature structural & molecular biology, 24(12), 1073.

Lundblad, V., & Szostak, J. W. (1989). A mutant with a defect in telomere elongation leads to senescence in yeast. Cell, 57(4), 633-643.

MacQueen, A. J., Phillips, C. M., Bhalla, N., Weiser, P., Villeneuve, A. M., & Dernburg, A. F. (2005). Chromosome sites play dual roles to establish homologous synapsis during meiosis in C. elegans. Cell, 123(6), 1037-1050.

Malik, H. S., Burke, W. D., & Eickbush, T. H. (2000). Putative telomerase catalytic subunits from Giardia lamblia and Caenorhabditis elegans. Gene, 251(2), 101-108.

Malone, C. J., Misner, L., Le Bot, N., Tsai, M. C., Campbell, J. M., Ahringer, J., & White, J. G. (2003). The C. elegans hook protein, ZYG-12, mediates the essential attachment between the centrosome and nucleus. Cell, 115(7), 825-836.

Marcand, S., Gilson, E., & Shore, D. (1997a). A protein-counting mechanism for telomere length regulation in yeast. Science, 275(5302), 986-990.

Marcand, S., Wotton, D., Gilson, E., & Shore, D. (1997b). Rap1p and telomere length regulation in yeast. In Ciba Found. Symp (Vol. 211, pp. 76-93).

McEachern, M. J., Krauskopf, A., & Blackburn, E. H. (2000). Telomeres and their control. Annual review of genetics, 34(1), 331-358.

Meier, B., Clejan, I., Liu, Y., Lowden, M., Gartner, A., Hodgkin, J., & Ahmed, S. (2006). trt-1 is the Caenorhabditis elegans catalytic subunit of telomerase. PLoS genetics, 2(2), e18.

Méjat, A., & Misteli, T. (2010). LINC complexes in health and disease. Nucleus, 1(1), 40-52.

Mekhail, K., & Moazed, D. (2010). The nuclear envelope in genome organization, expression and stability. Nature Reviews Molecular Cell Biology, 11(5), 317.

Meuwissen, R. L., Offenberg, H. H., Dietrich, A. J., Riesewijk, A., van Iersel, M., & Heyting, C. (1992). A coiled-coil related protein specific for synapsed regions of meiotic prophase chromosomes. The EMBO journal, 11(13), 5091-5100.

Meyer, A., & Zardoya, R. (2003). Recent advances in the (molecular) phylogeny of vertebrates. Annual Review of Ecology, Evolution, and Systematics, 34(1), 311-338.

Miki, F., Kurabayashi, A., Tange, Y., Okazaki, K., Shimanuki, M., & Niwa, O. (2004). Two-hybrid search for proteins that interact with Sad1 and Kms1, two membrane-

bound components of the spindle pole body in fission yeast. Molecular Genetics and Genomics, 270(6), 449-461.

Moens, P. B., Kolas, N. K., Tarsounas, M., Marcon, E., Cohen, P. E., & Spyropoulos, B. (2002). The time course and chromosomal localization of recombination-related proteins at meiosis in the mouse are compatible with models that can resolve the early DNA-DNA interactions without reciprocal recombination. Journal of cell science, 115(8), 1611-1622.

Morimoto, A., Shibuya, H., Zhu, X., Kim, J., Ishiguro, K. I., Han, M., & Watanabe, Y. (2012). A conserved KASH domain protein associates with telomeres, SUN1, and dynactin during mammalian meiosis. J Cell Biol, 198(2), 165-172.

Moses, M. J. (1956). Chromosomal structures in crayfish spermatocytes. The Journal of biophysical and biochemical cytology, 2(2), 215.

Moses, M. J. (1980). New cytogenetic studies on mammalian meiosis. Animal models in human reproduction. Raven Press, New York Y. 169, 190.

Moyzis, R. K., Buckingham, J. M., Cram, L. S., Dani, M., Deaven, L. L., Jones, M. D., Meyne, J., Ratliff, R. L., & Wu, J. R. (1988). A highly conserved repetitive DNA sequence, (TTAGGG) n, present at the telomeres of human chromosomes. Proceedings of the National Academy of Sciences, 85(18), 6622-6626.

Murphy, S. P., Gumber, H. K., Mao, Y., & Bass, H. W. (2014). A dynamic meiotic SUN belt includes the zygotene-stage telomere bouquet and is disrupted in chromosome segregation mutants of maize (Zea mays L.). Frontiers in plant science, 5, 314.

Naito, T., Matsuura, A., & Ishikawa, F. (1998). Circular chromosome formation in a fission yeast mutant defective in two ATM homologues. Nature genetics, 20(2), 203.

Nakamura, T. M., Cooper, J. P., & Cech, T. R. (1998). Two modes of survival of fission yeast without telomerase. Science, 282(5388), 493-496.

Nimmo, E. R., Pidoux, A. L., Perry, P. E., & Allshire, R. C. (1998). Defective meiosis in telomere-silencing mutants of Schizosaccharomyces pombe. Nature, 392(6678), 825.

Niwa, O., Shimanuki, M. and Miki, F. (2000). Telomere-led bouquet formation facilitates homologous chromosome pairing and restricts ectopic interaction in fission yeast meiosis. EMBO J. 19, 3831-3840.

Offenberg, H. H., Schalk, J. A., Meuwissen, R. L., van Aalderen, M., Kester, H. A., Dietrich, A. J., & Heyting, C. (1998). SCP2: a major protein component of the axial

elements of synaptonemal complexes of the rat. Nucleic acids research, 26(11), 2572-2579.

Palm, W., & de Lange, T. (2008). How shelterin protects mammalian telomeres. Annual review of genetics, 42, 301-334.

Pawlowski, W. P., Golubovskaya, I. N., & Cande, W. Z. (2003). Altered nuclear distribution of recombination protein RAD51 in maize mutants suggests the involvement of RAD51 in meiotic homology recognition. The Plant Cell, 15(8), 1807-1816.

Pei, J., & Grishin, N. V. (2007). PROMALS: towards accurate multiple sequence alignments of distantly related proteins. Bioinformatics, 23(7), 802-808.

Pei, J., Kim, B. H., & Grishin, N. V. (2008). PROMALS3D: a tool for multiple protein sequence and structure alignments. Nucleic acids research, 36(7), 2295-2300.

Pendlebury, D. F., Fujiwara, Y., Tesmer, V. M., Smith, E. M., Shibuya, H., Watanabe, Y., & Nandakumar, J. (2017). Dissecting the telomere–inner nuclear membrane interface formed in meiosis. Nature structural & molecular biology, 24(12), 1064.

Penkner, A., Tang, L., Novatchkova, M., Ladurner, M., Fridkin, A., Gruenbaum, Y., Schweizer, D., Loidl, J., & Jantsch, V. (2007). The nuclear envelope protein Matefin/SUN-1 is required for homologous pairing in C. elegans meiosis. Developmental cell, 12(6), 873-885.

Petronczki, M., Siomos, M. F., & Nasmyth, K. (2003). Un menage a quatre: the molecular biology of chromosome segregation in meiosis. Cell, 112(4), 423-440.

Pettersen, E. F., Goddard, T. D., Huang, C. C., Couch, G. S., Greenblatt, D. M., Meng, E. C., & Ferrin, T. E. (2004). UCSF Chimera—a visualization system for exploratory research and analysis. Journal of computational chemistry, 25(13), 1605-1612.

Philippe, H., Derelle, R., Lopez, P., Pick, K., Borchiellini, C., Boury-Esnault, N., Vacelet, J., Renard, E,. Houliston, E,. Quéinnec, E., Da Silva, C., Wincker, P., Le Guyader, H., Leys, S., Jackson, D. J., Schreiber, F., Erpenbeck, D., Morgenstern, B., Wörheide, G., & Manuel, M. (2009). Phylogenomics revives traditional views on deep animal relationships. Current Biology, 19(8), 706-712.

Phillips CM, Meng X, Zhang L, Chretien JH, Urnov FD, Dernburg AF (2009) Identification of chromosome sequence motifs that mediate meiotic pairing and synapsis in C. elegans. Nat Cell Biol 11:934–942

Phillips, C. M., & Dernburg, A. F. (2006). A family of zinc-finger proteins is required for chromosome-specific pairing and synapsis during meiosis in C. elegans. Developmental cell, 11(6), 817-829.

Phillips, C. M., Wong, C., Bhalla, N., Carlton, P. M., Weiser, P., Meneely, P. M., & Dernburg, A. F. (2005). HIM-8 binds to the X chromosome pairing center and mediates chromosome-specific meiotic synapsis. Cell, 123(6), 1051-1063.

Pich, U., Fritsch, R., & Schubert, I. (1996). Closely relatedAllium species (Alliaceae) share a very similar satellite sequence. Plant Systematics and Evolution, 202(3-4), 255-264.

Pradillo, M., Evans, D., & Graumann, K. (2019). The nuclear envelope in higher plant mitosis and meiosis. Nucleus, 10(1), 55-66.

Prieler, S., Penkner, A., Borde, V., & Klein, F. (2005). The control of Spo11's interaction with meiotic recombination hotspots. Genes & development, 19(2), 255-269.

Raible, F., & Arendt, D. (2004). Metazoan evolution: some animals are more equal than others. Current Biology, 14(3), R106-R108.

Raices, M., Verdun, R. E., Compton, S. A., Haggblom, C. I., Griffith, J. D., Dillin, A., & Karlseder, J. (2008). C. elegans telomeres contain G-strand and C-strand overhangs that are bound by distinct proteins. Cell, 132(5), 745-757.

Razafsky, D., & Hodzic, D. (2009). Bringing KASH under the SUN: the many faces of nucleo-cytoskeletal connections. The Journal of cell biology, 186(4), 461-472.

Richards, E. J., & Ausubel, F. M. (1988). Isolation of a higher eukaryotic telomere from Arabidopsis thaliana. Cell, 53(1), 127-136.

Robert, X., & Gouet, P. (2014). Deciphering key features in protein structures with the new ENDscript server. Nucleic acids research, 42(W1), W320-W324.

Romanienko, P. J., & Camerini-Otero, R. D. (2000). The mouse Spo11 gene is required for meiotic chromosome synapsis. Molecular cell, 6(5), 975-987.

Ronquist, F., Teslenko, M., Van Der Mark, P., Ayres, D. L., Darling, A., Höhna, S., Larget, B., Liu, L., Suchard, M. A., & Huelsenbeck, J. P. (2012). MrBayes 3.2: efficient Bayesian phylogenetic inference and model choice across a large model space. Systematic biology, 61(3), 539-542.

Sanford, C., & Perry, M. D. (2001). Asymmetrically distributed oligonucleotide repeats in the Caenorhabditis elegans genome sequence that map to regions important for meiotic chromosome segregation. Nucleic acids research, 29(14), 2920-2926.

Sato, A., Isaac, B., Phillips, C. M., Rillo, R., Carlton, P. M., Wynne, D. J., Kasad, R. A. & Dernburg, A. F. (2009). Cytoskeletal forces span the nuclear envelope to coordinate meiotic chromosome pairing and synapsis. Cell, 139(5), 907-919.

Schalk, J. A., Dietrich, A. J., Vink, A. C., Offenberg, H. H., van Aalderen, M., & Heyting, C. (1998). Localization of SCP2 and SCP3 protein molecules within synaptonemal complexes of the rat. Chromosoma, 107(8), 540-548.

Scherthan, H. (2001). A bouquet makes ends meet. Nature reviews Molecular cell biology, 2(8), 621.

Scherthan, H. (2007). Telomere attachment and clustering during meiosis. Cellular & Molecular Life Sciences, 64(2).

Scherthan, H., Weich, S., Schwegler, H., Heyting, C., Härle, M., & Cremer, T. (1996). Centromere and telomere movements during early meiotic prophase of mouse and man are associated with the onset of chromosome pairing. The Journal of Cell Biology, 134(5), 1109-1125.

Schindelin, J., Arganda-Carreras, I., Frise, E., Kaynig, V., Longair, M., Pietzsch, T., Preibisch, S., Rueden, C., Saalfeld, S., Schmid, B., Tinevez, J., White, D. J., Hartenstein, V., Eliceiri, K., Tomancak, P., & Tinevez, J. Y. (2012). Fiji: an open-source platform for biological-image analysis. Nature methods, 9(7), 676.

Schmekel, K., & Daneholt, B. (1995). The central region of the synaptonemal complex revealed in three dimensions. Trends in cell biology, 5(6), 239-242.

Schramm, S., Fraune, J., Naumann, R., Hernandez-Hernandez, A., Höög, C., Cooke, H. J., Alsheimer, M., & Benavente, R. (2011). A novel mouse synaptonemal complex protein is essential for loading of central element proteins, recombination, and fertility. PLoS genetics, 7(5), e1002088.

Schmitt, J., Benavente, R., Hodzic, D., Höög, C., Stewart, C. L., & Alsheimer, M. (2007). Transmembrane protein Sun2 is involved in tethering mammalian meiotic telomeres to the nuclear envelope. Proceedings of the National Academy of Sciences, 104(18), 7426-7431.

Sheehan, M. J., & Pawlowski, W. P. (2009). Live imaging of rapid chromosome movements in meiotic prophase I in maize. Proceedings of the National Academy of Sciences, 106(49), 20989-20994.

Shibuya, H., & Watanabe, Y. (2014). The meiosis-specific modification of mammalian telomeres. Cell Cycle, 13(13), 2024-2028.

Shibuya, H., Hernández-Hernández, A., Morimoto, A., Negishi, L., Höög, C., & Watanabe, Y. (2015). MAJIN links telomeric DNA to the nuclear membrane by exchanging telomere cap. Cell, 163(5), 1252-1266.

Shibuya, H., Ishiguro, K. I., & Watanabe, Y. (2014). The TRF1-binding protein TERB1 promotes chromosome movement and telomere rigidity in meiosis. Nature cell biology, 16(2), 145.

Shtessel, L., Lowden, M. R., Cheng, C., Simon, M., Wang, K., & Ahmed, S. (2013). Caenorhabditis elegans POT-1 and POT-2 repress telomere maintenance pathways. G3: Genes, Genomes, Genetics, 3(2), 305-313.

Starr, D. A. (2009). A nuclear-envelope bridge positions nuclei and moves chromosomes. J Cell Sci, 122(5), 577-586.

Starr, D. A., & Fischer, J. A. (2005). KASH'n Karry: The KASH domain family of cargo-specific cytoskeletal adaptor proteins. Bioessays, 27(11), 1136-1146.

Starr, D. A., & Fridolfsson, H. N. (2010). Interactions between nuclei and the cytoskeleton are mediated by SUN-KASH nuclear-envelope bridges. Annual review of cell and developmental biology, 26, 421-444.

Starr, D. A., & Han, M. (2002). Role of ANC-1 in tethering nuclei to the actin cytoskeleton. Science, 298(5592), 406-409.

Storlazzi, A., Tessé, S., Gargano, S., James, F., Kleckner, N., & Zickler, D. (2003). Meiotic double-strand breaks at the interface of chromosome movement, chromosome remodeling, and reductional division. Genes & development, 17(21), 2675-2687.

Tarsounas, M., Morita, T., Pearlman, R. E., & Moens, P. B. (1999). RAD51 and DMC1 form mixed complexes associated with mouse meiotic chromosome cores and synaptonemal complexes. The Journal of cell biology, 147(2), 207-220.

Telford, M. J., Budd, G. E., & Philippe, H. (2015). Phylogenomic insights into animal evolution. Current Biology, 25(19), R876-R887.

Tomita, K., & Cooper, J. P. (2007). The telomere bouquet controls the meiotic spindle. Cell, 130(1), 113-126.

Trelles-Sticken, E., Adelfalk, C., Loidl, J., & Scherthan, H. (2005). Meiotic telomere clustering requires actin for its formation and cohesin for its resolution. The Journal of cell biology, 170(2), 213-223.

Trelles-Sticken, E., Loidl, J., & Scherthan, H. (1999). Bouquet formation in budding yeast: initiation of recombination is not required for meiotic telomere clustering. Journal of Cell Science, 112(5), 651-658.

Tzur, Y. B., Wilson, K. L., & Gruenbaum, Y. (2006). SUN-domain proteins:'Velcro'that links the nucleoskeleton to the cytoskeleton. Nature reviews Molecular cell biology, 7(10), 782.

Varas, J., Graumann, K., Osman, K., Pradillo, M., Evans, D. E., Santos, J. L., & Armstrong, S. J. (2015). Absence of SUN 1 and SUN 2 proteins in Arabidopsis thaliana leads to a delay in meiotic progression and defects in synapsis and recombination. The plant journal, 81(2), 329-346.

Voet, T., Liebe, B., Labaere, C., Marynen, P., & Scherthan, H. (2003). Telomere-independent homologue pairing and checkpoint escape of accessory ring chromosomes in male mouse meiosis. The Journal of cell biology, 162(5), 795-808.

von Wettstein, D., Rasmussen, S. W., & Holm, P. B. (1984). The synaptonemal complex in genetic segregation. Annual review of genetics, 18(1), 331-411.

Wanat, J. J., Kim, K. P., Koszul, R., Zanders, S., Weiner, B., Kleckner, N., & Alani, E. (2008). Csm4, in collaboration with Ndj1, mediates telomere-led chromosome dynamics and recombination during yeast meiosis. PLoS genetics, 4(9), e1000188.

Wang, Y., Chen, Y., Chen, J., Wang, L., Nie, L., Long, J., Chang, H., Wu, J., Huang, C., & Lei, M. (2019). The meiotic TERB1-TERB2-MAJIN complex tethers telomeres to the nuclear envelope. Nature communications, 10(1), 564.

Weiner, B. M., & Kleckner, N. (1994). Chromosome pairing via multiple interstitial interactions before and during meiosis in yeast. Cell, 77(7), 977-991.

Wilkins, A. S., & Holliday, R. (2009). The evolution of meiosis from mitosis. Genetics, 181(1), 3-12.

Wettstein, R. & Sotelo, J. R., 1967. Electron microscope serial reconstruction of the spermatocytes I nuclei at pachytene. J. Microsc. 6: 557–576.

Woglar, A., & Jantsch, V. (2014). Chromosome movement in meiosis I prophase of Caenorhabditis elegans. Chromosoma, 123(1-2), 15-24.

Wynne, D. J., Rog, O., Carlton, P. M., & Dernburg, A. F. (2012). Dynein-dependent processive chromosome motions promote homologous pairing in C. elegans meiosis. J Cell Biol, 196(1), 47-64.

Yoon, S., Choi, E. H., Kim, J. W., & Kim, K. P. (2018). Structured illumination microscopy imaging reveals localization of replication protein A between chromosome lateral elements during mammalian meiosis. Experimental & molecular medicine, 50(8), 112.

Yoshida, Kayo, et al. "The mouse RecA-like gene Dmc1 is required for homologous chromosome synapsis during meiosis." Molecular cell 1.5 (1998): 707-718.

Yuan, L., Pelttari, J., Brundell, E., Björkroth, B., Zhao, J., Liu, J. G., Brismar, H. Daneholt, B. & Höög, C. (1998). The synaptonemal complex protein SCP3 can form multistranded, cross-striated fibers in vivo. The Journal of cell biology, 142(2), 331-339.

Zeng, X., Li, K., Yuan, R., Gao, H., Luo, J., Liu, F., Wu, Y., Wu, G., & Yan, X. (2018). Nuclear envelope-associated chromosome dynamics during meiotic prophase I. Frontiers in cell and developmental biology, 5, 121.

Zhang, J., Tu, Z., Watanabe, Y., & Shibuya, H. (2017). Distinct TERB1 domains regulate different protein interactions in meiotic telomere movement. Cell reports, 21(7), 1715-1726.

Zhang, Q., Skepper, J. N., Yang, F., Davies, J. D., Hegyi, L., Roberts, R. G., Weissberg, P.L., Ellis, J. A., & Shanahan, C. M. (2001). Nesprins: a novel family of spectrin-repeat-containing proteins that localize to the nuclear membrane in multiple tissues. Journal of cell science, 114(24), 4485-4498.

Zhao, Y., Su, H., Zhou, J., Feng, H., Zhang, K. Q., & Yang, J. (2015). The APSES family proteins in fungi: characterizations, evolution and functions. Fungal Genetics and Biology, 81, 271-280.

Zhong, Z., Shiue, L., Kaplan, S., & de Lange, T. (1992). A mammalian factor that binds telomeric TTAGGG repeats in vitro. Molecular and cellular biology, 12(11), 4834-4843.

Zhou, K., Rolls, M. M., Hall, D. H., Malone, C. J., & Hanna-Rose, W. (2009). A ZYG-12–dynein interaction at the nuclear envelope defines cytoskeletal architecture in the C. elegans gonad. The Journal of cell biology, 186(2), 229-241.

Zhou, X., Graumann, K., & Meier, I. (2015). The plant nuclear envelope as a multifunctional platform LINCed by SUN and KASH. Journal of experimental botany, 66(6), 1649-1659.

Zickler, D. (2006). From early homologue recognition to synaptonemal complex formation. Chromosoma, 115(3), 158-174.

Zickler, D., & Kleckner, N. (1998). The leptotene-zygotene transition of meiosis. Annual review of genetics, 32(1), 619-697.

Zickler, D., & Kleckner, N. (2015). Recombination, pairing, and synapsis of homologs during meiosis. Cold Spring Harbor perspectives in biology, 7(6), a016626.

Chapter 10 Supplementary Information

Table 10-1 Species, taxonomic rank, and protein accession numbers of candidate TERB1 homologues in metazoans obtained using PSI-BLAST

Species name	Taxonomic rank	Accesion number
Mus musculus	Metazoa; Deusterostoma; Chordata; Vertebrata; Mammalia	NP_851289
Cavia porcellus	Metazoa; Deusterostoma; Chordata; Vertebrata; Mammalia	XP_003471985
Homo sapiens	Metazoa; Deusterostoma; Chordata; Vertebrata; Mammalia	NP_001129977
Chrysemys picta bellii	Metazoa; Deuterostoma; Chordata Vertebrata; Testudines	XP_008173404
Monopterus albus	Metazoa; Deuterostoma; Chordata; Vertebrata; Actinopterygii	XP_020468880
Pogona vitticeps	Metazoa; Deuterostoma; Chordata; Vertebrata; Lepidosauria	XP_020670034
Scleropages formosus	Metazoa; Deuterostoma; Chordata; Vertebrata; Actinopterygii	XP_018607988
Alligator mississippiens	Metazoa; Deuterostoma; Chordata; Vertebrata; Archosauria	XP_019348499
Columba livia	Metazoa; Deuterostoma; Chordata; Vertebrata; Archosauria	XP_021137726
Callorhincus milii	Metazoa; Deuterostoma; Chordata; Vertebrata; Chondrichthyes	XP_007906058
Latimeria chalumnae	Metazoa; Deuterostoma; Chordata; Vertebrata; Coelacanthimorpha	XP_014348702
Gekko japonicus	Metazoa; Deuterostoma; Chordata; Vertebrata; Lepidosauria	XP_015279750
Chelonya mydas	Metazoa; Deuterostoma; Chordata; Vertebrata; Testudines	XP_007058728
Danio rerio	Metazoa; Deuterostoma; Chordata;Vertebrata; Actinopterygii	NP_001082851
Xenopus tropicalis	Metazoa; Deuterostoma; Chordata;Vertebrata; Amphibia	XP_017948679
Xenopus laevis	Metazoa; Deuterostoma; Chordata;Vertebrata; Amphibia	OCT57393
Acanthaster planci	Metazoa; Eumetazoa; Bilateria; Deuterostomia; Echinodermata	XP_022081545
Limulus polyphemus	Metazoa; Eumetazoa; Bilateria; Protostomia; Ecdysozoa; Panarthropoda; Arthropoda	XP_022246046
Capitella teleta	Metazoa; Eumetazoa; Bilateria; Protostomia; Lophotrochozoa; Annelida	ELU13718
Lingula anatina	Metazoa; Eumetazoa; Bilateria; Protostomia; Lophotrochozoa; Brachiopoda	XP_013407283
Crassostrea virginica	Metazoa; Eumetazoa; Bilateria; Protostomia; Lophotrochozoa; Mollusca; Bivalvia	XP_022286282
Mizuhopecten yessoensis	Metazoa; Eumetazoa; Bilateria; Protostomia; Lophotrochozoa; Mollusca; Bivalvia	OWF54743
Aplysia californica	Metazoa; Eumetazoa; Bilateria; Protostomia; Lophotrochozoa; Mollusca; Gastropoda	XP_005109353
Lottia gigantea	Metazoa; Eumetazoa; Bilateria; Protostomia; Lophotrochozoa; Mollusca; Gastropoda	XP_009053858
Elysia chlorotica	Metazoa; Eumetazoa; Bilateria; Protostomia; Lophotrochozoa; Mollusca; Gastropoda	RUS80343/EGW08_011882
Hydra vulgaris	Metazoa; Eumetazoa; Cnidaria; Hydrozoa	XP_012561908
Amphimedon queenslandica	Metazoa; Porifera; Demospongiae	XP_019850131

Sarcophilus harrisii	Metazoa; Deuterostoma; Chordata; Vertebrata; Mammalia	XP_012395745
Ornithorhynchus anatinus	Metazoa; Deuterostoma; Chordata; Vertebrata Mammalia; Monotremata	XP_007665674
Salmo salar	Metazoa; Deuterostoma; Chordata; Vertebrata; Actinopterygii	XP_014004017
Apteryx australis mantelli	Metazoa; Deuterostoma; Chordata; Vertebrata; Archosauria	XP_013796592
Rhincodon typus	Metazoa; Deuterostoma; Chordata; Vertebrata; Chondrichthyes	XP_020383869
Branchiostoma belcheri	Metazoa; Deuterostoma; Chordata;Cephalochordata	XP_019613458
Branchiostoma floridae	Metazoa; Deuterostoma; Chordata;Cephalochordata	XP_002588932
Strongylocentrotus purpuratus	Metazoa; Eumetazoa; Bilateria; Deuterostomia; Echinodermata	XP_003731208
Saccoglossus kowalevskii	Metazoa; Eumetazoa; Bilateria; Deuterostomia; Hemichordata	XP_006825363
Priapulus caudatus	Metazoa; Eumetazoa; Bilateria; Protostomia; Ecdysozoa	XP_014672679
Crassostrea gigas	Metazoa; Eumetazoa; Bilateria; Protostomia; Lophotrochozoa; Mollusca; Bivalvia	XP_019919025
Zootermopsis nevadensis	Metazoa; Eumetazoa; Bilateria; Protostomia; Ecdysozoa; Arthropoda; Hexapoda; Insecta	XP_021926856
Parasteatoda tepidariorum	Metazoa; Eumetazoa; Bilateria; Protostomia; Ecdysozoa; Arthropoda; Chelicerata; Arachnida;	XP_015915639
Octopus bimaculoides	Metazoa; Eumetazoa; Bilateria; Protostomia; Lophotrochozoa; Mollusca; Cephalopada	KOF89697
Dendronephthya gigantea	Metazoa; Eumetazoa; Cnidaria; Anthozoa	XP_028414065
Acropora digitifera	Metazoa; Eumetazoa; Cnidaria; Anthozoa	XP_015752571
Exaiptasia pallida	Metazoa; Eumetazoa; Cnidaria; Anthozoa	KXJ09956
Nematostella vectensis	Metazoa; Eumetazoa; Cnidaria; Anthozoa	XP_001626728
Orbicella faveolata	Metazoa; Eumetazoa; Cnidaria; Anthozoa	XP_020616593
Stylophora pistillata	Metazoa; Eumetazoa; Cnidaria; Anthozoa	XP_022802203
Pocillopora damicornis	Metazoa; Eumetazoa; Cnidaria; Anthozoa	XP_027049808
Trichoplax adherens	Metazoa; Placozoa; Trichoplax	XP_002117303

Table 10-2 Species, taxonomic rank, and protein accession numbers of candidate TERB2 homologues in metazoans obtained using PSI-BLAST.

Species name	Taxonomy rank	Accesion number
Mus Musculus	Metazoa; Deuterostoma; Chordata; Vertebrata; Mammalia	NP_083190
Branchiostoma belcheri	Metazoa; Deuterostoma; Chordata; Cephalochordata	XP_019615255
Monopterus albus	Metazoa; Chordata;Craniata; Vertebrata; Actinopterygii	XP_020462382
Latimeria chalumnae	Metazoa; Deuterostoma; Chordata; Vertebrata; Coelacanthimorpha	XP_006013910
Gekko japanicus	Metazoa; Deuterostoma; Chordata; Vertebrata; Lepidosauria	XP_01526237
Pogona vitticeps	Metazoa; Deuterostoma; Chordata; Vertebrata; Lepidosauria	XP_020663749
Scleropages formosus	Metazoa; Deuterostoma; Chordata; Vertebrata; Actinopterygii	XP_018595098

Salmo salar	Metazoa; Deuterostoma; Chordata; Vertebrata; Actinopterygii	XP_014030940
Alligator mississippiensis	Metazoa; Deuterostoma; Chordata; Vertebrata; Archosauria	XP_014455423
Apteryx rowi	Metazoa; Deuterostoma; Chordata; Vertebrata; Archosauria	XP_025914060
Apteryx austalis mantelli	Metazoa; Deuterostoma; Chordata; Vertebrata; Archosauria	XP_013811644
Columba livia	Metazoa; Deuterostoma; Chordata; Vertebrata; Archosauria	XP_021139078
Callorhinchus millii	Metazoa; Deuterostoma; Chordata; Vertebrata; Chondrichthyes	XP_007906225
Bos taurus	Metazoa; Deuterostoma; Chordata; Vertebrata; Mammalia	NP_001070546
Capra hircus	Metazoa; Deuterostoma; Chordata; Vertebrata; Mammalia	XP_005686283
Cavia porcellus	Metazoa; Deuterostoma; Chordata; Vertebrata; Mammalia	XP_003471804
Homo sapiens	Metazoa; Deuterostoma; Chordata; Vertebrata; Mammalia	NP_689661
Sarcophilus harrisii	Metazoa; Deuterostoma; Chordata; Vertebrata; Mammalia	XP_012401909
Chelonya mydas	Metazoa; Deuterostoma; Chordata; Vertebrata; Testudines	XP_007056532
Xenopus laevis	Metazoa; Deuterostoma; Chordata;Vertebrata; Amphibia	XP_018110167
Xenopus tropicalis	Metazoa; Deuterostoma; Chordata;Vertebrata; Amphibia	XP_017947896
Rhincodon typus	Metazoa; Deuterostoma; Vertebrata; Chondrichthyes	XP_020378706
Chrysemys picta bellii	Metazoa; Deuterstoma; Chordata; Vertebrata; Testudines	XP_008165062
Acanthaster planci	Metazoa; Eumetazoa; Bilateria; Deuterostomia; Echinodermata	XP_022105193
Apostichopus japonicus	Metazoa; Eumetazoa; Bilateria; Deuterostomia; Echinodermata	PIK5153
Strongylocentrotus purpuratus	Metazoa; Eumetazoa; Bilateria; Deuterostomia; Echinodermata	XP_011664353
Saccoglossus kowalevskii	Metazoa; Eumetazoa; Bilateria; Deuterostomia; Hemichordata	XP_002730738
Centruroides sculpturatus	Metazoa; Eumetazoa; Bilateria; Protostomia; Ecdysozoa; Panarthropoda; Arthropoda	XP_023233003
Limulus polyphemus	Metazoa; Eumetazoa; Bilateria; Protostomia; Ecdysozoa; Panarthropoda; Arthropoda	XP_022250037
Capitella teleta	Metazoa; Eumetazoa; Bilateria; Protostomia; Lophotrochozoa; Annelida	ELT95246
Crassostrea gigas	Metazoa; Eumetazoa; Bilateria; Protostomia; Lophotrochozoa; Mollusca; Bivalvia	XP_019930121
Crassostrea virginica	Metazoa; Eumetazoa; Bilateria; Protostomia; Lophotrochozoa; Mollusca; Bivalvia	XP_022329935
Mizuhopecten yessoensis	Metazoa; Eumetazoa; Bilateria; Protostomia; Lophotrochozoa; Mollusca; Bivalvia	XP_021360479
Aplysia californica	Metazoa; Eumetazoa; Bilateria; Protostomia; Lophotrochozoa; Mollusca; Gastropoda	XP_005090461
Lottia gigantea	Metazoa; Eumetazoa; Bilateria; Protostomia; Lophotrochozoa; Mollusca; Gastropoda	XP_009048665
Elysia chlorotica	Metazoa; Eumetazoa; Bilateria; Protostomia; Lophotrochozoa; Mollusca; Gastropoda	RUS7892277EGW08_013300
Acropora digitifera	Metazoa; Eumetazoa; Cnidaria; Anthozoa	XP_015753906
Orbicella faveolata	Metazoa; Eumetazoa; Cnidaria; Anthozoa	XP_020630061
Dendronephthya gigantea	Metazoa; Eumetazoa; Cnidaria; Anthozoa	XP_028398919
Pocillopora damicornis	Metazoa; Eumetazoa; Cnidaria; Anthozoa	XP_027045077
Stylophora pistillata	Metazoa; Eumetazoa; Cnidaria; Anthozoa	XP_022784010
Hydra vulgaris	Metazoa; Eumetazoa; Cnidaria; Hydrozoa	XP_002169769
Lingula anatina	Metazoa; Lophotrochozoa; Brachiopoda	XP_013380855
Trichoplax adherens	Metazoa; Placozoa; Trichoplax	XP_002110273

Amphimedon queenslandica	Metazoa; Porifera; Demospongiae	XP_019856173

Table 10-3 Species, taxonomic rank, and protein accession numbers of candidate MAJIN homologues in metazoans obtained using PSI-BLAST

Species name	Taxonomic rank	Accesion number
Mus musculus	Metazoa; Deuterostoma; Chordata; Vertebrata; Mammalia	NP_001159391
Callorhinchus milii	Metazoa; Deuterostoma; Chordata; Vertebrata; Chondrichthyes	XP_007883186
Chelonia mydas	Metazoa; Deuterostoma; Chordata; Vertebrata; Testudines	XP_007052730
Gekko japonicus	Metazoa; Chordata; Craniata; Vertebrata; Reptilia	XP_015282829
Alligator mississippiensis	Metazoa; Deuterostoma; Chordata; Vertebrata; Archosauria	KYO31280
Pogona vitticeps	Metazoa; Deuterostoma; Chordata; Vertebrata; Lepidosauria	XP_020652836
Branchiostoma belcheri	Metazoa; Deuterostoma; Chordata; Cephalochordata	XP_019625986
Branchiostoma floridae	Metazoa; Deuterostoma; Chordata; Cephalochordata	XP_002606604
Rhincodon typus	Metazoa; Deuterostoma; Vertebrata; Chondrichthyes	XP_020370007
Danio rerio	Metazoa; Deuterostoma; Chordata;Vertebrata; Actinopterygii	XP_017212702
Monopterus albus	Metazoa; Deuterostoma; Chordata; Vertebrata; Actinopterygii	XP_020465821
Salmo salar	Metazoa; Deuterostoma; Chordata; Vertebrata; Actinopterygii	XP_014012104
Latimeria chalumnae	Metazoa; Deuterostoma; Chordata; Vertebrata; Coelacanthimorpha	XP_014349143
Xenopus leavis	Metazoa; Deuterostoma; Chordata; Vertebrata; Amphibia	OCT81751
Xenopus tropicalis	Metazoa; Deuterostoma; Chordata; Vertebrata; Amphibia	OCA37246
Apteryx australis mantelli	Metazoa; Deuterostoma; Chordata; Vertebrata; Archosauria	XP_013799140
Columba livia	Metazoa; Deuterostoma; Chordata; Vertebrata; Archosauria	XP_013224740
Scleropages formosus	Metazoa; Deuterostoma; Chordata; Vertebrata; Archosauria	XP_018592548
Bos taurus	Metazoa; Deuterostoma; Chordata; Vertebrata; Mammalia	XP_015316798
Capra hircus	Metazoa; Deuterostoma; Chordata; Vertebrata; Mammalia	XP_017899084
Cavia porcellus	Metazoa; Deuterostoma; Chordata; Vertebrata; Mammalia	XP_013006196
Homo sapiens	Metazoa; Deuterostoma; Chordata; Vertebrata; Mammalia	XP_005273975
Saimiri boliviensis	Metazoa; Deuterostoma; Chordata; Vertebrata; Mammalia	XP_010346585
Ornithorhynchus anatinus	Metazoa; Deuterostoma; Chordata; Vertebrata; Mammalia; Monotrema	XP_007662640
Sarcophilus harrisii	Metazoa; Deuterostoma; Chordata; Vertebrata; Mammalia	XP_012408262
Acanthaster planci	Metazoa; Eumetazoa; Bilateria; Deuterostomia; Echinodermata	XP_022090649
Apostichopus japonicus	Metazoa; Eumetazoa; Bilateria; Deuterostomia; Echinodermata	PIK39444
Strongylocentrotus purpuratus	Metazoa; Eumetazoa; Bilateria; Deuterostomia; Echinodermata	XP_011668546
Saccoglossus kowalevskii	Metazoa; Eumetazoa; Bilateria; Deuterostomia; Hemichordata	XP_006812193
Priapulus caudatus	Metazoa; Eumetazoa; Bilateria; Protostomia; Ecdysozoa	XP_014676280
Capitella teletea	Metazoa; Eumetazoa; Bilateria; Protostomia; Lophotrochozoa; Annelida	ELT98474.1
Cassostrea gigas	Metazoa; Eumetazoa; Bilateria; Protostomia; Lophotrochozoa; Mollusca; Bivalvia	XP_011454168

Cassostrea virginica	Metazoa; Eumetazoa; Bilateria; Protostomia; Lophotrochozoa; Mollusca; Bivalvia	XP_022338123
Mizuhopecten yessoensis	Metazoa; Eumetazoa; Bilateria; Protostomia; Lophotrochozoa; Mollusca; Bivalvia	XP_021345218
Aplysia californica	Metazoa; Eumetazoa; Bilateria; Protostomia; Lophotrochozoa; Mollusca; Gastropoda	XP_012946253
Elysia chlorotica	Metazoa; Eumetazoa; Bilateria; Protostomia; Lophotrochozoa; Mollusca; Gastropoda	RUS71040 /EGW08_021198
Lottia gigantea	Metazoa; Eumetazoa; Bilateria; Protostomia; Lophotrochozoa; Mollusca; Gastropoda	XP_009058794
Acropora digitifera	Metazoa; Eumetazoa; Cnidaria; Anthozoa	XP_015763651
Orbicella faveolata	Metazoa; Eumetazoa; Cnidaria; Anthozoa	XP_020615173
Dendronephthya gigantea	Metazoa; Eumetazoa; Cnidaria; Anthozoa	RMX50144
Stylophora pistillata	Metazoa; Eumetazoa; Cnidaria; Anthozoa	XP_022790937
Hydra vulgaris	Metazoa; Eumetazoa; Cnidaria; Hydrozoa	XP_012563853
Lingula anatina	Metazoa; Lophotrochozoa; Brachiopoda	XP_013401921
Trichoplax adherens	Metazoa; Placozoa; Trichoplax	XP_002109914
Amphimedon queenslandica	Metazoa; Porifera; Demospongiae	XP_019850558

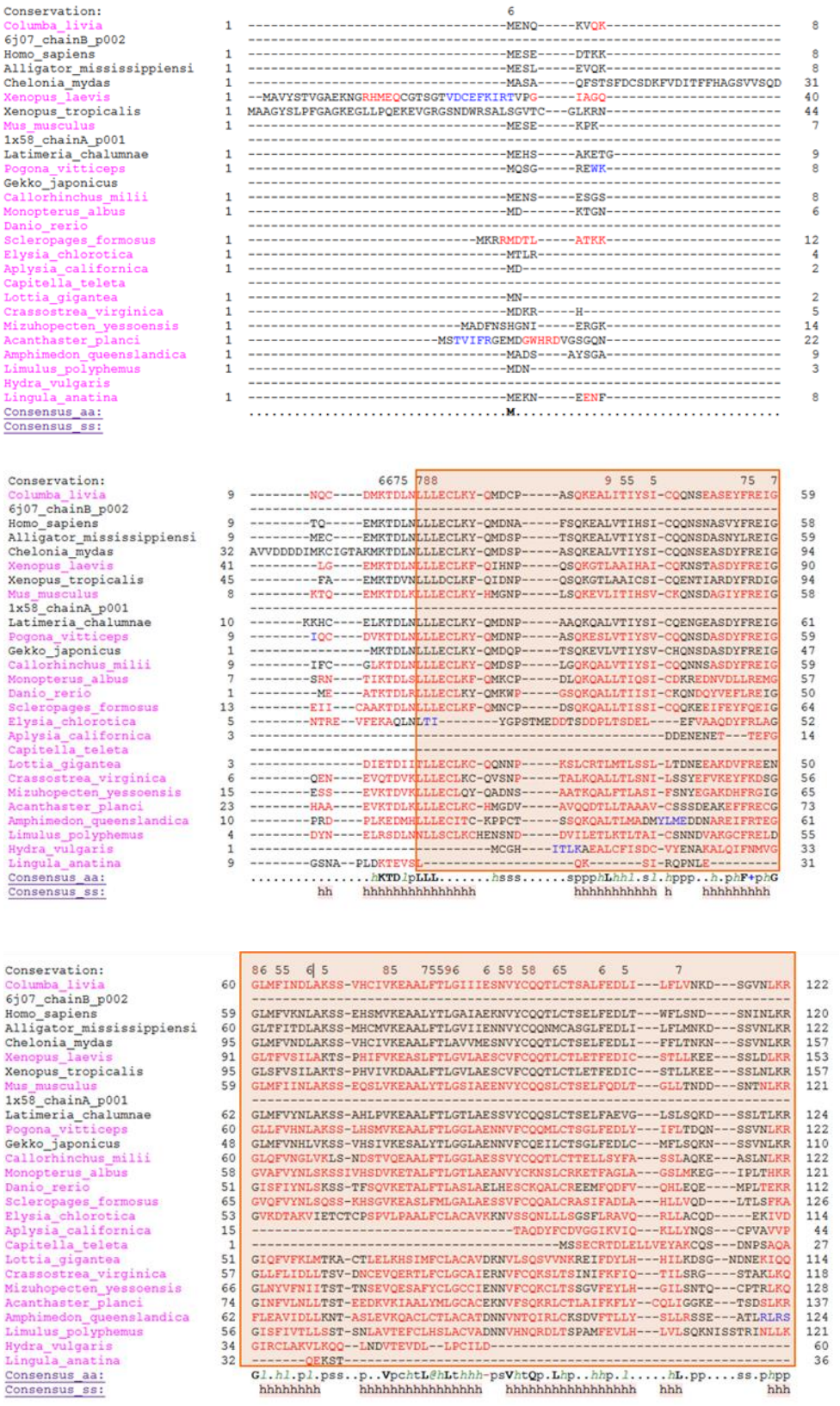
Conservation:
Columba_livia
6j07_chainB_p002
Homo_sapiens
Alligator_mississippiensi
Chelonia_mydas
Xenopus_laevis
Xenopus_tropicalis
Mus_musculus
1x58_chainA_p001
Latimeria_chalumnae
Pogona_vitticeps
Gekko_japonicus
Callorhinchus_milii
Monopterus_albus
Danio_rerio
Scleropages_formosus
Elysia_chlorotica
Aplysia_californica
Capitella_teleta
Lottia_gigantea
Crassostrea_virginica
Mizuhopecten_yessoensis
Acanthaster_planci
Amphimedon_queenslandica
Limulus_polyphemus
Hydra_vulgaris
Lingula_anatina
Consensus_aa:
Consensus_ss:


Conservation:
Columba_livia 123 MSVYVILVLVSNNKSGQTYVRDTGCIGLLLQLFRTTLS---------TSEMNLS---------DENT-- 171
6j07_chainB_p002
Homo_sapiens 121 MSVYVILVLVSNNRTGQTLVRETGCITVLSRLFRTVIS---------KHELDLS---------DKNV-- 169
Alligator_mississippiensi 123 MSVYVVLVLVSNNKSGQTHVRETGCIGVLLQLFRTALS---------ISEITLS---------DENI-- 171
Chelonia_mydas 158 MSVYVILVLVSNNKSGQTHIRETGCIGVLLQLFRTTLS---------ISEMNLS---------DENI-- 206
Xenopus_laevis 154 MSVYLFMVLVSNNRAGQTHSRISGCIDVLLCLFREIPS---------SCNIDVP---------DGTL-- 202
Xenopus_tropicalis 158 MSLYLFMVLVSNNRAGQTHSRISGCIDVLLCLFREMPS---------SCNIDVP---------NRAK-- 206
Mus_musculus 122 MSVYVLLVLVSNNRNGQTLVREVGCIEVLSQMFRTVLS---------NYELNLS---------DNSV-- 170
1x58_chainA_p001
Latimeria_chalumnae 125 MAVYVVLVLVSNNKTGQTFTRKTGCIDLLLNLFRTTFP---------ISENAIR---------ENM-- 172
Pogona_vitticeps 123 LSVYVLLVLVSNNKSGQTSVRKSGCLDVLLQLFRTILS---------VSEVNLL---------DQN--- 170
Gekko_japonicus 111 MSVYVLLVLVSNNKNGQTYVRESGCLDVLLQLFRTTLS---------ISEMNLS---------DNAI-- 159
Callorhinchus_milii 123 IAVYVILVLVSHNKFGQGLARTTGCIDILLILFRSSFP---------ISNKHSI---------HQNI-- 171
Monopterus_albus 122 VSVYLLSVLVANNKLGQILAQTTSCLDILLHLFRTTFP---------TSRDTTLR---------LATA-- 171
Danio_rerio 113 VAVYMLSVLVANNRCGQTLAKTSRCIEALLRLFRQNFP---------------V---------PGES-- 155
Scleropages_formosus 127 TVVYMVSALVASNRLGQTLARHSGCVSALLRLFSTSFP---------STSDCEK---------PRMA-- 175
Elysia_chlorotica 115 SAAFFLACVVADNGRGQQLIYETGCLRELLNILRRYLH---------------------------EP-- 154
Aplysia_californica 45 AALFCLACVVKENGIGQALCWQTGCLQDLINLLRSSTV---------------------------NE-- 84
Capitella_teleta 28 QAFRSIASLCSKQAPSQKELSTPQIFAYLKDVVHRELT---------------------------- 65
Lottia_gigantea 115 TAIFLLLCIVASNSVGQSLANESQCIDDLIMIFRKLLE----------NTAK---------WKTS-- 160
Crassostrea_virginica 119 TATFFLINLVSNNGEGQVLVKQSQCLSALMELLSFSLP---------RNMIGTDENDTDFDWLDGRG-- 176
Mizuhopecten_yessoensis 129 TATFFLLNLVSNNGQGQALVRTSRCLSDLLQLLRKTFP---------KTEVFNR---------QESTES 179
Acanthaster_planci 138 TSAFLLLCLVTNNGEGQNLARTSHCLEALLKLFRTSYPLAPHTSGLPGQMWMDSS---------DTDC-- 196
Amphimedon_queenslandica 125 GTVVLLANIMNNNSQGQKMARETKLLYKLIDMFKSLIQ---------EKDDLIA---------DPIL-- 173
Limulus_polyphemus 122 SAAFLLMILVAQNSSGQKLLTEKGCLHDLIYLYQSTYPL-------LVVEIKRH---------EIQS-- 172
Hydra_vulgaris 61 ----TLTIVFTDCNSNKDCASEMGIVNDLVDCLRLKII---------------------------- 94
Lingula_anatina
Consensus_aa:
Consensus_ss:

Conservation:
Columba_livia 172 ------NQCYQLWSSVCSTLCACVNNPQNEDNQNICCSV-FPYAKEWL----ESCTEPE----IVRPICS 226
6j07_chainB_p002
Homo_sapiens 170 ------FQSYQLWSSVCSTLCVCVNNPQNDENQMFCCSL-FPHANEWL----KNCTTPE----IIRPICS 224
Alligator_mississippiensi 172 ------NQHYELWSSVCSTLCACVNNPQNEENQKICSSV-FPQTKQWL----DRCIEPE----IVRPICS 226
Chelonia_mydas 207 ------NQYYQLWSSVCSTLCACVNNPQNEDNQNTCCSV-FPHAKDWL----QSCIKPE----IVRPICS 261
Xenopus_laevis 203 ------NRSYQLWSSACSGLCACANNPQNDENQKLCCTA-FSQAKDLL----KNSINPE----IVRPVCS 257
Xenopus_tropicalis 207 ------NWSYQLWSSVCSGLCACVNNPQNDENQKLCCSV-FPQAKDLL----KHSNDPE----IVRPVCS 261
Mus_musculus 171 ------FQSYLLWSSVCSTLCVCVNNPQNDENQMLCCSL-FPCVNEWL----MNCMRPE----VIRPICS 225
1x58_chainA_p001
Latimeria_chalumnae 173 ------SQYYELWSSVSSALCACVNNPQNEENQRICITV-FPIAKEWL----QKCIRRE----IIRPICS 227
Pogona_vitticeps 171 ------INHYHLWSSVCSTLCACVNNPQNEDNQKICTLV-FPHAKDWL----QNCVKSQ----IIRPICS 225
Gekko_japonicus 160 ------NQSYQLWSSVCSALSACVNNPQNEDNQKSCSLV-FPYAKDCL----QCCTKPE----IVRPICS 214
Callorhinchus_milii 172 ------SQCYELWSSIGSTLCACVNNPQNEENQRICTTV-FLFARDCL----QKYPRQE----IIRPICS 226
Monopterus_albus 172 ------TQTHQLWTSVSSALCGCVNNPQNEEGQRICVTA-FPILKIWL----QQMALPRT--EIFQPIC 228
Danio_rerio 156 ------YEQLQLWTTVSSALCGSVNNPQNEENQNVCMSV-FPEIKPWL----QEVALPRA--ELAQPLC 212
Scleropages_formosus 176 ------SQLYQLWASLSSAICGCVNNPQNEENQQMCMSI-FPVIKLWL----QNFGQSRN--DVIQPIC 232
Elysia_chlorotica 155 ------HTDDSKWSIVTRAVAVCVNNPQNERNQGVCCSV-LPLALKFI----STEPQNS----SIRHILA 209
Aplysia_californica 85 ------SEDENLWSSITSAIGVSVNNPQNEENQRMCCSV-LPHVLKVI----SRGKRTH----VDKHALG 139
Capitella_teleta 66 ------PMKTRKSAAFLLLCLVKNN---KENQRLCANV-LPFVLKSI----LNQTDTE----NLRQLVT 116
Lottia_gigantea 161 -------YKGLWCSLNSALSICVNNPQNDSNQRKCCIL-FPQAFKCL----SENNDPD----ILRPVLA 213
Crassostrea_virginica 177 ------PTSLELWTSVVNAICVSINNPQNDENQKMCGLQ-LPFIMSLF----EKHRDEPL----LGRPLMP 232
Mizuhopecten_yessoensis 180 WFEDVGMTSLELWSSVASTLCMCVNNPRNDENQGRCGLE-LGFMFSLI----QHCDNPS----VLRPLLS 240
Acanthaster_planci 197 ------KKQLDLWTVVTSTLSGCVNNPQNEANQLMCSSVAFATAIDII----GKTRNPT----IIRLVSS 252
Amphimedon_queenslandica 174 ------INY---FQNIGNGLSVACDNPQNELNQCQCISI-FPVAVHVLGLAAEGCCDLEGELVVLKSVIN 233
Limulus_polyphemus 173 ------FPSFDLWQAVNGALCFAVNNPQNEENQTICSML-FPVSLKIL----KHETNYN----VLRAVSI 227
Hydra_vulgaris 95 ------HNVQLKCLIC-- 104
Lingula_anatina 37 ----------------------DTPEN-------CSV----HEKCL----TKCNGEEE---AIR--CN 62
Consensus_aa:
Consensus_ss:

Conservation:
Columba_livia 227 FVGLTVANNSYVQKYFVSVG---GLDTLA---KVLIKLM------HDSCMS------HSSTKLAVVVTKT 278
6j07_chainB_p002
Homo_sapiens 225 FIGLTLANNTYVQKYFVSVG---GLDVLS---QVLMQLE------SDSHET------LSSAKLAVVVTKT 276
Alligator_mississippiensi 227 FVGLTVANNSHVQKYFVSIG---GLDILA---KALVKLV------DDSFRN------YTSTKLAVVVTKT 278
Chelonia_mydas 262 FVGLTVANNSRVQEYFVSVG---GLDILA---EVLIKLV------RDSSKS------YSSAKLAVVVTKT 313
Xenopus_laevis 258 FISLAVANNSIVQDYFASVG---GLDTLA---DLFLQLV------SNLQRG------LSSSKLAVVLTKT 309
Xenopus_tropicalis 262 FISFVVADNSFVQEYFASIG---GLDTLA---DLFLQLV------SNLQR--------RSSKLAVVVMKT 311
Mus_musculus 226 FIGLTLANNTHAQNCFVSSG---GLDVLC---QVLVQLE------SDSHNT------LSSAKLAVIVTKT 277
1x58_chainA_p001
Latimeria_chalumnae 228 FVSLTVANNEYAQNYFAMVG---GLDALA---MVLVKLV------DDALKS------YLSSELAVMVSKT 279
Pogona_vitticeps 226 FIMLTVANNSRIQQFFVSLG---GLAVLD---NLLDKLI------PKSFEN------CSNTKLAVIVTKT 277
Gekko_japonicus 215 FIGLTVANNSRLQQFFVSIG---GLTMLD---VLLAKLI------YNSSGN------SSSTKLAVVVTKT 266
Callorhinchus_milii 227 FVGLTVANNTYAQDCFSNVG---GLDTLA---EVLVKLI------DEAGRN------CSTAKLAVILTKT 278
Monopterus_albus 229 FIAMAVANNASVQESFSASG---GLETLT---LALVRLA------SAVDHS------VWSCQLCVILSKT 280
Danio_rerio 213 FIGMTVANNPCAQEYFVSVG---GLDSLS---DTLTRVL------SQSTHS------ASVCKMATIITKT 264
Scleropages_formosus 233 FITMAVASHSIAQDYFASVG---GLSMLA---QCVARLA------IESSIE------HSAFKAAITMTRA 284
Elysia_chlorotica 210 VITAVVSNNVSNQNRVRNCG---GLEEIA---NLV-KHQ------HRNHRD------LRVSSIVYAV-TA 259
Aplysia_californica 140 LINLVVANNAANQERMRNCD---GVGALM---RYVQSCH-------TSETR------GPRPALQICALSA 190
Capitella_teleta 117 FVGAITTENEHNQDRVNQCN---GLDVMV---HAL--LR------STVRDI------KQCMPLVLAIIGT 166
Lottia_gigantea 214 LLGLSVANNGCNQDIVRRCG---GIEVLI--SQIKIWIQ-------LVHTD------CDYLSLAVNGVGT 265
Crassostrea_virginica 233 LLVFVVSNNSTNQNHVRRSG---GLKILC---MTLKQWY------EKFTDS------ELMKDVVHIITT 283
Mizuhopecten_yessoensis 241 LVGFSVASNARNQDQVRQCG---GLLVLI--ARLKVALDLALCQNSETDSR------TEHINLAVTIART 299
Acanthaster_planci 253 FLSLTISNNVSNQDKFGLLG---GLEAMV---NLLHAVV------GDLLCQP----DQDAAQAAVQLANT 306
Amphimedon_queenslandica 234 VFTSCIANNGNTQDKLYKVG---GLRVMT---RMLIKQK------EKTITGGEDEKRQERLEFISCLMQA 291
Limulus_polyphemus 228 FLALTVSANMQNQEILVEYG---ALAVIKDCLQNFIHCV------VTSHCNQG--LQVGPISAAIGVMNY 286
Hydra_vulgaris 105 -IAECVHENEKCQKAFLQSN---GIPV-------VIGLM------STKQD-------ETISKVGMTILQS 150
Lingula_anatina 63 -------LTDHTGTCFSTVDRASSLPVIC---SNIERMP-----VVEINQG------VEFAKPKIVVNKK 111
Consensus_aa:
Consensus_ss:

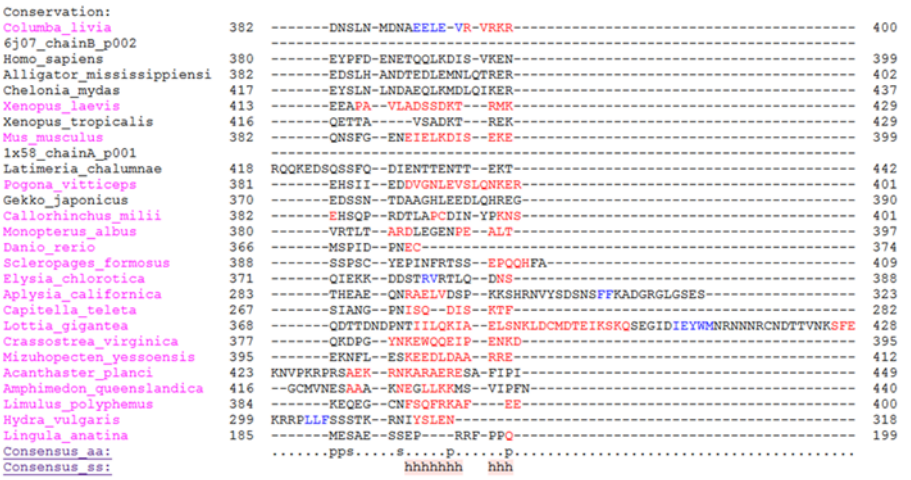
Conservation:
Columba_livia 382 -------DNSLN-MDNAEELE-VR-VRKR---------- 400
6j07_chainB_p002
Homo_sapiens 380 -------EYPFD-ENETQQLKDIS-VKEN---------- 399
Alligator_mississippiensi 382 -------EDSLH-ANDTEDLEMNLQTRER---------- 402
Chelonia_mydas 417 -------EYSLN-LNDAEQLKMDLQIKER---------- 437
Xenopus_laevis 413 -------EEAPA--VLADSSDKT---RMK---------- 429
Xenopus_tropicalis 416 -------QETTA-----VSADKT---REK---------- 429
Mus_musculus 382 -------QNSFG--ENEIELKDIS--EKE---------- 399
1x58_chainA_p001
Latimeria_chalumnae 418 RQQKEDSQSSFQ--DIENTTENTT--EKT---------- 442
Pogona_vitticeps 381 -------EHSII--EDDVGNLEVSLQNKER---------- 401
Gekko_japonicus 370 -------EDSSN--TDAAGHLEEDLQHREG---------- 390
Callorhinchus_milii 382 -------EHSQP--RDTLAPCDIN-YPKNS---------- 401
Monopterus_albus 380 -------VRTLT--ARDLEGENPE--ALT---------- 397
Danio_rerio 366 -------MSPID--PNEC---------- 374
Scleropages_formosus 388 -------SSPSC--YEPINFRTSS--EPQQHFA---------- 409
Elysia_chlorotica 371 -------QIEKK--DDSTRVRTLQ--DNS---------- 388
Aplysia_californica 283 -------THEAE--QNRAELVDSP--KKSHRNVYSDSNSFFKADGRGLGSES---------- 323
Capitella_teleta 267 -------SIANG--PNISQ--DIS--KTF---------- 282
Lottia_gigantea 368 -------QDTTDNDPNTIILQKIA--ELSNKLDCMDTEIKSKQSEGIDIEYWMNRNNNRCNDTTVNKSFE 428
Crassostrea_virginica 377 -------QKDPG--YNKEWQQEIP--ENKD---------- 395
Mizuhopecten_yessoensis 395 -------EKNFL--ESKEEDLDAA--RRE---------- 412
Acanthaster_planci 423 KNVPKRPRSAEK--RNKARAERESA-FIPI---------- 449
Amphimedon_queenslandica 416 --GCMVNESAAA--KNEGLLKKMS--VIPFN---------- 440
Limulus_polyphemus 384 -------KEQEG--CNFSQFRKAF----EE---------- 400
Hydra_vulgaris 299 KRRPLLFSSSTK--RNIYSLEN---------- 318
Lingula_anatina 185 -------MESAE--SSEP----RRF-PPQ---------- 199
Consensus_aa:
Consensus_ss:
hhhhhhh hhh


Conservation:
Columba_livia 401 ----------SMQDY-------WKKAK---------- 410
6j07_chainB_p002
Homo_sapiens 400 ----------NLEEH-------WRKAK---------- 409
Alligator_mississippiensi 403 ----------NLEVY-------WKKAK---------- 412
Chelonia_mydas 438 ----------NLEDY-------WKKVK---------- 447
Xenopus_laevis 430 ----------QMFDY-------WKKAK---------- 439
Xenopus_tropicalis 430 ----------QMFDY---------WKK---------- 437
Mus_musculus 400 ----------TLREH-------WKAAK---------- 409
1x58_chainA_p001
Latimeria_chalumnae 443 ----------TLPSG-------QDFAANYSDQLGVVQ---------- 462
Pogona_vitticeps 402 ----------NLEDY-------RNEAK---------- 411
Gekko_japonicus 391 ----------IIEDY-------RVKAK---------- 400
Callorhinchus_milii 402 ----------CLKGY-------WKFAQ---------- 411
Monopterus_albus 398 ----------NLERY-------RSSAR---------- 407
Danio_rerio 375 ----------DREGQ-------WRSAG---------- 384
Scleropages_formosus 410 ----------PSCNMESY-------WSFSN---------- 422
Elysia_chlorotica 389 ----------RVTRR-------QRLHS---------- 398
Aplysia_californica 333 SPRILASPNKYLSELQNM-------YKVCHRQMASLTQDSDVLEAAIGQQGRGDGPNMQINNQRKEAYAA 395
Capitella_teleta 283 ----------ETGD---------STN---------- 289
Lottia_gigantea 499 YHTSILVTHPQINQYQKHFRPPADPRQSTL---------- 528
Crassostrea_virginica 396 ----------IGENI-------LKKMN---------- 405
Mizuhopecten_yessoensis 413 ----------NGKKM-------LLKID---------- 422
Acanthaster_planci 450 ----------G-------KQRAETEGVPDGNKVPSRHKNAEQE---------- 475
Amphimedon_queenslandica 441 ----------TRINEW-------LEKAETQLQKPPLYSPSLGPADTTNKD---------- 473
Limulus_polyphemus 401 ----------RIKEE-------TCATN---------- 410
Hydra_vulgaris 319 ----------VVTSQ-------VYDTN---------- 328
Lingula_anatina 200 ----------TVQ---------- 202
Consensus_aa:
Consensus_ss:
hhhhh hhhhh

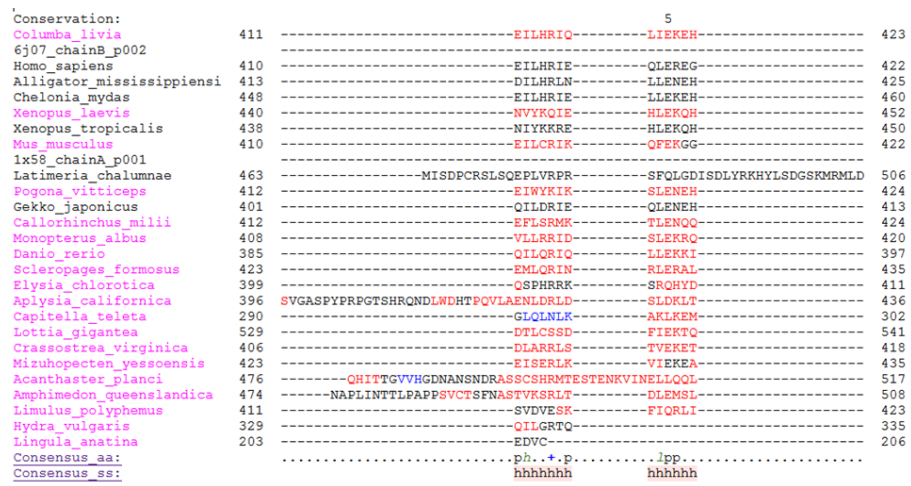
Conservation:
5
Columba_livia 411 ----------EILHRIQ---------LIEKEH---------- 423
6j07_chainB_p002
Homo_sapiens 410 ----------EILHRIE---------QLEREG---------- 422
Alligator_mississippiensi 413 ----------DILHRLN---------LLENEH---------- 425
Chelonia_mydas 448 ----------EILHRIE---------LLEKEH---------- 460
Xenopus_laevis 440 ----------NVYKQIE---------HLEKQH---------- 452
Xenopus_tropicalis 438 ----------NIYKKRE---------HLEKQH---------- 450
Mus_musculus 410 ----------EILCRIK---------QFEKGG---------- 422
1x58_chainA_p001
Latimeria_chalumnae 463 ----------MISDPCRSLSQEPLVRPR---------SFQLGDISDLYRKHYLSDGSKMRMLD 506
Pogona_vitticeps 412 ----------EIWYKIK---------SLENEH---------- 424
Gekko_japonicus 401 ----------QILDRIE---------QLENEH---------- 413
Callorhinchus_milii 412 ----------EFLSRMK---------TLENQQ---------- 424
Monopterus_albus 408 ----------VLLRRID---------SLEKRQ---------- 420
Danio_rerio 385 ----------QILQRIQ---------LLEKKI---------- 397
Scleropages_formosus 423 ----------EMLQRIN---------RLERAL---------- 435
Elysia_chlorotica 399 ----------QSPHRRK---------SRQHYD---------- 411
Aplysia_californica 396 SVGASPYPRPGTSHRQNDLWDHTPQVLAENLDRLD---------SLDKLT---------- 436
Capitella_teleta 290 ----------GLQLNLK---------AKLKEM---------- 302
Lottia_gigantea 529 ----------DTLCSSD---------FIEKTQ---------- 541
Crassostrea_virginica 406 ----------DLARRLS---------TVEKET---------- 418
Mizuhopecten_yessoensis 423 ----------EISERLK---------VIEKEA---------- 435
Acanthaster_planci 476 --------QHITTGVVHGDNANSNDRASSCSHRMTESTENKVINELLQQL---------- 517
Amphimedon_queenslandica 474 ------NAPLINTTLPAPPSVCTSFNASTVKSRLT---------DLEMSL---------- 508
Limulus_polyphemus 411 ----------SVDVESK---------FIQRLI---------- 423
Hydra_vulgaris 329 ----------QILGRTQ---------- 335
Lingula_anatina 203 ----------EDVC---------- 206
Consensus_aa:
Consensus_ss:
hhhhhhh hhhhhh


Conservation:
Columba_livia 424 ----------NKER---------- 427
6j07_chainB_p002
Homo_sapiens 423 ----------NEEE---------- 426
Alligator_mississippiensi 426 ----------YEDTCRSFHTRETEHSNQKRYLVKAAEHVQHKETTWKKNVCQKFCNQRDRNGDENPK 482
Chelonia_mydas 461 ----------DEET---------- 464
Xenopus_laevis 453 ----------KEEN---------- 456
Xenopus_tropicalis 451 ----------EEEN---------- 454
Mus_musculus 423 ----------KEEK---------- 426
1x58_chainA_p001
Latimeria_chalumnae 507 VTPDVGVYKNCCEQLQK---------- 523
Pogona_vitticeps 425 ----------QKEK---------- 428
Gekko_japonicus 414 ----------QEEK---------- 417
Callorhinchus_milii 425 ----------EELA---------- 428
Monopterus_albus 421 ----------EAED---------- 424
Danio_rerio 398 ----------GKKL---------- 401
Scleropages_formosus 436 ----------AGDF---------- 439
Elysia_chlorotica 412 ----------INSL---------- 415
Aplysia_californica 437 ----------SFM---------- 439
Capitella_teleta 303 ----------DNLL---------- 306
Lottia_gigantea 542 ----------AHYS---------- 545
Crassostrea_virginica 419 ----------ESRT---------- 422
Mizuhopecten_yessoensis 436 ----------EEKS---------- 439
Acanthaster_planci 518 ----------HEEK---------- 521
Amphimedon_queenslandica 509 ----------AEEK---------- 512
Limulus_polyphemus 424 ----------ATRN---------- 427
Hydra_vulgaris
Lingula_anatina
Consensus_aa:
Consensus_ss:
Conservation:
Columba_livia 428 --------VQG---------- 441
6j07_chainB_p002
Homo_sapiens 427 --------IQR---------- 440
Alligator_mississippiensi 483 LCQTDKTRKQRCEISPESCKEIWRHVDLSVTESDAGIHTKSPLMDRTRRKIFV---------- 542
Chelonia_mydas 465 --------VRR---------- 478
Xenopus_laevis 457 --------VKRQIFADV---------- 481
Xenopus_tropicalis 455 --------VRRQIFSDV---------- 479
Mus_musculus 427 --------QQN---------- 444
1x58_chainA_p001
Latimeria_chalumnae 524 --------TEDRP---------- 540
Pogona_vitticeps 429 --------MRR---------- 443
Gekko_japonicus 418 --------VRR---------- 435
Callorhinchus_milii 429 --------TNRFM---------- 448
Monopterus_albus 425 ---------- 433
Danio_rerio 402 --------WERDPE---------- 419
Scleropages_formosus 440 --------QGSIG---------- 458
Elysia_chlorotica 416 --------QNR---------- 418
Aplysia_californica
Capitella_teleta 307 --------NYTNI---------- 314
Lottia_gigantea 546 --------LNEKKNR---------- 552
Crassostrea_virginica 423 --------DFISAAEI---------- 445
Mizuhopecten_yessoensis 440 --------LALQQTGQGKEPVKERGCGILSATPYKNNLLFQLQQEREERKRMESIAFRMHVPSPHVQQYG 501
Acanthaster_planci 522 --------SIRQRLEDEKKVLEEREEARARSRGAAKEAALVITKELERQYTEQKL---DKTPEDEGEQPE 580
Amphimedon_queenslandica 513 --------ERRRCLEIELE---------- 550
Limulus_polyphemus 428 --------DHERRGNAET---------- 458
Hydra_vulgaris 336 ---------- 353
Lingula_anatina 207 ---------- 213
Consensus_aa:
Consensus_ss:
Conservation:
Columba_livia 442 ----------TEAS-KYYEVNPAD-PKIY---------- 466
6j07_chainB_p002
Homo_sapiens 441 ----------ISIQNTWKHLHADRIGRGS---------- 467
Alligator_mississippiensi 543 ----------MPTASKYHEVDASD-QTSH---------- 568
Chelonia_mydas 479 ----------MQMTPKYRKMNASD-QKAN---------- 504
Xenopus_laevis 482 ----------ISGDNQAEPERNHM-DLPC---------- 505
Xenopus_tropicalis 480 ----------ISGDNQAEPEENHM-DLPC---------- 503
Mus_musculus 445 ----------IQTNLKRLCADSTG-GTRA---------- 468
1x58_chainA_p001
Latimeria_chalumnae 541 ----------RQIFVDNDRIQKPA-GTTSS---------- 570
Pogona_vitticeps 444 ----------LQNTSVHLKANA---SKQL---------- 465
Gekko_japonicus 436 ----------MQTTSKHLQVNA---SGQS---------- 457
Callorhinchus_milii 449 ----------PSVNEELQAYHSVY-PGLQ---------- 472
Monopterus_albus 434 ----------S----------NEGL---------- 444
Danio_rerio 420 ----------VECDDELWEGSVMR-KVKG---------- 443
Scleropages_formosus 459 ----------DPAQYRVARDMGEG-DLLL---------- 482
Elysia_chlorotica
Aplysia_californica
Capitella_teleta
Lottia_gigantea
Crassostrea_virginica 446 ----------NPGSSKEI-GKKCG-NILP---------- 468
Mizuhopecten_yessoensis 502 LEPRPCLSEENFPVHRGTFIESDRQRLHHQSLC-CSTPDSSCHRKGFGQNPNMYCVNNCPEYTCGNQDVD 570
Acanthaster_planci 581 GTKSATP-EKQFLSPSMKNVEQRLEALEKSLND-ISSV---------- 624
Amphimedon_queenslandica 551 KPKR-------FKTRGEKNSMTRYKH---------- 575
Limulus_polyphemus 459 ----------HETLLSFNTGPKNG-QSRK---------- 482
Hydra_vulgaris 354 ----------ERPALTKKQGISHNIYPPT---------- 378
Lingula_anatina 214 ----------RRWTHKENIHPEQH-YTVA---------- 240
Consensus_aa:
Consensus_ss:

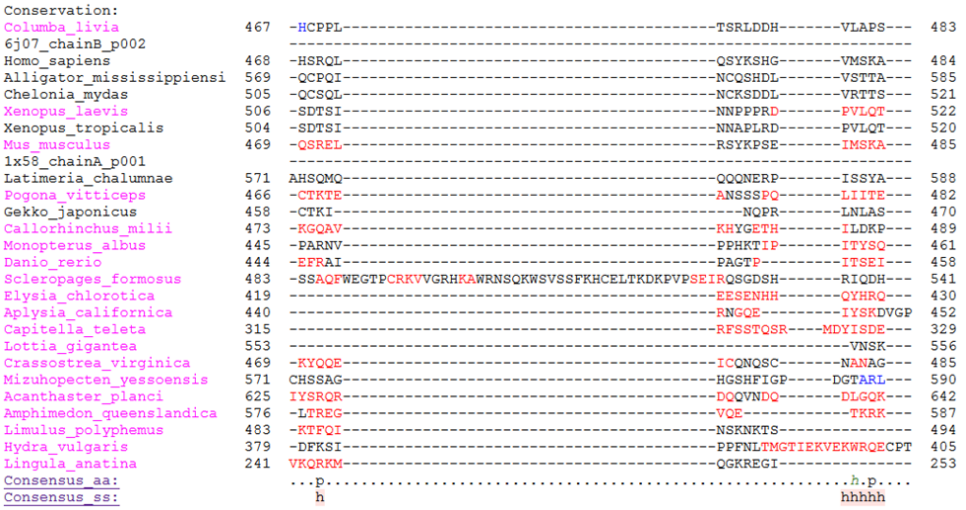
Conservation:
Columba_livia 467 -HCPPL----------TSRLDDH-------VLAPS--- 483
6j07_chainB_p002
Homo_sapiens 468 -HSRQL----------QSYKSHG-------VMSKA--- 484
Alligator_mississippiensi 569 -QCPQI----------NCQSHDL-------VSTTA--- 585
Chelonia_mydas 505 -QCSQL----------NCKSDDL-------VRTTS--- 521
Xenopus_laevis 506 -SDTSI----------NNPPPRD-------PVLQT--- 522
Xenopus_tropicalis 504 -SDTSI----------NNAPLRD-------PVLQT--- 520
Mus_musculus 469 -QSREL----------RSYKPSE-------IMSKA--- 485
1x58_chainA_p001
Latimeria_chalumnae 571 AHSQMQ----------QQQNERP-------ISSYA--- 588
Pogona_vitticeps 466 -CTKTE----------ANSSSPQ-------LIITE--- 482
Gekko_japonicus 458 -CTKI----------NQPR-------LNLAS--- 470
Callorhinchus_milii 473 -KGQAV----------KHYGETH-------ILDKP--- 489
Monopterus_albus 445 -PARNV----------PPHKTIP-------ITYSQ--- 461
Danio_rerio 444 -EFRAI----------PAGTP--------ITSEI--- 458
Scleropages_formosus 483 -SSAQFWEGTPCRKVVGRHKAWRNSQKWSVSSFKHCELTKDKPVPSEIRQSGDSH-------RIQDH--- 541
Elysia_chlorotica 419 ----------EESENHH-------QYHRQ--- 430
Aplysia_californica 440 ----------RNGQE--------IYSKDVGP 452
Capitella_teleta 315 ----------RFSSTQSR----MDYISDE--- 329
Lottia_gigantea 553 ----------VNSK--- 556
Crassostrea_virginica 469 -KYQQE----------ICQNQSC------NANAG--- 485
Mizuhopecten_yessoensis 571 CHSSAG----------HGSHFIGP-----DGTARL--- 590
Acanthaster_planci 625 IYSRQR----------DQQVNDQ------DLGQK--- 642
Amphimedon_queenslandica 576 -LTREG----------VQE----------TKRK--- 587
Limulus_polyphemus 483 -KTFQI----------NSKNKTS---------- 494
Hydra_vulgaris 379 -DFKSI----------PPFNLTMGTIEKVEKWRQECPT 405
Lingua_anatina 241 VKQRKM----------QGKREGI---------- 253
Consensus_aa:
Consensus_ss:

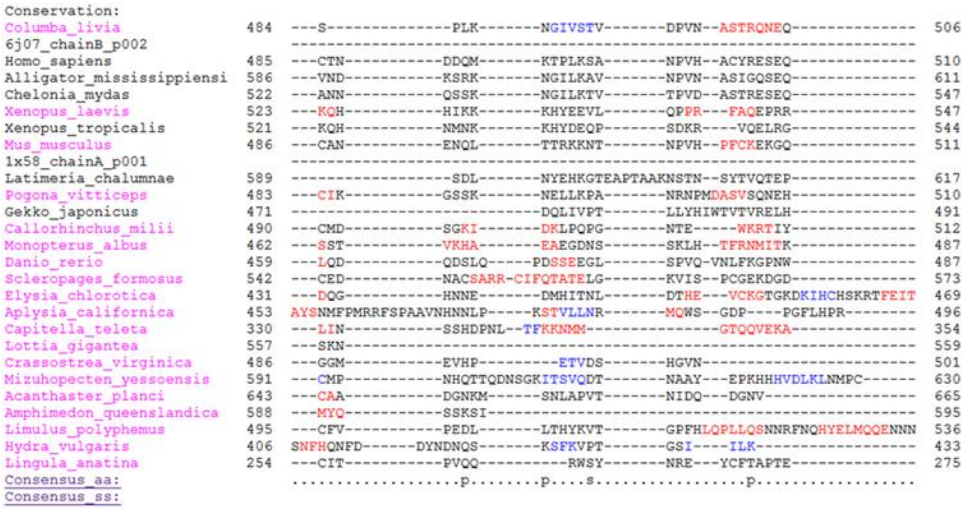
Conservation:
Columba_livia 484 ---S----------PLK-------NGIVSTV-------DPVN--ASTRQNEQ---------- 506
6j07_chainB_p002
Homo_sapiens 485 ---CTN----------DDQM-------KTPLKSA-------NPVH--ACYRESEQ---------- 510
Alligator_mississippiensi 586 ---VND----------KSRK-------NGILKAV-------NPVN--ASIGQSEQ---------- 611
Chelonia_mydas 522 ---ANN----------QSSK-------NGILKTV-------TPVD--ASTRESEQ---------- 547
Xenopus_laevis 523 ---KQH----------HIKK-------KHYEEVL-------QPPR---FAQEPRR---------- 547
Xenopus_tropicalis 521 ---KQH----------NMNK-------KHYDEQP-------SDKR----VQELRG---------- 544
Mus_musculus 486 ---CAN----------ENQL-------TTRKKNT-------NPVH--PFCKEKGQ---------- 511
1x58_chainA_p001
Latimeria_chalumnae 589 ----------SDL-------NYEHKGTEAPTAAKNSTN--SYTVQTEP---------- 617
Pogona_vitticeps 483 ---CIK----------GSSK-------NELLKPA-------NRNPMDASVSQNEH---------- 510
Gekko_japonicus 471 ----------DQLIVPT-------LLYHIWTVTVRELH---------- 491
Callorhinchus_milii 490 ---CMD----------SGKI-------DKLPQPG-------NTE-----WKRTIY---------- 512
Monopterus_albus 462 ---SST----------VKHA-------EAEGDNS-------SKLH--TFRNMITK---------- 487
Danio_rerio 459 ---LQD----------QDSLQ-----PDSSEEGL-------SPVQ-VNLFKGPNW---------- 487
Scleropages_formosus 542 ---CED----------NACSARR-CIFQTATELG-------KVIS--PCGEKDGD---------- 573
Elysia_chlorotica 431 ---DQG----------HNNE-------DMHITNL-------DTHE---VCKGTGKDKIHCHSKRTFEIT 469
Aplysia_californica 453 AYSNMFPMRRFSPAAVNHNNLP-----KSTVLLNR-------MQWS--GDP----PGFLHPR-------- 496
Capitella_teleta 330 ---LIN----------SSHDPNL--TFKKNMM----------GTQQVEKA---------- 354
Lottia_gigantea 557 ---SKN---------- 559
Crassostrea_virginica 486 ---GGM----------EVHP---------ETVDS-------HGVN---------- 501
Mizuhopecten_yessoensis 591 ---CMP----------NHQTTQDNSGKITSVQDT-------NAAY---EPKHHHVDLKLNMPC------ 630
Acanthaster_planci 643 ---CAA----------DGNKM------SNLAPVT-------NIDQ---DGNV---------- 665
Amphimedon_queenslandica 588 ---MYQ----------SSKSI---------- 595
Limulus_polyphemus 495 ---CFV----------PEDL-------LTHYKVT-------GPFHLQPLLQSNNRFNQHYELMQQENNN 536
Hydra_vulgaris 406 SNFHQNFD------DYNDNQS-------KSFKVPT-------GSI----ILK---------- 433
Lingua_anatina 254 ---CIT----------PVQQ----------RWSY-------NRE---YCFTAPTE---------- 275
Consensus_aa:
Consensus_ss:

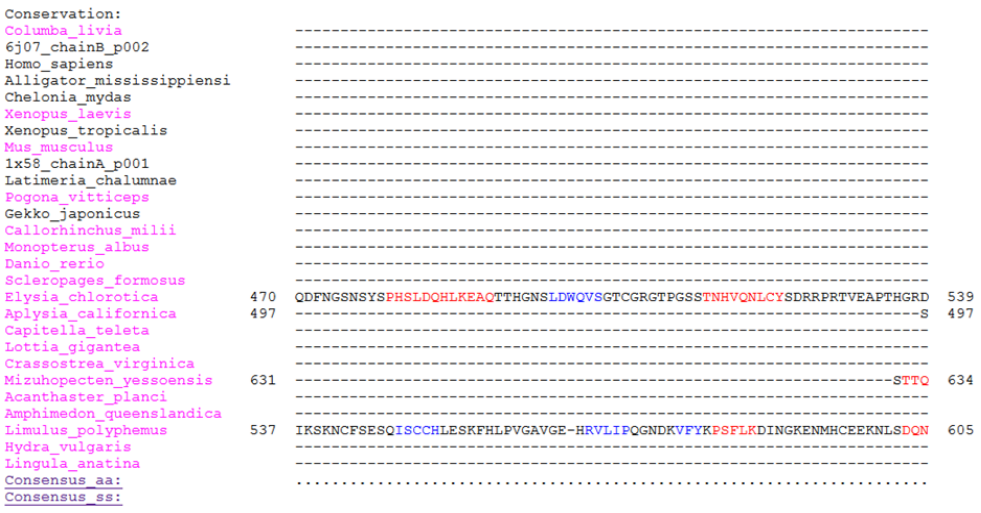
Conservation:
Columba_livia
6j07_chainB_p002
Homo_sapiens
Alligator_mississippiensi
Chelonia_mydas
Xenopus_laevis
Xenopus_tropicalis
Mus_musculus
1x58_chainA_p001
Latimeria_chalumnae
Pogona_vitticeps
Gekko_japonicus
Callorhinchus_milii
Monopterus_albus
Danio_rerio
Scleropages_formosus
Elysia_chlorotica 470 QDFNGSNSYSPHSLDQHLKEAQTTHGNSLDWQVSGTCGRGTPGSSTNHVQNLCYSDRRPRTVEAPTHGRD 539
Aplysia_californica 497 S 497
Capitella_teleta
Lottia_gigantea
Crassostrea_virginica
Mizuhopecten_yessoensis 631 STTQ 634
Acanthaster_planci
Amphimedon_queenslandica
Limulus_polyphemus 537 IKSKNCFSESQISCCHLESKFHLPVGAVGE-HRVLIPQGNDKVFYKPSFLKDINGKENMHCEEKNLSDQN 605
Hydra_vulgaris
Lingua_anatina
Consensus_aa:
Consensus_ss:

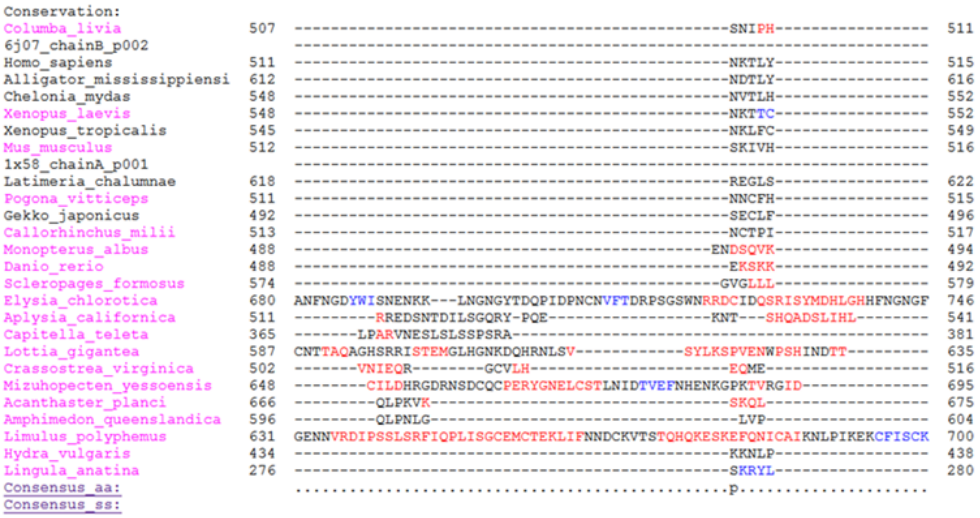
Conservation:
Columba_livia 507 -----SNIPH----- 511
6j07_chainB_p002
Homo_sapiens 511 -----NKTLY----- 515
Alligator_mississippiensi 612 -----NDTLY----- 616
Chelonia_mydas 548 -----NVTLH----- 552
Xenopus_laevis 548 -----NKTTC----- 552
Xenopus_tropicalis 545 -----NKLFC----- 549
Mus_musculus 512 -----SKIVH----- 516
1x58_chainA_p001
Latimeria_chalumnae 618 -----REGLS----- 622
Pogona_vitticeps 511 -----NNCFH----- 515
Gekko_japonicus 492 -----SECLF----- 496
Callorhinchus_milii 513 -----NCTPI----- 517
Monopterus_albus 488 -----ENDSQVK----- 494
Danio_rerio 488 -----EKSKK----- 492
Scleropages_formosus 574 -----GVGLLL----- 579
Elysia_chlorotica 680 ANFNGDYWISNENKK---LNGNGYTDQPIDPNCNVFTDRPSGSWNRRDCIDQSRISYMDHLGHHFNGNGF 746
Aplysia_californica 511 ---------RREDSNTDILSGQRY-PQE-----KNT---SHQADSLIHL-------- 541
Capitella_teleta 365 -------LPARVNESLSLSSPSRA----------- 381
Lottia_gigantea 587 CNTTAQAGHSRRISTEMGLHGNKDQHRNLSV-----SYLKSPVENWPSHINDTT-------- 635
Crassostrea_virginica 502 -------VNIEQR--------GCVLH----------EQME----------- 516
Mizuhopecten_yessoensis 648 --------CILDHRGDRNSDCQCPERYGNELCSTLNIDTVEFNHENKGPKTVRGID---------- 695
Acanthaster_planci 666 ---------QLPKVK----------SKQL----------- 675
Amphimedon_queenslandica 596 ---------QLPNLG----------LVP----------- 604
Limulus_polyphemus 631 GENNVRDIPSSLSRFIQPLISGCEMCTEKLIFNNDCKVTSTQHQKESKEFQNICAIKNLPIKEKCFISCK 700
Hydra_vulgaris 434 -----KKNLP----------- 438
Lingula_anatina 276 -----SKRYL----------- 280
Consensus_aa:
Consensus_ss:


Conservation:
Columba_livia 512 ----------SLNELQTGIVLQRH---------- 525
6j07_chainB_p002
Homo_sapiens 516 ----------KAKSSCN------QNLH---------- 526
Alligator_mississippiensi 617 ----------SVDKLQRGSVLSHL---------- 630
Chelonia_mydas 553 ----------SADKLQTGSVQKGH---------- 566
Xenopus_laevis 553 ----------RTDS------KKTK---------- 560
Xenopus_tropicalis 550 ----------RINY------KETR---------- 557
Mus_musculus 517 ----------ETTP------SCAQ---------- 524
1x58_chainA_p001
Latimeria_chalumnae 623 ----------STSK------ARLE---------- 630
Pogona_vitticeps 516 ----------SKSS------IAKR---------- 523
Gekko_japonicus
Callorhinchus_milii 518 ----------KRNL------DYRY---------- 525
Monopterus_albus 495 ----------KISL------STLK---------- 502
Danio_rerio 493 ----------REHK------QKRE---------- 500
Scleropages_formosus 580 ----------HKPDQ------AGCSS---------- 589
Elysia_chlorotica 747 -SDYSNGQLIGNGHSDSRSGQLNVS------NCIDHRNQSFNDNSHSDPRNRNEAGMENIGHHSGNLHSY 809
Aplysia_californica 542 ----------LRGGTFQSSFTSHGLVPDLTMNCNEVHKDIPNEAARTGDVSSP---------- 584
Capitella_teleta 382 ----------PLY------NRHELPKDVMQMVD---------- 398
Lottia_gigantea 636 ----------HQGIPKESSYNYRNNSTALASCCQDHHDQRQLTHDRS---------- 672
Crassostrea_virginica 517 ----------NQNTG------HPSPN---------- 526
Mizuhopecten_yessoensis 696 ----------QVTDVTTDNS------RCESAGR---------- 712
Acanthaster_planci 676 ----------CDRVN------KYIRN---------- 685
Amphimedon_queenslandica 605 ----------YTSTP---------- 609
Limulus_polyphemus 701 FQEQNIMSDESGCKHCYQSQWFEDT------KNNSTEKQITDNISKTKKHPEEKGSIPLEACNCFCCHKE 764
Hydra_vulgaris 439 ----------KFTE------NFQE---------- 446
Lingula_anatina 281 ----------NFQD------SIIESSN---------- 291
Consensus_aa:
Consensus_ss:
hhhh

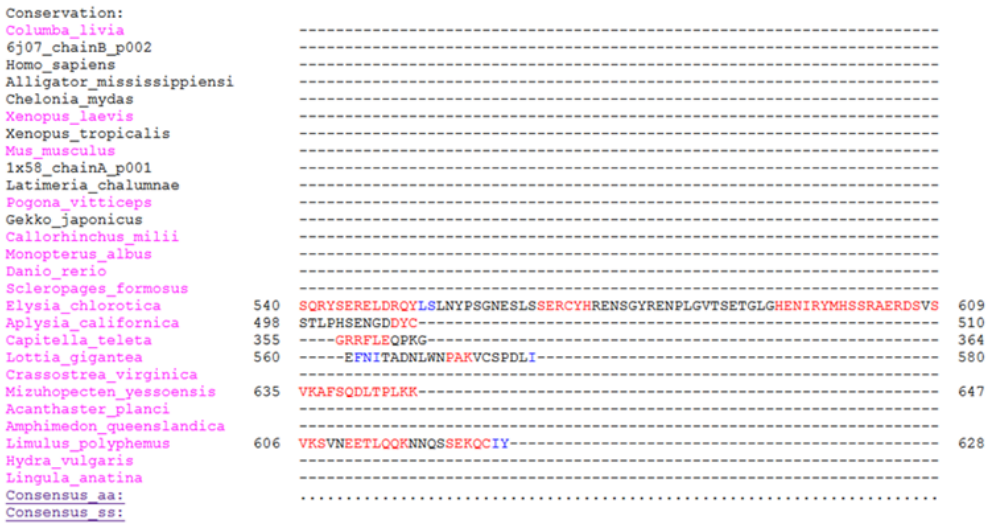
Conservation:
Columba_livia
6j07_chainB_p002
Homo_sapiens
Alligator_mississippiensi
Chelonia_mydas
Xenopus_laevis
Xenopus_tropicalis
Mus_musculus
1x58_chainA_p001
Latimeria_chalumnae
Pogona_vitticeps
Gekko_japonicus
Callorhinchus_milii
Monopterus_albus
Danio_rerio
Scleropages_formosus
Elysia_chlorotica 540 SQRYSERELDRQYLSLNYPSGNESLSSERCYHRENSGYRENPLGVTSETGLGHENIRYMHSSRAERDSVS 609
Aplysia_californica 498 STLPHSENGDDYC---------- 510
Capitella_teleta 355 ----GRRFLEQPKG---------- 364
Lottia_gigantea 560 -----EFNITADNLWNPAKVCSPDLI---------- 580
Crassostrea_virginica
Mizuhopecten_yessoensis 635 VKAFSQDLTPLKK---------- 647
Acanthaster_planci
Amphimedon_queenslandica
Limulus_polyphemus 606 VKSVNEETLQQKNNQSSEKQCIY---------- 628
Hydra_vulgaris
Lingula_anatina
Consensus_aa:
Consensus_ss:


Conservation:
Columba_livia
6j07_chainB_p002
Homo_sapiens
Alligator_mississippiensi
Chelonia_mydas
Xenopus_laevis
Xenopus_tropicalis
Mus_musculus
1x58_chainA_p001
Latimeria_chalumnae
Pogona_vitticeps
Gekko_japonicus
Callorhinchus_milii
Monopterus_albus
Danio_rerio
Scleropages_formosus
Elysia_chlorotica
Aplysia_californica
Capitella_teleta
Lottia_gigantea
Crassostrea_virginica
Mizuhopecten_yessoensis
Acanthaster_planci
Amphimedon_queenslandica
Limulus_polyphemus
Hydra_vulgaris
Lingula_anatina
Consensus_aa:
Consensus_ss:


Conservation:
Columba_livia
6j07_chainB_p002
Homo_sapiens
Alligator_mississippiensi
Chelonia_mydas
Xenopus_laevis
Xenopus_tropicalis
Mus_musculus
1x58_chainA_p001
Latimeria_chalumnae
Pogona_vitticeps
Gekko_japonicus
Callorhinchus_milii
Monopterus_albus
Danio_rerio
Scleropages_formosus
Elysia_chlorotica
Aplysia_californica
Capitella_teleta
Lottia_gigantea
Crassostrea_virginica
Mizuhopecten_yessoensis
Acanthaster_planci
Amphimedon_queenslandica
Limulus_polyphemus
Hydra_vulgaris
Lingula_anatina
Consensus_aa:
Consensus_ss:

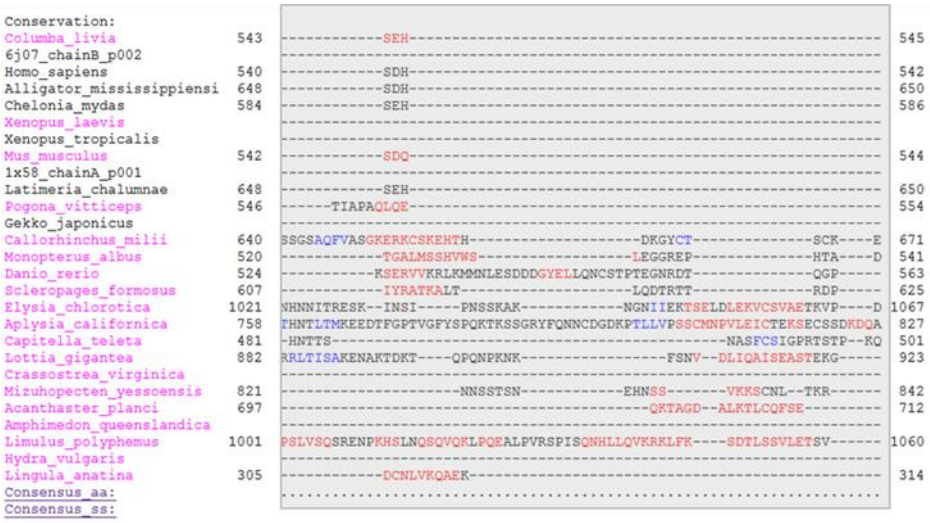
Conservation:
Columba_livia
6j07_chainB_p002
Homo_sapiens
Alligator_mississippiensi
Chelonia_mydas
Xenopus_laevis
Xenopus_tropicalis
Mus_musculus
1x58_chainA_p001
Latimeria_chalumnae
Pogona_vitticeps
Gekko_japonicus
Callorhinchus_milii
Monopterus_albus
Danio_rerio
Scleropages_formosus
Elysia_chlorotica
Aplysia_californica
Capitella_teleta
Lottia_gigantea
Crassostrea_virginica
Mizuhopecten_yessoensis
Acanthaster_planci
Amphimedon_queenslandica
Limulus_polyphemus
Hydra_vulgaris
Lingula_anatina
Consensus_aa:
Consensus_ss:

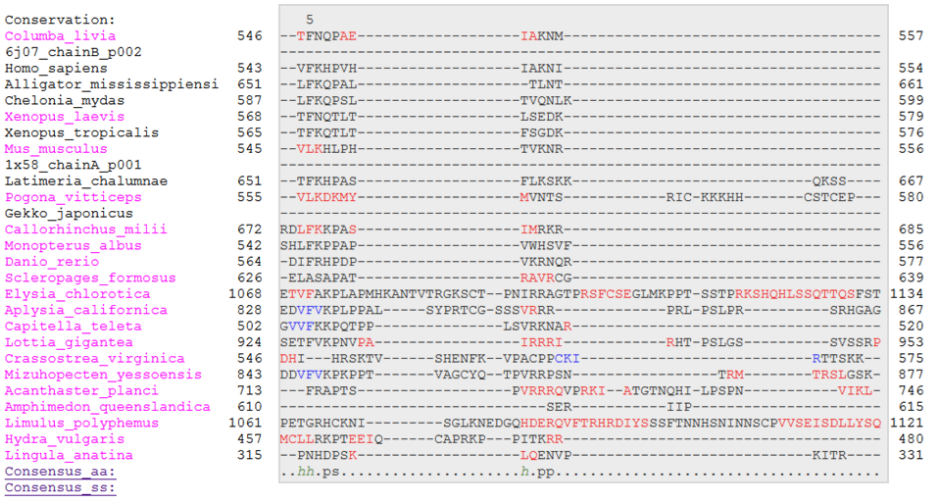
Conservation:
Columba_livia
6j07_chainB_p002
Homo_sapiens
Alligator_mississippiensi
Chelonia_mydas
Xenopus_laevis
Xenopus_tropicalis
Mus_musculus
1x58_chainA_p001
Latimeria_chalumnae
Pogona_vitticeps
Gekko_japonicus
Callorhinchus_milii
Monopterus_albus
Danio_rerio
Scleropages_formosus
Elysia_chlorotica
Aplysia_californica
Capitella_teleta
Lottia_gigantea
Crassostrea_virginica
Mizuhopecten_yessoensis
Acanthaster_planci
Amphimedon_queenslandica
Limulus_polyphemus
Hydra_vulgaris
Lingula_anatina
Consensus_aa:
Consensus_ss:

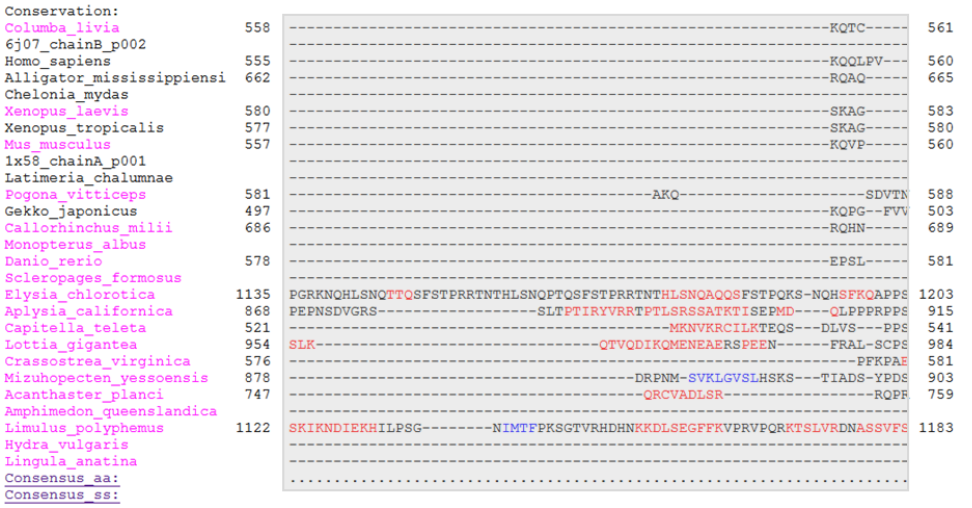
Conservation:
Columba_livia 558 KQTC 561
6j07_chainB_p002
Homo_sapiens 555 KQQLPV 560
Alligator_mississippiensi 662 RQAQ 665
Chelonia_mydas
Xenopus_laevis 580 SKAG 583
Xenopus_tropicalis 577 SKAG 580
Mus_musculus 557 KQVP 560
1x58_chainA_p001
Latimeria_chalumnae
Pogona_vitticeps 581 AKQ SDVTN 588
Gekko_japonicus 497 KQPG--FVV 503
Callorhinchus_milii 686 RQHN 689
Monopterus_albus
Danio_rerio 578 EPSL 581
Scleropages_formosus
Elysia_chlorotica 1135 PGRKNQHLSNQTTQSFSTPRRTNTHLSNQPTQSFSTPRRTNTHLSNQAQQSFSTPQKS-NQHSFKQAPPS 1203
Aplysia_californica 868 PEPNSDVGRS SLTPTIRYVRRTPTLSRSSATKTISEPMD QLPPPRPPS 915
Capitella_teleta 521 MKNVKRCILKTEQS---DLVS---PPS 541
Lottia_gigantea 954 SLK QTVQDIKQMENEAERSPEEN FRAL-SCPS 984
Crassostrea_virginica 576 PFKPAE 581
Mizuhopecten_yessoensis 878 DRPNM-SVKLGVSLHSKS---TIADS-YPDS 903
Acanthaster_planci 747 QRCVADLSR RQPR 759
Amphimedon_queenslandica
Limulus_polyphemus 1122 SKIKNDIEKHILPSG NIMTFPKSGTVRHDHNKKDLSEGFFKVPRVPQRKTSLVRDNASSVFS 1183
Hydra_vulgaris
Lingula_anatina
Consensus_aa:
Consensus_ss:

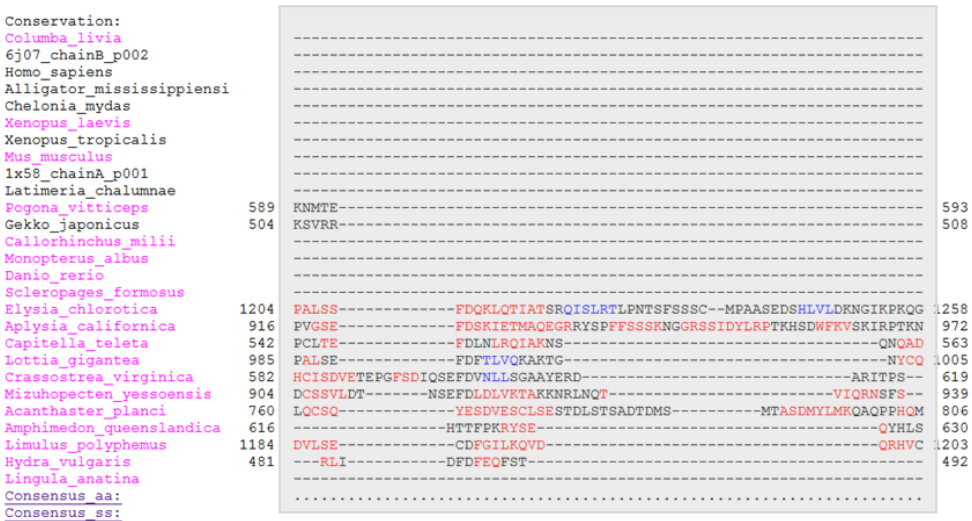
Conservation:
Columba_livia
6j07_chainB_p002
Homo_sapiens
Alligator_mississippiensi
Chelonia_mydas
Xenopus_laevis
Xenopus_tropicalis
Mus_musculus
1x58_chainA_p001
Latimeria_chalumnae
Pogona_vitticeps 589 KNMTE 593
Gekko_japonicus 504 KSVRR 508
Callorhinchus_milii
Monopterus_albus
Danio_rerio
Scleropages_formosus
Elysia_chlorotica 1204 PALSS FDQKLQTIATSRQISLRTLPNTSFSSSC--MPAASEDSHLVLDKNGIKPKQG 1258
Aplysia_californica 916 PVGSE FDSKIETMAQEGRRYSPFFSSSKNGGRSSIDYLRPTKHSDWFKVSKIRPTKN 972
Capitella_teleta 542 PCLTE FDLNLRQIAKNS QNQAD 563
Lottia_gigantea 985 PALSE FDFTLVQKAKTG NYCQ 1005
Crassostrea_virginica 582 HCISDVETEPGFSDIQSEFDVNLLSGAAYERD ARITPS-- 619
Mizuhopecten_yessoensis 904 DCSSVLDT NSEFDLDLVKTAKKNRLNQT VIQRNSFS-- 939
Acanthaster_planci 760 LQCSQ YESDVESCLSESTDLSTSADTDMS MTASDMYLMKQAQPPHQM 806
Amphimedon_queenslandica 616 HTTFPKRYSE QYHLS 630
Limulus_polyphemus 1184 DVLSE CDFGILKQVD QRHVC 1203
Hydra_vulgaris 481 RLI DFDFEQFST 492
Lingula_anatina
Consensus_aa:
Consensus_ss:

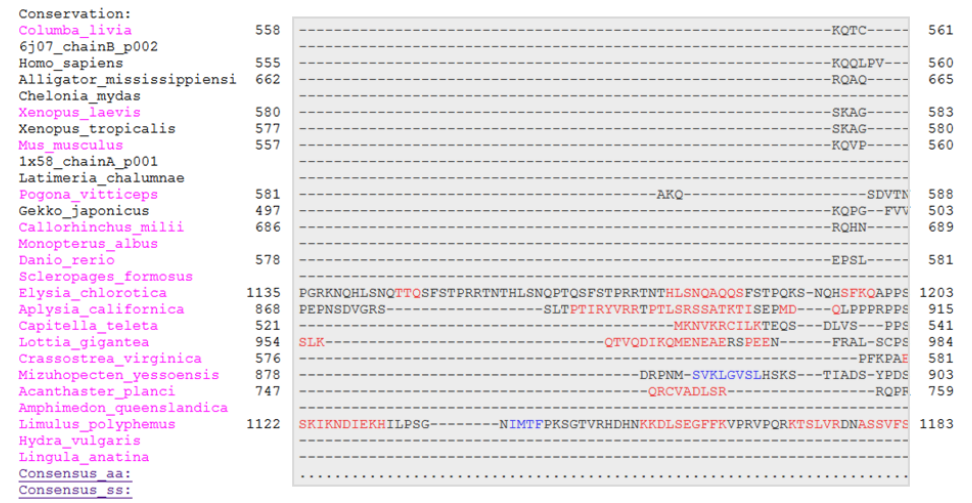
Conservation:
Columba_livia 558 KQTC 561
6j07_chainB_p002
Homo_sapiens 555 KQQLPV 560
Alligator_mississippiensi 662 RQAQ 665
Chelonia_mydas
Xenopus_laevis 580 SKAG 583
Xenopus_tropicalis 577 SKAG 580
Mus_musculus 557 KQVP 560
1x58_chainA_p001
Latimeria_chalumnae
Pogona_vitticeps 581 AKQ SDVTN 588
Gekko_japonicus 497 KQPG--FVV 503
Callorhinchus_milii 686 RQHN 689
Monopterus_albus
Danio_rerio 578 EPSL 581
Scleropages_formosus
Elysia_chlorotica 1135 PGRKNQHLSNQTTQSFSTPRRTNTHLSNQPTQSFSTPRRTNTHLSNQAQQSFSTPQKS-NQHSFKQAPPS 1203
Aplysia_californica 868 PEPNSDVGRS SLTPTIRYVRRTPTLSRSSATKTISEPMD QLPPPRPPS 915
Capitella_teleta 521 MKNVKRCILKTEQS---DLVS---PPS 541
Lottia_gigantea 954 SLK QTVQDIKQMENEAERSPEEN FRAL-SCPS 984
Crassostrea_virginica 576 PFKPAE 581
Mizuhopecten_yessoensis 878 DRPNM-SVKLGVSLHSKS---TIADS-YPDS 903
Acanthaster_planci 747 QRCVADLSR RQPR 759
Amphimedon_queenslandica
Limulus_polyphemus 1122 SKIKNDIEKHILPSG NIMTFPKSGTVRHDHNKKDLSEGFFKVPRVPQRKTSLVRDNASSVFS 1183
Hydra_vulgaris
Lingula_anatina
Consensus_aa:
Consensus_ss:

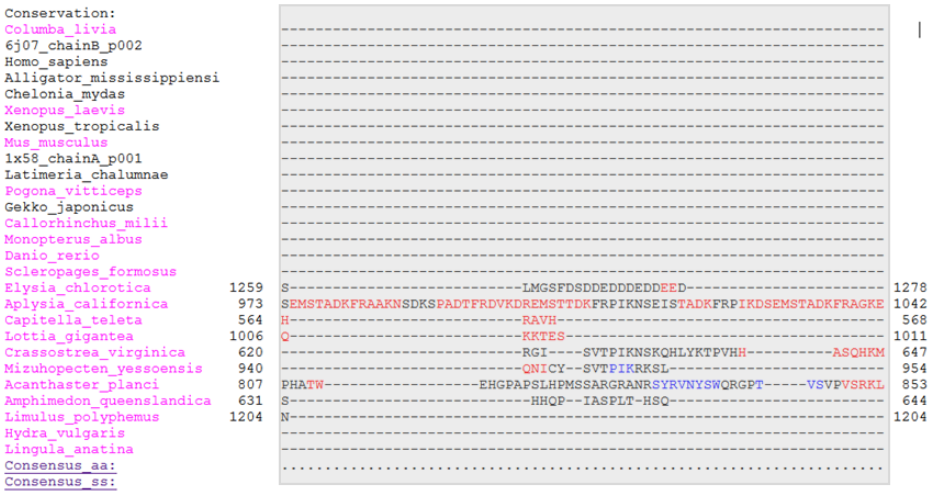
Conservation:
Columba_livia
6j07_chainB_p002
Homo_sapiens
Alligator_mississippiensi
Chelonia_mydas
Xenopus_laevis
Xenopus_tropicalis
Mus_musculus
1x58_chainA_p001
Latimeria_chalumnae
Pogona_vitticeps
Gekko_japonicus
Callorhinchus_milii
Monopterus_albus
Danio_rerio
Scleropages_formosus
Elysia_chlorotica 1259 S-----LMGSFDSDDEDDDEDDEED----- 1278
Aplysia_californica 973 SEMSTADKFRAAKNSDKSPADTFRDVKDREMSTTDKFRPIKNSEISTADKFRPIKDSEMSTADKFRAGKE 1042
Capitella_teleta 564 H-----RAVH----- 568
Lottia_gigantea 1006 Q-----KKTES----- 1011
Crassostrea_virginica 620 -----RGI----SVTPIKNSKQHLYKTPVHH---------ASQHKM 647
Mizuhopecten_yessoensis 940 -----QNICY--SVTPIKRKSL----- 954
Acanthaster_planci 807 PHATW----------EHGPAPSLHPMSSARGRANRSYRVNYSWQRGPT-----VSVPVSRKL 853
Amphimedon_queenslandica 631 S-----HHQP--IASPLT-HSQ----- 644
Limulus_polyphemus 1204 N----------
Hydra_vulgaris
Lingula_anatina
Consensus_aa:
Consensus_ss:


Conservation:
Columba_livia
6j07_chainB_p002
Homo_sapiens
Alligator_mississippiensi
Chelonia_mydas
Xenopus_laevis
Xenopus_tropicalis
Mus_musculus
1x58_chainA_p001
Latimeria_chalumnae
Pogona_vitticeps
Gekko_japonicus
Callorhinchus_milii
Monopterus_albus
Danio_rerio
Scleropages_formosus
Elysia_chlorotica 1279 -DNTLYQSSTSDVDSTRSDSSNTHHKD----------NPA 1307
Aplysia_californica 1043 SDRSSEDRFRATRESDRSSEDRFRATRESDRSSEDRFRATRESDRSSEDRFRPNKENNEPTADCFRSSQN 1112
Capitella_teleta 569 ---TWLQKS----- 574
Lottia_gigantea 1012 ---TKQTESHSSGLNSAGTSS----- 1029
Crassostrea_virginica 648 KMFRHTYYHNERTGLQTPRFS----- 668
Mizuhopecten_yessoensis 955 ---PIKELQREN---DRTRIREDRPNVGSTPCSVKSIDRM----------TDHFHDENYCENYSD 1003
Acanthaster_planci 854 SELTNLSVSHHGIGRDSITKA----- 874
Amphimedon_queenslandica 645 ---PLVAPS-------TPKRQ----- 655
Limulus_polyphemus 1205 ----------HSVNKQP----- 1211
Hydra_vulgaris
Lingula_anatina
Consensus_aa:
Consensus_ss:

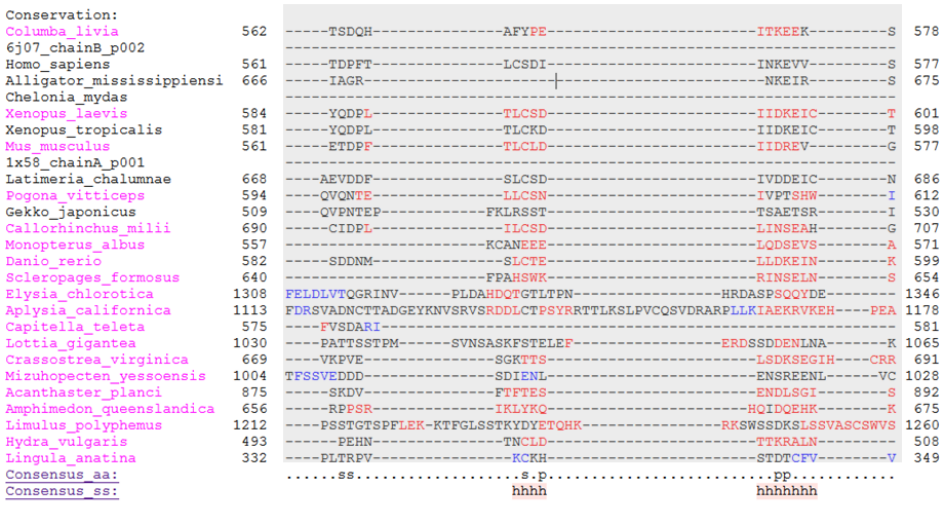
Conservation:
Columba_livia 562 -----TSDQH----------AFYPE----------ITKEEK--------S 578
6j07_chainB_p002
Homo_sapiens 561 -----TDPFT----------LCSDI----------INKEVV--------S 577
Alligator_mississippiensi 666 -----IAGR----------NKEIR--------S 675
Chelonia_mydas
Xenopus_laevis 584 -----YQDPL----------TLCSD----------IIDKEIC--------T 601
Xenopus_tropicalis 581 -----YQDPL----------TLCKD----------IIDKEIC--------T 598
Mus_musculus 561 -----ETDPF----------TLCLD----------IIDREV--------G 577
1x58_chainA_p001
Latimeria_chalumnae 668 ----AEVDDF----------SLCSD----------IVDDEIC--------N 686
Pogona_vitticeps 594 ----QVQNTE----------LLCSN----------IVPTSHW--------I 612
Gekko_japonicus 509 ----QVPNTEP----------FKLRSST----------TSAETSR--------I 530
Callorhinchus_milii 690 -----CIDPL----------ILCSD----------LINSEAH--------G 707
Monopterus_albus 557 ----------KCANEEE----------LQDSEVS--------A 571
Danio_rerio 582 -----SDDNM----------SLCTE----------LLDKEIN--------K 599
Scleropages_formosus 640 ----------FPAHSWK----------RINSELN--------S 654
Elysia_chlorotica 1308 FELDLVTQGRINV------PLDAHDQTGTLTPN----------HRDASPSQQYDE-------- 1346
Aplysia_californica 1113 FDRSVADNCTTADGEYKNVSRVSRDDLCTPSYRRTTLKSLPVCQSVDRARPLLKIAEKRVKEH----PEA 1178
Capitella_teleta 575 ----FVSDARI----------
Lottia_gigantea 1030 ----PATTSSTPM------SVNSASKFSTELEF----------ERDSSDDENLNA-------K 1065
Crassostrea_virginica 669 ----VKPVE----------SGKTTS----------LSDKSEGIH----CRR 691
Mizuhopecten_yessoensis 1004 TFSSVEDDD----------SDIENL----------ENSREENL------VC 1028
Acanthaster_planci 875 -----SKDV----------FTFTES----------ENDLSGI--------S 892
Amphimedon_queenslandica 656 -----RPPSR----------IKLYKQ----------HQIDQEHK--------K 675
Limulus_polyphemus 1212 ----PSSTGTSPFLEK-KTFGLSSTKYDYETQHK----------RKSWSSDKSLSSVASCSWVS 1260
Hydra_vulgaris 493 ------PEHN----------TNCLD----------TTKRALN---------- 508
Lingula_anatina 332 ----PLTRPV----------KCKH----------STDTCFV--------V 349
Consensus_aa:
Consensus_ss:

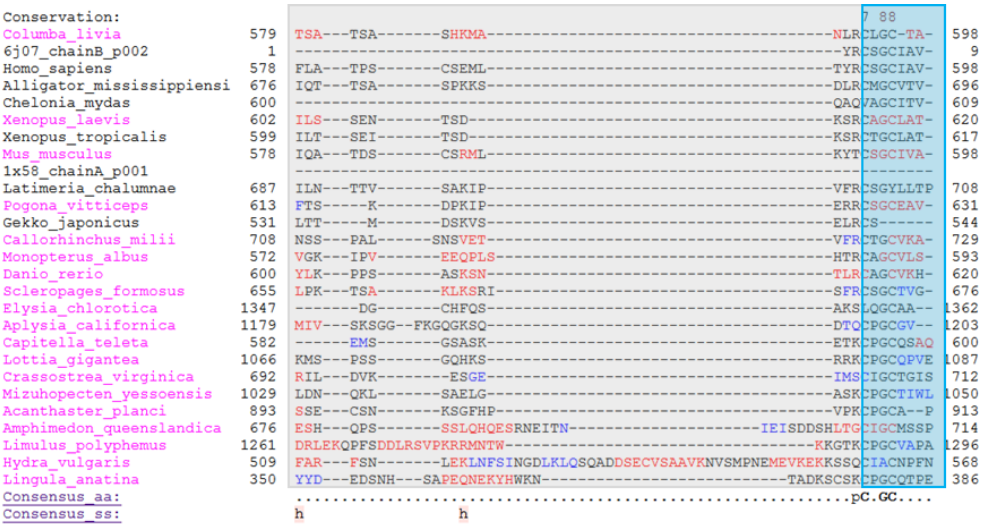
Conservation:
Columba_livia 579 TSA---TSA-------SHKMA---------- 598
6j07_chainB_p002 1 ---------- 9
Homo_sapiens 578 FLA---TPS-------CSEML---------- 598
Alligator_mississippiensi 676 IQT---TSA-------SPKKS---------- 696
Chelonia_mydas 600 ---------- 609
Xenopus_laevis 602 ILS---SEN-------TSD---------- 620
Xenopus_tropicalis 599 ILT---SEI-------TSD---------- 617
Mus_musculus 578 IQA---TDS-------CSRML---------- 598
1x58_chainA_p001
Latimeria_chalumnae 687 ILN---TTV-------SAKIP---------- 708
Pogona_vitticeps 613 FTS-----K-------DPKIP---------- 631
Gekko_japonicus 531 LTT-----M-------DSKVS---------- 544
Callorhinchus_milii 708 NSS---PAL------SNSVET---------- 729
Monopterus_albus 572 VGK---IPV-------EEQPLS---------- 593
Danio_rerio 600 YLK---PPS-------ASKSN---------- 620
Scleropages_formosus 655 LPK---TSA-------KLKSRI---------- 676
Elysia_chlorotica 1347 -------DG-------CHFQS---------- 1362
Aplysia_californica 1179 MIV---SKSGG--FKGQGKSQ---------- 1203
Capitella_teleta 582 ------EMS-------GSASK---------- 600
Lottia_gigantea 1066 KMS---PSS-------GQHKS---------- 1087
Crassostrea_virginica 692 RIL---DVK--------ESGE---------- 712
Mizuhopecten_yessoensis 1029 LDN---QKL-------SAELG---------- 1050
Acanthaster_planci 893 SSE---CSN-------KSGFHP---------- 913
Amphimedon_queenslandica 676 ESH---QPS-------SSLQHQESRNEITN---------- 714
Limulus_polyphemus 1261 DRLEKQPFSDDLRSVPKRRMNTW---------- 1296
Hydra_vulgaris 509 FAR---FSN-------LEKLNFSINGDLKLQSQADDSECVSAAVKNVSMPNEMEVKEKKSSQ 568
Lingula_anatina 350 YYD---EDSNH---SAPEQNEKYHWKN---------- 386
Consensus_aa:
Consensus_ss:

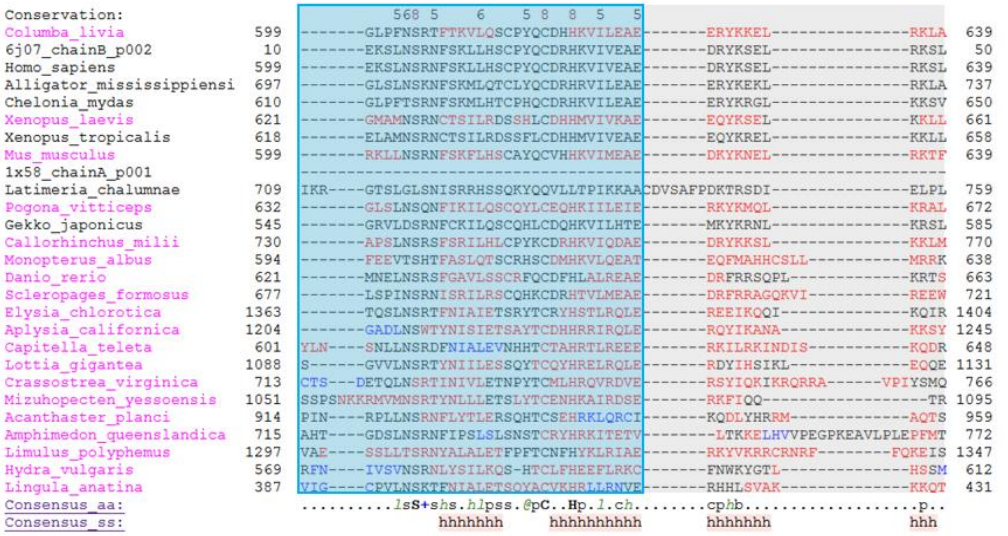
Conservation:
Columba_livia 599 -------GLPFNSRTFTKVLQSCPYQCDHHKVILEAE------- 639
6j07_chainB_p002 10 -------EKSLNSRNFSKLLHSCPYQCDRHKVIVEAE------- 50
Homo_sapiens 599 -------EKSLNSRNFSKLLHSCPYQCDRHKVIVEAE------- 639
Alligator_mississippiensi 697 -------GLSLNSKNFSKMLQTCLYQCDRHRVILEAE------- 737
Chelonia_mydas 610 -------GLPFTSRNFSKMLHTCPHQCDRHKVILEAE------- 650
Xenopus_laevis 621 -------GMAMNSRNCTSILRDSSHLCDHHMVIVKAE------- 661
Xenopus_tropicalis 618 -------ELAMNSRNCTSILRDSSFLCDHHMVIVEAE------- 658
Mus_musculus 599 -------RKLLNSRNFSKFLHSCAYQCVHHKVIMEAE------- 639
1x58_chainA_p001
Latimeria_chalumnae 709 IKR----GTSLGLSNISRRHSSQKYQQVLLTPIKKAA 745
Pogona_vitticeps 632 -------GLSLNSQNFIKILQSCQYLCEQHKIILEIE------- 672
Gekko_japonicus 545 -------GRVLDSRNFCKILQSCQHLCDQHKVILHTE------- 585
Callorhinchus_milii 730 -------APSLNSRSFSRILHLCPYKCDRHKVIQDAE------- 770
Monopterus_albus 594 -------FEEVTSHTFASLQTSCRHSCDMHKVLQEAT------- 638
Danio_rerio 621 -------MNELNSRSFGAVLSSCRFQCDFHLALREAE------- 663
Scleropages_formosus 677 -------LSPINSRNISRILRSCQHKCDRHTVLMEAE------- 721
Elysia_chlorotica 1363 -------TQSLNSRTFNIAIETSRYTCRYHSTLRQLE------- 1404
Aplysia_californica 1204 -------GADLNSWTYNISIETSAYTCDHHRRIRQLE------- 1245
Capitella_teleta 601 YLN----SNLLNSRDFNIALEVNHHTCTAHRTLREEE------- 648
Lottia_gigantea 1088 S------GVVLNSRTYNIILESSQYTCQYHRELRQLE------- 1131
Crassostrea_virginica 713 CTS---DETQLNSRTINIVLETNPYTCMLHRQVRDVE------- 766
Mizuhopecten_yessoensis 1051 SSPSNKKRMVMNSRTYNLLLETSLYTCENHKAIRDSE------- 1095
Acanthaster_planci 914 PIN----RPLLNSRNFLYTLERSQHTCSEHRKLQRCI------- 959
Amphimedon_queenslandica 715 AHT----GDSLNSRNFIPSLSLSNSTCRYHRKITETV-------- 772
Limulus_polyphemus 1297 VAE----SSLLTSRNYALALETFPFTCNFHYKLRIAE------- 1347
Hydra_vulgaris 569 RFN----IVSVNSRNLYSILKQS-HTCLFHEEFLRKC------- 612
Lingula_anatina 387 VIG----CPVLNSKTFNIALETSQYACVKHRLLRNVE------- 431
Consensus_aa:
Consensus_ss:

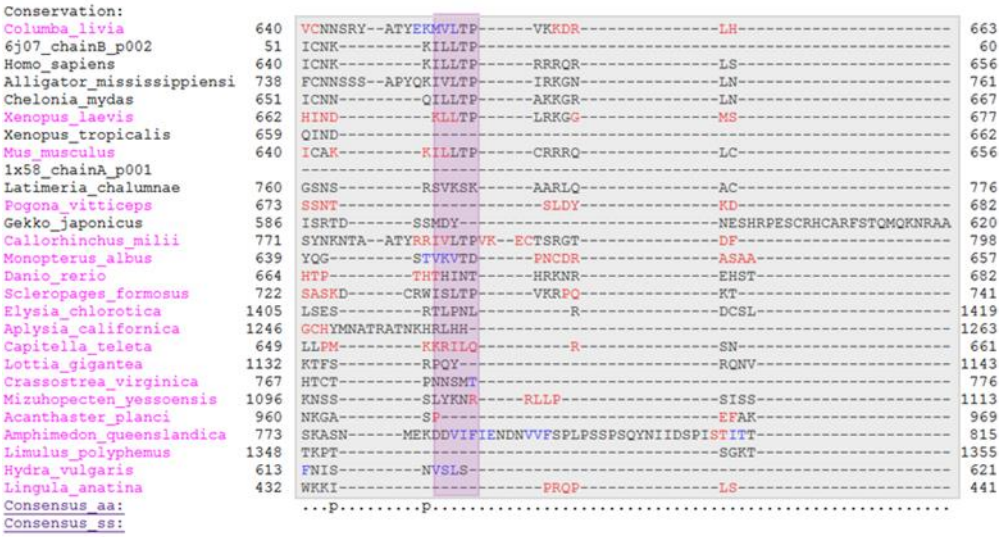
Conservation:
Columba_livia 640 VCNNSRY--ATYEKMVLTP------VKKDR---------- 663
6j07_chainB_p002 51 ICNK---------KILLTP---------- 60
Homo_sapiens 640 ICNK---------KILLTP------RRRQR---------- 656
Alligator_mississippiensi 738 FCNNSSS--APYQKIVLTP------IRKGN---------- 761
Chelonia_mydas 651 ICNN---------QILLTP------AKKGR---------- 667
Xenopus_laevis 662 HIND---------KLLTP------LRKGG---------- 677
Xenopus_tropicalis 659 QIND---------- 662
Mus_musculus 640 ICAK---------KILLTP------CRRRQ---------- 656
1x58_chainA_p001
Latimeria_chalumnae 760 GSNS---------RSVKSK------AARLQ---------- 776
Pogona_vitticeps 673 SSNT---------SLDY---------- 682
Gekko_japonicus 586 ISRTD-------SSMDY---------- 620
Callorhinchus_milii 771 SYNKNTA--ATYRRIVLTPVK--ECTSRGT---------- 798
Monopterus_albus 639 YQG---------STVKVTD------PNCDR---------- 657
Danio_rerio 664 HTP---------THTHINT------HRKNR---------- 682
Scleropages_formosus 722 SASKD------CRWISLTP------VKRPQ---------- 741
Elysia_chlorotica 1405 LSES---------RTLPNL---------- 1419
Aplysia_californica 1246 GCHYMNATRATNKHRLHH---------- 1263
Capitella_teleta 649 LLPM---------KKRILQ---------- 661
Lottia_gigantea 1132 KTFS---------RPQY---------- 1143
Crassostrea_virginica 767 HTCT---------PNNSMT---------- 776
Mizuhopecten_yessoensis 1096 KNSS---------SLYKNR------RLLP---------- 1113
Acanthaster_planci 960 NKGA---------SP---------- 969
Amphimedon_queenslandica 773 SKASN------MEKDDVIFIENDNVVFSPLPSSPSQYNIIDSPI 815
Limulus_polyphemus 1348 TKPT---------- 1355
Hydra_vulgaris 613 FNIS---------NVSLS---------- 621
Lingula_anatina 432 WKKI---------PRQP---------- 441
Consensus_aa:
Consensus_ss:

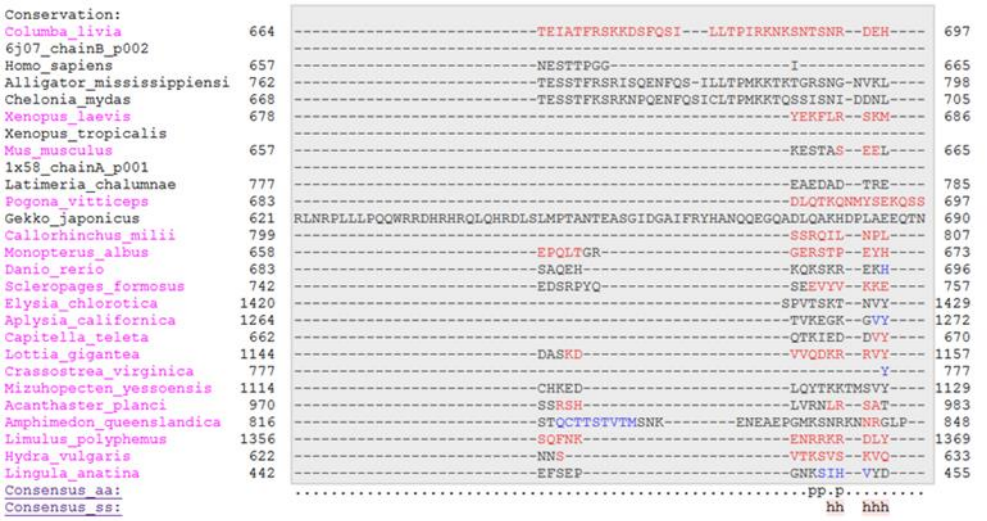
Conservation:
Columba_livia 664 TEIATFRSKKDSFQSI---LLTPIRKNKSNTSNR--DEH---- 697
6j07_chainB_p002
Homo_sapiens 657 NESTTPGG----------I---------- 665
Alligator_mississippiensi 762 TESSTFRSRISQENFQS-ILLTPMKKTKTGRSNG-NVKL---- 798
Chelonia_mydas 668 TESSTFKSRKNPQENFQSICLTPMKKTQSSISNI-DDNL---- 705
Xenopus_laevis 678 YEKFLR--SKM---- 686
Xenopus_tropicalis
Mus_musculus 657 KESTAS--EEL---- 665
1x58_chainA_p001
Latimeria_chalumnae 777 EAEDAD--TRE---- 785
Pogona_vitticeps 683 DLQTKQNMYSEKQSS 697
Gekko_japonicus 621 RLNRPLLLPQQWRRDHRHRQLQHRDLSLMPTANTEASGIDGAIFRYHANQQEGQADLQAKHDPLAEEQTN 690
Callorhinchus_milii 799 SSRQIL--NPL---- 807
Monopterus_albus 658 EPQLTGR----------GERSTP--EYH---- 673
Danio_rerio 683 SAQEH----------KQKSKR--EKH---- 696
Scleropages_formosus 742 EDSRPYQ----------SEEVYV--KKE---- 757
Elysia_chlorotica 1420 SPVTSKT--NVY---- 1429
Aplysia_californica 1264 TVKEGK--GVY---- 1272
Capitella_teleta 662 QTKIED--DVY---- 670
Lottia_gigantea 1144 DASKD----------VVQDKR--RVY---- 1157
Crassostrea_virginica 777 Y---- 777
Mizuhopecten_yessoensis 1114 CHKED----------LQYTKKTMSVY---- 1129
Acanthaster_planci 970 SSRSH----------LVRNLR--SAT---- 983
Amphimedon_queenslandica 816 STQCTTSTVTMSNK--------ENEAEPGMKSNRKNNRGLP-- 848
Limulus_polyphemus 1356 SQFNK----------ENRRKR--DLY---- 1369
Hydra_vulgaris 622 NNS----------VTKSVS--KVQ---- 633
Lingula_anatina 442 EFSEP----------GNKSIH--VYD---- 455
Consensus_aa:
Consensus_ss:

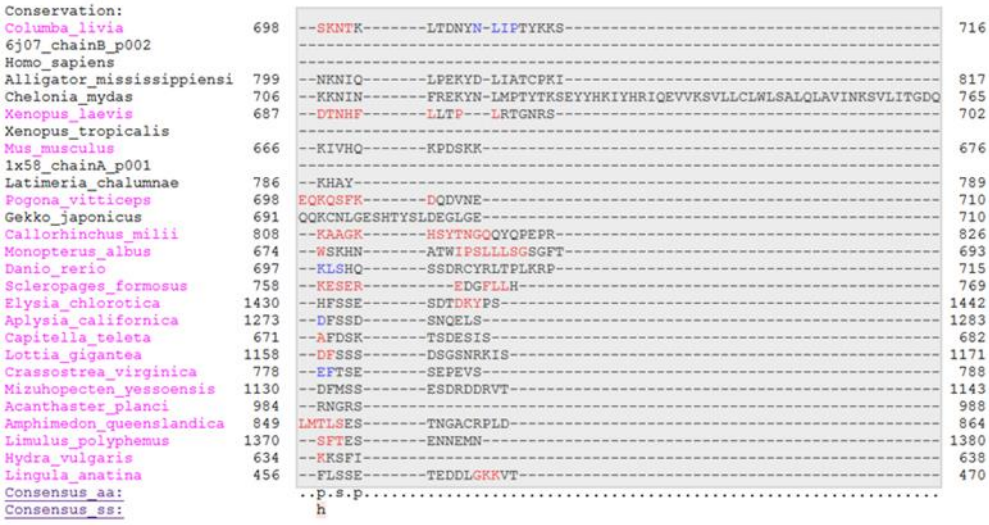
Conservation:
Columba_livia 698 --SKNTK-------LTDNYN-LIPTYKKS---------- 716
6j07_chainB_p002
Homo_sapiens
Alligator_mississippiensi 799 --NKNIQ-------LPEKYD-LIATCPKI---------- 817
Chelonia_mydas 706 --KKNIN-------FREKYN-LMPTYTKSEYYHKIYHRIQEVVKSVLLCLWLSALQLAVINKSVLITGDQ 765
Xenopus_laevis 687 --DTNHF-------LLTP---LRTGNRS---------- 702
Xenopus_tropicalis
Mus_musculus 666 --KIVHQ-------KPDSKK---------- 676
1x58_chainA_p001
Latimeria_chalumnae 786 --KHAY---------- 789
Pogona_vitticeps 698 EQKQSFK-------DQDVNE---------- 710
Gekko_japonicus 691 QQKCNLGESHTYSLDEGLGE---------- 710
Callorhinchus_milii 808 --KAAGK-------HSYTNGQQYQPEPR---------- 826
Monopterus_albus 674 --WSKHN-------ATWIPSLLLSGSGFT---------- 693
Danio_rerio 697 --KLSHQ-------SSDRCYRLTPLKRP---------- 715
Scleropages_formosus 758 --KESER----------EDGFLLH---------- 769
Elysia_chlorotica 1430 --HFSSE-------SDTDKYPS---------- 1442
Aplysia_californica 1273 --DFSSD-------SNQELS---------- 1283
Capitella_teleta 671 --AFDSK-------TSDESIS---------- 682
Lottia_gigantea 1158 --DFSSS-------DSGSNRKIS---------- 1171
Crassostrea_virginica 778 --EFTSE-------SEPEVS---------- 788
Mizuhopecten_yessoensis 1130 --DFMSS-------ESDRDDRVT---------- 1143
Acanthaster_planci 984 --RNGRS---------- 988
Amphimedon_queenslandica 849 LMTLSES-------TNGACRPLD---------- 864
Limulus_polyphemus 1370 --SFTES-------ENNEMN---------- 1380
Hydra_vulgaris 634 --KKSFI---------- 638
Lingula_anatina 456 --FLSSE-------TEDDLGKKVT---------- 470
Consensus_aa:
Consensus_ss:

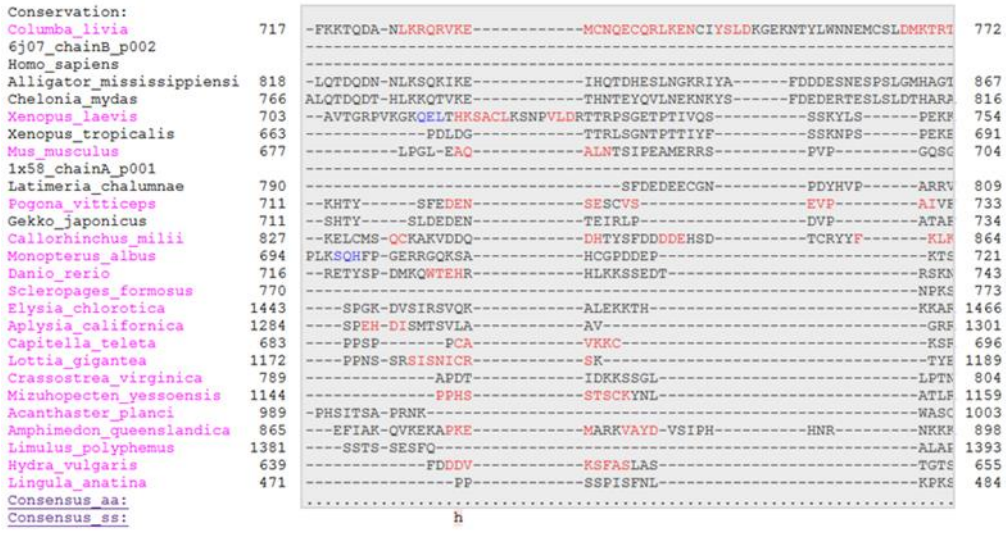
Conservation:
Columba_livia 717 -FKKTQDA-NLKRQRVKE----------MCNQECQRLKENCIYSLDKGEKNTYLWNNEMCSLDMKTRI 772
6j07_chainB_p002
Homo_sapiens
Alligator_mississippiensi 818 -LQTDQDN-NLKSQKIKE----------IHQTDHESLNGKRIYA------FDDDESNESPSLGMHAGI 867
Chelonia_mydas 766 ALQTDQDT-HLKKQTVKE----------THNTEYQVLNEKNKYS------FDEDERTESLSLDTHARA 816
Xenopus_laevis 703 --AVTGRPVKGKQELTHKSACLKSNPVLDRTTRPSGETPTIVQS---------SSKYLS------PEKF 754
Xenopus_tropicalis 663 ----------PDLDG----------TTRLSGNTPTTIYF---------SSKNPS------PEKE 691
Mus_musculus 677 ----------LPGL-EAQ----------ALNTSIPEAMERRS---------PVP---------GQSG 704
1x58_chainA_p001
Latimeria_chalumnae 790 ----------SFDEDEECGN---------PDYHVP------ARRV 809
Pogona_vitticeps 711 --KHTY------SFEDEN----------SESCVS----------EVP---------AIVE 733
Gekko_japonicus 711 --SHTY-----SLDEDEN----------TEIRLP----------DVP---------ATAE 734
Callorhinchus_milii 827 --KELCMS-QCKAKVDDQ----------DHTYSFDDDDEHSD---------TCRYYF-------KLK 864
Monopterus_albus 694 PLKSQHFP-GERRGQKSA----------HCGPDDEP----------KTS 721
Danio_rerio 716 --RETYSP-DMKQWTEHR----------HLKKSSEDT----------RSKN 743
Scleropages_formosus 770 ----------NPKS 773
Elysia_chlorotica 1443 ----SPGK-DVSIRSVQK----------ALEKKTH----------KKAR 1466
Aplysia_californica 1284 ----SPEH-DISMTSVLA----------AV----------GRF 1301
Capitella_teleta 683 ----PPSP-------PCA----------VKKC----------KSF 696
Lottia_gigantea 1172 ----PPNS-SRSISNICR----------SK----------TYE 1189
Crassostrea_virginica 789 ----------APDT----------IDKKSSGL----------LPTN 804
Mizuhopecten_yessoensis 1144 ----------PPHS----------STSCKYNL----------ATLF 1159
Acanthaster_planci 989 -PHSITSA-PRNK----------WASC 1003
Amphimedon_queenslandica 865 ---EFIAK-QVKEKAPKE----------MARKVAYD-VSIPH---------HNR---------NKKF 898
Limulus_polyphemus 1381 ----SSTS-SESFQ----------ALAE 1393
Hydra_vulgaris 639 ----------FDDDV----------KSFASLAS----------TGTS 655
Lingula_anatina 471 ----------PP----------SSPISFNL----------KPKS 484
Consensus_aa:
Consensus_ss:

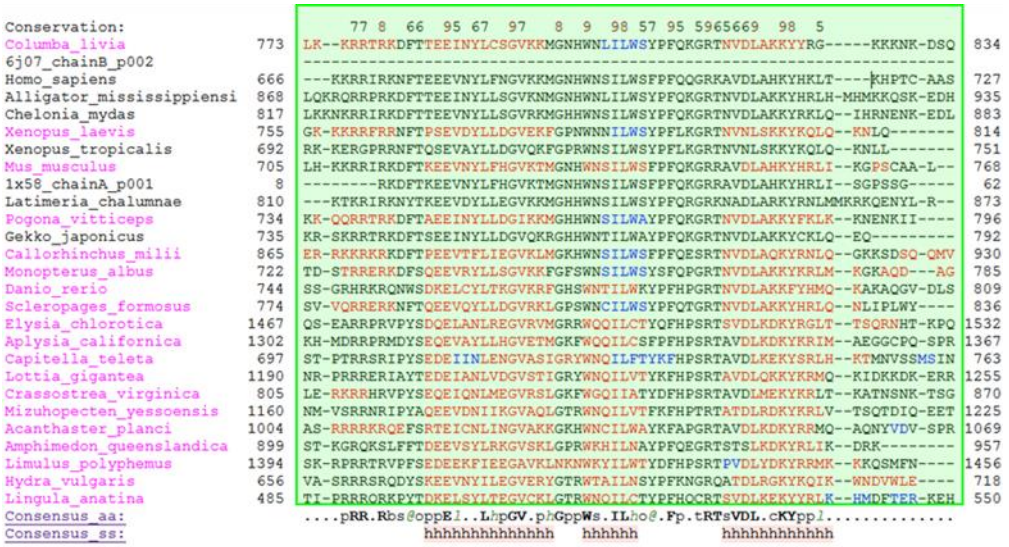

Figure 10-1 Multiple sequence alignment of candidate TERB1 sequences by PROMALS3D.

The sequences with magenta names are colored according to their predicted secondary structures (red: alpha-helix; blue: beta-strand). The sequences with black names belong to the same taxonomic groups of the nearest magenta sequence above them in the alignment. The first line in each block shows conservation indices for positions with a conservation index above 4. The highlighted rectangles in the alignment indicates domain/motif boundaries in mouse TERB1 protein. Each color represents a domain: ARM repeat domain (orange), TRFB domain (grey), T2B; binding site of TERB2 (light blue), TRF1-binding motif (violet) and MYB domain (green).

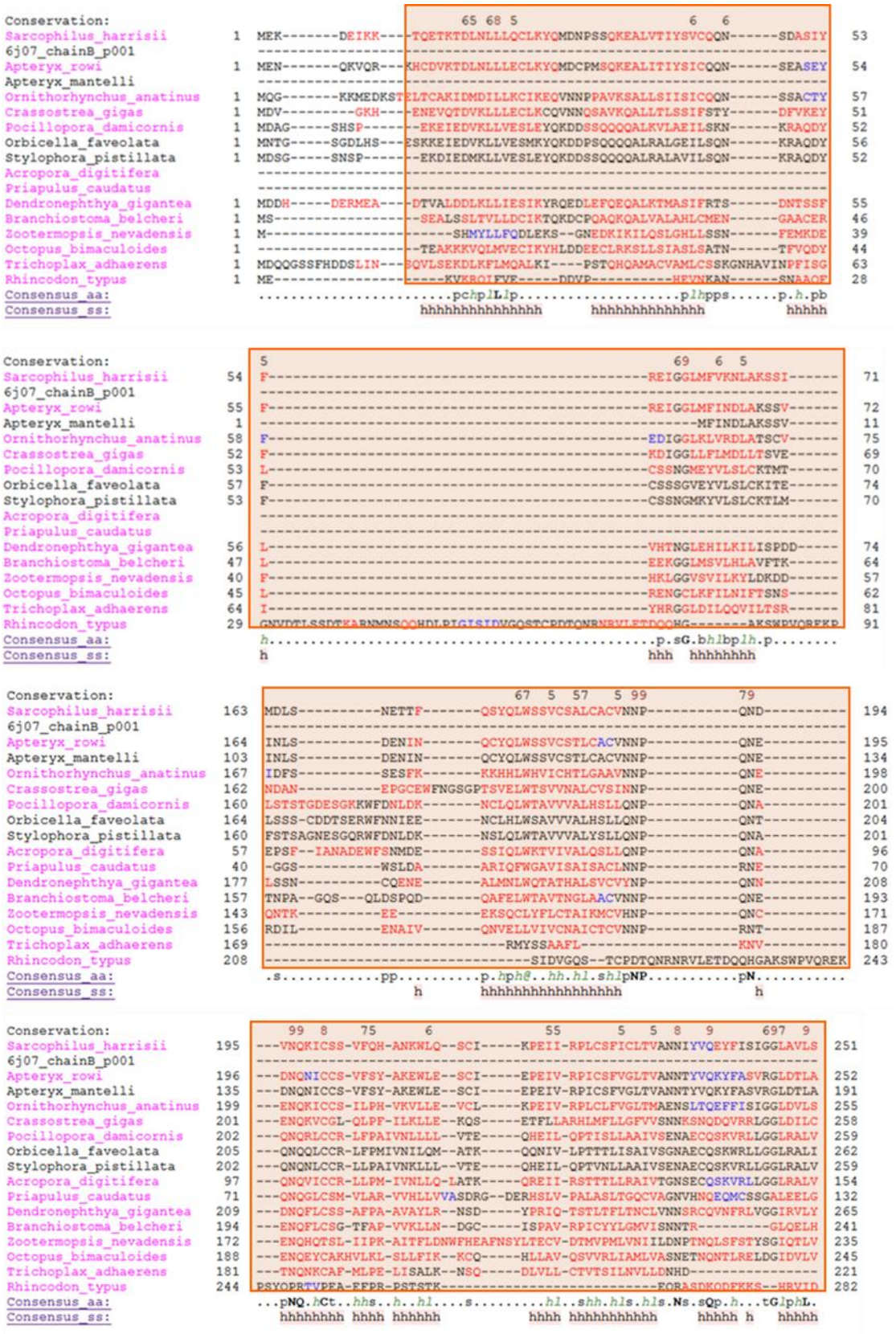


Conservation:
Sarcophilus_harrisii 163 MDLS----------NETTF-------QSYQLWSSVCSALCACVNNP----------QND---------- 194
6j07_chainB_p001
Apteryx_rowi 164 INLS----------DENIN-------QCYQLWSSVCSTLCACVNNP----------QNE---------- 195
Apteryx_mantelli 103 INLS----------DENIN-------QCYQLWSSVCSTLCACVNNP----------QNE---------- 134
Ornithorhynchus_anatinus 167 IDFS----------SESFK-------KKHHLWHVICHTLGAAVNNP----------QNE---------- 198
Crassostrea_gigas 162 NDAN----------EPGCEWFNGSGPTSVELWTSVVNALCVSINNP----------QNE---------- 200
Pocillopora_damicornis 160 LSTSTGDESGKKWFDNLDK-------NCLQLWTAVVVALHSLLQNP----------QNA---------- 201
Orbicella_faveolata 164 LSSS-CDDTSERWFNNIEE-------NCLHLWSAVVVALHSLLQNP----------QNT---------- 204
Stylophora_pistillata 160 FSTSAGNESGQRWFDNLDK-------NSLQLWTAVVVALYSLLQNP----------QNA---------- 201
Acropora_digitifera 57 EPSF--IANADEWFSNMDE-------SSIQLWKTVIVALQSLLQNP----------QNA---------- 96
Priapulus_caudatus 40 -GGS----------WSLDA-------ARIQFWGAVISAISACLNNP----------RNE---------- 70
Dendronephthya_gigantea 177 LSSN----------CQENE-------ALMNLWQTATHALSVCVYNP----------QNN---------- 208
Branchiostoma_belcheri 157 TNPA--GQS---QLDSPQD-------QAFELWTAVTNGLAACVNNP----------QNE---------- 193
Zootermopsis_nevadensis 143 QNTK----------EE----------EKSQCLYFLCTAIKMCVHNP----------QNC---------- 171
Octopus_bimaculoides 156 RDIL----------ENAIV-------QNVELLVIVCNAICTCVNNP----------RNT---------- 187
Trichoplax_adhaerens 169 ----------RMYSSAAFL----------KNV---------- 180
Rhincodon_typus 208 ----------SIDVGQS--TCPDTQNRNRVLETDQQHGAKSWPVQREH 243
Consensus_aa:
Consensus_ss:
Conservation:
Sarcophilus_harrisii 195 ---VNQKICSS-VFQH-ANKWLQ--SCI-----KPEII-RPLCSFICLTVANNIYVQEYFISIGGLAVLS 251
6j07_chainB_p001
Apteryx_rowi 196 ---DNQNICCS-VFSY-AKEWLE--SCI-----EPEIV-RPICSFVGLTVANNTYVQKYFASVRGLDTLA 252
Apteryx_mantelli 135 ---DNQNICCS-VFSY-AKEWLE--SCI-----EPEIV-RPICSFVGLTVANNTYVQKYFASVRGLDTLA 191
Ornithorhynchus_anatinus 199 ---ENQKICCS-ILPH-VKVLLE--VCL-----KPEIV-RPLCLFVGLTMAENSLTQEFFISIGGLDVLS 255
Crassostrea_gigas 201 ---ENQKVCGL-QLPF-ILKLLE--KQS-----ETFLLARHLMFLLGFVVSNNKSNQDQVRRLGGLDILC 258
Pocillopora_damicornis 202 ---QNQRLCCR-LFPAIVNLLLL--VTE-----QHEIL-QPTISLLAAIVSENAECQSKVRLLGGLRALV 259
Orbicella_faveolata 205 ---QNQQLCCR-LFPMIVNILQM--ATK-----QQNIV-LPTTTLISAIVSGNAECQSKWRLLGGLRALI 262
Stylophora_pistillata 202 ---QNQNLCCR-LLPAIVNKLLL--VTE-----QHEIL-QPTVNLLAAIVSENAECQSKVRLLGGLRALV 259
Acropora_digitifera 97 ---QNQVICCR-LLPM-IVNLLQ-LATK-----QREII-RSTTTLLRAIVTGNSECQSKVRLLGGLRALV 154
Priapulus_caudatus 71 ---QNQGLCSM-VLAR-VVHLLVVASDRG--DERHSLV-PALASLTGQCVAGNVHNQEQMCSSGALEELG 132
Dendronephthya_gigantea 209 ---DNQFLCSS-AFPA-AVAYLR--NSD-----YPRIQ-TSTLTFLTNCLVNNSRCQVNFRLVGGIRVLY 265
Branchiostoma_belcheri 194 ---ENQFLCSG-TFAP-VVKLLN--DGC-----ISPAV-RPICYYLGMVISNNTR---------GLQELH 241
Zootermopsis_nevadensis 172 ---ENQHQTSL-IIPK-AITFLDNWFHEAFNSYLTECV-DTMVPMLVNIILDNPTNQLSFSTYSGIQTLV 235
Octopus_bimaculoides 188 ---ENQEYCAKHVLKL-SLLFIK--KCQ-----HLLAV-QSVVRLIAMLVASNETNQNTLRELDGIDVLV 245
Trichoplax_adhaerens 181 ---TNQNKCAF-MLPE-LISALK--NSQ-----DLVLL-CTVTSILNVLLDNHD---------------- 221
Rhincodon_typus 244 PSYQPRTVPPA-EFPR-PSTSTK----------EQRASDKQDFKKS--HRVID 282
Consensus_aa:
Consensus_ss:
Conservation:
Sarcophilus_harrisii 252 EVL--IKLEHDSHDNVASAKLAVVVTKTLDACIA---------DNPA-VGVVLAKYHIVSKLLTLLLHE 308
6j07_chainB_p001
Apteryx_rowi 253 KVL--IKLMHDSYMSHSSTKLAVVVTKTLDACIA---------NDST-MGVVLAKYHTVSELLKLLPND 309
Apteryx_mantelli 192 KVL--IKLMHDSYMSHSSTKLAVVVTKTLDACIA---------NDST-MGVVLAKYHTVSELLKLLPND 248
Ornithorhynchus_anatinus 256 DVL--IKLTRESHQSISSAKLAVNVTNAINVCIA---------DNSP-GSVVLARHHVVPKLLTLLLLE 312
Crassostrea_gigas 259 MIL--KQWYEKSSS--EVLKEVVHIITTIDSCIS---------DNAD-SANMLGKSGAIQILANVIHND 313
Pocillopora_damicornis 260 IRL--KQVVDLKEHVEQDILFMERVVNTLGSIIAGHVICQESAADLGL-VTLLLKCFAVISQ--ATCFDD 324
Orbicella_faveolata 263 NQL--KEHVEHKEPAVQDISFLEHVVNTIGSAIAGHAVCLDSSADLGL-VSLLIKCLD-ISQ--TPGVDD 326
Stylophora_pistillata 260 ILL--KQVVDLKEHAERDILFMGRIINTLGSVIAGHVICQDSAADLGL-VTLLLKCLALITP--ATQVDG 324
Acropora_digitifera 155 NVL--KECINEKQLCDQDLHFIEHVVSTIGSATA---------GHGM-CQESTAELGLVSLLVKCLEMS 211
Priapulus_caudatus 133 RVF--RRLSQLSCSGRSMQILAC-IANAIDACVT---------DYCQ-GSILVGSLGVVEALVQLLAEP 188
Dendronephthya_gigantea 266 DIF---REDLLAGGQIPSTVLQILIL-TIDAAVR---------DNDM-CRDSIAEMEIVPLLLQSLQLC 320
Branchiostoma_belcheri 242 QL----------KAVPLMVQLLSLN 256
Zootermopsis_nevadensis 236 IGL--NTLESWQEAPLNIETVKVKIICLLDAAIC---------GNIV-NSEQATVLGVIPLLLKMLQNF 292
Octopus_bimaculoides 246 NIIKLYTLATDNVYNADYLKTAVLLTSALDTCLL---------GNALYTERVITKLKSVIRVK--LPRE 303
Trichoplax_adhaerens 222 NIL--KQWHKDMKSTI----------TLK----------ALYHLI-----MISNS 249
Rhincodon_typus 283 NIF--KRP----------APN 291
Consensus_aa:
Consensus_ss:
Conservation:
Sarcophilus_harrisii 309 S--LDSGE-------KFSIILTLGHCTEACEENQLQLFKN-----NGLPLMIQVLT-ESQN-EELNKAAT 362
6j07_chainB_p001
Apteryx_rowi 310 T--LDTGE-------KISIILTIGHCTEVCEENQYELLKN-----NGLPLMIQVLT-ESQD-EELNKAAT 363
Apteryx_mantelli 249 T--LDTGE-------KISIILTIGHCTEVCEENQYELLKN-----NGLPLMIQVLT-ESQD-EELNKAAT 302
Ornithorhynchus_anatinus 313 S--LNSGE-------KTSVMLTLAYCTAACEENLHHLLQN-----NGLNFLIDSIS-DPCY-EALGNIVF 366
Crassostrea_gigas 314 C--LDTED-------KIKVTITLGHAMENSATNRKLFLEA----GNSLQDVVHILT-SSED-EELVKALK 368
Pocillopora_damicornis 325 A--AAKQF-------KTKCILALSICIDQSERNQQLLRDG-----GGVEALIELLT-KEQS-EEFRRVAI 378
Orbicella_faveolata 327 A--VSKTF-------RTKCILALSICVDQCERNQRQLRDR-----EGVERLVELLA-QEQS-EEFRRVAI 380
Stylophora_pistillata 325 A--AAKQF-------KTKCILALSICIDQSERNQQQLRDS-----GGVAALIELLT-EEQS-EEFRRVAI 378
Acropora_digitifera 212 S--CPSLSSLATRQFRTKCILALSICVEQCDWKEAIVESNQRDRIPGCETQIPHLTQEAET-QTESHDAQ 278
Priapulus_caudatus 189 SAETDITH-------KTKFLLTLAHLVDDNDENRQRAVDA-----HGVPVIVKCLA-ETGD-PEFSRTAQ 244
Dendronephthya_gigantea 321 F--ASPKF-------KIQCLITLSACIEGCDSSCKQFLTN-----DGMLTVVKVLT-ENQNCEELQKSAL 375
Branchiostoma_belcheri 257 L--QDPQL-------QLQVLLTILHLTEMNKDIQHQLISA-----GGLSVVLHSMA-RNQS-AEYNKAAT 310
Zootermopsis_nevadensis 293 ----------TDQAIRRAYCFNR------KRTPK--DLY---------LKWRST 319
Octopus_bimaculoides 304 M----YGE-------NIKAILI---------DKEKYKKLKE----------KCQI-EHP-----GFVVQ 336
Trichoplax_adhaerens 250 F----VDE-------EVANCL----CETECVTILSE----------LQI-NSEV-NVLAELAD 285
Rhincodon_typus 292 S---RKRS-------KQNYKDSLILCSDLIDTEINSTLTS-----PAPSL---------- 326
Consensus_aa:
Consensus_ss:

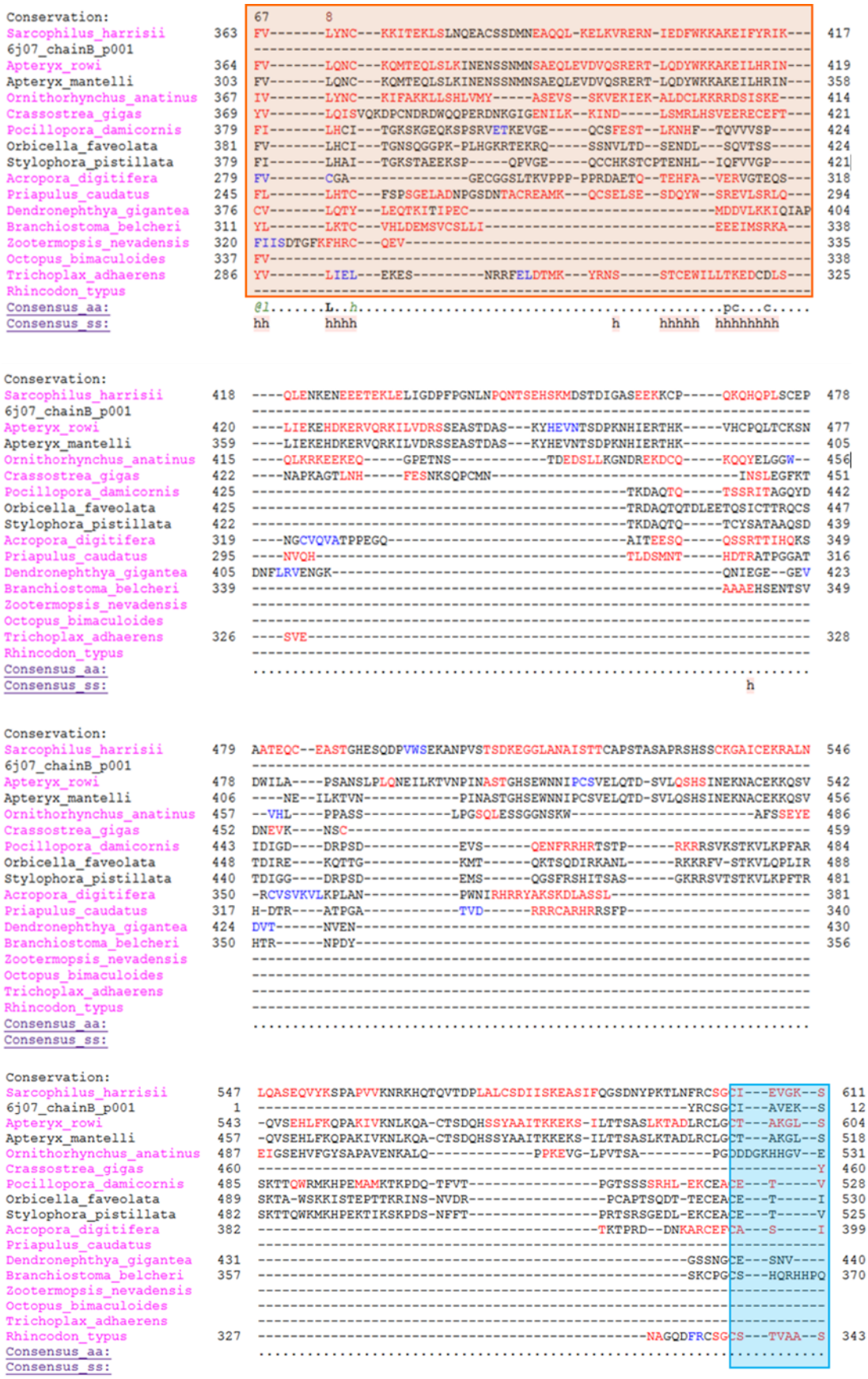
Conservation:
Sarcophilus_harrisii 363 FV-------LYNC---KKITEKLSLNQEACSSDMNEAQQL-KELKVRERN-IEDFWKKAKEIFYRIK--- 417
6j07_chainB_p001
Apteryx_rowi 364 FV-------LQNC---KQMTEQLSLKINENSSNMNSAEQLEVDVQSRERT-LQDYWKKAKEILHRIN--- 419
Apteryx_mantelli 303 FV-------LQNC---KQMTEQLSLKINENSSNMNSAEQLEVDVQSRERT-LQDYWKKAKEILHRIN---
Ornithorhynchus_anatinus 367 IV-------LYNC---KIFAKKLLSHLVMY-----ASEVS--SKVEKIEK-ALDCLKKRRDSISKE---- 414
Crassostrea_gigas 369 YV-------LQISVQKDPCNDRDWQQPERDNKGIGENILK--KIND-----LSMRLHSVEERECEFT--- 421
Pocillopora_damicornis 379 FI-------LHCI---TGKSKGEQKSPSRVETKEVGE-----QCSFEST--LKNHF--TQVVVSP----- 424
Orbicella_faveolata 381 FV-------LHCI---TGNSQGGPK-PLHGKRTEKRQ-----SSNVLTD--SENDL---SQVTSS----- 424
Stylophora_pistillata 379 FI-------LHAI---TGKSTAEEKSP-----QPVGE-----QCCHKSTCPTENHL--IQFVVGP----- 421
Acropora_digitifera 279 FV-------CGA--------------GECGGSLTKVPPP-PPRDAETQ--TEHFA--VERVGTEQS--- 318
Priapulus_caudatus 245 FL-------LHTC---FSPSGELADNPGSDNTACREAMK---QCSELSE--SDQYW--SREVLSRLQ--- 294
Dendronephthya_gigantea 376 CV-------LQTY---LEQTKITIPEC-------------------------------MDDVLKKIQIAP 404
Branchiostoma_belcheri 311 YL-------LKTC---VHLDEMSVCSLLI-----------------------------EEEIMSRKA--- 338
Zootermopsis_nevadensis 320 FIISDTGFKFHRC---QEV-- 335
Octopus_bimaculoides 337 FV-- 338
Trichoplax_adhaerens 286 YV-------LIEL---EKES---------NRRFELDTMK---YRNS-----STCEWILLTKEDCDLS--- 325
Rhincodon_typus
Consensus_aa:
Consensus_ss:
Conservation:
Sarcophilus_harrisii 418 ----QLENKENEEETEKLELIGDPFPGNLNPQNTSEHSKMDSTDIGASEEKKCP-----QKQHQPLSCEP 478
6j07_chainB_p001
Apteryx_rowi 420 ----LIEKEHDKERVQRKILVDRSSEASTDAS---KYHEVNTSDPKNHIERTHK-----VHCPQLTCKSN 477
Apteryx_mantelli 359 ----LIEKEHDKERVQRKILVDRSSEASTDAS---KYHEVNTSDPKNHIERTHK---------------- 405
Ornithorhynchus_anatinus 415 ----QLKRKEEKEQ-----GPETNS------------TDEDSLLKGNDREKDCQ-----KQQYELGGW-- 456
Crassostrea_gigas 422 ----NAPKAGTLNH-----FESNKSQPCMN-----------------------------INSLEGFKT 451
Pocillopora_damicornis 425 --TKDAQTQ-----TSSRITAGQYD 442
Orbicella_faveolata 425 --TRDAQTQTDLEETQSICTTRQCS 447
Stylophora_pistillata 422 --TKDAQTQ-----TCYSATAAQSD 439
Acropora_digitifera 319 ----NGCVQVATPPEGQ-----------------------------AITEESQ-----QSSRTTIHQKS 349
Priapulus_caudatus 295 ----NVQH-------------------------------------TLDSMNT-----HDTRATPGGAT 316
Dendronephthya_gigantea 405 DNFLRVENGK---QNIEGE--GEV 423
Branchiostoma_belcheri 339 --AAAEHSENTSV 349
Zootermopsis_nevadensis
Octopus_bimaculoides
Trichoplax_adhaerens 326 ----SVE---------- 328
Rhincodon_typus
Consensus_aa:
Consensus_ss:
Conservation:
Sarcophilus_harrisii 479 AATEQC--EASTGHESQDPVWSEKANPVSTSDKEGGLANAISTTCAPSTASAPRSHSSCKGAICEKRALN 546
6j07_chainB_p001
Apteryx_rowi 478 DWILA----PSANSLPLQNEILKTVNPINASTGHSEWNNIPCSVELQTD-SVLQSHSINEKNACEKKQSV 542
Apteryx_mantelli 406 ----NE--ILKTVN-----------PINASTGHSEWNNIPCSVELQTD-SVLQSHSINEKNACEKKQSV 456
Ornithorhynchus_anatinus 457 --VHL----PPASS-----------LPGSQLESSGGNSKW----------------------AFSSEYE 486
Crassostrea_gigas 452 DNEVK----NSC---------- 459
Pocillopora_damicornis 443 IDIGD----DRPSD-----------EVS------QENFRRHRTSTP------RKRRSVKSTKVLKPFAR 484
Orbicella_faveolata 448 TDIRE----KQTTG-----------KMT------QKTSQDIRKANL------RKKRFV-STKVLQPLIR 488
Stylophora_pistillata 440 TDIGG----DRPSD-----------EMS------QGSFRSHITSAS------GKRRSVTSTKVLKPFTR 481
Acropora_digitifera 350 -RCVSVKVLKPLAN-----------PWNIRHRRYAKSKDLASSL---------- 381
Priapulus_caudatus 317 H-DTR----ATPGA-----------TVD------RRRCARHRRSFP---------- 340
Dendronephthya_gigantea 424 DVT------NVEN---------- 430
Branchiostoma_belcheri 350 HTR------NPDY---------- 356
Zootermopsis_nevadensis
Octopus_bimaculoides
Trichoplax_adhaerens
Rhincodon_typus
Consensus_aa:
Consensus_ss:
Conservation:
Sarcophilus_harrisii 547 LQASEQVYKSPAPVVKNRKHQTQVTDPLALCSDIISKEASIFQGSDNYPKTLNFRCSGCI---EVGK--S 611
6j07_chainB_p001 1 ----------YRCSGCI---AVEK--S 12
Apteryx_rowi 543 -QVSEHLFKQPAKIVKNLKQA-CTSDQHSSYAAITKKEKS-ILTTSASLKTADLRCLGCT---AKGL--S 604
Apteryx_mantelli 457 -QVSEHLFKQPAKIVKNLKQA-CTSDQHSSYAAITKKEKS-ILTTSASLKTADLRCLGCT---AKGL--S 518
Ornithorhynchus_anatinus 487 EIGSEHVFGYSAPAVENKALQ----------PPKEVG-LPVTSA---------PGDDDGKHHGV--E 531
Crassostrea_gigas 460 ----------Y 460
Pocillopora_damicornis 485 SKTTQWRMKHPEMAMKTKPDQ-TFVT----------PGTSSSSRHL-EKCEACE---T-----V 528
Orbicella_faveolata 489 SKTA-WSKKISTEPTTKRINS-NVDR----------PCAPTSQDT-TECEACE---T-----I 530
Stylophora_pistillata 482 SKTTQWKMKHPEKTIKSKPDS-NFFT----------PRTSRSGEDL-EKCEACE---T-----V 525
Acropora_digitifera 382 ----------TKTPRD--DNKARCEPCA---S-----I 399
Priapulus_caudatus
Dendronephthya_gigantea 431 ----------GSSNGCE---SNV---- 440
Branchiostoma_belcheri 357 ----------SKCPGCS---HQRHHPQ 370
Zootermopsis_nevadensis
Octopus_bimaculoides
Trichoplax_adhaerens
Rhincodon_typus 327 ----------NAGQDFRCSGCS---TVAA--S 343
Consensus_aa:
Consensus_ss:

Figure 10-2 Multiple sequence alignment of candidate TERB1 sequences that lack a MYB-domain by Promals3D.

Multiple sequence alignment of candidate TERB1 sequences that lack a MYB-domain by Promals3D. The sequences with magenta names are colored according to predicted secondary structures (red: alpha-helix, blue: beta-strand). The sequences with black names belong to the same taxonomic group of the nearest magenta sequence above them. The first line in each block shows conservation indices for positions with a conservation index above 4. The highlighted rectangles in the alignment correspond to the mouse TERB1 N-terminal ARM repeat domain (orange) and TERB2-binding site in TERB1 (light blue).

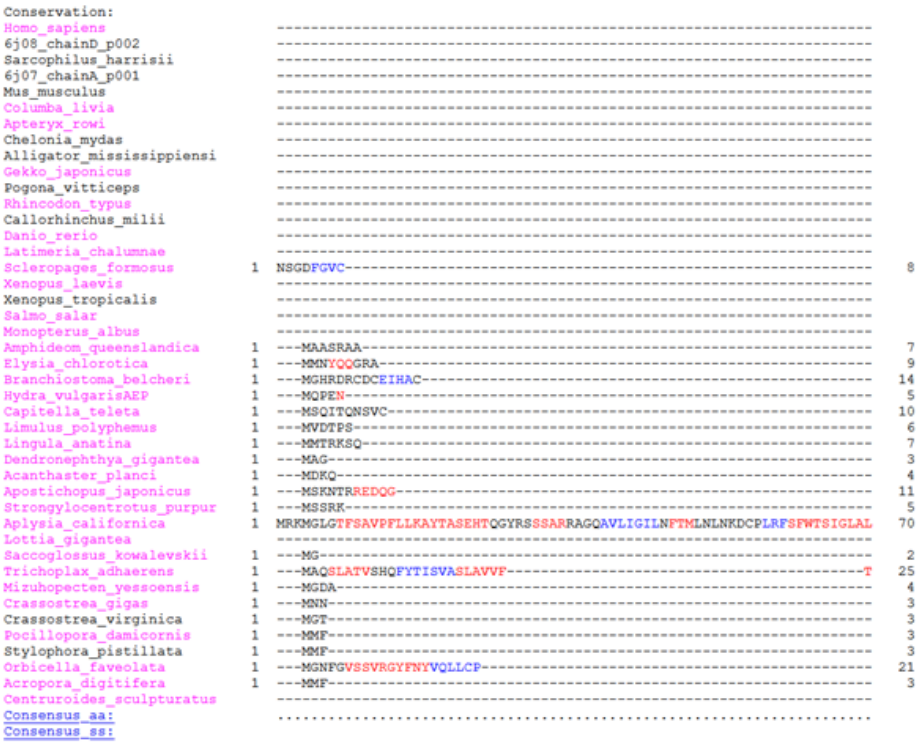
Conservation:
Homo_sapiens
6j08_chainD_p002
Sarcophilus_harrisii
6j07_chainA_p001
Mus_musculus
Columba_livia
Apteryx_rowi
Chelonia_mydas
Alligator_mississippiensi
Gekko_japonicus
Pogona_vitticeps
Rhincodon_typus
Callorhinchus_milii
Danio_rerio
Latimeria_chalumnae
Scleropages_formosus
Xenopus_laevis
Xenopus_tropicalis
Salmo_salar
Monopterus_albus
Amphideom_queenslandica
Elysia_chlorotica
Branchiostoma_belcheri
Hydra_vulgarisAEP
Capitella_teleta
Limulus_polyphemus
Lingula_anatina
Dendronephthya_gigantea
Acanthaster_planci
Apostichopus_japonicus
Strongylocentrotus_purpur
Aplysia_californica
Lottia_gigantea
Saccoglossus_kowalevskii
Trichoplax_adhaerens
Mizuhopecten_yessoensis
Crassostrea_gigas
Crassostrea_virginica
Pocillopora_damicornis
Stylophora_pistillata
Orbicella_faveolata
Acropora_digitifera
Centruroides_sculpturatus
Consensus_aa:
Consensus_ss:


Conservation:
Homo_sapiens
6j08_chainD_p002
Sarcophilus_harrisii
6j07_chainA_p001
Mus_musculus
Columba_livia
Apteryx_rowi
Chelonia_mydas
Alligator_mississippiensi
Gekko_japonicus
Pogona_vitticeps
Rhincodon_typus
Callorhinchus_milii
Danio_rerio
Latimeria_chalumnae
Scleropages_formosus
Xenopus_laevis
Xenopus_tropicalis
Salmo_salar
Monopterus_albus
Amphideom_queenslandica
Elysia_chlorotica
Branchiostoma_belcheri
Hydra_vulgarisAEP
Capitella_teleta
Limulus_polyphemus
Lingula_anatina
Dendronephthya_gigantea
Acanthaster_planci
Apostichopus_japonicus
Strongylocentrotus_purpur
Aplysia_californica
Lottia_gigantea
Saccoglossus_kowalevskii
Trichoplax_adhaerens
Mizuhopecten_yessoensis
Crassostrea_gigas
Crassostrea_virginica
Pocillopora_damicornis
Stylophora_pistillata
Orbicella_faveolata
Acropora_digitifera
Centruroides_sculpturatus
Consensus_aa:
Consensus_ss:

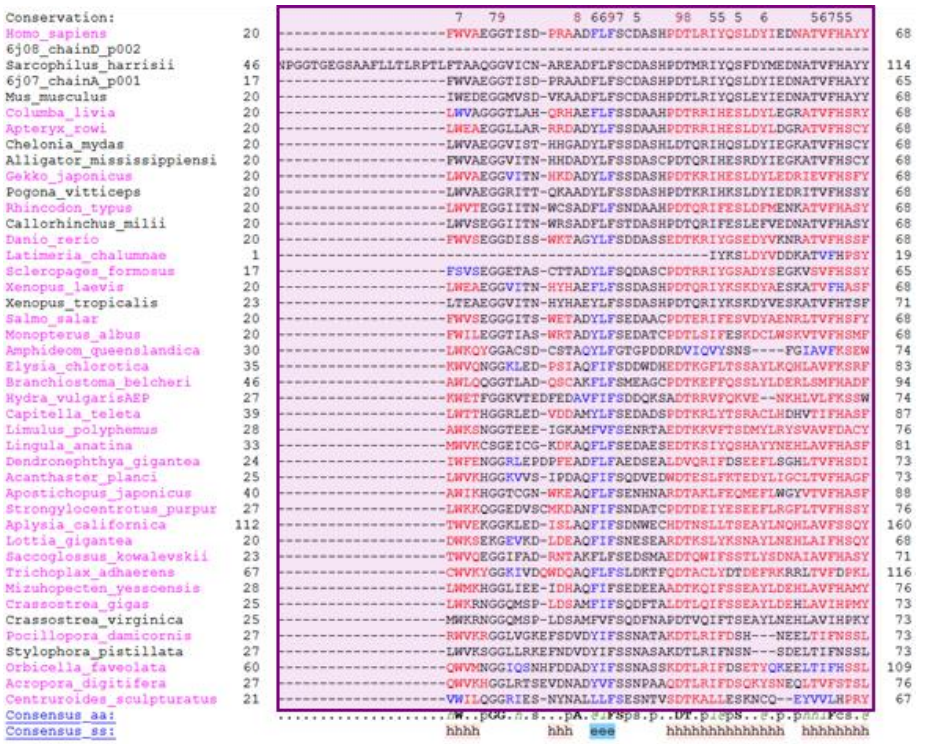
Conservation:
Homo_sapiens
6j08_chainD_p002
Sarcophilus_harrisii
6j07_chainA_p001
Mus_musculus
Columba_livia
Apteryx_rowi
Chelonia_mydas
Alligator_mississippiensi
Gekko_japonicus
Pogona_vitticeps
Rhincodon_typus
Callorhinchus_milii
Danio_rerio
Latimeria_chalumnae
Scleropages_formosus
Xenopus_laevis
Xenopus_tropicalis
Salmo_salar
Monopterus_albus
Amphideom_queenslandica
Elysia_chlorotica
Branchiostoma_belcheri
Hydra_vulgarisAEP
Capitella_teleta
Limulus_polyphemus
Lingula_anatina
Dendronephthya_gigantea
Acanthaster_planci
Apostichopus_japonicus
Strongylocentrotus_purpur
Aplysia_californica
Lottia_gigantea
Saccoglossus_kowalevskii
Trichoplax_adhaerens
Mizuhopecten_yessoensis
Crassostrea_gigas
Crassostrea_virginica
Pocillopora_damicornis
Stylophora_pistillata
Orbicella_faveolata
Acropora_digitifera
Centruroides_sculpturatus
Consensus_aa:
Consensus_ss:

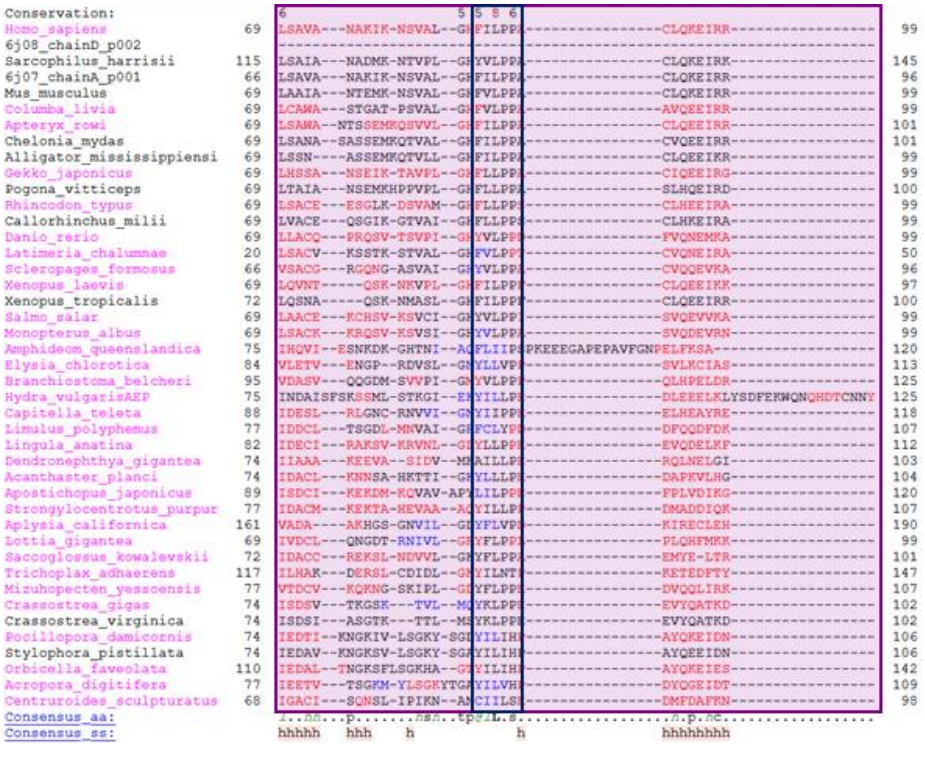
Conservation:
Homo_sapiens
6j08_chainD_p002
Sarcophilus_harrisii
6j07_chainA_p001
Mus_musculus
Columba_livia
Apteryx_rowi
Chelonia_mydas
Alligator_mississippiensi
Gekko_japonicus
Pogona_vitticeps
Rhincodon_typus
Callorhinchus_milii
Danio_rerio
Latimeria_chalumnae
Scleropages_formosus
Xenopus_laevis
Xenopus_tropicalis
Salmo_salar
Monopterus_albus
Amphideom_queenslandica
Elysia_chlorotica
Branchiostoma_belcheri
Hydra_vulgarisAEP
Capitella_teleta
Limulus_polyphemus
Lingula_anatina
Dendronephthya_gigantea
Acanthaster_planci
Apostichopus_japonicus
Strongylocentrotus_purpur
Aplysia_californica
Lottia_gigantea
Saccoglossus_kowalevskii
Trichoplax_adhaerens
Mizuhopecten_yessoensis
Crassostrea_gigas
Crassostrea_virginica
Pocillopora_damicornis
Stylophora_pistillata
Orbicella_faveolata
Acropora_digitifera
Centruroides_sculpturatus
Consensus_aa:
Consensus_ss:

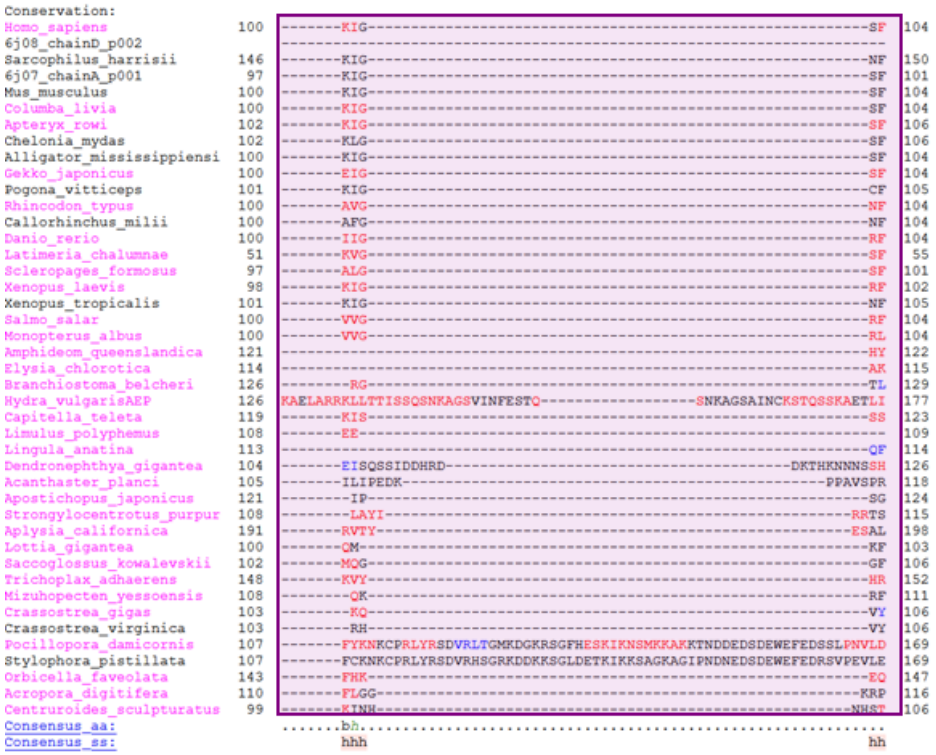
Conservation:
Homo_sapiens 100 -------KIG----------SF 104
6j08_chainD_p002
Sarcophilus_harrisii 146 -------KIG----------NF 150
6j07_chainA_p001 97 -------KIG----------SF 101
Mus_musculus 100 -------KIG----------SF 104
Columba_livia 100 -------KIG----------SF 104
Apteryx_rowi 102 -------KIG----------SF 106
Chelonia_mydas 102 -------KLG----------SF 106
Alligator_mississippiensi 100 -------KIG----------SF 104
Gekko_japonicus 100 -------EIG----------SF 104
Pogona_vitticeps 101 -------KIG----------CF 105
Rhincodon_typus 100 -------AVG----------NF 104
Callorhinchus_milii 100 -------AFG----------NF 104
Danio_rerio 100 -------IIG----------RF 104
Latimeria_chalumnae 51 -------KVG----------SF 55
Scleropages_formosus 97 -------ALG----------SF 101
Xenopus_laevis 98 -------KIG----------RF 102
Xenopus_tropicalis 101 -------KIG----------NF 105
Salmo_salar 100 -------VVG----------RF 104
Monopterus_albus 100 -------VVG----------RL 104
Amphideom_queenslandica 121 ----------HY 122
Elysia_chlorotica 114 ----------AK 115
Branchiostoma_belcheri 126 --------RG----------TL 129
Hydra_vulgarisAEP 126 KAELARRKLLTTISSQSNKAGSVINFESTQ----------SNKAGSAINCKSTQSSKAETLI 177
Capitella_teleta 119 -------KIS----------SS 123
Limulus_polyphemus 108 -------EE---------- 109
Lingula_anatina 113 ----------QF 114
Dendronephthya_gigantea 104 -------EISQSSIDDHRD----------DKTHKNNNSSH 126
Acanthaster_planci 105 -------ILIPEDK----------PPAVSPR 118
Apostichopus_japonicus 121 --------IP----------SG 124
Strongylocentrotus_purpur 108 -------LAYI----------RRTS 115
Aplysia_californica 191 -------RVTY----------ESAL 198
Lottia_gigantea 100 -------QM----------KF 103
Saccoglossus_kowalevskii 102 -------MQG----------GF 106
Trichoplax_adhaerens 148 -------KVY----------HR 152
Mizuhopecten_yessoensis 108 -------QK----------RF 111
Crassostrea_gigas 103 --------KQ----------VY 106
Crassostrea_virginica 103 --------RH----------VY 106
Pocillopora_damicornis 107 -------FYKNKCPRLYRSDVRLTGMKDGKRSGFHESKIKNSMKKAKKTNDDEDSDEWEFEDSSLPNVLD 169
Stylophora_pistillata 107 -------FCKNKCPRLYRSDVRHSGRKDDKKSGLDETKIKKSAGKAGIPNDNEDSDEWEFEDRSVPEVLE 169
Orbicella_faveolata 143 -------FHK----------EQ 147
Acropora_digitifera 110 -------FLGG----------KRP 116
Centruroides_sculpturatus 99 -------KINH----------NHST 106
Consensus_aa:
Consensus_ss:

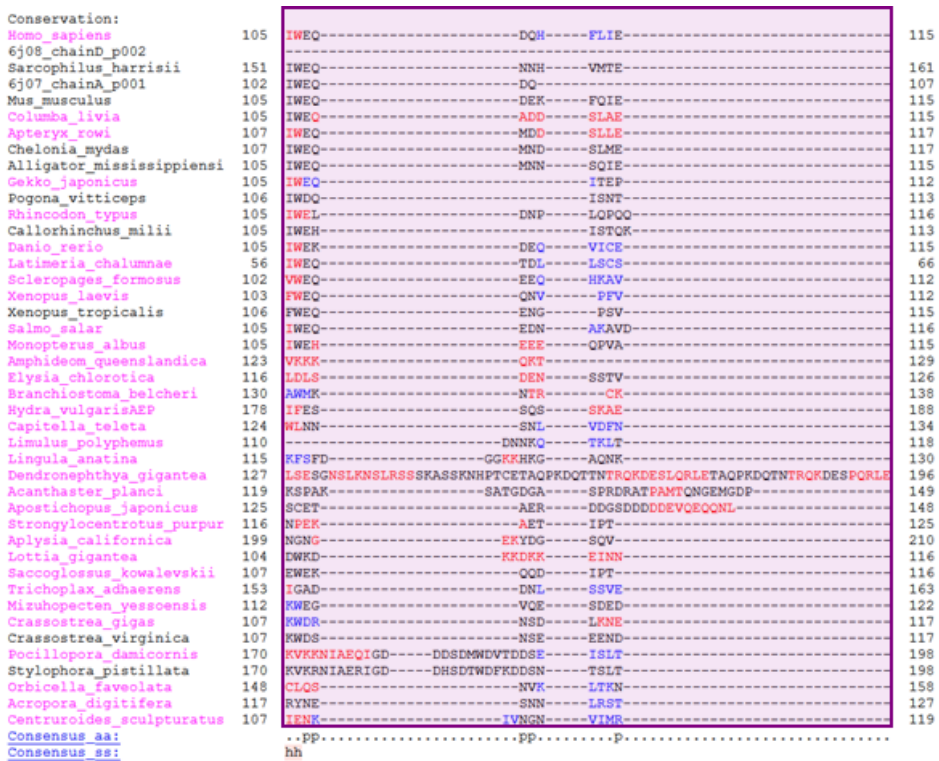
Conservation:
Homo_sapiens 105 IWEQ----------DQH----FLIE---------- 115
6j08_chainD_p002
Sarcophilus_harrisii 151 IWEQ----------NNH----VMTE---------- 161
6j07_chainA_p001 102 IWEQ----------DQ---------- 107
Mus_musculus 105 IWEQ----------DEK----FQIE---------- 115
Columba_livia 105 IWEQ----------ADD----SLAE---------- 115
Apteryx_rowi 107 IWEQ----------MDD----SLLE---------- 117
Chelonia_mydas 107 IWEQ----------MND----SLME---------- 117
Alligator_mississippiensi 105 IWEQ----------MNN----SQIE---------- 115
Gekko_japonicus 105 IWEQ----------ITEP---------- 112
Pogona_vitticeps 106 IWDQ----------ISNT---------- 113
Rhincodon_typus 105 IWEL----------DNP----LQPQQ---------- 116
Callorhinchus_milii 105 IWEH----------ISTQK---------- 113
Danio_rerio 105 IWEK----------DEQ----VICE---------- 115
Latimeria_chalumnae 56 IWEQ----------TDL----LSCS---------- 66
Scleropages_formosus 102 VWEQ----------EEQ----HKAV---------- 112
Xenopus_laevis 103 FWEQ----------QNV------PFV---------- 112
Xenopus_tropicalis 106 FWEQ----------ENG------PSV---------- 115
Salmo_salar 105 IWEQ----------EDN----AKAVD---------- 116
Monopterus_albus 105 IWEH----------EEE----QPVA---------- 115
Amphideom_queenslandica 123 VKKK----------QKT---------- 129
Elysia_chlorotica 116 LDLS----------DEN----SSTV---------- 126
Branchiostoma_belcheri 130 AWMK----------NTR------CK---------- 138
Hydra_vulgarisAEP 178 IFES----------SQS----SKAE---------- 188
Capitella_teleta 124 WLNN----------SNL----VDFN---------- 134
Limulus_polyphemus 110 ----------DNNKQ----TKLT---------- 118
Lingula_anatina 115 KFSFD----------GGKKHKG----AQNK---------- 130
Dendronephthya_gigantea 127 LSESGNSLKNSLRSSSKASSKNHPTCETAQPKDQTTNTRQKDESLQRLETAQPKDQTNTRQKDESPQRLE 196
Acanthaster_planci 119 KSPAK----------SATGDGA----SPRDRATPAMTQNGEMGDP---------- 149
Apostichopus_japonicus 125 SCET----------AER----DDGSDDDDDEVQEQQNL---------- 148
Strongylocentrotus_purpur 116 NPEK----------AET----IPT---------- 125
Aplysia_californica 199 NGNG----------EKYDG----SQV---------- 210
Lottia_gigantea 104 DWKD----------KKDKK----EINN---------- 116
Saccoglossus_kowalevskii 107 EWEK----------QQD----IPT---------- 116
Trichoplax_adhaerens 153 IGAD----------DNL----SSVE---------- 163
Mizuhopecten_yessoensis 112 KWEG----------VQE----SDED---------- 122
Crassostrea_gigas 107 KWDR----------NSD----LKNE---------- 117
Crassostrea_virginica 107 KWDS----------NSE----EEND---------- 117
Pocillopora_damicornis 170 KVKKNIAEQIGD-----DDSDMWDVTDDSE----ISLT---------- 198
Stylophora_pistillata 170 KVKRNIAERIGD-----DHSDTWDFKDDSN----TSLT---------- 198
Orbicella_faveolata 148 CLQS----------NVK----LTKN---------- 158
Acropora_digitifera 117 RYNE----------SNN----LRST---------- 127
Centruroides_sculpturatus 107 IENK----------IVNGN----VIMR---------- 119
Consensus_aa:
Consensus_ss:

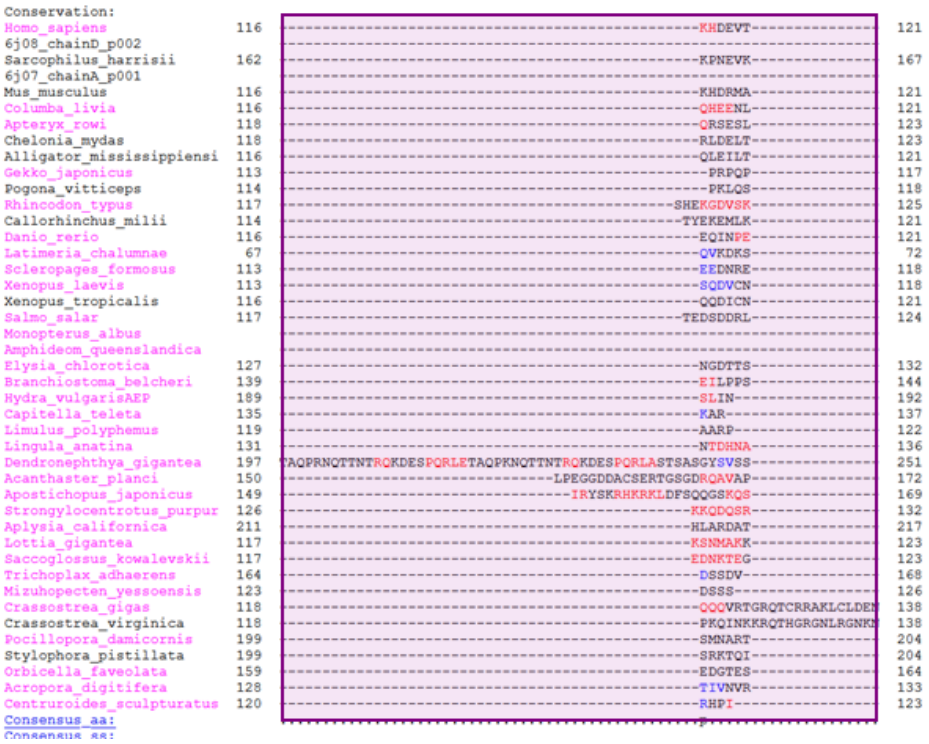
Conservation:
Homo_sapiens 116 KHDEVT 121
6j08_chainD_p002
Sarcophilus_harrisii 162 KPNEVK 167
6j07_chainA_p001
Mus_musculus 116 KHDRMA 121
Columba_livia 116 QHEENL 121
Apteryx_rowi 118 QRSESL 123
Chelonia_mydas 118 RLDELT 123
Alligator_mississippiensi 116 QLEILT 121
Gekko_japonicus 113 PRPQP 117
Pogona_vitticeps 114 PKLQS 118
Rhincodon_typus 117 SHEKGDVSK 125
Callorhinchus_milii 114 TYEKEMLK 121
Danio_rerio 116 EQINPE 121
Latimeria_chalumnae 67 QVKDKS 72
Scleropages_formosus 113 EEDNRE 118
Xenopus_laevis 113 SQDVCN 118
Xenopus_tropicalis 116 QQDICN 121
Salmo_salar 117 TEDSDDRL 124
Monopterus_albus
Amphidecm_queenslandica
Elysia_chlorotica 127 NGDTTS 132
Branchiostoma_belcheri 139 EILPPS 144
Hydra_vulgarisAEP 189 SLIN 192
Capitella_teleta 135 KAR 137
Limulus_polyphemus 119 AARP 122
Lingula_anatina 131 NTDHNA 136
Dendronephthya_gigantea 197 TAQPRNQTTNTRQKDESPQRLETAQPKNQTTNTRQKDESPQRLASTSASGYSVSS 251
Acanthaster_planci 150 LPEGGDDACSERTGSGDRQAVAP 172
Apostichopus_japonicus 149 IRYSKRHKRKLDFSQQGSKQS 169
Strongylocentrotus_purpur 126 KKQDQSR 132
Aplysia_californica 211 HLARDAT 217
Lottia_gigantea 117 KSNMAKK 123
Saccoglossus_kowalevskii 117 EDNKTEG 123
Trichoplax_adhaerens 164 DSSDV 168
Mizuhopecten_yessoensis 123 DSSS 126
Crassostrea_gigas 118 QQQVRTGRQTCRRAKLCLDEN 138
Crassostrea_virginica 118 PKQINKKRQTHGRGNLRGNKN 138
Pocillopora_damicornis 199 SMNART 204
Stylophora_pistillata 199 SRKTQI 204
Orbicella_faveolata 159 EDGTES 164
Acropora_digitifera 128 TIVNVR 133
Centruroides_sculpturatus 120 RHPI 123
Consensus aa:
Consensus ss:

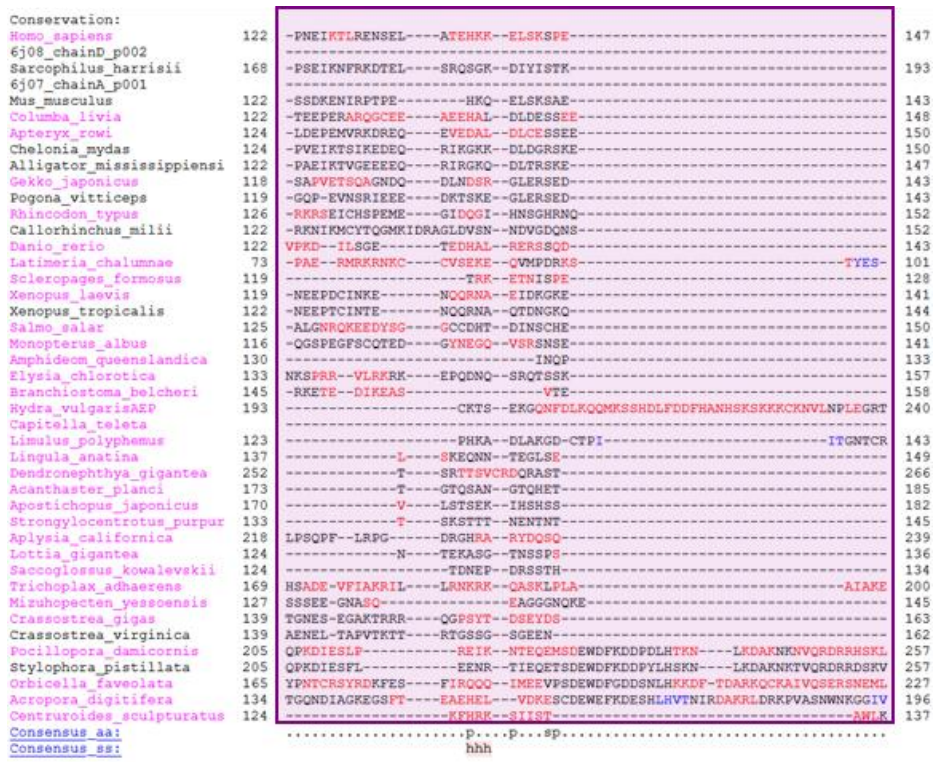
Conservation:
Homo_sapiens 122 PNEIKTLRENSEL ATEHKR ELSKSPE 147
6j08_chainD_p002
Sarcophilus_harrisii 168 PSEIKNFRKDTEL SRQSGK DIYISTK 193
6j07_chainA_p001
Mus_musculus 122 SSDKENIRPTPE HKQ ELSKSAE 143
Columba_livia 122 TEEPERARQGCEE AEEHAL DLDESSEE 148
Apteryx_rowi 124 LDEPEMVRKDREQ EVEDAL DLCESSEE 150
Chelonia_mydas 124 PVEIKTSIKEDEQ RIKGKK DLDGRSKE 150
Alligator_mississippiensi 122 PAEIKTVGEEEEQ RIRGKQ DLTRSKE 147
Gekko_japonicus 118 SAPVETSQAGNDQ DLNDSR GLERSED 143
Pogona_vitticeps 119 GQP EVNSRIEEE DKTSKE GLERSED 143
Rhincodon_typus 126 RKRSEICHSPEME GIDQGI HNSGHRNQ 152
Callorhinchus_milii 122 RKNIKMCYTQGMKIDRAGLDVSN NDVGDQNS 152
Danio_rerio 122 VPKD ILSGE TEDHAL RERSSQD 143
Latimeria_chalumnae 73 PAE RMRKRNKC CVSEKE QVMPDRKS TYES 101
Scleropages_formosus 119 TRK ETNISPE 128
Xenopus_laevis 119 NEEPDCINKE NQQRNA EIDKGKE 141
Xenopus_tropicalis 122 NEEPTCINTE NQQRNA QTDNGKQ 144
Salmo_salar 125 ALGNRQKEEDYSG GCCDHT DINSCHE 150
Monopterus_albus 116 QGSPEGFSCQTED GYNEGQ VSRSNSE 141
Amphidecm_queenslandica 130 INQP 133
Elysia_chlorotica 133 NKSPRR VLRKRK EPQDNQ SRQTSSK 157
Branchiostoma_belcheri 145 RKETE DIKEAS VTE 158
Hydra_vulgarisAEP 193 CKTS EKGQNFDLKQQMKSSHDLFDDFHANHSKSKKKCKNVLNPLEGRT 240
Capitella_teleta
Limulus_polyphemus 123 PHKA DLAKGD CTPI ITGNTCR 143
Lingula_anatina 137 L SKEQNN TEGLSE 149
Dendronephthya_gigantea 252 T SRTTSVCRD QRAST 266
Acanthaster_planci 173 T GTQSAN GTQHET 185
Apostichopus_japonicus 170 V LSTSEK IHSHSS 182
Strongylocentrotus_purpur 133 T SKSTTT NENTNT 145
Aplysia_californica 218 LPSQPF LRPG DRGHRA RYDQSQ 239
Lottia_gigantea 124 N TEKASG TNSSPS 136
Saccoglossus_kowalevskii 124 TDNEP DRSSTH 134
Trichoplax_adhaerens 169 HSADE VFIAKRIL LRNKRR QASKLPLA AIAKE 200
Mizuhopecten_yessoensis 127 SSSEE GNASQ EAGGGNQKE 145
Crassostrea_gigas 139 TGNES EGAKTRRR QGPSYT DSEYDS 163
Crassostrea_virginica 139 AENEL TAPVTKTT RTGSSG SGEEN 162
Pocillopora_damicornis 205 QPKDIESLP REIK NTEQEMSDEWDFKDDPDLHTKN LKDAKNKNVQRDRRHSKL 257
Stylophora_pistillata 205 QPKDIESFL EENR TIEQETSDEWDFKDDPYLHSKN LKDAKNKTVQRDRRDSKV 257
Orbicella_faveolata 165 YPNTCRSYRDKFES FIRQQQ IMEEVPSDEWDPGDDSNLHKKDF TDARKQCKAIVQSERSNEML 227
Acropora_digitifera 134 TGQNDIAGKEGSFT EAEHEL VDKESCDEWEFKDESHLHVTNIRDAKRLDRKPVASNWNKGGIV 196
Centruroides_sculpturatus 124 KFHRK SIIST AWLK 137
Consensus aa:
Consensus ss:
hhh


Conservation:
Homo_sapiens
6j08_chainD_p002
Sarcophilus_harrisii
6j07_chainA_p001
Mus_musculus
Columba_livia
Apteryx_rowi
Chelonia_mydas
Alligator_mississippiensi
Gekko_japonicus
Pogona_vitticeps
Rhincodon_typus
Callorhinchus_milii
Danio_rerio
Latimeria_chalumnae
Scleropages_formosus
Xenopus_laevis
Xenopus_tropicalis
Salmo_salar
Monopterus_albus
Amphidecm_queenslandica
Elysia_chlorotica
Branchiostoma_belcheri
Hydra_vulgarisAEP
Capitella_teleta
Limulus_polyphemus
Lingula_anatina
Dendronephthya_gigantea
Acanthaster_planci
Apostichopus_japonicus
Strongylocentrotus_purpur
Aplysia_californica
Lottia_gigantea
Saccoglossus_kowalevskii
Trichoplax_adhaerens
Mizuhopecten_yessoensis
Crassostrea_gigas
Crassostrea_virginica
Pocillopora_damicornis
Stylophora_pistillata
Orbicella_faveolata
Acropora_digitifera
Centruroides_sculpturatus
Consensus_aa:
Consensus_ss:

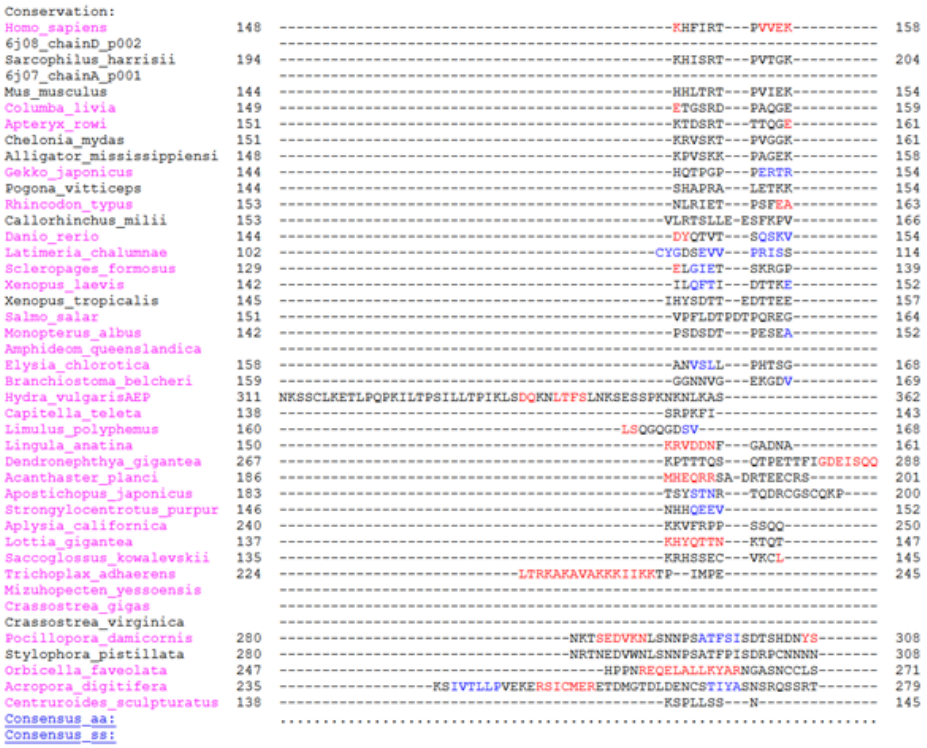
Conservation:
Homo_sapiens
6j08_chainD_p002
Sarcophilus_harrisii
6j07_chainA_p001
Mus_musculus
Columba_livia
Apteryx_rowi
Chelonia_mydas
Alligator_mississippiensi
Gekko_japonicus
Pogona_vitticeps
Rhincodon_typus
Callorhinchus_milii
Danio_rerio
Latimeria_chalumnae
Scleropages_formosus
Xenopus_laevis
Xenopus_tropicalis
Salmo_salar
Monopterus_albus
Amphidecm_queenslandica
Elysia_chlorotica
Branchiostoma_belcheri
Hydra_vulgarisAEP
Capitella_teleta
Limulus_polyphemus
Lingula_anatina
Dendronephthya_gigantea
Acanthaster_planci
Apostichopus_japonicus
Strongylocentrotus_purpur
Aplysia_californica
Lottia_gigantea
Saccoglossus_kowalevskii
Trichoplax_adhaerens
Mizuhopecten_yessoensis
Crassostrea_gigas
Crassostrea_virginica
Pocillopora_damicornis
Stylophora_pistillata
Orbicella_faveolata
Acropora_digitifera
Centruroides_sculpturatus
Consensus_aa:
Consensus_ss:


Conservation:
Homo_sapiens 159 ----------QMYFP----------LQNY 167
6j08_chainD_p002
Sarcophilus_harrisii 205 ----------QLYYP----------LQNY 213
6j07_chainA_p001
Mus_musculus 155 ----------QMCFP----------LHSY 163
Columba_livia 160 ----------FPYRT----------LHEY 168
Apteryx_rowi 162 ----------FAYHA----------LQEY 170
Chelonia_mydas 162 ----------PAYCP----------LQDY 170
Alligator_mississippiensi 159 ----------LSCYP----------LQDY 167
Gekko_japonicus 155 ----------LAYVP----------LQDY 163
Pogona_vitticeps 155 ----------QPYIP----------LQDY 163
Rhincodon_typus 164 ----------TTCHV----------QQMY 172
Callorhinchus_milii 167 ----------SCCHL----------QQMY 175
Danio_rerio 155 ----------CSCCE----------MRQY 163
Latimeria_chalumnae 115 ----------PSCCH----------LQHY 123
Scleropages_formosus 140 ----------FTCCN----------TQHY 148
Xenopus_laevis 153 ----------VRCYT----------LQNY 161
Xenopus_tropicalis 158 ----------VTFYT----------LQNY 166
Salmo_salar 165 ----------ALCCE----------VQHY 173
Monopterus_albus 153 ----------LLCGN----------LQDY 161
Amphideom_queenslandica
Elysia_chlorotica 169 ----------QRNGT----------IGCT 177
Branchiostoma_belcheri 170 ----------VSLAD----------SEK- 177
Hydra_vulgarisAEP 363 ----------EVISTD----------LNVS 372
Capitella_teleta
Limulus_polyphemus 169 ----------LMTCN----------SEL- 176
Lingula_anatina 162 ----------DQEKE----------TTER 170
Dendronephthya_gigantea 289 TNASTGGDFSESSAATSVVSMNEDQKVGRAVSEKLKSEVPKIIFVGEERSLRDITDSAGGPYFTTKLSST 358
Acanthaster_planci 202 ----------DSKDHST----------RRHSH 213
Apostichopus_japonicus 201 --------FQFCNGVEENR----------KDNDV 216
Strongylocentrotus_purpur
Aplysia_californica 251 ----------GPCGA----------ERAQH 260
Lottia_gigantea 148 ----------PVSTR----------TRSTV 157
Saccoglossus_kowalevskii 146 ----------ESRNA----------TKQNF 155
Trichoplax_adhaerens 246 ----------NCDDF----------TFP---- 253
Mizuhopecten_yessoensis
Crassostrea_gigas 168 ----------TTERQ----------QSA---- 175
Crassostrea_virginica 167 ----------TKGQH----------QSG---- 174
Pocillopora_damicornis 309 ----------QADEKQQGQGGYHLQKPVEQDREQQMHCGD---CQELHTSHSQHTEQGESCLDDTKSRN 364
Stylophora_pistillata 309 ----------QADQKQQGQSGYNSKKLTEQDREQQMHSGD---CQEMYSSHAQDGEQRESFLDDTKLKY 364
Orbicella_faveolata 272 ----------ESERKSFCENHSQNLMDHEREQDLYCGEY----QRKLESAGFEGVEERESLLSDSQKAT 326
Acropora_digitifera 280 ----------ADEIKLFTNSTDSQLMGLE----------DKGSFLEGTCLKNQL 313
Centruroides_sculpturatus 146 ----------FTSSCSS----------IDWG--- 156
Consensus_aa:
Consensus_ss:
Homo_sapiens 168 P----------VNNM---------- 172
6j08_chainD_p002
Sarcophilus_harrisii 214 P----------VNNM---------- 218
6j07_chainA_p001
Mus_musculus 164 P----------VNNM---------- 168
Columba_livia 169 P----------VNNM---------- 173
Apteryx_rowi 171 P----------VNNM---------- 175
Chelonia_mydas 171 P----------VNNM---------- 175
Alligator_mississippiensi 168 P----------VNNM---------- 172
Gekko_japonicus 164 P----------ASNM---------- 168
Pogona_vitticeps 164 P----------ASNM---------- 168
Rhincodon_typus 173 P----------VNNM---------- 177
Callorhinchus_milii 176 P----------VNNM---------- 180
Danio_rerio 164 P----------VNNM---------- 168
Latimeria_chalumnae 124 P----------VNNM---------- 128
Scleropages_formosus 149 P----------VNNM---------- 153
Xenopus_laevis 162 P----------VNNM---------- 166
Xenopus_tropicalis 167 P----------VNNM---------- 171
Salmo_salar 174 P----------VNNM---------- 178
Monopterus_albus 162 P----------VNYM---------- 166
Amphideom_queenslandica
Elysia_chlorotica 178 P----------PHRPQTRRSLPKETHLE---------- 195
Branchiostoma_belcheri 178 P----------LAAGSSEYVTAVTGTSSSTILQAKRSQDHREGILQPTDCSDERTSNEEVTE------- 229
Hydra_vulgarisAEP 373 P----------SNSMKLASLKMQPKRTRKSINYHETSEVISTDLNVSPYDSMKLASLRMHPKRTRKSIN 431
Capitella_teleta
Limulus_polyphemus 177 ----------LSKL---------- 180
Lingula_anatina 171 I----------TNGD---------- 175
Dendronephthya_gigantea 359 PN--------ESSV---------- 364
Acanthaster_planci 214 K----------IDSA---------- 218
Apostichopus_japonicus 217 P----------LLEL---------- 221
Strongylocentrotus_purpur
Aplysia_californica 261 P----------ASDS---------- 265
Lottia_gigantea 158 P----------SLHK---------- 162
Saccoglossus_kowalevskii 156 P---------- 156
Trichoplax_adhaerens 254 ----------ENVV---------- 257
Mizuhopecten_yessoensis 146 ----------NKIQ---------- 149
Crassostrea_gigas 176 ----------VVPRE---------- 180
Crassostrea_virginica 175 ----------DRMKK---------- 179
Pocillopora_damicornis 365 KVSPDKGIRPDFLSSM---------- 380
Stylophora_pistillata 365 KVSPDKGFRPRFLSSM---------- 380
Orbicella_faveolata 327 WET-------PKSHSLSKF---------- 338
Acropora_digitifera 314 S----------SFSSAMAKS---------- 323
Centruroides_sculpturatus 157 ----------LFLR---------- 160
Consensus_aa:
Consensus_ss:
h

Figure 10-3 Multiple sequence alignment of TERB2 sequences with PROMALS3D.

The sequences with magenta names are colored according to predicted secondary structures (red: alpha-helix, blue: beta-strand). The sequences with black names

belong to the same taxonomic group as the nearest magenta sequence above them. The first line in each block shows conservation indices for positions with a conservation index above 4. The highlighted rectangles in the alignment correspond to the mouse TERB2 N-terminal domain (violet) and MAJIN-binding site (pink). The highly conserved motif [F/YxLxP] detected in all TERB2 N-terminal sequences is shown in the dark blue rectangle.

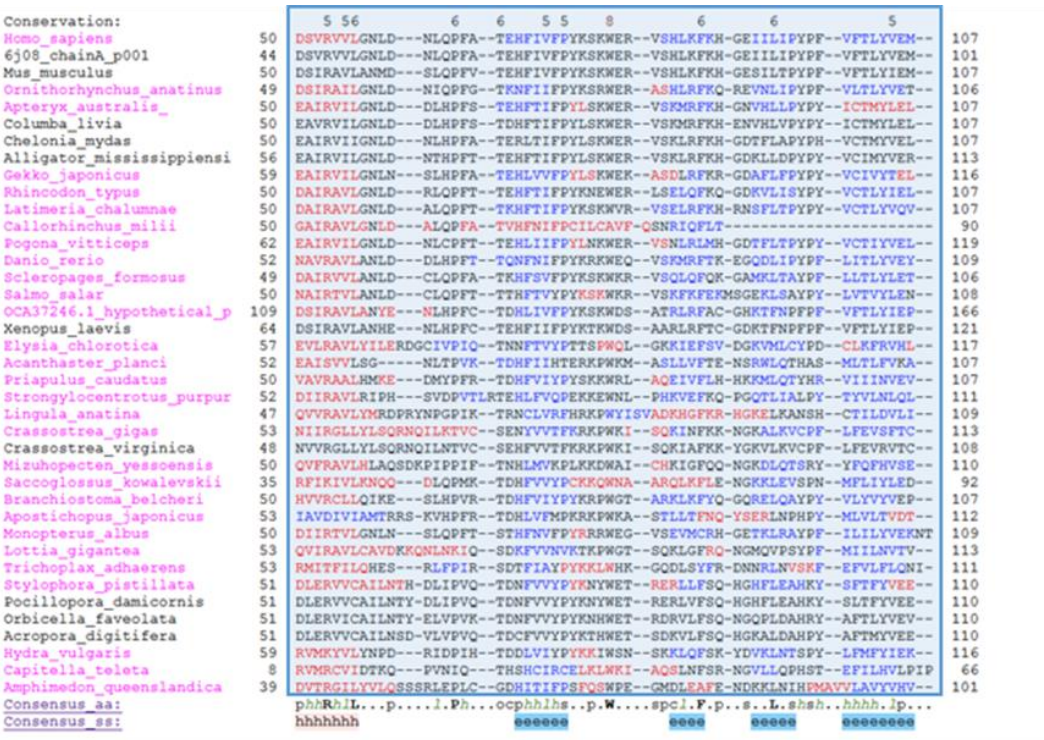

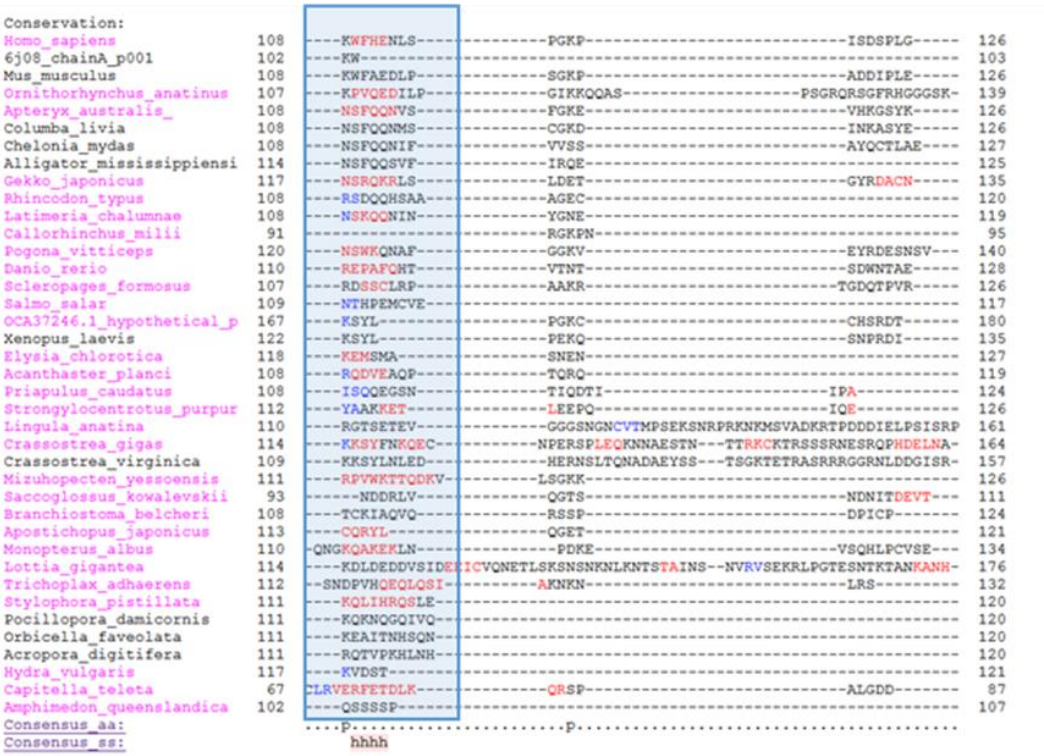

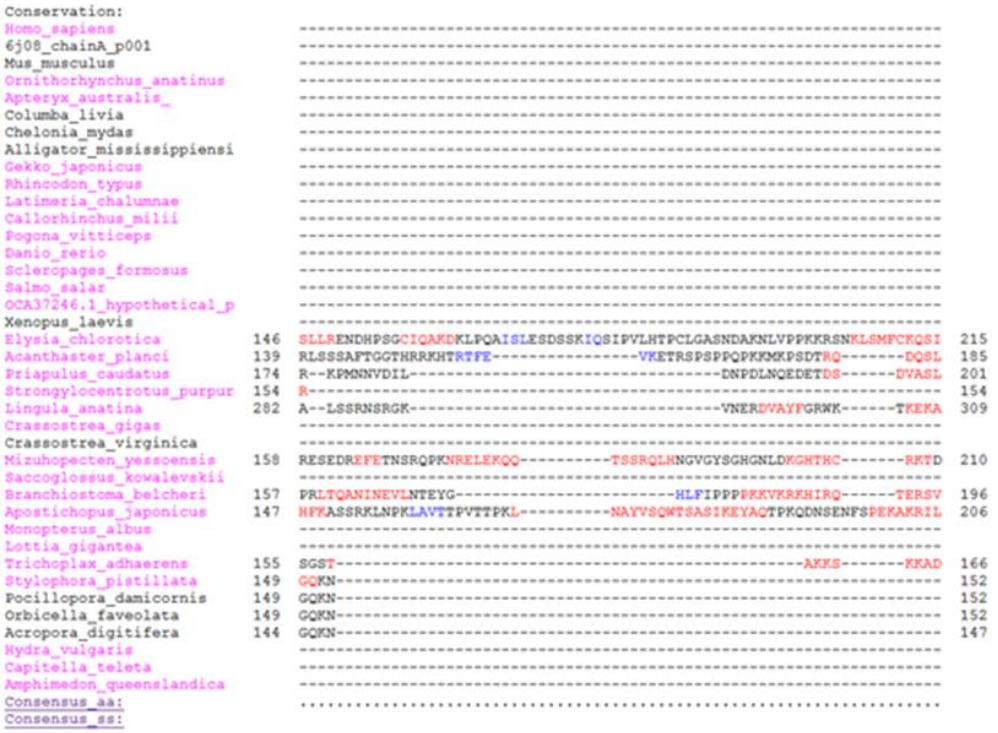
Conservation:
Homo_sapiens
6j08_chainA_p001
Mus_musculus
Ornithorhynchus_anatinus
Apteryx_australis_
Columba_livia
Chelonia_mydas
Alligator_mississippiensi
Gekko_japonicus
Rhincodon_typus
Latimeria_chalumnae
Callorhinchus_milii
Pogona_vitticeps
Danio_rerio
Scleropages_formosus
Salmo_salar
OCA37246.1_hypothetical_p
Xenopus_laevis
Elysia_chlorotica 146 SLLRENDHPSGCIQAKDKLPQAISLESDSSKIQSIPVLHTPCLGASNDAKNLVPPKKRSNKLSMFCKQSI 215
Acanthaster_planci 139 RLSSSAFTGGTHRRKHTRTFE----------VKETRSPSPPQPKKMKPSDTRQ-------DQSL 185
Priapulus_caudatus 174 R--KPMNNVDIL----------DNPDLNQEDETDS------DVASL 201
Strongylocentrotus_purpur 154 R 154
Lingula_anatina 282 A--LSSRNSRGK----------VNERDVAYFGRWK------TKEKA 309
Crassostrea_gigas
Crassostrea_virginica
Mizuhopecten_yessoensis 158 RESEDREFETNSRQPKNRELEKQQ----------TSSRQLHNGVGYSGHGNLDKGHTHC-------RKTD 210
Saccoglossus_kowalevskii
Branchiostoma_belcheri 157 PRLTQANINEVLNTEYG----------HLFIPPPPKKVKRKHIRQ------TERSV 196
Apostichopus_japonicus 147 HFKASSRKLNPKLAVTTPVTTPKL----------NAYVSQWTSASIKEYAQTPKQDNSENFSPEKAKRIL 206
Monopterus_albus
Lottia_gigantea
Trichoplax_adhaerens 155 SGST----------AKKS-------KKAD 166
Stylophora_pistillata 149 GQKN---------- 152
Pocillopora_damicornis 149 GQKN---------- 152
Orbicella_faveolata 149 GQKN---------- 152
Acropora_digitifera 144 GQKN---------- 147
Hydra_vulgaris
Capitella_teleta
Amphimedon_queenslandica
Consensus_aa:
Consensus_ss:


Conservation:
Homo_sapiens
6j08_chainA_p001
Mus_musculus
Ornithorhynchus_anatinus
Apteryx_australis_
Columba_livia
Chelonia_mydas
Alligator_mississippiensi
Gekko_japonicus
Rhincodon_typus
Latimeria_chalumnae
Callorhinchus_milii
Pogona_vitticeps
Danio_rerio
Scleropages_formosus
Salmo_salar
OCA37246.1_hypothetical_p
Xenopus_laevis
Elysia_chlorotica 216 DDSAQQLHALSAVNKSTKICLELNPTVRLADVMKVRNATVDTSVRRSRVDPSETSEVQSQSISTTYKLRP 285
Acanthaster_planci 186 EQQDVQHRAY--LLR----------RRDRVPD--TNERQQHTI-KNYHLRS 221
Priapulus_caudatus 202 MS-ATNMRLMEAVRNKTRVL----------SNGNCSDKTPS--CRAVQEHCL-AEKATKG 247
Strongylocentrotus_purpur 155 -------KLIQEG---------- 160
Lingula_anatina 310 -----HRKLTGNPLK----------NRNSEG---------- 325
Crassostrea_gigas 196 -----KKLLVKRRPNSCEKVVPVMSCDQD-ETSSSSENEDESEEQSEEEYHQPKKRKAAKKCQSGGDWA 259
Crassostrea_virginica 189 -----KRTIKHQRLPSKEVTVELSCDQD----VTSSSSSENEESNSEDEVRSKQKKKKMACKSQFAGDWM 249
Mizuhopecten_yessoensis 211 NRELQRRELQKRNCYAREQENKETVSK-----GKNRTASSDSEDDQLESRR--CLRRSARISDISSKEID 273
Saccoglossus_kowalevskii
Branchiostoma_belcheri 197 RTQEHEAVDQSKELPVT----------QADETP---------- 219
Apostichopus_japonicus 207 SDIATQLRPSSVQQPAANT----------PFSILQNRKRV----------AVKK 240
Monopterus_albus 160 ----------DEI---------- 162
Lottia_gigantea 246 ----------KVVKETEKTQKLPKNK 261
Trichoplax_adhaerens 167 ----------CDRGKK----------DQLPGALE---------- 180
Stylophora_pistillata
Pocillopora_damicornis
Orbicella_faveolata
Acropora_digitifera
Hydra_vulgaris
Capitella_teleta
Amphimedon_queenslandica
Consensus_aa:
Consensus_ss:

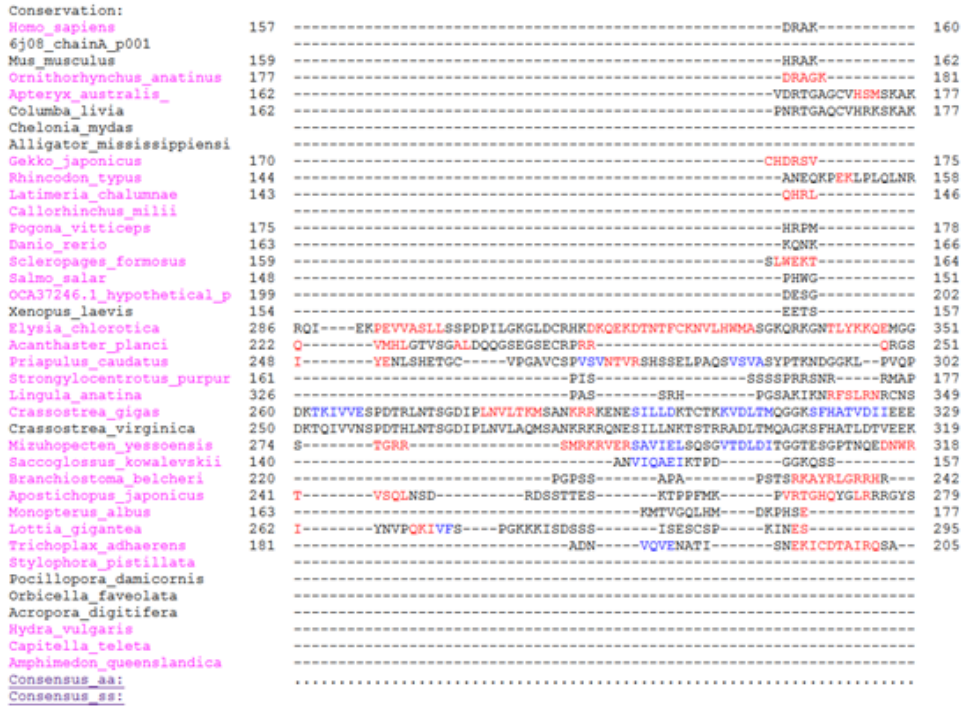
Conservation:
Homo_sapiens 157 ----------DRAK---------- 160
6j08_chainA_p001
Mus_musculus 159 ----------HRAK---------- 162
Ornithorhynchus_anatinus 177 ----------DRAGK---------- 181
Apteryx_australis_ 162 ----------VDRTGAGCVHSMSKAK 177
Columba_livia 162 ----------PNRTGAQCVHRKSKAK 177
Chelonia_mydas
Alligator_mississippiensi
Gekko_japonicus 170 ----------CHDRSV---------- 175
Rhincodon_typus 144 ----------ANEQKPEKLPLQLNR 158
Latimeria_chalumnae 143 ----------QHRL---------- 146
Callorhinchus_milii
Pogona_vitticeps 175 ----------HRPM---------- 178
Danio_rerio 163 ----------KQNK---------- 166
Scleropages_formosus 159 ----------SLWEKT---------- 164
Salmo_salar 148 ----------PHWG---------- 151
OCA37246.1_hypothetical_p 199 ----------DESG---------- 202
Xenopus_laevis 154 ----------EETS---------- 157
Elysia_chlorotica 286 RQI----EKPEVVASLLSSPDPILGKGLDCRHKDKQEKDTNTFCKNVLHWMASGKQRKGNTLYKKQEMGG 351
Acanthaster_planci 222 Q--------VMHLGTVSGALDQQGSEGSECRPRR---------- QRGS 251
Priapulus_caudatus 248 I--------YENLSHETGC-----VPGAVCSPVSVNTVRSHSSELPAQSVSVASYPTKNDGGKL--PVQP 302
Strongylocentrotus_purpur 161 ----------PIS----------SSSSPRRSNR-----RMAP 177
Lingula_anatina 326 ----------PAS-------SRH--------PGSAKIKNRFSLRNRCNS 349
Crassostrea_gigas 260 DKTKIVVESPDTRLNTSGDIPLNVLTKMSANKRRKENESILLDKTCTKKVDLTMQGGKSFHATVDIIEEE 329
Crassostrea_virginica 250 DKTQIVVNSPDTHLNTSGDIPLNVLAQMSANKRKRQNESILLNKTSTRRADLTMQAGKSFHATLDTVEEK 319
Mizuhopecten_yessoensis 274 S--------TGRR----------SMRKRVERSAVIELSQSGVTDLDITGGTESGPTNQEDNWR 318
Saccoglossus_kowalevskii 140 ----------ANVIQAEIKTPD-------GGKQSS--------- 157
Branchiostoma_belcheri 220 ----------PGPSS-------APA--------PSTSRKAYRLGRRKR--- 242
Apostichopus_japonicus 241 T--------VSQLNSD----------RDSSTTES-------KTPPFMK------PVRTGHQYGLRRRGYS 279
Monopterus_albus 163 ----------KMTVGQLHM----DKPHSE---------- 177
Lottia_gigantea 262 I--------YNVPQKIVFS----PGKKKISDSSS-------ISESCSP-----KINES---------- 295
Trichoplax_adhaerens 181 ----------ADN-----VQVENATI-------SNEKICDTAIRQSA-- 205
Stylophora_pistillata
Pocillopora_damicornis
Orbicella_faveolata
Acropora_digitifera
Hydra_vulgaris
Capitella_teleta
Amphimedon_queenslandica
Consensus_aa:
Consensus_ss:

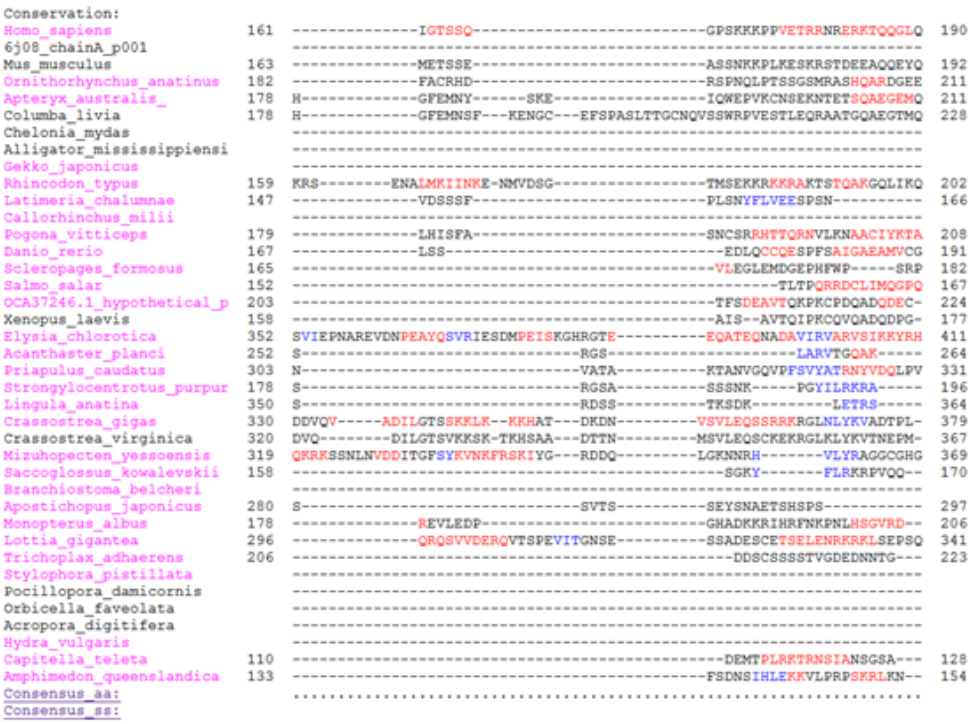
Conservation:
Homo_sapiens 161 ----------IGTSSQ----------GPSKKKPPVETRRNRERKTQQGLQ 190
6j08_chainA_p001
Mus_musculus 163 ----------METSSE----------ASSNKKPLKESKRSTDEEAQQEYQ 192
Ornithorhynchus_anatinus 182 ----------FACRHD----------RSPNQLPTSSGSMRASHQARDGEE 211
Apteryx_australis_ 178 H----------GFEMNY------SKE----------IQWEPVKCNSEKNTETSQAEGEMQ 211
Columba_livia 178 H----------GFEMNSF---KENGC---EFSPASLTTGCNQVSSWRPVESTLEQRAATGQAEGTMQ 228
Chelonia_mydas
Alligator_mississippiensi
Gekko_japonicus
Rhincodon_typus 159 KRS--------ENALMKIINKE-NMVDSG----------TMSEKKRKKRAKTSTQAKGQLIKQ 202
Latimeria_chalumnae 147 ----------VDSSSF----------PLSNYFLVEESPSN---------- 166
Callorhinchus_milii
Pogona_vitticeps 179 ----------LHISFA----------SNCSRRHTTQRNVLKNAACIYKTA 208
Danio_rerio 167 ----------LSS----------EDLQCCQESPFSAIGAEAMVCG 191
Scleropages_formosus 165 ----------VLEGLEMDGEPHFWP-----SRP 182
Salmo_salar 152 ----------TLTPQRRDCLIMQGPQ 167
OCA37246.1_hypothetical_p 203 ----------TFSDEAVTQKPKCPDQADQDEC- 224
Xenopus_laevis 158 ----------AIS--AVTQIPKCQVQADQDPG- 177
Elysia_chlorotica 352 SVIEPNAREVDNPEAYQSVRIESDMPEISKGHRGTE----------EQATEQNADAVIRVARVSIKKYRH 411
Acanthaster_planci 252 S----------RGS----------LARVTGQAK----- 264
Priapulus_caudatus 303 N----------VATA----------KTANVGQVPFSVYATRNYVDQLPV 331
Strongylocentrotus_purpur 178 S----------RGSA----------SSSNK-----PGYILRKRA----- 196
Lingula_anatina 350 S----------RDSS----------TKSDK---------LETRS----- 364
Crassostrea_gigas 330 DDVQV-----ADILGTSSKKLK--KKHAT---DKDN---------VSVLEQSSRRKRGLNLYKVADTPL- 379
Crassostrea_virginica 320 DVQ--------DILGTSVKKSK-TKHSAA---DTTN---------MSVLEQSCKEKRGLKLYKVTNEPM- 367
Mizuhopecten_yessoensis 319 QRRKSSNLNVDDITGFSYKVNKFRSKIYG---RDDQ---------LGKNNRH-------VLYRAGGCGHG 369
Saccoglossus_kowalevskii 158 ----------SGKY-------FLRKRPVQQ-- 170
Branchiostoma_belcheri
Apostichopus_japonicus 280 S----------SVTS----------SEYSNAETSHSPS---------- 297
Monopterus_albus 178 ----------REVLEDP----------GHADKKRIHRFNKPNLHSGVRD-- 206
Lottia_gigantea 296 ----------QRQSVVDERQVTSPEVITGNSE----------SSADESCETSELENRKRKLSEPSQ 341
Trichoplax_adhaerens 206 ----------DDSCSSSSTVGDEDNNTG--- 223
Stylophora_pistillata
Pocillopora_damicornis
Orbicella_faveolata
Acropora_digitifera
Hydra_vulgaris
Capitella_teleta 110 ----------DEMTPLRKTRNSIANSGSA--- 128
Amphimedon_queenslandica 133 ----------FSDNSIHLEKKVLPRPSKRLKN-- 154
Consensus_aa:
Consensus_ss:


Conservation:
Homo_sapiens 191 ET 192
6j08_chainA_p001
Mus_musculus 193 DT 194
Ornithorhynchus_anatinus 212 AAPSRSPLYVPVAEESVA QQGS 233
Apteryx_australis_ 212 LP 213
Columba_livia 229 LL 230
Chelonia_mydas
Alligator_mississippiensi
Gekko_japonicus
Rhincodon_typus 203 PS 204
Latimeria_chalumnae
Callorhinchus_milii
Pogona_vitticeps 209 KPRLQKDMIYLPQNQPEEMP HRCCGPA 235
Danio_rerio 192 TK 193
Scleropages_formosus 183 ET 184
Salmo_salar 168 SR 169
OCA37246.1_hypothetical_p
Xenopus_laevis
Elysia_chlorotica 412 QKTQSLKAKQTFDENGDGAVGNEGKESPQKKSLDREKNRPWRNFFCFEMQDSDMVEVHNNGSVITSPSYS 481
Acanthaster_planci 265 QEHVRDI SHPHEAEPRVGATANVPSRP 291
Priapulus_caudatus 332 WPTVPTMETANEYVSRLPVQPV-PVSVETASSSHGQLSVKPFLTSVSHCSINNGQLPVQPISEAMEAALC 400
Strongylocentrotus_purpur 197 LRV TTSNNTSNNS NMLQRGGSHTIPPDDKRLDE 229
Lingula_anatina 365 VKLR IKKHPLSKNK AHITRAVSLTTDSMRNKADAF 399
Crassostrea_gigas 380 MNLPSLEN SLNEP SSNLTQQLNFKHTFL 407
Crassostrea_virginica 368 MNLPSVEN SLNNS PPNVTQQLNFKDT 393
Mizuhopecten_yessoensis 370 TERPPLIMELPEVSPSDGTAEIPNKSKRKRPSDTDQTLTKDQTNSSTERCGGLTASIPNNKPTYDNVQTT 439
Saccoglossus_kowalevskii 171 SNEEP SSKRPV 181
Branchiostoma_belcheri
Apostichopus_japonicus
Monopterus_albus
Lottia_gigantea 342 SQNSQSEGFPEKRGRGRPRK LDQASLL 368
Trichoplax_adhaerens
Stylophora_pistillata
Pocillopora_damicornis
Orbicella_faveolata
Acropora_digitifera
Hydra_vulgaris
Capitella_teleta
Amphimedon_queenslandica
Consensus_aa:
Consensus_ss:
Conservation:
Homo_sapiens
6j08_chainA_p001
Mus_musculus
Ornithorhynchus_anatinus
Apteryx_australis_
Columba_livia
Chelonia_mydas
Alligator_mississippiensi
Gekko_japonicus
Rhincodon_typus
Latimeria_chalumnae
Callorhinchus_milii
Pogona_vitticeps
Danio_rerio
Scleropages_formosus
Salmo_salar
OCA37246.1_hypothetical_p
Xenopus_laevis
Elysia_chlorotica 482 SAGQGRKRRNKSPVQYDNKLDGRNNSEVKKQRQQILRSCSPKKKLYNSETGFGSFRNLNITEGYRSPQIL 551
Acanthaster_planci 292 AYPQGGAVQHDTHHV LQPAQHD 313
Priapulus_caudatus 401 CSRQFPAWPVAEAVEEAKRSGRQLPVKPVPVSVSTFMNYVGQLPVEPGSASVDIARSYSEPIPVQPAVTT 470
Strongylocentrotus_purpur 230 AGMLDGWDEQTGRR NRDRI DIERQKRERSPELESG 264
Lingula_anatina 400 SVSSHVKHKLSDK SNRNV ALERQRS 424
Crassostrea_gigas 408 SPGGESSLKSKEGWKNAHNSLTPLSRFNR SEP 439
Crassostrea_virginica 394 FLSPSTISKEESNVVDSSLTPLRRFDR NEH 423
Mizuhopecten_yessoensis 440 VNPRRNQDGSSDSRQSGTDSQSLRDGRRKQNTSQSNGHKRLLGSSIKVQRSSDSPKGHRAHTRSSEPPKG 509
Saccoglossus_kowalevskii
Branchiostoma_belcheri
Apostichopus_japonicus
Monopterus_albus
Lottia_gigantea 369 ALKEQKKAAK 378
Trichoplax_adhaerens
Stylophora_pistillata
Pocillopora_damicornis
Orbicella_faveolata
Acropora_digitifera
Hydra_vulgaris
Capitella_teleta
Amphimedon_queenslandica
Consensus_aa:
Consensus_ss:


Conservation:
Homo_sapiens
6j08_chainA_p001
Mus_musculus
Ornithorhynchus_anatinus
Apteryx_australis_
Columba_livia
Chelonia_mydas
Alligator_mississippiensi
Gekko_japonicus
Rhincodon_typus
Latimeria_chalumnae
Callorhinchus_milii
Pogona_vitticeps
Danio_rerio
Scleropages_formosus
Salmo_salar
OCA37246.1_hypothetical_p
Xenopus_laevis
Elysia_chlorotica 552 KESSTTSQYYRQKLCEKQKIRTELKTVCAEGDSAKRNSQTRSSPRLGNKLNSNNIVTLYTNFIETASHLQ 621
Acanthaster_planci 314 GAQYQL 319
Priapulus_caudatus 471 MTTASNNSGQPPVQAAPVT----LQAHGNYGDQSQFHPTSMETDSNCFGQLPQAAVTMETARHYSDQLLV 536
Strongylocentrotus_purpur 265 FSRLVQGKAAVGPERFPRVNESADR 289
Lingula_anatina 425 LNHVEVQENRMQNSSV 440
Crassostrea_gigas 440 EKGANGRNK--- 448
Crassostrea_virginica 424 EEGTNKKSKG-- 433
Mizuhopecten_yessoensis 510 RKSASPAKDVKIPTRSLTSSKGHRSQARSVTPSKGHRGRLRSATPSKSLRGQLRSATPSSHRNGMRSATT 579
Saccoglossus_kowalevskii
Branchiostoma_belcheri 243 SVDT 246
Apostichopus_japonicus
Monopterus_albus
Lottia_gigantea 379 KKYVVNPETRNLMMLRRIVE 398
Trichoplax_adhaerens
Stylophora_pistillata
Pocillopora_damicornis
Orbicella_faveolata
Acropora_digitifera
Hydra_vulgaris
Capitella_teleta
Amphimedon_queenslandica
Consensus_aa:
Consensus_ss:


Conservation:
Homo_sapiens
6j08_chainA_p001
Mus_musculus
Ornithorhynchus_anatinus
Apteryx_australis_
Columba_livia
Chelonia_mydas
Alligator_mississippiensi
Gekko_japonicus
Rhincodon_typus
Latimeria_chalumnae
Callorhinchus_milii
Pogona_vitticeps
Danio_rerio
Scleropages_formosus
Salmo_salar
OCA37246.1_hypothetical_p
Xenopus_laevis
Elysia_chlorotica 622 PNLRSPKGTSGHELPTVETKQNTVKRSAHQTQNLSVRKSPKQSANGRMSEPIVSKKITRNSPNLRKRKSD 691
Acanthaster_planci
Priapulus_caudatus 537 HPAPVSIYPVRCYRSQ----------IPAPALGGCVTSYHSTGPAQTNAASLEVAWQCHDS 587
Strongylocentrotus_purpur 290 DHSHVECT----------GDQGPMPARPSDGGAARVGVPGH---- 320
Lingula_anatina 441 IKHKGTRVQL----------QPPPGRSSPRKSKSTPAVLSD------ 471
Crassostrea_gigas 449 RSVNFPV 455
Crassostrea_virginica 434 INFPV 438
Mizuhopecten_yessoensis 580 SIARRGRMRSATPSEGHRIRLRSAISSKAQSDHLRPATLSKSLRGRKRLATPSEESERLLNMTHPEEHGI 649
Saccoglossus_kowalevskii
Branchiostoma_belcheri 247 PISGRPRKIHLHSR---- 260
Apostichopus_japonicus 298 GRRDVAYL------- 305
Monopterus_albus 207 SESPG 211
Lottia_gigantea 399 SSDESEKKRL----------RLRLPLSNQIRKSPRIQQKGSKDKWSNKN 437
Trichoplax_adhaerens 224 SNRNIVTTALACDEA 238
Stylophora_pistillata
Pocillopora_damicornis
Orbicella_faveolata
Acropora_digitifera
Hydra_vulgaris
Capitella_teleta
Amphimedon_queenslandica
Consensus_aa:
Consensus_ss:

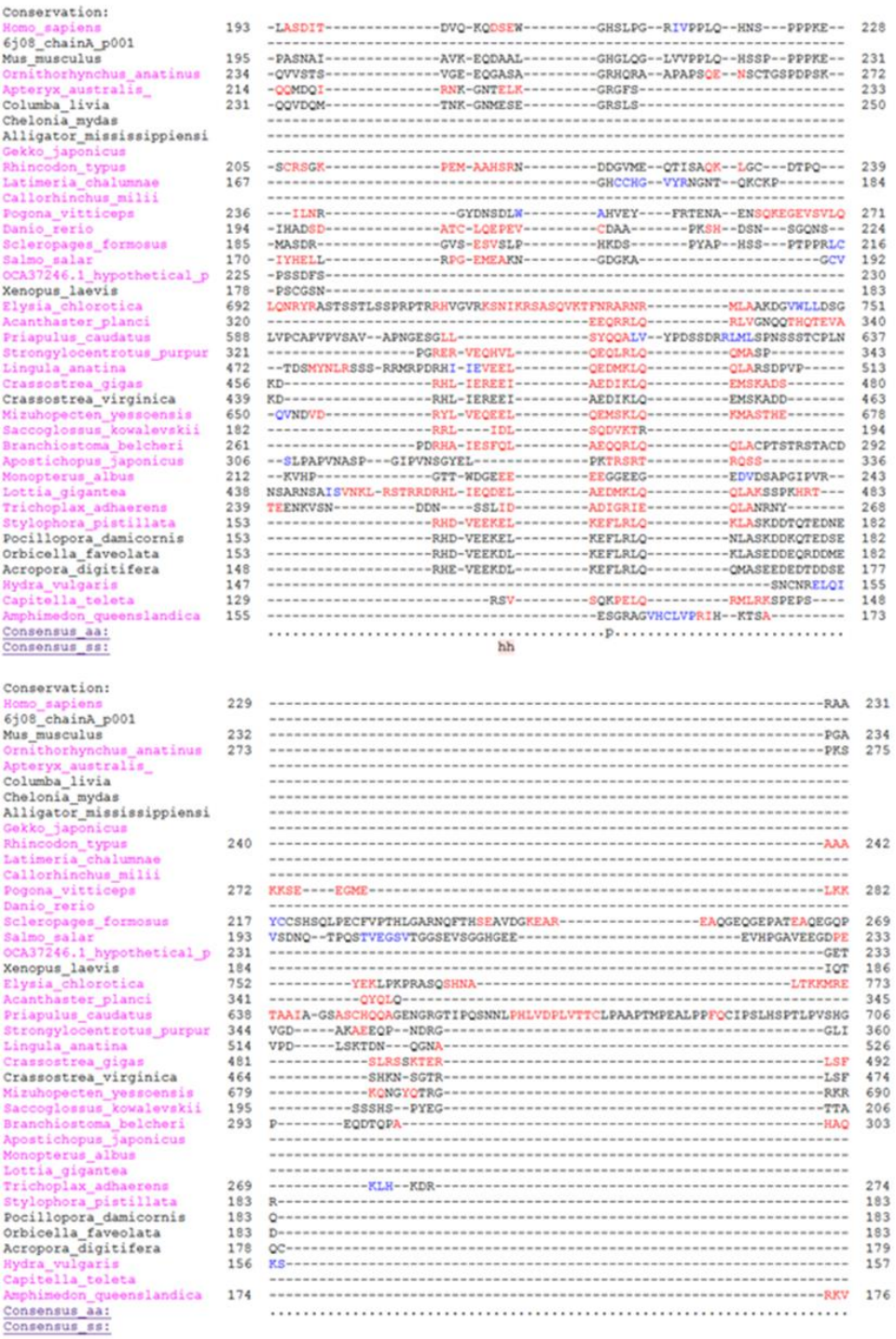
Conservation:
Homo_sapiens 193 -LASDIT-------------DVQ-KQDSEW---------GHSLPG--RIVPPLQ--HNS---PPPKE-- 228
6j08_chainA_p001
Mus_musculus 195 -PASNAI-------------AVK-EQDAAL---------GHGLQG--LVVPPLQ--HSSP--PPPKE-- 231
Ornithorhynchus_anatinus 234 -QVVSTS-------------VGE-EQGASA---------GRHQRA--APAPSQE--NSCTGSPDPSK-- 272
Apteryx_australis_ 214 -QQMDQI-------------RNK-GNTELK---------GRGFS---------- 233
Columba_livia 231 -QQVDQM-------------TNK-GNMESE---------GRSLS---------- 250
Chelonia_mydas
Alligator_mississippiensi
Gekko_japonicus
Rhincodon_typus 205 -SCRSGK-------------PEM-AAHSRN---------DDGVME--QTISAQK--LGC---DTPQ--- 239
Latimeria_chalumnae 167 ----------GHCCHG--VYRNGNT--QKCKP-------- 184
Callorhinchus_milii
Pogona_vitticeps 236 ---ILNR---------------GYDNSDLN---------AHVEY----FRTENA--ENSQKEGEVSVLQ 271
Danio_rerio 194 -IHADSD-------------ATC-LQEPEV---------CDAA-------PKSH--DSN---SGQNS-- 224
Scleropages_formosus 185 -MASDR-------------GVS-ESVSLP---------HKDS-------PYAP--HSS---PTPPRLC 216
Salmo_salar 170 -IYHELL-------------RPG-EMEAKN---------GDGKA---------GCV 192
OCA37246.1_hypothetical_p 225 -PSSDFS---------- 230
Xenopus_laevis 178 -PSCGSN---------- 183
Elysia_chlorotica 692 LQNRYRASTSSTLSSPRPTRRHVGVRKSNIKRSASQVKTFNRARNR---------MLAAKDGVWLLDSG 751
Acanthaster_planci 320 ----------EEQRRLQ---------RLVGNQQTHQTEVA 340
Priapulus_caudatus 588 LVPCAPVPVSAV--APNGESGLL---------SYQQALV--YPDSSDRRLMLSPNSSSTCPLN 637
Strongylocentrotus_purpur 321 ----------PGRER-VEQHVL---------QEQLRLQ---------QMASP--------- 343
Lingula_anatina 472 --TDSMYNLRSSS-RRMRPDRHI-IEVEEL---------QEDMKLQ---------QLARSDPVP----- 513
Crassostrea_gigas 456 KD----------RHL-IEREEI---------AEDIKLQ---------EMSKADS------- 480
Crassostrea_virginica 439 KD----------RHL-IEREEI---------AEDIKLQ---------EMSKADD------- 463
Mizuhopecten_yessoensis 650 -QVNDVD----------RYL-VEQEEL---------QEMSKLQ---------KMASTHE------- 678
Saccoglossus_kowalevskii 182 ----------RRL----IDL---------SQDVKTR---------- 194
Branchiostoma_belcheri 261 ----------PDRHA-IESFQL---------AEQQRLQ---------QLACPTSTRSTACD 292
Apostichopus_japonicus 306 --SLPAPVNASP---GIPVNSGYEL----------PKTRSRT---------RQSS---------- 336
Monopterus_albus 212 --KVHP----------GTT-WDGEEE---------EEGGEEG---------EDVDSAPGIPVR-- 243
Lottia_gigantea 438 NSARNSAISVNKL-RSTRRDRHL-IEQDEL---------AEDMKLQ---------QLAKSSPKHRT--- 483
Trichoplax_adhaerens 239 TEENKVSN----------DDN----SSLID---------ADIGRIE---------QLANRNY------- 268
Stylophora_pistillata 153 ----------RHD-VEEKEL---------KEFLRLQ---------KLASKDDTQTEDNE 182
Pocillopora_damicornis 153 ----------RHD-VEEKEL---------KEFLRLQ---------NLASKDDKQTEDSE 182
Orbicella_faveolata 153 ----------RHD-VEEKDL---------KEFLRLQ---------KLASEDDEQRDDME 182
Acropora_digitifera 148 ----------RHE-VEEKDL---------KEFLRLQ---------QMASEEDEDTDDSE 177
Hydra_vulgaris 147 ----------SNCNRELQI 155
Capitella_teleta 129 ----------RSV---------SQKPELQ---------RMLRKSPEPS---- 148
Amphimedon_queenslandica 155 ----------ESGRAGVHCLVPRIH--KTSA--------- 173
Consensus_aa:
Consensus_ss:
hh
Conservation:
Homo_sapiens 229 ----------RAA 231
6j08_chainA_p001
Mus_musculus 232 ----------PGA 234
Ornithorhynchus_anatinus 273 ----------PKS 275
Apteryx_australis_
Columba_livia
Chelonia_mydas
Alligator_mississippiensi
Gekko_japonicus
Rhincodon_typus 240 ----------AAA 242
Latimeria_chalumnae
Callorhinchus_milii
Pogona_vitticeps 272 KKSE----EGME----------LKK 282
Danio_rerio
Scleropages_formosus 217 YCCSHSQLPECFVPTHLGARNQFTHSEAVDGKEAR----------EAQGEQGEPATEAQEGQP 269
Salmo_salar 193 VSDNQ--TPQSTVEGSVTGGSEVSGGHGEE----------EVHPGAVEEGDPE 233
OCA37246.1_hypothetical_p 231 ----------GET 233
Xenopus_laevis 184 ----------IQT 186
Elysia_chlorotica 752 ----------YEKLPKPRASQSHNA----------LTKKMRE 773
Acanthaster_planci 341 ----------QYQLQ---------- 345
Priapulus_caudatus 638 TAAIA-GSASCHQQAGENGRGTIPQSNNLPHLVDPLVTTCLPAAPTMPEALPPFQCIPSLHSPTLPVSHG 706
Strongylocentrotus_purpur 344 VGD-----AKAEEQP--NDRG----------GLI 360
Lingula_anatina 514 VPD-----LSKTDN---QGNA---------- 526
Crassostrea_gigas 481 ----------SLRSSKTER----------LSF 492
Crassostrea_virginica 464 ----------SHKN-SGTR----------LSF 474
Mizuhopecten_yessoensis 679 ----------KQNGYQTRG----------RKR 690
Saccoglossus_kowalevskii 195 ----------SSSHS--PYEG----------TTA 206
Branchiostoma_belcheri 293 P--------EQDTQPA----------HAQ 303
Apostichopus_japonicus
Monopterus_albus
Lottia_gigantea
Trichoplax_adhaerens 269 ----------KLH--KDR---------- 274
Stylophora_pistillata 183 R---------- 183
Pocillopora_damicornis 183 Q---------- 183
Orbicella_faveolata 183 D---------- 183
Acropora_digitifera 178 QC---------- 179
Hydra_vulgaris 156 KS---------- 157
Capitella_teleta
Amphimedon_queenslandica 174 ----------RKV 176
Consensus_aa:
Consensus_ss:

Figure 10-4.-Multiple sequence alignment of MAJIN sequences carried out using the PROMALS3D.

The sequences with magenta names are colored according to predicted secondary structures (red: alpha-helix, blue: beta-strand). The sequences with black names belong to the same taxonomic group of the nearest magenta sequence above. The first line in each block shows conservation indices for positions with a conservation index above 4. The highlighted rectangles in the alignment correspond to the mouse MAJIN N-terminal domain (blue) and TM domain (in dark green).

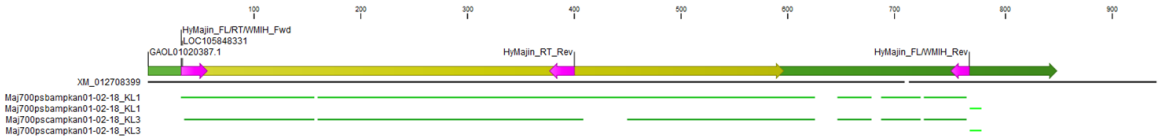

Figure 10-5 *Hydra Vulgaris* MAJIN transcript model.

Schematic representation of the blastn performed with transcript model of hydra vulgaris XM_012708399 vs independent cloning sequences obtained after amplification and sequencing of *Hydra vulgaris* AEP Majin, shown at the right side of the panel. The horizontal green lines are the regions with ≥ 90 % identity between query and the respect sequences analyzed. The primers used for hydra Majin are shown in fuchsia and the coding region of the transcript is depicted in yellow while the whole mRNA prediction is in dark green. After the amplification we obtained a 735 bp sequence corresponding to 186 amino acids residues.

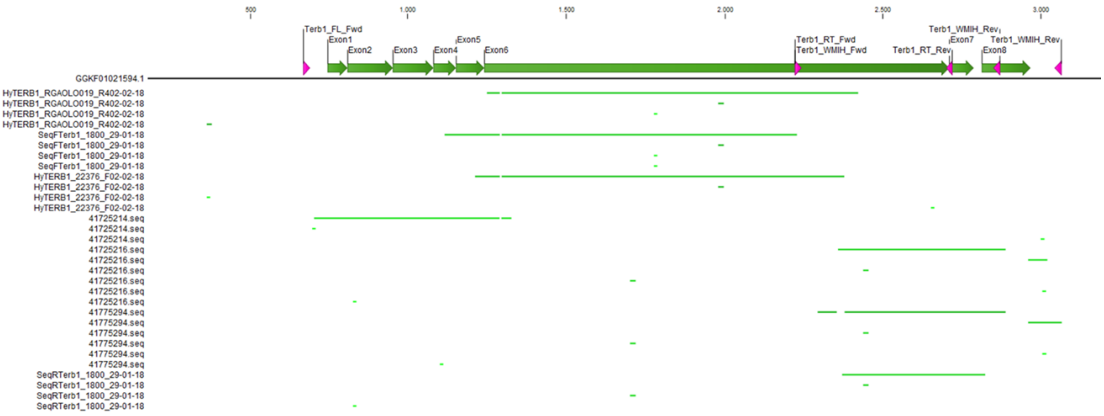

Figure 10-6 Prediction of the full open reading frame of *Hydra Vulgaris* TERB1

Schematic representation of the blastn performed with the assembled transcript sequence GGKF01021594 as query vs independent cloning sequences obtained after amplification and sequencing of hydra vulgaris AEP Terb1 shown at the right side of the panel. The horizontal green lines are the regions with ≥ 90 % identity between query and the respect sequences analyzed. The assembled transcript sequence GGKF01021594 was annotated with the primers (fuscia) used in this analysis and the exons (green) from the genomic reference sequence (GenBank ID: NW_004171015). The predicted ORF sequence of hydra Terb1 was obtained combining all the sequence in 2218 bp which correspond to 738 amino acids residues.

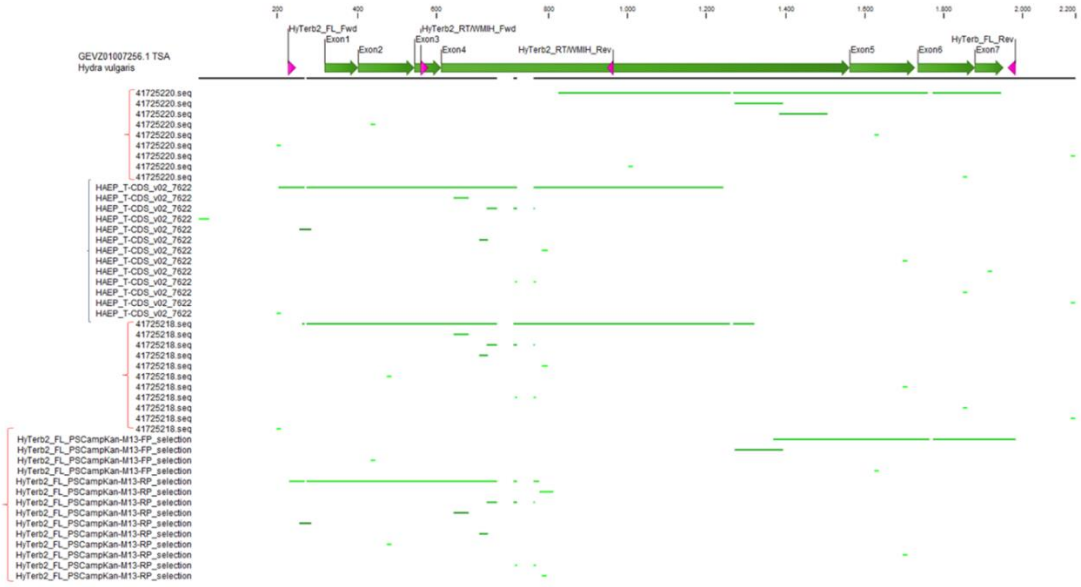

Figure 10-7 Prediction of the full open reading frame of *Hydra Vulgaris* TERB2

Schematic illustration of blastn performed with the assembled transcript sequence GEVZ01007256 as query vs HAEP_T-CDS_v02_7622 (transcript sequence from *Hydra vulgaris* AEP Compagen database) (blue brackets) and the independent cloning sequences obtained after amplification and sequencing (red brackets) of *Hydra vulgaris* AEP Terb2, shown at the right side of the panel. The horizontal green lines are the regions with ≥ 90 % identity between query and the respect sequences analyzed. The assembled transcript sequence GEVZ01007256 was annotated with the primers (fuchsia) used in this analysis and the exons (green) from the genomic reference sequence (GenBank ID: NW_00417053). The predicted ORF sequence of hydra Terb2 was obtained combining all the sequence in 2134 bp corresponding to 591 amino acid residues.

Affidavit

I hereby declare that my thesis entitled: „ Investigating the murine meiotic telomere complex TERB1-TERB2-MAJIN: spatial organization and evolutionary history" is the result of my own work. I did not receive any help or support from commercial consultants. All sources and / or materials applied are listed and specified in the thesis.

Furthermore I verify that the thesis has not been submitted as part of another examination process neither in identical nor in similar form.

Besides I declare that if I do not hold the copyright for figures and paragraphs, I obtained it from the rights holder and that paragraphs and figures have been marked according to law or for figures taken from the internet the hyperlink has been added accordingly.

Würzburg, den 20 May, 2020

_____

Signature PhD-student

Peer-reviewed articles obtained in this thesis

da Cruz, I., Brochier-Armanet, C., & Benavente, R. (2020). The TERB1-TERB2-MAJIN complex of mouse meiotic telomeres dates back to the common ancestor of metazoans. BMC Evolutionary Biology, 20(1), 1-11.

Dunce, J. M., Milburn, A. E., Gurusaran, M., **da Cruz, I**., Sen, L. T., Benavente, R., & Davies, O. R. (2018). Structural basis of meiotic telomere attachment to the nuclear envelope by MAJIN-TERB2-TERB1. Nature communications, 9(1), 5355.

Others peer-reviewed articles

da Cruz, I., Rodriguez-Casuriaga, R., Santinaque, F. F., Farias, J., Curti, G., Capoano, C. A., Folle, G. A., Benavente, R., Sotelo-Silveira, J. R., Geisinger, A. (2016). Transcriptome analysis of highly purified mouse spermatogenic cell populations: gene expression signatures switch from meiotic-to postmeiotic-related processes at pachytene stage. BMC Genomics,17(1),294.

Acknowledgments

The Ph.D. journey has been a truly life-changing experience for me, and it would not have been possible without the support I have received from many people.

Firstly, I owe my deepest gratitude to my supervisor Prof. Ricardo Benavente for his support and encouragement to undertake this Ph.D. abroad. Also for accepting me as a Ph.D. student in his group and to be part of exciting projects and collaborations. His guidance and freedom helped me to frame my research and have been the backbone of my professional growth.

I am indebted to my collaboration partners Owen Davies and Céline Brochier-Armanet with whom the publications of the work performed in this thesis would not have been possible to accomplish. Thank you also for the learning experience and fruitful discussions along the process.

I would like to thank Prof. Manfred Alsheimer for generous advice in experimental design and for constructive insights that helped me to improve the quality of my research.

Special thanks to my second supervisor Prof. Christian Stigloher for his time dedicated in taking over my thesis reports and for his support and advice.

This work would not have either been accomplished without the technical support of Elisabeth Meyer-Natus who took very good care of the hydra culture and without Marcus Behringer for his assistance in the acquisition of the images with SIM microscope.

I would also like to express my gratitude to Ines Subouta, Brooke Morriswood, and Elena Bencurova who have contributed to proof-reading my work and for receiving valuable remarks and honest criticism.

I would like to express my faithful thanks to all my dear colleagues from Zoology I. Being part of the Department was always a joy and inspiration for me. Thank you all for being so generous and attentive.

There are no words great enough to thank my colleagues Marie-Christin Splinder who have unwavering supported me. Thank you for being the face in the audience when I was nervous and for the long talks, laugh and fun in the lab.

I gratefully acknowledge the funding support from the DAAD scholarship that allowed me to pursue my biggest ambitions to obtain a doctoral degree abroad. Finally, I am deeply grateful for the unconditional support and infinite love of my family and friends to pursuit my dreams on this journey.